

WL-TR-97-1003

HIGH DEFINITION DISPLAY BASED ON THE
DIGITAL MICROMIRROR DEVICE (DMD)
SPATIAL LIGHT MODULATOR

JACK M. YOUNSE

TEXAS INSTRUMENTS
P.O. BOX 655012
DALLAS TX 75265

JANUARY 1997

FINAL REPORT FOR 03/09/90 - 08/30/96



UNCLASSIFIED

APPROVED FOR PUBLIC RELEASE; DISTRIBUTION IS UNLIMITED.

19970225 106

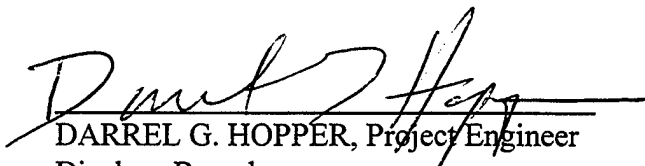
AVIONICS DIRECTORATE
WRIGHT LABORATORY
AIR FORCE MATERIEL COMMAND
WRIGHT PATTERSON AFB OH 45433-7623

NOTICE

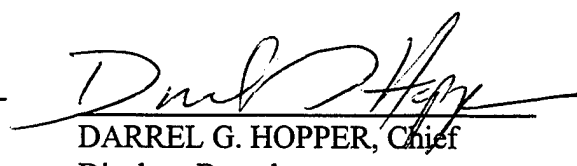
WHEN GOVERNMENT DRAWINGS, SPECIFICATIONS, OR OTHER DATA ARE USED FOR ANY PURPOSE OTHER THAN IN CONNECTION WITH A DEFINITE GOVERNMENT-RELATED PROCUREMENT, THE UNITED STATES GOVERNMENT INCURS NO RESPONSIBILITY OR ANY OBLIGATION WHATSOEVER. THE FACT THAT THE GOVERNMENT MAY HAVE FORMULATED OR IN ANY WAY SUPPLIED THE SAID DRAWINGS, SPECIFICATIONS, OR OTHER DATA, IS NOT TO BE REGARDED BY IMPLICATION, OR OTHERWISE IN ANY MANNER CONSTRUED, AS LICENSING THE HOLDER, OR ANY OTHER PERSON OR CORPORATION; OR AS CONVEYING ANY RIGHTS OR PERMISSION TO MANUFACTURE, USE, OR SELL ANY PATENTED INVENTION THAT MAY IN ANY WAY BE RELATED THERETO.

THIS REPORT IS RELEASABLE TO THE NATIONAL TECHNICAL INFORMATION SERVICE (NTIS). AT NTIS, IT WILL BE AVAILABLE TO THE GENERAL PUBLIC, INCLUDING FOREIGN NATIONS.

THIS TECHNICAL REPORT HAS BEEN REVIEWED AND IS APPROVED FOR PUBLICATION.



DARREL G. HOPPER, Project Engineer
Displays Branch
Avionics Directorate



DARREL G. HOPPER, Chief
Displays Branch
Avionics directorate

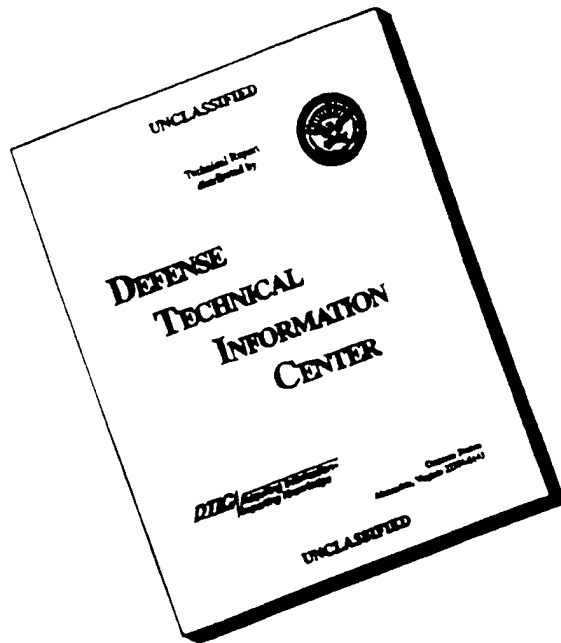


RICHARD D. HUNZIKER, Acting Chief
Electro-Optic Technology Division
Avionics Directorate

IF YOUR ADDRESS HAS CHANGED, IF YOU WISH TO BE REMOVED FROM OUR MAILING LIST, OR IF THE ADDRESSEE IS NO LONGER EMPLOYED BY YOUR ORGANIZATION PLEASE NOTIFY WL/AAJD WRIGHT-PATTERSON AFB OH 45433- 7511 TO HELP MAINTAIN A CURRENT MAILING LIST.

Copies of this report should not be returned unless return is required by security considerations, contractual obligations, or notice on a specific document.

DISCLAIMER NOTICE



THIS DOCUMENT IS BEST QUALITY AVAILABLE. THE COPY FURNISHED TO DTIC CONTAINED A SIGNIFICANT NUMBER OF PAGES WHICH DO NOT REPRODUCE LEGIBLY.

| REPORT DOCUMENTATION PAGE | | | Form Approved OMB No. 0704-0188 | |
|--|---|--|---|--|
| Public reporting burden for this collection of information is estimated to average 1 hour per response, including the time for reviewing instructions, searching existing data sources, gathering and maintaining the data needed, and completing and reviewing the collection of information. Send comments regarding this burden estimate or any other aspect of this collection of information, including suggestions for reducing this burden, to Washington Headquarters Services, Directorate for Information Operations and Reports, 1215 Jefferson Davis Highway, Suite 1204, Arlington, VA 22202-4302, and to the Office of Management and Budget, Paperwork Reduction Project (0704-0188), Washington, DC 20503. | | | | |
| 1. AGENCY USE ONLY (Leave blank) | 2. REPORT DATE January 1997 | 3. REPORT TYPE AND DATES COVERED Final 03/09/90 - 08/30/96 | | |
| 4. TITLE AND SUBTITLE High Definition Display Based on The Digital Micromirror Device (DMD) Spatial Light Modulator | | | 5. FUNDING NUMBERS C: MDA972-90-C-0008 PE: 62708E PR: DARK TA: 02 WU: 04 | |
| 6. AUTHOR(S) Jack M. Younse | | | | |
| 7. PERFORMING ORGANIZATION NAME(S) AND ADDRESS(ES) TEXAS INSTRUMENTS P. O. BOX 655012 DALLAS TX 75265 | | | 8. PERFORMING ORGANIZATION REPORT NUMBER | |
| 9. SPONSORING/MONITORING AGENCY NAME(S) AND ADDRESS(ES) AVIONICS DIRECTORATE WRIGHT LABORATORY AIR FORCE MATERIEL COMMAND WRIGHT PATTERSON AFB OH 45433-7511 POC: Darrel G. Hopper, Displays Branch WL/AAJD, (937) 255-8267 | | | 10. SPONSORING/MONITORING AGENCY REPORT NUMBER WL-TR-97-1003 | |
| 11. SUPPLEMENTARY NOTES | | | | |
| 12a. DISTRIBUTION AVAILABILITY STATEMENT APPROVED FOR PUBLIC RELEASE; DISTRIBUTION IS UNLIMITED. | | | 12b. DISTRIBUTION CODE | |
| 13. ABSTRACT (Maximum 200 words) This report describes the effort over a six year period to develop a high definition display using the Texas Instrument (TI) Digital Micromirror Device (DMD) [formerly deformable mirror device]. The majority of this work carried out at TI in Dallas, Texas and it's subcontractor, the David Sarnoff Research Center (Sarnoff) in Princeton, New Jersey. The program began in March 1990 and ended in March 1996 with the delivery of an HD projection display to the Government. This program resulted in the world's largest micro-electro-mechanical system (MEMS) device, from the standpoint of the number of moving mechanical structures (2,359,296 mirrors), built on a single monolithic chip. Three of these chips were used to build a truly digital high-definition front projection display. | | | | |
| 14. SUBJECT TERMS Large Displays, Cockpit Display, Laser Optics, High Definition, Digital Micromirror, Frame Sequential, Projection DisplayDigital Light Processing (DLP) | | | 15. NUMBER OF PAGES 280 | |
| | | | 16. PRICE CODE | |
| 17. SECURITY CLASSIFICATION OF REPORT Unclassified | 18. SECURITY CLASSIFICATION OF THIS PAGE Unclassified | 19. SECURITY CLASSIFICATION OF ABSTRACT Unclassified | 20. LIMITATION OF ABSTRACT SAR | |

TABLE OF CONTENTS

| | |
|--|-----------|
| 1. EXECUTIVE OVERVIEW | 1 |
| 1.1 PROGRAM OBJECTIVE | 1 |
| 1.2 PROGRAM DESCRIPTION | 1 |
| 1.3 PROGRAM GOALS | 2 |
| 1.4 PROGRAM MANAGEMENT | 3 |
| 1.5 DMD TECHNOLOGY OVERVIEW (REF 1) | 3 |
| 1.5.1 DMD Fabrication | 5 |
| 1.5.1.1 Surface Micromachining (ref 2) | 5 |
| 1.5.1.2 Back-end Assembly (ref 2) | 7 |
| 1.5.2 DMD Architecture | 7 |
| 1.5.3 DMD Grayscale Using Pulse Width Modulation Technique | 8 |
| 1.5.4 Darkfield Optics | 9 |
| 1.5.5 DMD Projector Systems | 9 |
| 1.5.5.1 Single-DMD NTSC/VGA Projector System | 9 |
| 1.5.5.2 Three-DMD High-Definition Projector System | 10 |
| 1.6 SUMMARY | 12 |
| 2. PHASE I - HD DMD PROJECTION DISPLAY TECHNOLOGY DEVELOPMENT | 13 |
| 2.1 768x576 UNDERLYING CMOS | 13 |
| 2.1.1 2T DRAM | 13 |
| 2.1.2 6T SRAM | 16 |
| 2.2 1920x1080 LAC MIRROR SUPERSTRUCTURE | 17 |
| 2.2.1 Description Task | 17 |
| 2.2.2 Design Goals | 17 |
| 2.2.3 LAC Design | 18 |
| 2.2.4 LAC Layout | 21 |
| 2.2.5 LAC Device | 21 |
| 2.2.6 LAC Device Package | 22 |
| 2.2.7 DMD Testing | 23 |
| 2.2.7.1 Electrical Testing of DMD CMOS | 23 |
| 2.2.7.2 Optical Testing of LAC Devices | 26 |
| 2.3 OPTICS AND ILLUMINATION SYSTEM | 27 |
| 2.3.1 Display Systems | 27 |
| 2.3.1.1 Self-Luminescent | 28 |
| 2.3.1.2 Light Valves | 29 |
| 2.3.2 System Requirements | 29 |
| 2.3.3 Monochrome Projection Schemes | 30 |
| 2.3.3.1 Off-Axis Projection | 30 |
| 2.3.3.2 A Re-Entrant Lens Configuration | 32 |
| 2.3.3.3 Parallel Light Illumination | 33 |
| 2.3.3.4 Use of a Coupling Prism with Parallel Illumination | 34 |
| 2.3.4 Light valve diffraction effects | 34 |
| 2.3.4.1 Throughput | 35 |
| 2.3.4.2 Contrast | 35 |
| 2.3.4.3 f# and MTF, a Classical Argument | 39 |
| 2.3.4.4 Light Use Efficiency | 40 |
| 2.3.5 The prototype | 43 |
| 2.3.6 Commercially available parts | 43 |

| | |
|--|-----------|
| 2.3.7 Performance | 44 |
| 2.3.7.1 Light Budget | 44 |
| 2.3.7.2 Light Uniformity | 46 |
| 2.3.7.3 Distortion and Other Aberrations | 46 |
| 2.3.7.4 Optical Tests | 47 |
| 2.3.8 Possible color displays | 47 |
| 2.3.8.1 Adaptability to a Color System | 47 |
| 2.3.8.2 Color Wheel | 47 |
| 2.3.8.3 Triple Projection | 48 |
| 2.3.8.4 Combining Prism | 48 |
| 2.3.9 Summary and Conclusions for Phase I Optics and Illumination System | 49 |
| 2.4 ELECTRONICS | 49 |
| 2.5 LAC DEVICE/SYSTEM PERFORMANCE | 50 |
| 2.6 PHASE I ISSUES/PROBLEMS | 56 |
| 2.6.1 Photolithography | 56 |
| 2.6.2 Hinge Integrity | 56 |
| 2.6.3 Sticking Mirrors | 56 |
| 2.7 RECOMMENDATION FOR HD DMD | 57 |
| 3. PHASE II - NTSC/VGA DMD PROJECTOR FABRICATION | 58 |
| 3.1 768x576 NTSC/VGA DMD | 58 |
| 3.1.1 DMD Underlying CMOS Structure | 58 |
| 3.1.1.1 DMD 2T DRAM Memory Structure | 58 |
| 3.1.1.2 DMD 6T SRAM Memory Structure | 58 |
| 3.1.2 DMD Mirror Superstructure | 59 |
| 3.1.2.1 DMD Mirror Response Time | 59 |
| 3.1.2.2 768x576 DMD Simulated Defect Rate | 60 |
| 3.2 NTSC/VGA PROJECTOR | 60 |
| 3.2.1 640x480 Projector Optics and Illumination System | 61 |
| 3.2.2 Color Wheel | 61 |
| 3.3 NTSC/VGA PROJECTOR ELECTRONICS | 62 |
| 3.3.1 Grayscale Using Pulse Width Modulation (PWM) | 62 |
| 3.4 PROJECTOR MECHANICAL SYSTEM | 63 |
| 3.4.1 System Block Diagram | 64 |
| 3.5 PROJECTOR PERFORMANCE/RESULTS | 65 |
| 3.5.1 Performance of DMD 640X480 NTSC/VGA Projector | 65 |
| 3.5.2 Other Projected Results | 66 |
| 3.6 LAMP FAILURE | 67 |
| 4. PHASE III - FULL HDD DMD PROJECTOR | 68 |
| 4.1 2048x1152 HD DMD | 70 |
| 4.1.1 HD DMD Layout | 71 |
| 4.1.2 HD DMD Photolithography | 71 |
| 4.1.3 HD DMD Package | 72 |
| 4.1.4 DMD Testing | 73 |
| 4.1.4.1 Electrical Testing | 73 |
| 4.1.4.2 Current State of the Electro-optical Test | 73 |
| 4.1.4.3 Current Test Procedure | 73 |
| 4.1.4.4 Artifacts and Defects | 73 |
| 4.1.4.5 Device Tracking, Documentation, and Test Results | 74 |
| 4.1.4.6 Areas for Test Automation and Improvements | 75 |

| | |
|--|-----|
| 4.1.5 Conventional B2 HD DMD Characterization Summary | 75 |
| 4.1.5.1 Tilt Angle Characterization | 76 |
| 4.1.5.2 Reflectivity Data | 77 |
| 4.1.5.3 Pixel Active Area | 77 |
| 4.1.5.4 Window Transmission | 77 |
| 4.1.5.5 Die Registration In Package | 78 |
| 4.1.5.6 Pulse Width Modulation (PWM) Efficiency | 78 |
| 4.1.5.7 Modeled Device Performance | 78 |
| 4.2 1920X1080 PROJECTOR OPTICS AND ILLUMINATION SYSTEM (SARNOFF) | 78 |
| 4.2.1 System Performance | 78 |
| 4.2.1.1 Brightness, contrast, uniformity | 78 |
| 4.2.1.2 Collection region | 79 |
| 4.2.1.3 Light distribution in the stop of the projection lens | 79 |
| 4.2.1.4 Screen uniformity | 79 |
| 4.2.1.5 Contrast | 88 |
| 4.2.1.6 Lamp life | 89 |
| 4.2.1.7 Colorimetry | 90 |
| 4.2.2 Light Budget | 96 |
| 4.2.3 Conclusion | 97 |
| 4.3 HDD DMD PROJECTOR SYSTEM ELECTRONICS | 97 |
| 4.3.1 Computer Control | 98 |
| 4.3.2 Data Formatter | 98 |
| 4.3.2.1 Input Receiver | 99 |
| 4.3.2.2 Test Buffer | 99 |
| 4.3.2.3 Channel Seaming | 99 |
| 4.3.2.4 Data Intensity, Contrast, and De-Gamma Function | 100 |
| 4.3.2.5 Formatter | 101 |
| 4.3.2.6 Output Driver | 101 |
| 4.3.2.7 Timing and Control | 101 |
| 4.3.3 Projector Electronics | 101 |
| 4.3.3.1 Projector I/O | 102 |
| 4.3.3.2 VRAM Control | 102 |
| 4.3.3.3 DMD Controller | 102 |
| 4.3.3.4 Red, Green, and Blue DMD Display | 103 |
| 4.3.4 Proscan Motion Adaptive Algorithm (Sarnoff) | 103 |
| 4.3.4.1 Purpose | 103 |
| 4.3.4.2 System Background (Interlaced Mode) | 103 |
| 4.3.4.3 System Description | 104 |
| 4.3.4.4 Nest Configuration | 104 |
| 4.3.4.5 Reference Documents | 105 |
| 4.3.5 PROSCAN Theory of Operation | 106 |
| 4.3.5.1 PROSCAN Definition | 106 |
| 4.3.5.2 PROSCAN Algorithm | 107 |
| 4.3.5.3 Motion Detector Description | 109 |
| 4.3.6 Board Level Implementation | 110 |
| 4.3.6.1 System Level Implementation of Proscan | 110 |
| 4.3.6.2 Board Orientation with Proscan | 112 |
| 4.3.6.3 NEST CONFIGURATION WITH PROSCAN | 112 |
| 4.3.7 Board Level Definition | 113 |
| 4.3.7.1 Input/Output Definitions | 113 |
| 4.3.7.2 Motion Signal Board | 117 |
| 4.3.7.3 Proscan Board | 119 |

| | |
|---|------------|
| 4.4 PROJECTOR PERFORMANCE..... | 123 |
| 5. HDD PROGRAM RESULTS | 124 |
| 5.1 SUMMARY..... | 124 |
| 5.1.1 Objective | 124 |
| 5.1.2 Approach..... | 124 |
| 5.1.3 Status..... | 124 |
| 5.1.4 Schedule/Tasks..... | 125 |
| 5.2 PERFORMANCE VS. GOALS | 125 |
| 5.3 RECOMMENDATIONS | 125 |
| 5.3.1 New "Hidden Hinge (HH3)" HD DMD | 126 |
| 5.3.2 DRAM CMOS STRUCTURE | 127 |
| 5.4 QRA | 128 |
| 5.5 MANUFACTURING..... | 129 |
| 5.6 DUAL-USE DISPLAY PRODUCTS | 130 |
| 5.7 BENEFITS TO SOCIETY | 130 |
| 5.8 CONCLUSION..... | 131 |
| 5.9 ACKNOWLEDGMENTS | 132 |

TABLE OF FIGURES

| | |
|--|----|
| FIGURE 1 HDD projector "House of Quality"..... | 2 |
| FIGURE 2 (a) DMD element with conventional torsion hinge suspension, and (b) mirror configuration with schematic of the SRAM cell | 4 |
| FIGURE 3 Picture of DMD mirrors | 5 |
| FIGURE 4 Micromirror element fabrication sequence | 6 |
| FIGURE 5 DMD chip architecture | 7 |
| FIGURE 6 Corner of DMD CMOS array | 8 |
| FIGURE 7 Pulse width modulation grayscale | 8 |
| FIGURE 8 DMD darkfield optics | 9 |
| FIGURE 9 DMD single-chip color projector display | 10 |
| FIGURE 10a HDD optics | 11 |
| FIGURE 10b HDD projector optics | 11 |
| FIGURE 11 DMD 2T DRAM cell | 14 |
| FIGURE 12 2T DRAM CMOS addressing circuitry | 15 |
| FIGURE 13 768 x 576 DMD DRAM | 15 |
| FIGURE 14 6T SRAM CMOS addressing circuitry | 16 |
| FIGURE 15 LAC chip patterns | 18 |
| FIGURE 16 HD DMD limited addressability chip (LAC) layout | 21 |
| FIGURE 17 First LAC device | 22 |
| FIGURE 18 LAC device package | 22 |
| FIGURE 19 First DMD tester hardware block diagram | 23 |
| FIGURE 20 First DMD software tester block diagram | 24 |
| FIGURE 21 Early DMD CMOS test data | 25 |
| FIGURE 22 Block diagram for optical testing of LAC DMDs | 26 |
| FIGURE 23 An off-axis projection system | 31 |
| FIGURE 24 A re-entrant projection lens | 32 |
| FIGURE 25 A simple parallel illumination system | 33 |
| FIGURE 26 Coupling prism with parallel illumination | 34 |

| | | |
|------------|---|----|
| FIGURE 27 | The complimentary pattern nestles about the projection lens as shown ----- | 36 |
| FIGURE 28 | The fraction of overlap as a function of lens f# for the orders 1-5 ----- | 37 |
| FIGURE 29 | The overlap of the image of the source at the zeroth order location in the complimentary pattern as a function of f# for DMD mirror tilts of 9 to 14 degrees ----- | 38 |
| FIGURE 30 | The overlap of the image of the source at the zeroth order location in the coplanar pattern as a function of mirror tilts for projection lens f# from 1.9 to 2.3 ----- | 39 |
| FIGURE 31 | The MTF in an aperture limited system ----- | 40 |
| FIGURE 32a | Collection fraction as a function of f# for various arc lengths, given a DMD diagonal of 37.5 mm ----- | 41 |
| FIGURE 32b | Collection fraction as a function of arc length for various DMD diagonal sizes, for a f/4 projection lens ----- | 42 |
| FIGURE 33 | Comparison of the overall efficiencies vs. f# for a 6-mm/W metal halide lamp and 2.3-mm, 28-lm/W Xenon arc lamp ----- | 42 |
| FIGURE 34 | By tilting and shifting the beams from diametrically opposite sides of the ellipse we fill in the central region ----- | 43 |
| FIGURE 35a | Pictures from LAC projector ----- | 51 |
| FIGURE 35b | Pictures from LAC projector - Con't ----- | 52 |
| FIGURE 35c | Pictures from LAC projector - Con't ----- | 53 |
| FIGURE 35d | Pictures from LAC projector - Con't ----- | 54 |
| FIGURE 35e | Pictures from LAC projector - Con't ----- | 55 |
| FIGURE 36 | 768 x 576 DMD Wafer ----- | 59 |
| FIGURE 37 | Typical DMD Mirror Response Time ----- | 59 |
| FIGURE 38 | DMD defect rate simulation ----- | 60 |
| FIGURE 39 | 640x 480 (NTSC/VGA) using the 768 x 576 DMD ----- | 61 |
| FIGURE 40 | Early three segment color wheel ----- | 62 |
| FIGURE 41 | Pulse width modulation timing shown for 7-bits ----- | 63 |
| FIGURE 42 | NTSC/VGA projector concept sketch ----- | 63 |
| FIGURE 43 | Block diagram for single-DMD projector system ----- | 64 |
| FIGURE 44 | NTSC/VGA DMD projector ----- | 64 |
| FIGURE 45 | First picture from 640 x 480 DMD projector (color) ----- | 65 |
| FIGURE 46 | Pictures taken from DMD NTSC/VGA projector ----- | 67 |
| FIGURE 47 | ARPA HD system/source block diagram ----- | 68 |
| FIGURE 48 | ARPA HD system ----- | 70 |
| FIGURE 49 | Comparison of NTSC and HDTV resolution ----- | 70 |
| FIGURE 50 | Chip architecture for the 2948 x 1152 HD DMD ----- | 71 |
| FIGURE 51 | HD 2048 x 1152 DMD reticle ----- | 71 |
| FIGURE 52 | Cut-and-repeat reticle composition technique used for 2048 x 1152 DMD ----- | 72 |
| FIGURE 53 | DMD ceramic package ----- | 72 |
| FIGURE 54 | The Sylvania and Philips 575 W, 7mm gap metal-halide lamps ----- | 80 |
| FIGURE 55 | Measured arc distribution for the 7 mm gap metal-halide lamp vs. the specification of the Hamamatsu for the same lamp ----- | 81 |
| FIGURE 56 | A comparison of the specifications for the Hamamatsu 575W metal-halide lamp with the 5 mm gap and the model that was used in the initial design of the projector ----- | 82 |
| FIGURE 57 | The Hamamatsu 575W metal-halide lamp with the 5 mm gap as measured ----- | 83 |
| FIGURE 58 | Profiles of various 5 mm gap metal-halide lamps ----- | 84 |
| FIGURE 59 | The ray distribution in the projection lens' stop for a 7 mm lamp ----- | 85 |
| FIGURE 60 | NOT USED | |
| FIGURE 61 | Surface plot of calculated screen brightness as a function of position ----- | 86 |
| FIGURE 62 | Contour plot of calculated screen brightness as a function of position ----- | 86 |
| FIGURE 63 | Surface plot of measured screen brightness as a function of position ----- | 87 |
| FIGURE 64 | Contour plot of the measured screen brightness as a function of position ----- | 88 |
| FIGURE 65 | Manufacturers lifetime data for two lamp types ----- | 90 |

| | | |
|------------|---|-----|
| FIGURE 66 | The response of a lossless filter set ----- | 91 |
| FIGURE 67 | The spectrum of the Hamamatsu 575W metal-halide lamp and the suppression of the Hg yellow line through the use of the filter set ----- | 92 |
| FIGURE 68 | A map of color temperature as a function of position in the arc of the 575W Hamamatsu metal-halide lamp ----- | 93 |
| FIGURE 69 | a map of X-Y color coordinates as a function of position in the arc of the 575W metal-halide lamp ----- | 94 |
| FIGURE 70 | CIE 1933 color diagram (color) ----- | 95 |
| FIGURE 71 | Formatter/Projector electronics ----- | 98 |
| FIGURE 72 | Data formatter block diagram ----- | 99 |
| FIGURE 73 | Input/Seamer/Display relationship ----- | 100 |
| FIGURE 74 | Projector electronics block diagram ----- | 102 |
| FIGURE 75 | DMD overall system diagram ----- | 104 |
| FIGURE 76 | Nest cabling diagram ----- | 105 |
| FIGURE 77 | VT diagram describing Proscan algorithm ----- | 106 |
| FIGURE 78 | Proscan generation algorithm based on a Thompson patent ----- | 107 |
| FIGURE 79a | Motion signal exceeding Difference signal ----- | 108 |
| FIGURE 79b | Difference signal exceeding Motion signal ----- | 108 |
| FIGURE 80 | Motion detector block diagram ----- | 110 |
| FIGURE 81 | Proscan board level interconnect ----- | 111 |
| FIGURE 82 | System block diagram with Proscan ----- | 112 |
| FIGURE 83 | Nest definition with Proscan ----- | 113 |
| FIGURE 84 | Input timing ----- | 114 |
| FIGURE 85 | Output timing ----- | 116 |
| FIGURE 86 | Detailed Motion Signal board block diagram ----- | 118 |
| FIGURE 87 | Detailed Proscan Processing board block diagram ----- | 120 |
| FIGURE 88 | Relationship between pixels on the PPB ----- | 121 |
| FIGURE 89 | Light reflected from the B2 mirror structure for both "on" and "off" states ----- | 126 |
| FIGURE 90 | "Hidden Hinge" DMD superstructure ----- | 127 |

TABLE OF TABLES

| | | |
|----------|--|----|
| TABLE 1 | HDD Technical Goals/Specifications ----- | 3 |
| TABLE 2 | CALMA LAC pixel types ----- | 19 |
| TABLE 3 | Properties of self-luminescent displays ----- | 28 |
| TABLE 4 | Properties of light valves ----- | 29 |
| TABLE 5 | System requirements ----- | 29 |
| TABLE 6 | Positions, radii, and f# of 1 to 1 transfer lenses in a parallel illumination system ----- | 33 |
| TABLE 7 | Total light in all orders up and including the designated orders and the percentage of the total resident in each order ----- | 35 |
| TABLE 8 | Complimentary pattern leakage for an f/3.1 lens ----- | 37 |
| TABLE 9 | Light collection parts specifications for the prototype ----- | 43 |
| TABLE 10 | Light budget calculations and measurements ----- | 45 |
| TABLE 11 | Light distribution ----- | 46 |
| TABLE 12 | The color coordinates of the dichroic filters ----- | 48 |
| TABLE 13 | Categorized mirror defects ----- | 74 |
| TABLE 14 | Characterization study to determine the limiting factors for the contrast ratio of the B2 HD DMD display ----- | 76 |
| TABLE 15 | Tilt angle characterization data for 1st HD DMDs ----- | 77 |
| TABLE 16 | The calculated screen brightness as a function of position ----- | 87 |

| | | |
|----------|---|-----|
| TABLE 17 | A map of the normalized brightness on the screen ----- | 88 |
| TABLE 18 | A map of the light output from the projector as measured on a Lambertian screen ----- | 89 |
| TABLE 19 | A map of contrast ratio ----- | 89 |
| TABLE 19 | The color coordinates for the primary colors and white, for three designs ----- | 92 |
| TABLE 20 | A light budget for currently existing projector, and with improved elements ----- | 96 |
| TABLE 21 | Reference documents ----- | 105 |
| TABLE 22 | Final HDD DMD projector results ----- | 123 |
| TABLE 23 | Performance - actual vs. goals for DMD based HDD projector ----- | 125 |
| TABLE 24 | DMD qualification data ----- | 128 |
| TABLE 25 | Dual-use applications of DMD based displays ----- | 130 |
| TABLE 26 | Estimated military display market ----- | 131 |

1. EXECUTIVE OVERVIEW

This report describes the effort over a six year period to develop a high definition display using the Texas Instrument (TI) Digital Micromirror Device (DMD) [formerly deformable mirror device]. The majority of this work was carried out at TI in Dallas, Texas and it's subcontractor, the David Sarnoff Research Center (Sarnoff) in Princeton, New Jersey. The program began in March 1990 and ended in March 1996 with the delivery of an HD projection display to the Government.

This program resulted in the world's largest micro-electro-mechanical system (MEMS) device, from the standpoint of the number of moving mechanical structures (2,359,296 mirrors), built on a single monolithic chip. Three of these chips were used to build a truly digital high-definition front projection display.

1.1 Program Objective

The objective of the program was to develop a prototype high definition projection display system based upon Texas Instruments' digital micromirror technology. The basic DMD torsion beam structure is based on a 1987 patent by Dr. Larry Hornbeck of TI. The program included the design and fabrication of a unique DMD chip for projection display application, peripheral address circuitry to interface with the DMD chip, a projection optical system optimized to suit the DMD's mode of operation, and a video system interface to the source of real time high definition video.

1.2 Program Description

A three-phase approach was established to meet this objective, as shown below:

- Phase I
 1. Design and fab DMD underlying CMOS array of 256x256 pixels or greater (actually 768x576)
 2. Layout and fab HD (1920x1080) DMD mirror test array, including a DMD package and drive electronics
 3. Develop DMD optics for use in testing the HD mirror array.
- Phase II
 4. Build 768x576 DMD by fabricating mirror array over the above memory array (added task)
 5. Build first NTSC/VGA (640x480) DMD front projector (added task funded by TI)
 6. Expand the design of the CMOS array to at least 1920x1080 pixels (actually 2048x1152)
 7. Complete design of HD optics
 8. Complete the design of HD DMD electronics and front-end video source electronics
 9. Provide DMD test capability (later expanded by TI)

- Phase III
 10. Complete layout and fab of HD 2048x1152 DMD
 11. Fab 3-DMD HD optics
 12. Fab and test DMD front-end electronics
 13. Complete HD projector mechanical design and fab
 14. Complete interlace-to-proscan electronics design, fab, and test
 15. Integrate the HD system
 16. Test, demonstrate, and deliver the HD projector

The details for each of these three phases will be discussed in the main body of this report.

1.3 Program Goals

At the beginning of the program, Quality Functional Deployment (QFD) was used to develop a "house of quality" for the HD projector. From this series of exercises came a set of design specifications for the prototype projector. Although too small to read, a copy of the HDD projector "house of quality" is shown in Figure 1 and some of the key parameters and their target values (goals) going into the program are shown in Table 1.

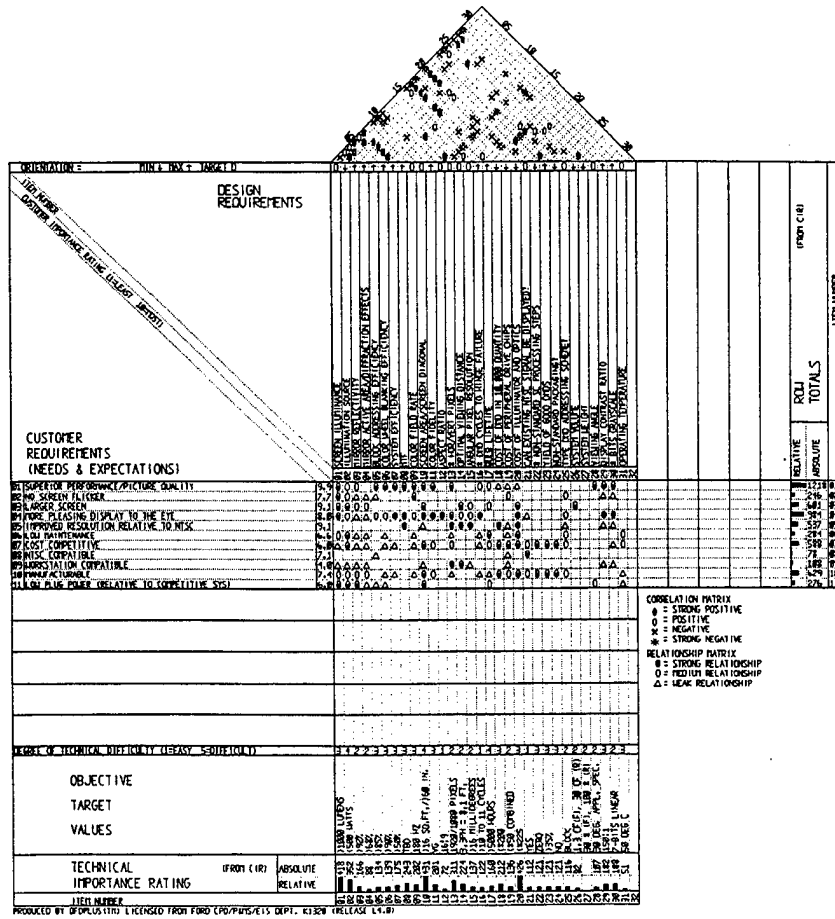


Figure 1. HDD projector "House of Quality".

Table 1

HDD Technical Goals/Specification

| <u>Projector Characteristic</u> | /----- Goals -----\ ----- | |
|-----------------------------------|------------------------------|-----------------------------|
| | <u>NTSC/VGA Proj</u> | <u>HDD Proj</u> |
| • No. of DMD pixels | 768 x 576 (1 DMD) | 1920 x 1080 (3 DMDs) |
| • No. active pixels used in proj | 640 x 480 | 1920 x 1080 |
| • Pixel size | 16 x 16 um | 16 x 16 um |
| • Pixel spacing (pitch) | 17 um | 17 um |
| • Pixel aperture (fill factor) | 74% | >75% |
| • Pixel response time | 10 us | 10 us |
| • Projector type | Front | Front |
| • Screen size | >52-inches | >60-inches |
| • Picture aspect ratio | 4:3 | 16:9 |
| • Color frame rate | 180 Hz | 60 Hz |
| • Screen Brightness | >200 lumens | >1000 lumens |
| • Light source | 1000 Watt, xenon arc | 575 Watt, Metal Halide |
| • Contrast ratio | >50:1 | >150:1 (DC) |
| • Grayscale capability per color | 8 bits (256 shades) | 7 bits (128 shades) |
| • Color generation method | Rotating color wheel | Color prism |
| • Pixel convergence | Self-aligned | Optically converged |
| • No. DMD hinge cycles to failure | > 1*10 ¹¹ cycles | > 1*10 ¹¹ cycles |

1.4 Program Management

This program was funded out of ARPA's ESTO under Dr. Lance Glasser, Director, and program managers Dr. Marko Slusarczuk (first half) and Dr. David Slobodin (second half). The program was run by Capt. Bert Dunlop (first half) and Robert Blanton (second half) out of the Cockpit Avionics Office at Wright Laboratory, directed by Dr. Darrel Hopper. The program manager at Texas Instruments was Dr. Jack Younse. The program manager at subcontractor Sarnoff was Dr. Phil Heyman.

1.5 DMD Technology Overview (ref 1)

The DMD spatial light modulator is an electromechanical semiconductor device with very small, highly reflective mechanical mirrors built over a SRAM CMOS memory chip. The aluminum alloy mirror superstructures are fabricated over each cell of an memory array. The mirror pixel cell (Figure 2) consists of individual hinge support posts, thin torsion hinges, a thicker mirror element, address electrodes, and landing pads. The mirrors are square, 17 μm center-to-center, and rotate + or - 10 degrees about a torsion beam.

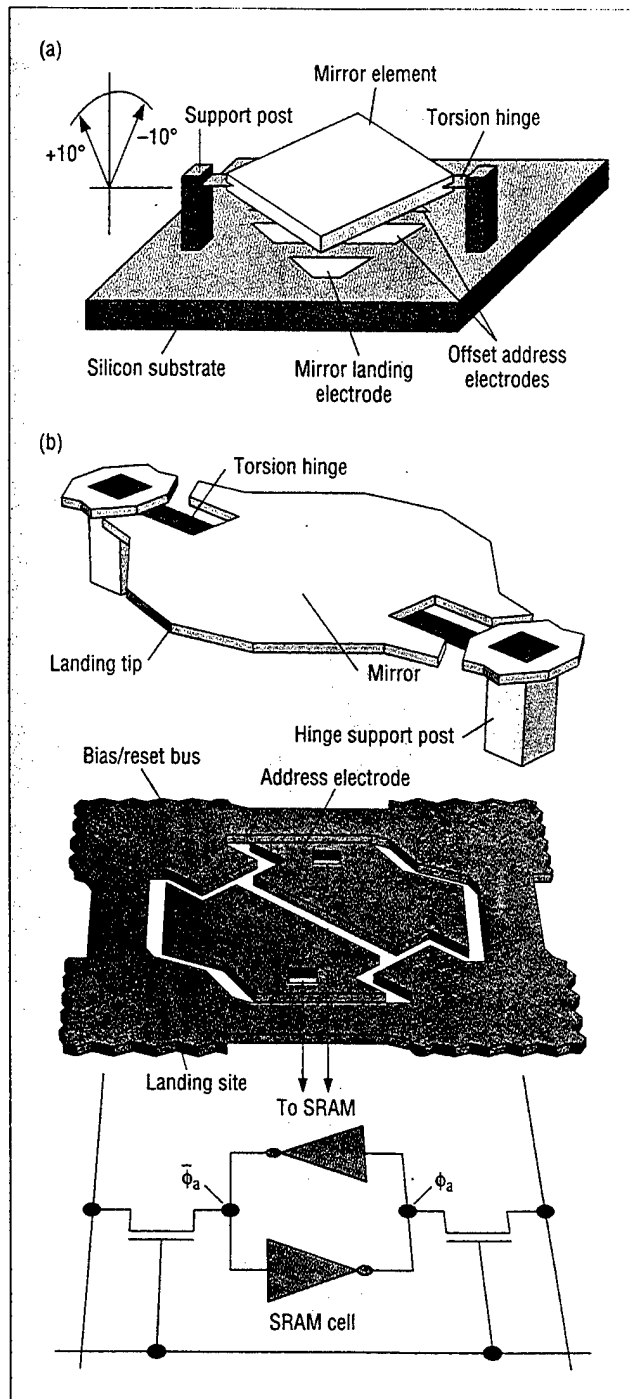


Figure 2. (a) DMD element with conventional torsion hinge suspension, and (b) mirror configuration with schematic of the SRAM cell.

The tristable mirror structure is used in a bistable mode, with the mirrors tilted either +10 degrees (on) or -10 degrees (off) during display operation. Mirrors are parked in the third (flat) state when the display is powered off. When the mirrors rotate in either direction, they are driven to landing pads that are at the same potential as the mirror structure. This operation results in excellent light uniformity across the DMD. Figure 3 shows a DMD section with mirrors in all three states (i.e., on, off, and flat).

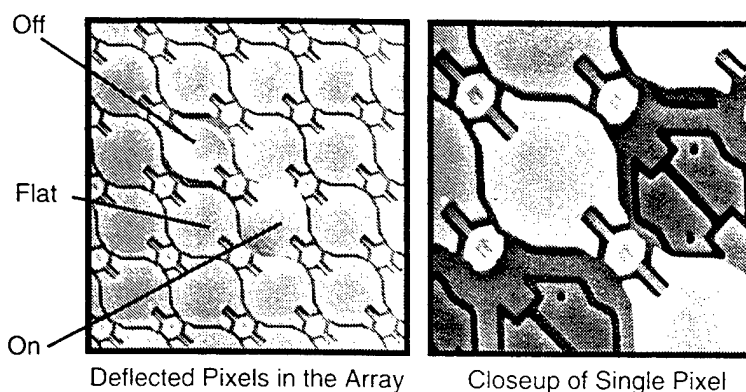


Figure 3. Picture of DMD mirrors.

In operation, the DMD mirrors have a built-in mechanical memory in that once they tilt + or -10 degrees, they stay electromechanically latched in that state until a reset signal is applied, regardless of the data in the underlying CMOS memory. This feature is used to great advantage because once the mirrors are simultaneously set to the desired state, new data for the next picture plane can be loaded into the underlying memory.

1.5.1 DMD Fabrication

1.5.1.1 Surface Micromachining (ref 2)

Over the underlying CMOS memory structure four photolithographically defined layers are surface micromachined to form the electrode, sacrificial layer, hinge, and mirrors. The sacrificial layer is an organic material that is plasma-ashed to form the air gap between the address electrodes and mirrors. The other three layers are formed from dry plasma etched, sputter-deposited aluminum. Structural details and the fabrication sequence for this process are shown in Figure 4.

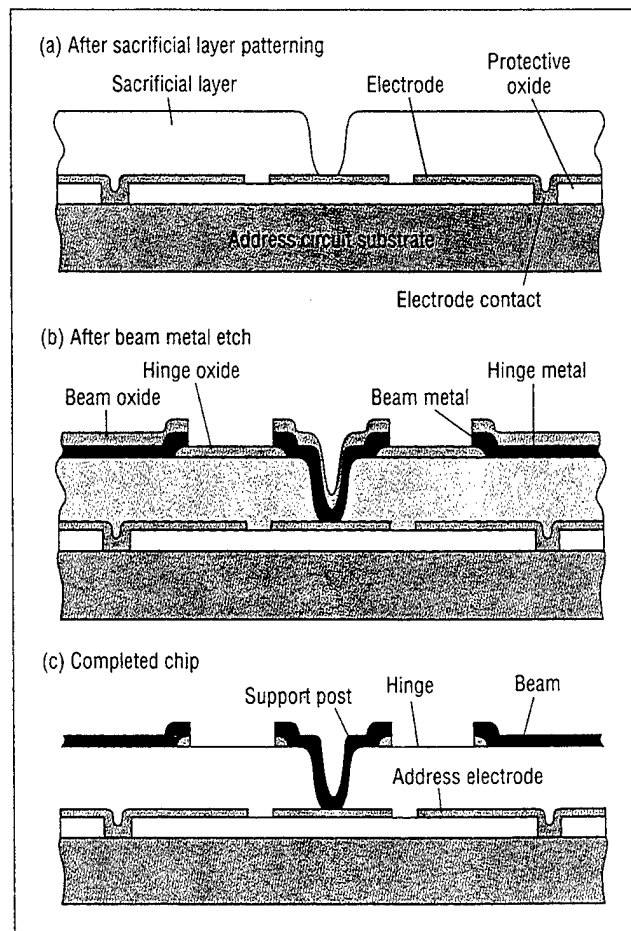


Figure 4. Micromirror element fabrication sequence.

DMD surface micromachining begins after contact openings for the address circuit electrode have been formed in the circuit's protective oxide. The address electrode film is then sputter deposited onto the oxide, lithographically patterned, and plasma etched. An organic sacrificial plagiaring layer is then spun over the electrode and patterned with vias, which will be used subsequently to form the support posts. Standard IC technology tightly controls the critical dimensions in the x and y directions. However, the z-axis dimension (i.e., thickness) must be equally tightly controlled to achieve reproducible, uniform mirror tilt angles.

Two metal layers are employed for the buried hinge process. The hinge aluminum alloy sputtered on top of the sacrificial layer is followed by a plasma-deposited masking oxide that is patterned to define the hinges. Deposition of a second aluminum alloy layer then buries the hinge oxide and forms the beam. This, in turn, is followed by still another plasma-deposited masking oxide, which is patterned to form the mirrors. The support posts consists of both the hinge and mirror metals.

Finally, a single aluminum plasma etching step patterns the hinges and mirrors. The mirror metal overlying the hinge region is etched away to expose the buried-hinge oxide, which functions as an etch stop. When the aluminum plasma etching has been completed, what remains are regions of hinge and mirror metal that have been simultaneously patterned.

1.5.1.2 Back-end Assembly (ref 2)

It is during back-end operations that the DMD device finally becomes a functional spatial light modulator (SLM). This occurs upon removal of the sacrificial layer. During the preliminary wafer sawing step, it is important that individual chips not be contaminated with particles, which can interfere with the DMD's mechanical operation. When wafer sawing is complete, the chips are placed in a plasma etching chamber, where isotropic etching creates an air gap by removing the sacrificial layer from under the mirrors and hinges, leaving them suspended in the ambient environment.

Although a familiar sequence of assembly operations is employed for the DMD- die attach, wire bond, window seal, and final test - the structure nevertheless requires special handling with special attention given to particle control and device handling during each assembly operation. The die attach and window sealing processes utilize adhesives with low outgassing properties, since adhesive outgassing can promote mirror stiction. A robust package is also required to maintain a proper ambient environment for the chip. In some applications, chip heat sinking and/or cooling may be necessary.

1.5.2 DMD Architecture

The DMD chip's architecture is shown in Figure 5. The chip is designed to handle large amounts of parallel input data. Data are fed into both the upper and lower portion of the chip simultaneously in packets of 16 columns per input pin. Row select circuitry is included on the left side of the chip to select the rows, both upper and lower sections, to which data are being written.

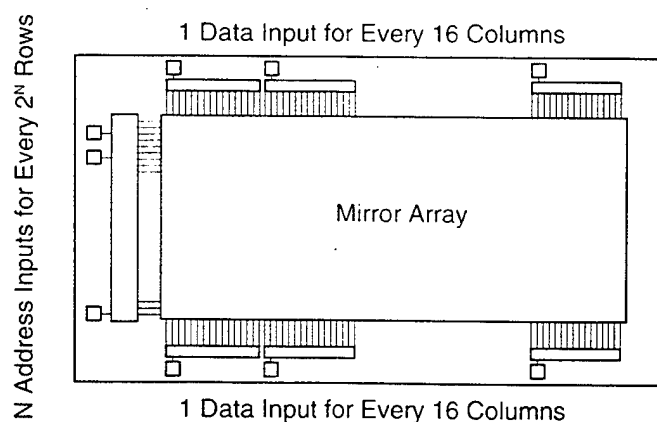


Figure 5. DMD chip architecture.

Figure 6 shows the underlying CMOS circuitry for the TI 768 x 576 DMD and illustrates the column drivers and bond pads for each 16 column input and the row encoder pads and drivers.

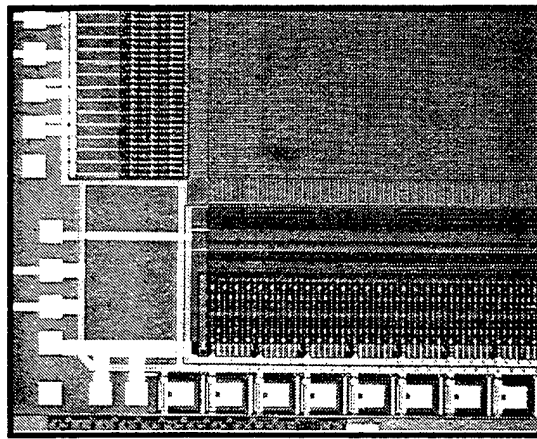


Figure 6. Corner of DMD CMOS memory array.

1.5.3 DMD Grayscale Using Pulse Width Modulation Technique

Grayscale using the bistable DMD is accomplished using pulse width modulation (PWM). For the projectors developed on this program, 8-bits (256 shades of gray) are generated using PWM. With PWM the digital data is loaded into the DMD in bit-planes, ranging from most-significant to least-significant bit. Effectively, the most-significant bit is loaded into the memory, the mirrors are set to either + or - 10 degrees depending on whether there is a binary "1" or "0" in the corresponding memory cell and left in this state for 1/2 the field period. Then the next-most-significant bit is loaded in and the mirrors set in the state representative of this new data for 1/4 the field time. This process continues until finally the least-significant bit is loaded in where the mirrors remain for 1/256 of the field time. When the light from an individual mirror is integrated over an entire field by the observer's eye, the pixel will appear to have one of 256 shades of gray ranging from black to white. The effect of this approach is illustrated in Figure 7, showing mirrors left "on" for the entire field, 1/2, 1/4, and 1/8 of the field time.

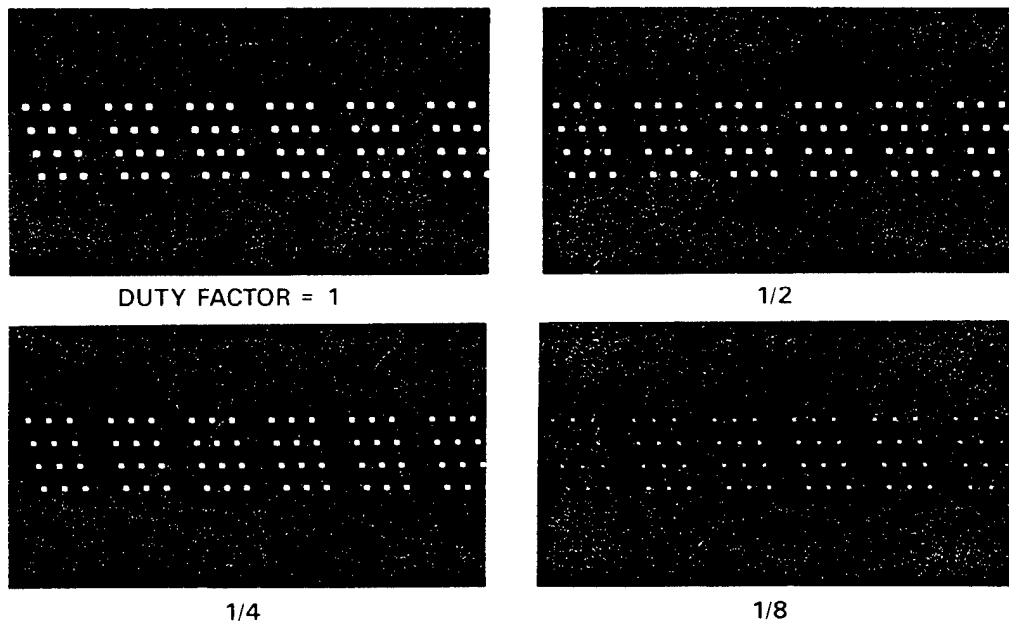


Figure 7. Pulse width modulation grayscale.

1.5.4 Darkfield Optics

The DMD is used in conjunction with darkfield optics to provide a highly efficient projection display. Figure 8 illustrates the darkfield optical approach. As shown, incoming light is incident on the device at 20 degrees from perpendicular to the plane of the chip. For mirrors tilted +10 degrees (on), light is reflected perpendicularly to the plane of the chip through the projection lens and onto the screen. A pixel on the screen is the same shape as the mirror and always remains spatially in the same location, with only its intensity changing. For mirrors tilted -10 degrees (off), light is reflected approximately -40 degrees from perpendicular to the plane of the chip and, as a result, misses the projection lens aperture. Likewise, surfaces on the chip, such as hinges and post tops, which tend to be flat, reflect light -20 degrees from perpendicular to the plane of the chip, and this light also misses the projection lens aperture. The goal is to trap all light not passing through the projection lens in a "dark trap."

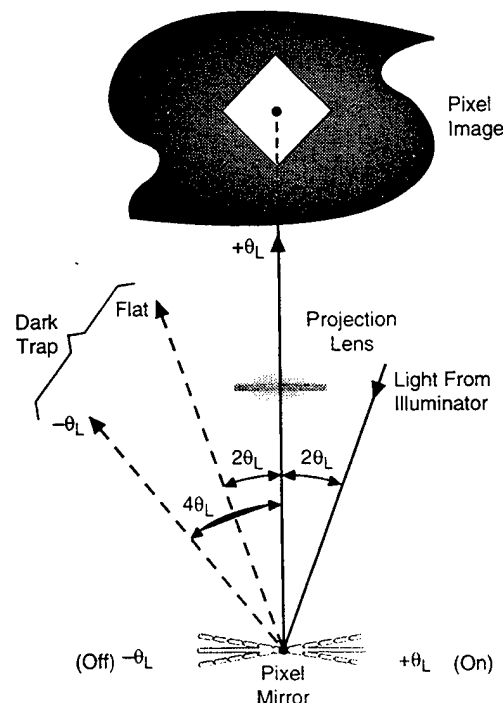


Figure 8. DMD darkfield optics.

1.5.5 DMD Projector Systems

During this program both a single-DMD NTSC/VGA (640x480 pixel) front projector and a three-DMD HDD (1920x1080) front projector system was built and delivered to the customer. These are discussed briefly below.

1.5.5.1 Single-DMD NTSC/VGA Projector System

Figure 9 shows a typical configuration for a fully digital, single-DMD projector. The digital picture data come from the DMD formatter/ picture buffer electronics and are then written to the DMD's CMOS memory array. A very bright and concentrated light source is conditioned by

condensing lenses and then directed onto the surface of the DMD, where it is modulated according to the position of the individual micromirrors and reflected either to the screen or to the dark trap. Because of the fast response time ($<20 \mu\text{s}$ on to off) of the DMD mirrors, color in the system is achieved by operating the DMD in color field-sequential mode, in which the "white" light from the source is filtered using a rotating color filter wheel to generate red, green, and blue light, respectively, for each third (5.6 ms) of a TV field. The system runs at 180 color fields/second.

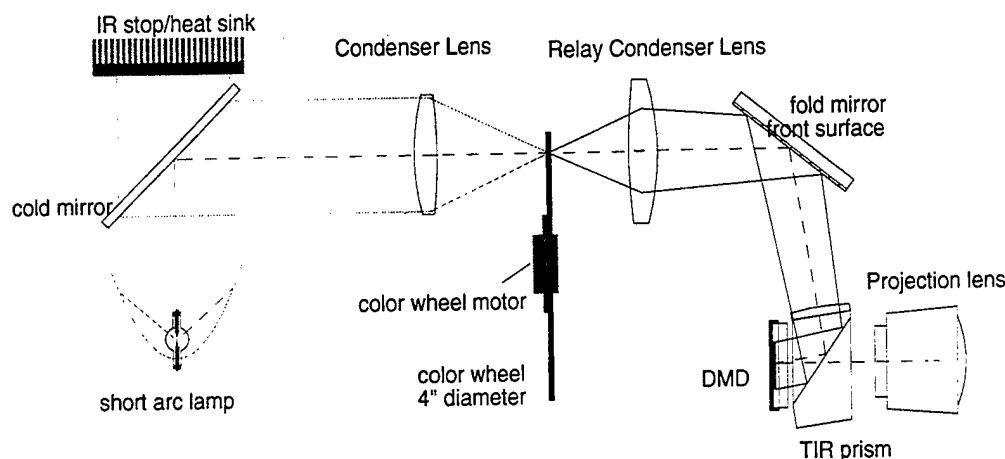


Figure 9. DMD single-chip color projection display.

1.5.5.2 Three-DMD High-Definition Projector System

The next logical step is to extend the DMD technology to a 16:9 aspect ratio, extended definition NTSC and/or PAL format to address nearer-term markets. However, DMD technology offers a new and revolutionary approach to projection TV that is directly applicable to HDTV. To this end, TI, with significant support from ARPA on this program, has extended the DMD technology for high-definition displays with a 2048 x 1152 (2,359,296 pixels) DMD. This high performance system uses three DMDs and a color prism to provide continuous "red", "green", and "blue" channels operating at 60 color fields/second.

Scaling this technology up to HD resolution offered new challenges for the semiconductor industry and TI in particular. This is due largely to the physical size (roughly 37 x 22 mm) of the chip and the photolithography requirements for writing such large patterns. In 1992, this task pushed technology close to the limits in areas of the DMD chip, package, electronics, and optics but is within the current state of the technology. Figures 10 a) and b) respectively, show the HDD optics and HDD projector head with the three (R-G-B) DMDs in place above the optical prism, illustrating how the picture is projected onto the large-area screen. A brief discussion of this effort follows.

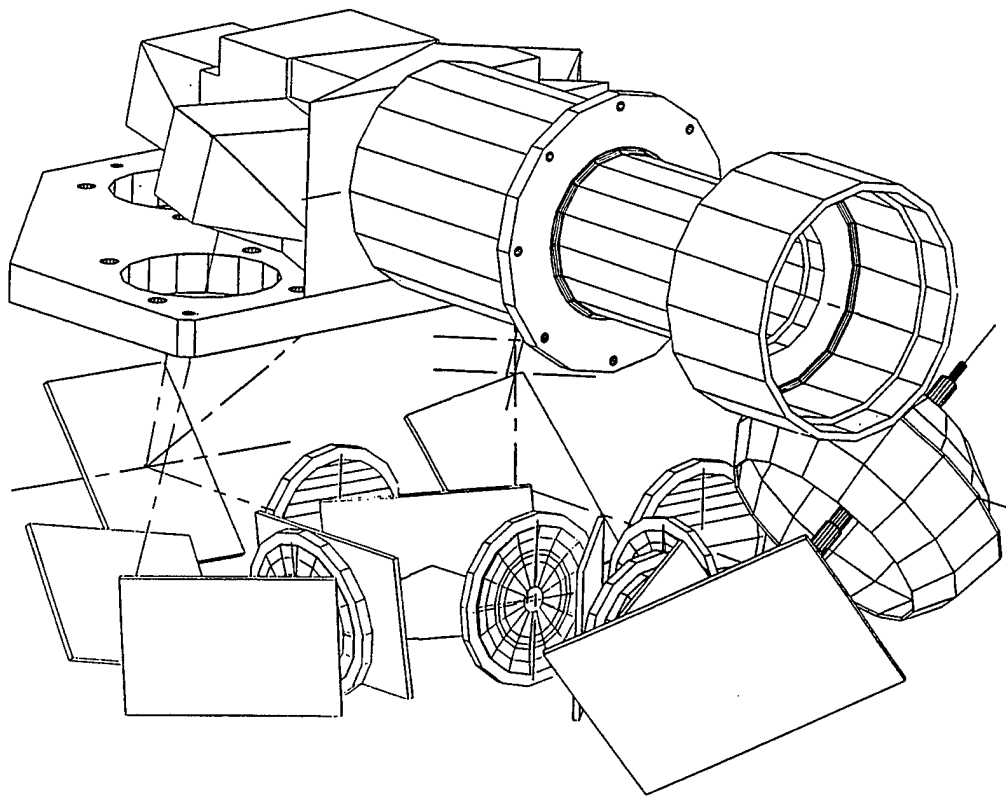


Figure 10a. HDD Optics.

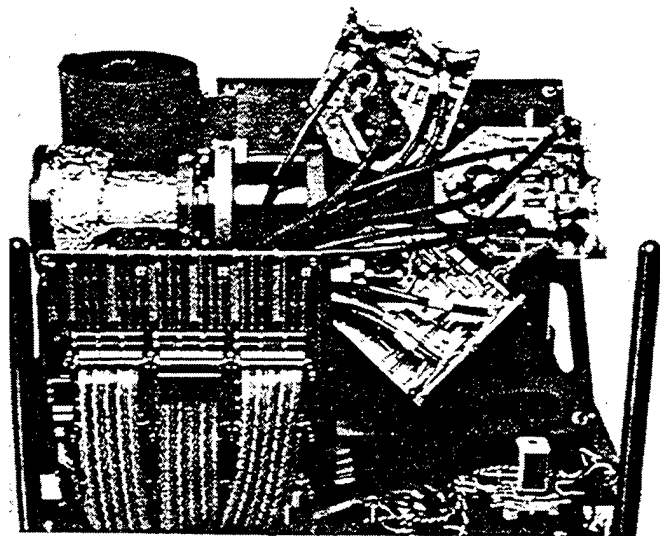


Figure 10b. HDD projector optics.

1.5.5.2.1 DMD Standard Pixel

The basic pixel cell for the HD DMD is the same as that used for the NTSC/VGA/PAL (768 x 576) resolution chip. A decision was made to optimize the standard 17 μm pitch pixel structure and then to step and repeat this "standard cell" to achieve at least ADTV/HDTV (1920 x 1080) formats.

1.5.5.2.2 HD Chip Configuration

Referring back to Figure 5, the HD chip has 2,048 pixels per row and 1,152 rows, although only 1920 x 1080 are used due to available video source material. The aspect ratio was chosen to be 16:9, which is consistent with most HDTV standards currently being discussed. As for the case of the NTSC chip, each input will handle 16 columns of data, so there are 120 input pads for both the upper and lower portions of the device. In addition, two 10 bit encoders are required to select the upper and lower rows where the data are to be written.

1.5.5.2.3 Chip Lithography

There are only a few available steppers today (in 1992) that can write patterns using standard 5X photomasks over such a large field of view and with the high resolution required for this HD DMD chip. Although 1X steppers, which might be able to handle the task, are just beginning to appear, such steppers place a heavy burden on the quality of the photomask reticle. So for this program, the HD chip uses reticle composition where the patterns are written in sections and spliced together in what is called a "step-and-repeat" process to provide a virtually "seamless" large-area DMD chip.

1.6 Summary

The DMD displays demonstrated recently resolve a number of major technical issues involved with building a truly digital high-definition display. DMD projection technology has shown excellent performance in resolution, brightness, contrast, response time, and color fidelity at both standard NTSC/VGA and HDTV resolutions. Because this technology is fabricated using mostly standard semiconductor processes, it has the potential to provide truly digital displays to the marketplace in the relative near future and offers the promise for a cost-effective display solution for HDTV.

The various program phases are discussed in more detail in the following sections.

References:

1. Jack M. Younse and David W. Monk, "The Digital Micromirror Device (DMD) and Its Transition to HDTV", SID/EuroDisplay '93, Sept. 1993, late-news papers, pp 613-616..
2. Michael A. Mignardi, "Digital Micromirror Array for Projection TV", Solid State Technology, July 1994, pp 63-66.

2. PHASE I - HD DMD PROJECTION DISPLAY TECHNOLOGY DEVELOPMENT

Phase I of the program concentrated in three primary areas of DMD technology; (1) the underlying CMOS memory structure, (2) the DMD mirror superstructure, and (3) optics and illumination components. These are discussed below.

2.1 768x576 Underlying CMOS

The contract stated that in Phase I a CMOS array of at least 256 x 256 pixels would be developed. But a decision was made early on to work with a CMOS area array which had a PAL format of 768 x 576 pixels or about one-fifth the size of the final HDD 1920 x 1080 device. This size chip was large enough to give us reasonable yield data for scaling up to the HD chip size and was also a usable format for building the first area DMD. Also, because modeling data indicated that dynamic RAM (DRAM) structures could have light handling limitations, it was decided to work on both DRAM and static RAM (SRAM) approaches to the underlying CMOS. The assumptions were that based on the results of this PAL CMOS chip, projections on performance, yield, and cost could be extrapolated for the future HDD 1920 x 1080 CMOS chip.

The approach for this effort was to:

- workout the design of the DMD CMOS array
- workout the DMOS-IV process requirements
- determine the feasibility of building a 2.0 million pixel DMD CMOS array based on the results of on the performance of the 442,368 pixel (768 x 576) CMOS array.

2.1.1 2T DRAM

The two-transistor (2T) DRAM design was based on an earlier DMD patent by Dr. Larry Hornbeck (U.S. Patent No. 5,142,405). The basic cell for this design is shown in Figure 11. In operation, the DRAM transistors, 101 and 301, are connected to corresponding address electrodes under the mirror and on opposite sides of the torsion beam axis. When a binary "1" is in the memory cell, transistor 101 places a TTL (+5V) voltage on the right-hand electrode, while transistor 301 places 0 volts on the left-hand electrode. With the mirror superstructure biased at -10 volts, this places a potential of 15 volts (magnitude) between the mirror plate and the right-hand electrode and only 10 volts between the mirror plate and the left-hand electrode. The generated electrostatic field is such as to cause the mirror to tilt +10-degrees to the right. For a binary "0" in the memory cell, the structure is such as to cause it to tilt -10-degrees to the left.

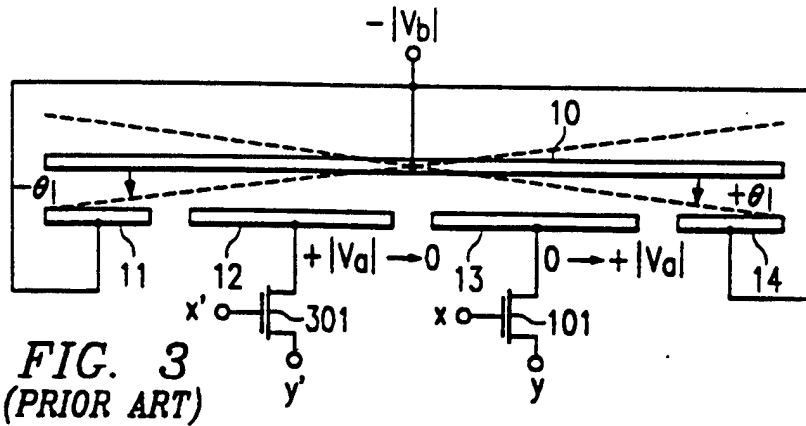


Figure 11. DMD 2T DRAM cell.

A functional diagram for the 768 x 576, 2T underlying DRAM circuit is shown in Figure 12, along with the row and column addressing circuitry. As shown, the circuit operates in a highly parallel fashion. First, the chip is divided vertically into two, 288 line, top and bottom sections which are driven in parallel from top and bottom column shift registers and parallel latches. Each 768 bit shift register is divided into 48 columns, each with its own data input. Along the left side of the chip are row decoders and drivers which selects two rows, one in the top and one in the bottom section, to be addressed. So the time required to write to the entire array is the time it takes to read in 16 data bits plus shift the line of data to the selected line and then repeat this process 288 times. Also, there are sense amplifiers and read/write I/O's used in electrically testing the CMOS circuitry.

A picture of the 768 x 576 DRAM CMOS chip with a magnified view of one corner is shown in Figure 13. This view shows several of the data inputs along the bottom of the chip, each driving 16 columns of the array. Also shown on the left side of the chip are bonding pads connected to the row decoder addressing circuitry.

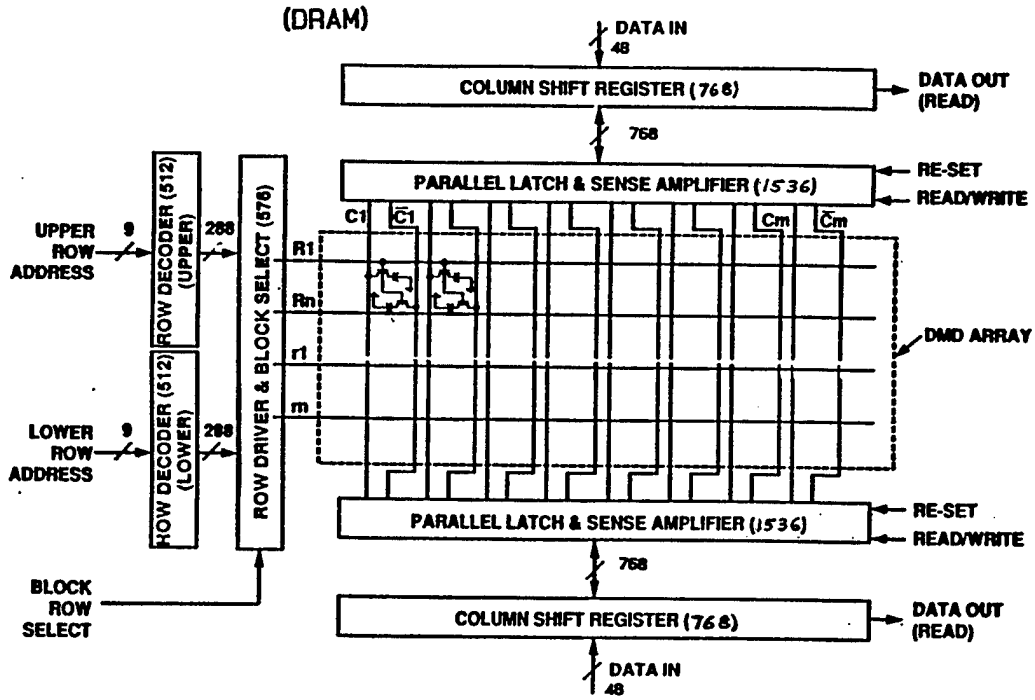


Figure 12. 2T DRAM CMOS addressing circuitry.

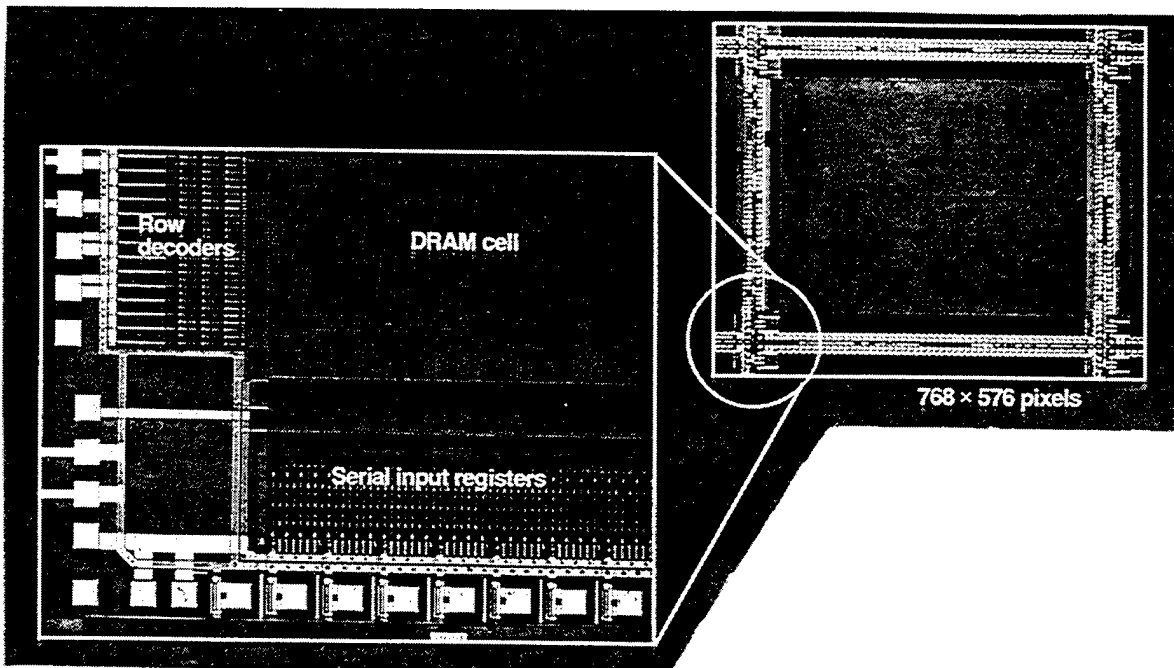


Figure 13. 768 x 576 DMD DRAM chip.

From the beginning it was clear that the DRAM structure could possibly have light capability limitations. This structure is dynamic in the sense that a capacitance is charged up and then discharges temporarily. The presence of light generates "carriers" in the silicon which accelerate the discharge rate of this capacitance and the more light the shorter the time constant for this voltage decay. For proper operation of the chip it is necessary for the first row of cells set to a "1" state to remain valid for the period of time it takes to address the rest of the chip and latch the mirrors. However, once the mirrors are exercised, they remain mechanically in their selected state, independent of the underlying CMOS circuitry, until they are electrically reset.

For the above reason, it was decided to take a dual approach to the underlying CMOS design. So in addition to the DRAM design, an effort was started in parallel but about 6-months lagging, on an SRAM design.

2.1.2 6T SRAM

The SRAM CMOS cell has six transistors (6T) connected in a "flip-flop" fashion so as to latch the signal at each cell. This feature overcomes the problem discussed above with the DRAM light limitation, but at a considerable cost (3X) in number of transistors. This in turn will impact yield of the chips and ultimately cost of the DMD.

The basic SRAM chip layout was the same as for the DRAM, shown in figure 12 except for the cell circuitry. The effort here was for the most part that of designing and optimizing a 6T cell and dropping it into the memory cell locations. This is shown in Figure 14.

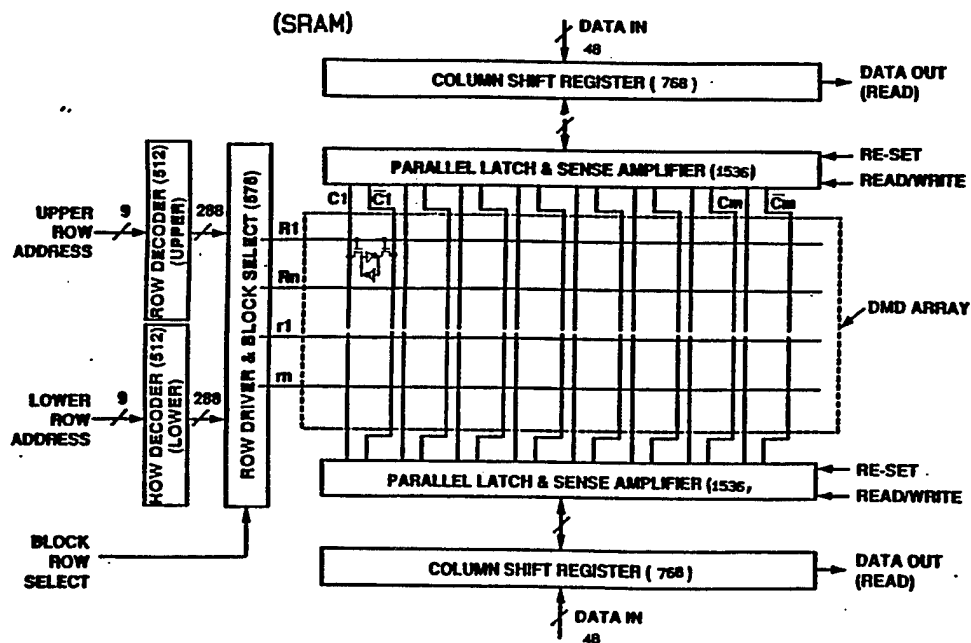


Figure 14. 6T SRAM CMOS addressing circuitry.

As will be discussed later in the results section, this design did provide the performance needed for operation in the presence of very bright illumination sources.

2.2 1920x1080 LAC Mirror Superstructure

While the decision was to start with a 768 x 576 CMOS chip, it was decided to see if we could indeed build a full HDD 1920 x 1080 DMD mirror superstructure, the world's largest Micro-Electromechanical Systems (MEMS) chip. The approach here was to:

- build a "faux" or "limited addressability chip" (LAC) with over 2-million mirrors (1920 x 1080 mirrors) fabricated over blank silicon and connected together in selected patterns that could be addressed through individual bond pads on the chip.
- optimize the pixel cell for a 17 um pitch in both the x and y dimensions
- keep the chip size to around 35 mm x 20 mm so the chip could be fabricated photolithographically in two halves using a single reticle composition (this is not the way we ended up doing it in the final chip)
- provide two layers of polysilicon and metal interconnections to provide "hard-wired" patterns that could be switched on and off
- use the DMD process flow identical to other fully addressable chips from electrode level through mirrors
- to assure that mega-pixel DMD mirror arrays are possible and get a feeling for what the yield might be for such a device
- use this HDD chip to support the development of high definition optics for DMD based projection displays.

2.2.1 Description Task

The Limited Addressability Chip (LAC) is a 1920 x 1080 element Deformable Mirror Device (DMD). It has no conventional address circuitry, but is comprised of pixels grouped in patterns which can be bondpad addressed. The LAC has three main purposes. It can be used for DMD process development and the generation of yield statistics, since DMD arrays of this size have never been built before. The functionality of the DMD superstructure can be determined without the additional complication of CMOS yield concerns. Second, the LAC can be used for optical system development and testing. LACs can be mounted in projection optics and operated without video conversion and CMOS drive electronics. Both the optical characteristics of the DMD array and the optical system can be studied. Finally, the LAC offers the only means of building a projection display with 1920 x 1080 pixels. The first fully addressable DMD display chips are constrained to smaller array sizes by the field size of the photolithography tools available in CMOS fabrication labs. However, a chip with limited addressability can be built in a process development lab such as the Semiconductor Processing (SPL) using reticle composition.

2.2.2 Design Goals

The LAC was intended to emulate the optical characteristics of a fully addressable display. Therefore, it was desired that the DMD superstructure, that part of the chip design from the electrode level up, look like an addressed chip. That is, there can be no electrode level interconnections which could lead to stray reflections that would not be present in the final chip. Additionally, several types of patterns were requested by the subcontractor which would permit a more thorough optical analysis of the DMD chip and projection system. The suggested chip and

patterns are shown in Figure 15. Among these patterns were some text, a spatial chip pattern, a Nyquist pattern, a radial or fan pattern, some bullseyes, a crosshair, some long straight lines, and a 16 element gray-scale bar.

Initially the array size and pixel dimensions were not specified. However, after some discussion 1920 x 1080 was chosen. It has the desired 16:9 ratio, it is an array size compatible with future workstation screens, and it provides an ambitious goal, being larger than arrays promoted by our competition in the HDD arena. Our goal for pixel size was to build the largest pixel we could. However, the largest DSW (direct step on wafer, a photolithography tool) field size available to us was 20 mm x 20 mm. This limited us to 17 μm pixel spacing, after taking into account the space occupied by leads and bondpads.

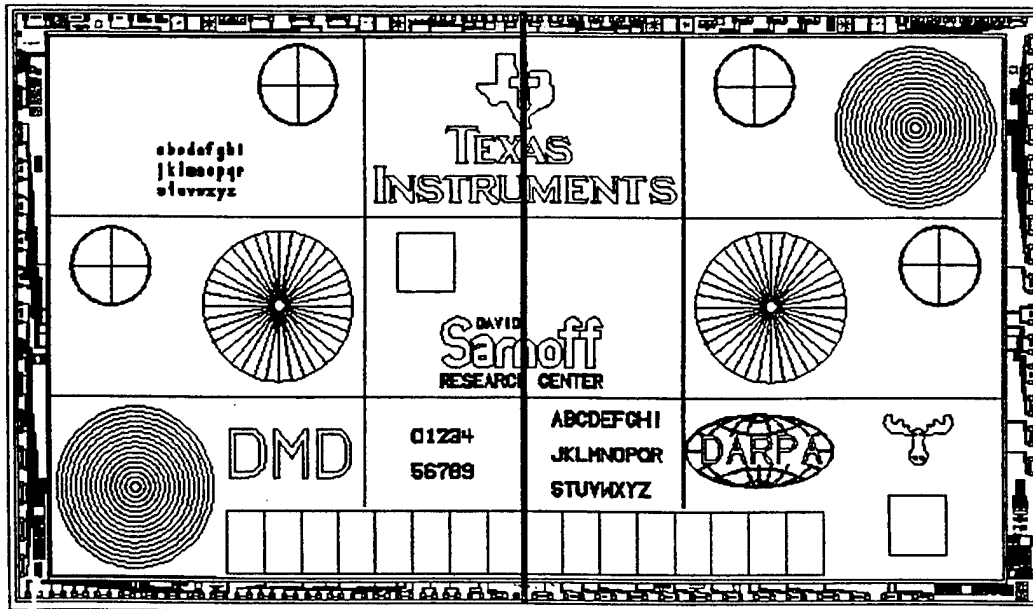


Figure 15. LAC chip patterns.

2.2.3 LAC Design

The above design goals, coupled with the bi-directional operation required for the mirrors, presented several design challenges, some of which were not recognized at the outset of the design phase. First, the requirement that no interconnects be present on the electrode level coupled with the bi-directional pixel operation forced us to use a double-level metal interconnection scheme. Second, the need to address patterns which can have arbitrarily shaped borders and which are multiply connected led to a novel interconnection scheme.

Since the patterns may have arbitrarily shaped borders with re-entrant curves, it was necessary to ensure that the pixels were connected in any desired direction (up, down, right, or left). It is necessary that the basic LAC pixel consist of a pair of leads (one for each direction of deflection) on each of the interconnect levels (POLY, which runs up and down, and METAL, which runs right and left). Each of these leads is connected by a tab to its twin in the neighboring pixels, creating an x-y grid of doubly-interconnected pixels. In addition, in each pixel the top lead and left lead are connected together by CONTACT1, as the bottom and right leads. Finally, two address electrodes providing the two directions of mirror tip, upper left and bottom right are connected to the METAL level interconnects by CONTACT2 contacts. Using this architecture both electrodes can be driven from any direction.

This basic pixel architecture gives rise to a fully connected array. In order to isolate addressable patterns from each other and from the background, it is necessary to "cut" the pattern from the background. This is accomplished through the use of the eight "directional pixels"; i.e., UP, DOWN, RIGHT, LEFT, UPRIGHT, UPLEFT, DOWNRIGHT, AND DOWNLEFT. Each of these is a pixel from which the interconnection tabs have been removed on all sides except those designated by the pixel's name. For example, UP has the POLY tabs removed from the bottom and the METAL tabs removed from both the right and left sides in such a way that they are connected only to the interior, the pattern is effectively severed from the background. Nested patterns such as the bullseyes are handled the same way, thus separating the patterns from each other, but leaving the pixels within a pattern full interconnected.

Because of the large number of patterns (approximately 90) and pixels involved, the placement of the directional pixels could not be accomplished manually. A layout algorithm was developed for the CALMA design terminal to do this task. Qualitatively, the program "walks" along the border of a pattern in a clockwise sense and determines what kind of pixel must be placed at each point. Boundaries (even curves) on the CALMA x (or y) direction one pixel distance (17µm), and determines what y (or x) pixel position best falls on the line segment. Next, the algorithm determines which kind of pixel must be placed in that position. This is determined from the angle the line forms with positive x axis as shown in Table 2. The "corner pixels" (UPRIGHT, UPLEFT, DOWNRIGHT, and DOWNLEFT) are inserted at appropriate slope changes to avoid isolation of pixels in the corners of patterns.

Table 2

CALMA LAC pixel types.

| PIXEL TYPE | SEGMENT ANGLE θ |
|------------|----------------------------------|
| UP | $135^\circ < \theta < 225^\circ$ |
| DOWN | $315^\circ < \theta < 45^\circ$ |
| LEFT | $45^\circ < \theta < 135^\circ$ |
| RIGHT | $225^\circ < \theta < 315^\circ$ |

Finally, there remains the problem of interconnection. To be able to address multiply connected (color-within-a-color) patterns, it is necessary to run leads from bondpads to the desired pattern without affecting pixels which are not part of that pattern. Two additional pixel types are required for this: VERTICAL and HORIZONTAL jumpers. The CONTACT1 contact between the POLY and METAL levels is removed in both of these pixels so that one level can be used for signal busing to the desired pattern, while the other level can be used to address the overlying mirror. The VERTICAL bus pixel has CONTACT2 contacts between the ELECTRODE level and the METAL level, so that signal can be bused elsewhere on the POLY pattern, while the overlying mirror is addressed by METAL which is connected to the pixels to the right and/or left of the bus pixel. Similarly, the HORIZONTAL bus pixel has contacts between ELECTRODE and POLY, so that the signal is bused horizontally on METAL, but the mirrors are addressed by POLY, which is connected to the pixels above and below the bus pixel.

Using combinations of the above eleven pixels we were able to lay out all the desired patterns. However, two unexpected difficulties remained. We initially intended to implement the pixel placement routine described above by literally removing basic pixels from the array and replacing them with the appropriate directional pixel. This leads to a data handling problem. The basic pixels were placed in the design as an AREF (array reference), so that only the size of the array (1920 x 1080) and the coordinates of its origin need to be saved. So the AREF must be reduced to 1920 x 1080, or over 2 million SREFs (structured references). That is, the coordinates of each of the pixels must be stored. The first time we tried this, we crashed the system. Another approach had to be found which left the array intact.

Basically we needed to remove unwanted pixel connections wherever a directional pixel was placed without removing the underlying basic pixel structure. An SREF on the CALMA, however, can only add data, not remove it. We settled on a color-reversal scheme. In this scheme, the pixel data drawn for the interconnect levels consists not of the POLY and METAL lead geometry's as is usual, but of the gaps between the leads. In other words, we designed INVERSE POLY and INVERSE METAL. Using this scheme, the inter-pixel tab connections can be removed by the addition of gaps in the position of the tabs. For example, The DOWN pixel consists of gaps at the top on the INVERSE POLY level. Thus when the DOWN pixel is superimposed on the basic pixel in the design, the connections to the pixel just above are removed. When the composite image is color-reversed at the end, a pixel disconnected at the top on the POLY level results.

The entire active array of the chip was designed using the pixel placement algorithm and color reversal. The bondpads, leads, and test structures were designed using the usual method of drawing the desired geometry's. The final reticle was made by merging the data in the periphery and the INVERSE data, after a final color-reversal, in the array.

2.2.4 LAC Layout

Figure 16 shows the actual layout for the LAC device with the address lines connected to the bond pads and use to exercise the various patterns on the LAC. The following addressable patterns were chosen to allow for fully testing the chip:

- Crosshairs: Single pixel width lines
- Bullseye: 16 concentric annuli, individually addressed; Grayscale and motion
- Radial: 36 radial segment for angular resolution; Grayscale and motion
- Nyquist: 120 x 120 array of pixels in groups of four; each group addressable for Nyquist checkerboards, vertical and horizontal bars
- Chirp: Pixels alternating in groups of 1, 2, 3, 10 vertically and horizontally
- Grayscale: 16 rectangles individually addressed; Grayscale and motion.

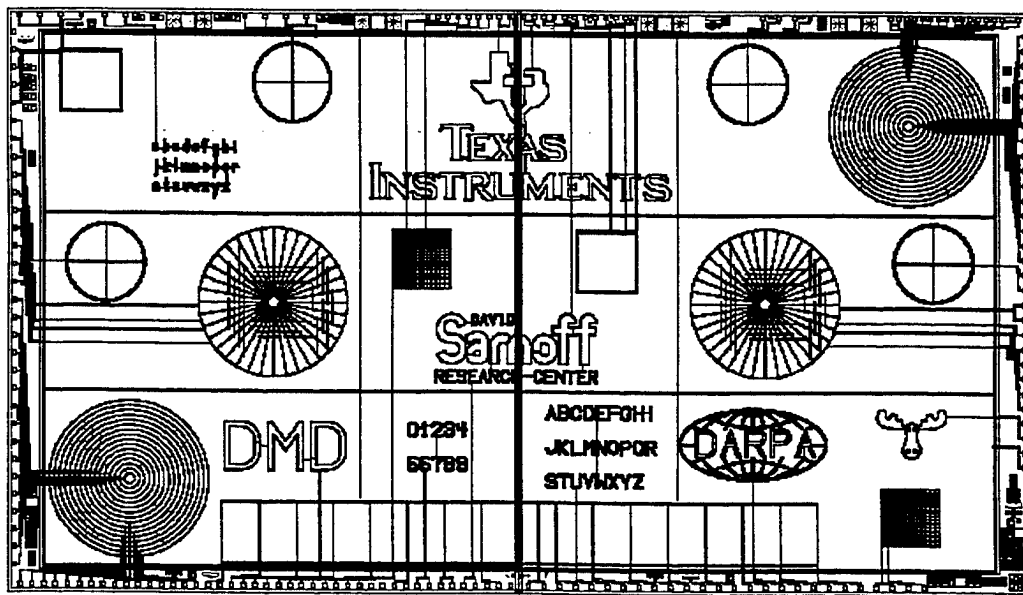


Figure 16. HD DMD limited addressability chip (LAC) layout.

2.2.5 LAC Device

A picture of the 1920 x 1080 LAC test device is shown in Figure 17. This figure shows the entire chip with >2-million mirrors and a blow-up of several of the mirrors. Actually, a couple of problems with these first devices can be seen in the picture; i.e., (1) over etching resulted in smaller mirrors and wider than 1 μm gaps, as well as narrow hinges, and (2) each mirror has a tapered edge. Regardless of this the devices worked.

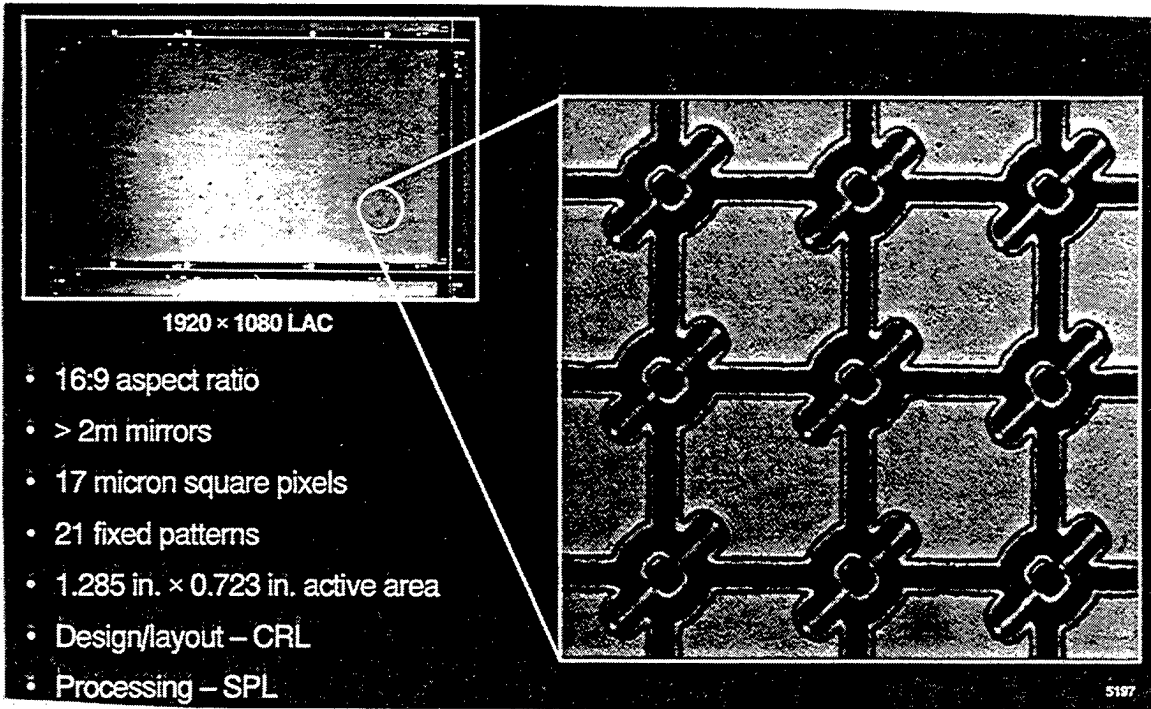


Figure 17. First LAC device.

2.2.6 LAC Device Package

It was necessary to design and fabricate a custom ceramic package for the very large LAC chip. A picture of the package with LAC device mounted is shown in Figure 18. The package has 184 pins and included a clear cover glass mounted at an angle to cut down on reflected light from the cover glass into the projector lens's aperture.

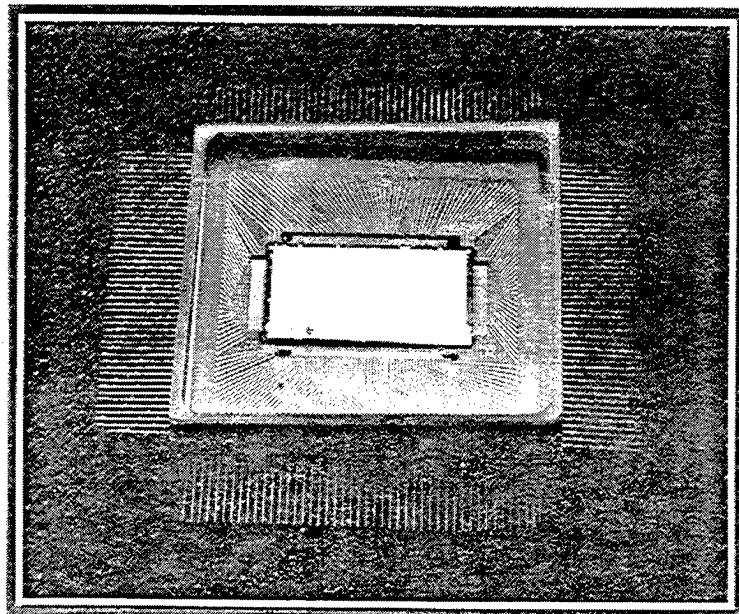


Figure 18. LAC device package.

2.2.7 DMD Testisng

Early stages of testing the DMD structures are described below:

2.2.7.1 Electrical Testing of DMD CMOS

Electrical characterization of the underlying CMOS structures in the early DMD devices provided unconvoluted design verifications, failure analysis, and yield information which could be extrapolated to the larger, future HDD devices. The scope of these tests encompasses initial testing after DRAM (or SRAM) fabrication, up to and including retest after subsequent processing steps. Besides providing feedback on the design and processing, it also provided early identification of devices which will not yield functional DMDs after mirror fabrication.

Both the DRAM and SRAM memory structure have built-in provisions for electrical testing, as shown in block diagrams of Figure 12 and 14 with the read/write output and sense amplifiers. The DMD features multi-input, multi-function shift registers with the last shift register stage brought out to a test port (read/write pin). Through proper mode control, these serial output ports provides read-back access, on a sequential basis, to the content of each memory cell and its associated peripheral circuitry. To a large extent this built-in readback architecture of the DMD dictated the test methodology for early DMD testing.

2.2.7.1.1 Hardware Test Setup

Setup for electrical test at wafer probe in shown in Figure 19. The test system is modular and can be readily customized to test either the DRAM or SRAM devices by using matching personality modules which are made up of a probe card and custom interconnect card.

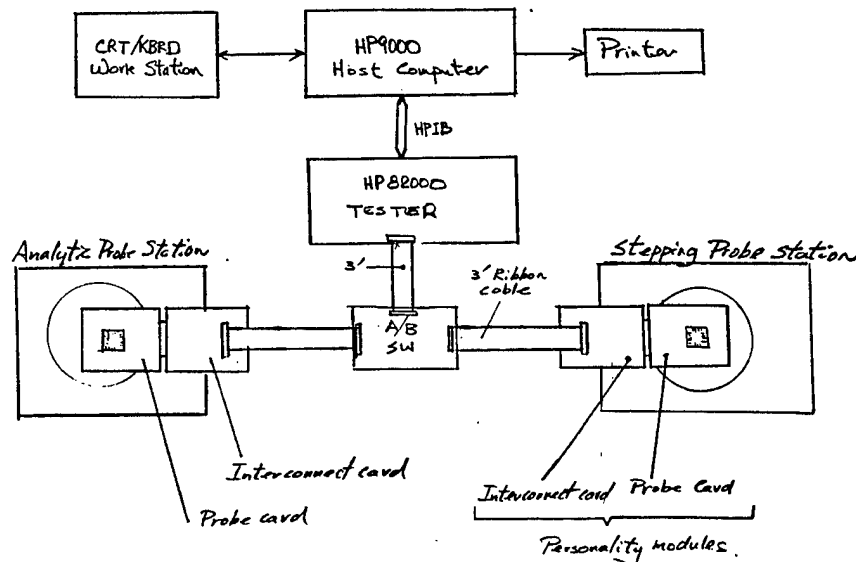


Figure 19. First DMD tester hardware block diagram.

The HP82000-D50 is a general purpose digital IC evaluation system. It features programmable timing and level setting on an individual channel basis. Each channel can be programmed as either input and/or output and backed up with 64K deep of dedicated memory. It can operate in either the Real Time Compare Acquire Data Mode. The human interface software for the tester resides in an HP9000-300 computer with communication between the two machines over a high speed HP-IB link.

The probe card is designed to provide landing on all signal power bond pads on both sides of the device. With the exception of "data input" pads, each probe has a circuit appearance on the card edge connector. Due to routing difficulty on the probe card, the "data input" probes are arranged in pairs, such that every two adjacent input pads receive identical signal input, hence reducing the number of circuit appearances at the card edge connector.

The interconnect card provides the cross-connect between unique pin assignments for each probe card and the fixed channel assignments prescribed by the HD82000 interface. The channel assignment on the HP82000 interface is fixed by design to maintain commonality.

2.2.7.1.2 Test Software

Test software was developed to customize the HP82000 for DMD memory testing. A simplified block diagram of the software elements used in early DMD testing is shown in Figure 20.

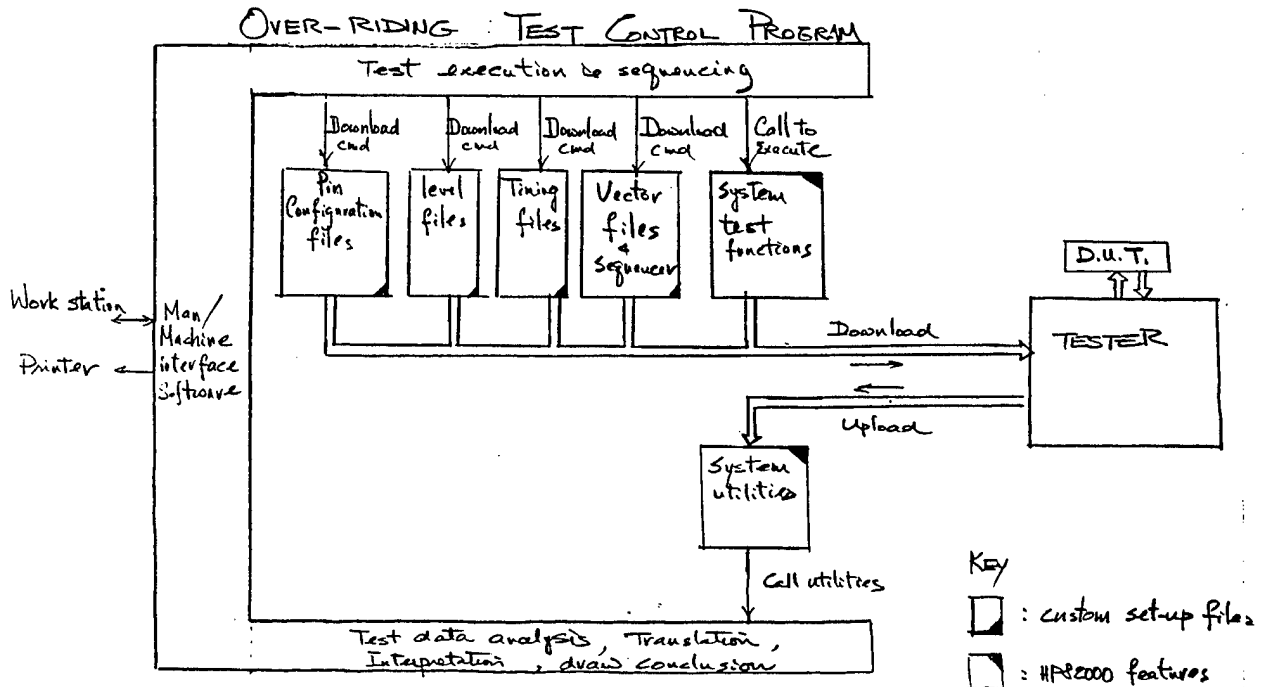


Figure 20. First DMD software tester block diagram.

The set of pin configuration, level, timing, and test vector files form the core of the test software. Devices can be tested manually by invoking the appropriate HP82000 test function. The test results can then be viewed in the result window in the form of error maps, state listings, or timing diagram. It goes without saying this method of testing, used with early DMD, was manpower and time intensive.

Additional testing software was developed to carry out a coordinated sequence of command executions, data extraction's, analysis, and translations. It also provides hardcopy listings for all test results performed on each device. These additions considerably improved the through-put time for electrical testing to approximately two minutes per device. Of course, in future production runs this testing will need to be automated to provide considerably faster operation.

In addition, software was developed to some artificial intelligence in rating the devices based on test results. Besides pass/fail information, it provides a rating factor for each device. It also packs relevant test results for each device into an 80 character record for storing and provides a consolidated listing for all devices on each wafer. Statistics are then accrued for the devices on a wafer.

2.2.7.1.3 Typical Test Data

Typical test data taken from the early DMD test system described above is shown in Figures 21.

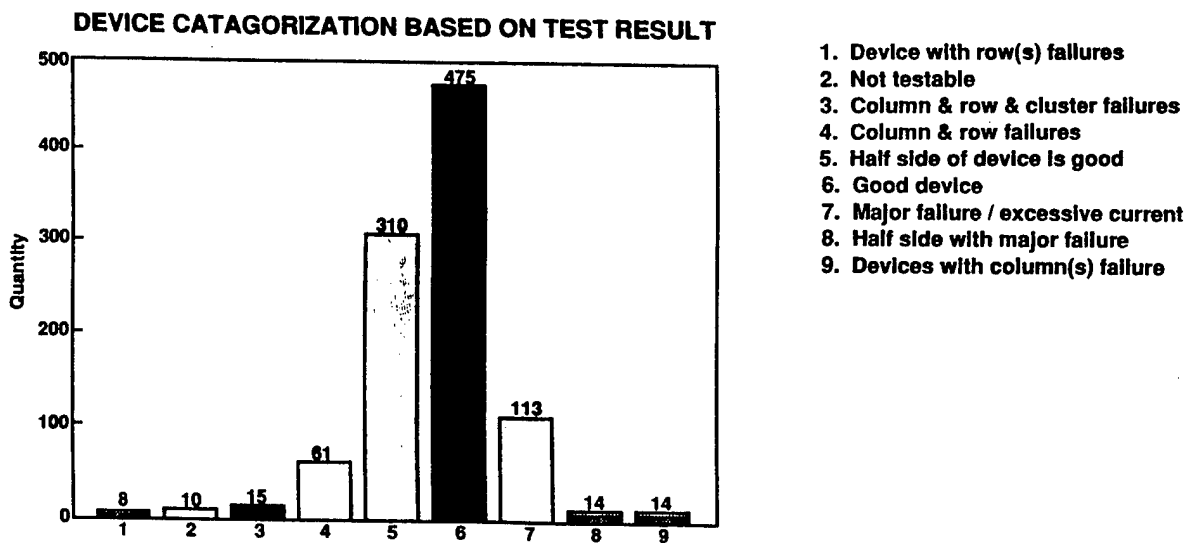


Figure 21. Early DMD CMOS test data.

2.2.7.2 Optical Testing of LAC Devices

Since the 1920 x 1080 LAC mirror was to be used only temporarily as a feasibility vehicle, testing was limited to illuminating the chips and observing visually the projected results. The block diagram for operating and testing the system is shown in Figure 22. As discussed above, the LAC had no CMOS addressing structure under the mirrors but rather had patterns of mirrors "wired" together with a lead going out to a bond pad for exciting (turning on) each pattern. Examples of this data will be shown later in this section of the report.

LIMITED ADDRESSABILITY DEVICE
DRIVE ELECTRONICS BLOCK DIAGRAM

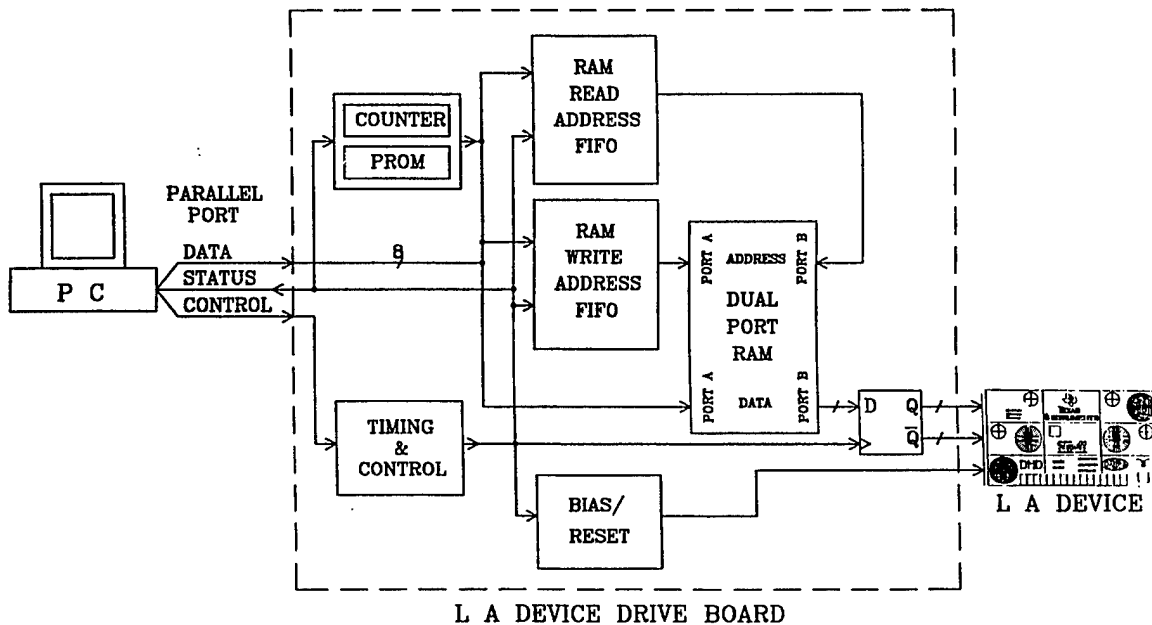


Figure 22. Block diagram for optical testing of LAC DMDs.

2.3 Optics and Illumination System

The following sub-report from Sarnoff describes the work performed as a subcontract to Texas Instruments (TI) under TI Purchase Order No. 109043636. Design criteria for a high-definition display system using the Texas Instruments Digital Micromirror Device (DMD) [formerly deformable mirror device] are presented. Perspectives are gained by examining both the optical behavior of the device and applications in which it may be employed. Technical detail has been reserved for the Appendices. An overview with some exposition is given in the main body.

Three general optical systems have been considered: one uses converging illumination, a second parallel illumination, and the third is re-entrant. The first of these three schemes is the simplest and most cost effective, particularly in a monochromatic implementation.

Overall system performance is of prime concern. Thus, closed-form estimates of lens throughput, contrast ratios, and ideal MTF's are derived for a given illumination source. The analytic expressions for reflector collection efficiencies are shown as a function of DMD diagonal, arc size, and projection lens $f\#$.

The analysis has been confirmed experimentally. A single-DMD monochrome laboratory prototype using only off-the-shelf components has been constructed. The prototype has been modified to implement a frame-sequential color display. Light efficiencies consistent with 3 lumens/Watt have been observed in the display which also maintains a contrast ratio of better than 140:1 and has less than 0.5% geometric distortion. Data pertaining to light budgets and illumination distributions have been collected. Further tests, such as those for local distortion and chromatic effects, that can be performed on the Limited Addressability Chip (LAC) are also discussed.

Full color projection schemes using three DMD's are of interest for Phase II. By using a coupling prism, a scheme has been found to increase the angular separation between the incoming illumination and the reflected image from the DMD. The rear end of the projection system can be compact, fitting within a cube, 8 in. on a side. However, in order to accommodate the color-combining elements, the back focal distance of the projection lens must be larger than the effective focal length. The required reverse telephoto lens is longer than a conventional enlarging lens.

Finally, radiation patterns from two commercially available projection screens are presented.

2.3.1 Display Systems

It is important to establish criteria for systems design. One aspect of this function is to determine what current systems are able to deliver in terms of performance. Displays fall into two broad groups: self-luminescent and illuminated. The latter may be generically referred to as light valves. Tables 3 and 4 present an overview of current display devices.

2.3.1.1 Self-Luminescent

Table 3

Properties of self-luminescent displays.

| Type | Resolution | Brightness | Contract | Efficiency | Reference |
|-----------------------|-------------------|--------------------------------|---|--|--|
| CRT - High Resolution | 2048 x 2048 | 30 fL | Better than 50:1, see boxes below | | |
| CRT - Commercial | | 80 fL | CRTs have their contrast ratio expressed in terms of ambient light levels. | Between 5 - 20 lm/W if deflection is ignored < 1 lm/W including deflection | Masterman, 1990, 1991 Goede, 1991 |
| CRT - Projection | 1000 - 2400 lines | 500 - 1620 lumens total output | In environments where the ambient light is orders of magnitude greater than that of the screen-25:1 | With 11 lm/W phosphor efficiency 2.7 lm/W is actually projected. Values do not include deflection energies | Matthies, 1991 Stoomer, 1989 |
| Electro-luminescent | 1000 x 1000 | 5 - 30 fL | 100:1 max | 0.8 - 30 lm/W | Goede, 1991 |
| Plasma | almost HDD | 200 fL max depends on color | | 1.5 lm/W max. | Goede, 1991 |

2.3.1.2 Light Valves

Table 4
Properties of light valves.

| Type | Resolution | Brightness | Contrast | Efficiency | Reference |
|--|-------------|---|---|---|--|
| Oil Film | 1024 x 1280 | 4000 - 56000 lm total output | Better than 50:1 | 0.5 lm/W | Good, 1971 Matthies, 1991 |
| Liquid Crystal types Twisted Nematic Polymer Dispersed Nematic Curvalinear Aligned Phase | 750 x 750 | Currently 250-W metal halide lamps are available. | 40:1 typical As high as 150:1 quoted Unknown value for the high efficiency Nematic Curvalinear Aligned Phase Liquid Crystals | 4.4 lm/W is the best achieved, using large-area Nematic Curvalinear Aligned Phase Liquid Crystals. Some systems are as low as 1 lm/W in color | Mori, 1988 Miyasaki, 1989 Bruce, 1991 Jones, 1991 Scheuble, 1991 |
| DMD | 1024 x 1920 | Better than 1000 lm in black and white | 140 - 190:1 | 3 lm/W est. | |

2.3.2 System Requirements

From the tables above we have constructed a reasonable set of design goals, displayed in Table 5 below, for the DMD display optics.

Table 5
System Requirements.

| | |
|----------------------|--------------|
| Aspect Ratio | 16:9 |
| Screen Diagonal | = or >60 in. |
| Display Area | 10.7 sq. ft. |
| Brightness | 100 fL |
| Total Light | 1100 lm |
| Efficiency | 3 lm/W |
| Resolution | 1920x1080 |
| Dynamic Range | 8 bits |
| Contrast Ratio | > 50:1 |
| Geometric Distortion | < 1% |

2.3.3 Monochrome Projection Schemes

The goal of Phase I of the development program was to show the feasibility of a black and white projector. Thus with one DMD, questions of optical access, resolution, and source matching were examined.

We examined: off-axis projection, use of a re-entrant projection lens, and parallel light illumination. All three designs image the light source in the limiting aperture of the system. In the first two cases the limiting aperture is within the lens, while in the last it is at the front focal plane. In all cases the stop is positioned at the point in the system where the illumination source is imaged. The light valve forms three images of the source; these are associated with the three possible mirror positions: tilted on, neutral, and tilted off. The stop is set to accept only the first of these three. Each of these schemes is described below.

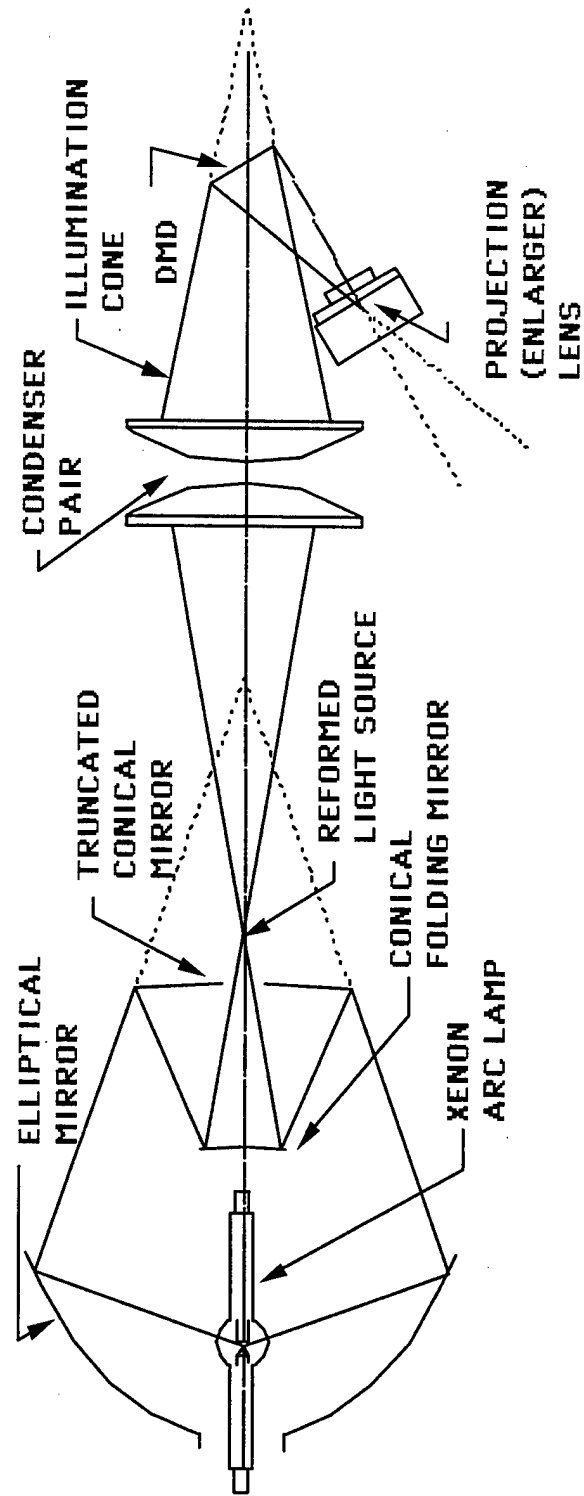
2.3.3.1 Off-Axis Projection

Figure 23 is a schematic of an off-axis projection system. The mirrors in the DMD form a blazed surface, thus converging light forms a skewed cone with its apex in the projection lens. Focused illumination reduces the aperture requirements of the projection lens. Since commercial lenses are rotationally symmetric, the angular requirements increase. Consequently, the prototype system used a Rodenstock 80-mm f/4 medium format enlarging lens.

No keystoneing will occur if the planes in which the image, object, and lenses lie are all parallel to each other. The centers of the object, lens, and image need not be all upon the optical axis. The scheme, however, effectively uses only one quadrant of the lens' angular field.

The off-axis, perspective control configuration allows the DMD to both be illuminated and have its image projected. The illuminating beam converges at the enlarging lens. We have thus implemented a Kohler-type projection system. The lens is both the limiting aperture and the stop. The stop prevents the unwanted beams from making their way to the screen.

THE UNFOLDED BLACK AND WHITE PROJECTION SYSTEM



An off axis projection system

Figure 23. An off-axis projection system.

2.3.3.2 A Re-Entrant Lens Configuration

The re-entrant lens scheme shown in Figure 24 allows one to illuminate and project through a single lens with at least two elements. A scheme such as this has been demonstrated recently by Mori et al. (1988), however, the configuration has a long history. The illumination is introduced as a point source in the space between the two elements. The light diverging toward the light valve is collimated by the back lens. The illuminated light valve reflects the light back toward the projection lenses; an image of the source is reformed in the region between the lenses. The system appears to be symmetric about the DMD. Thus the reflected light refocuses in the same plane at which the point source was introduced. It is in this plane that one must place the stop.

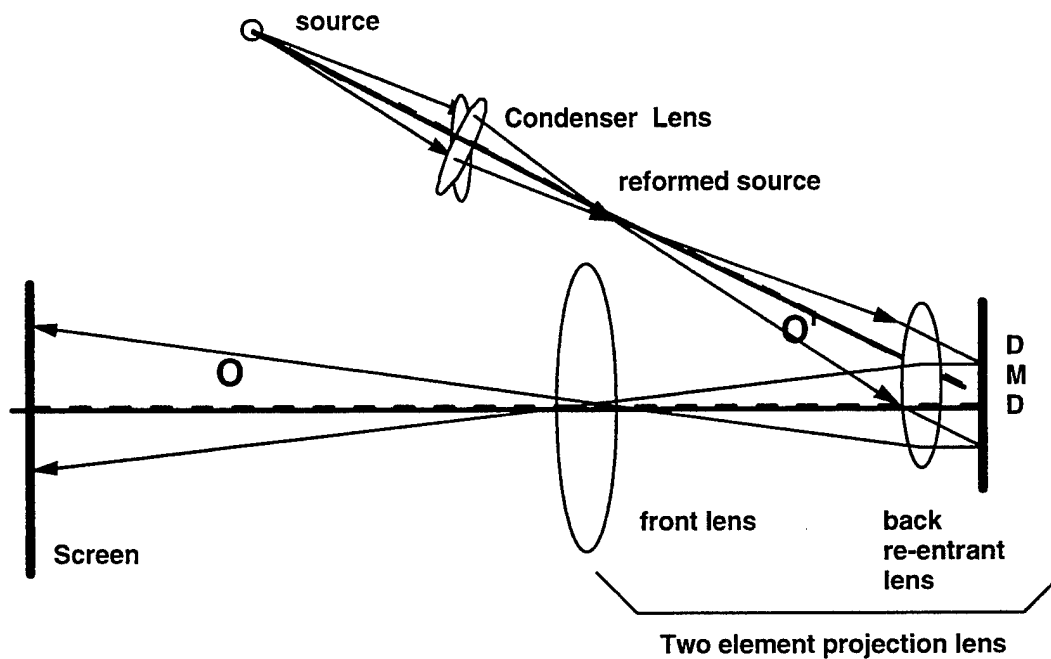
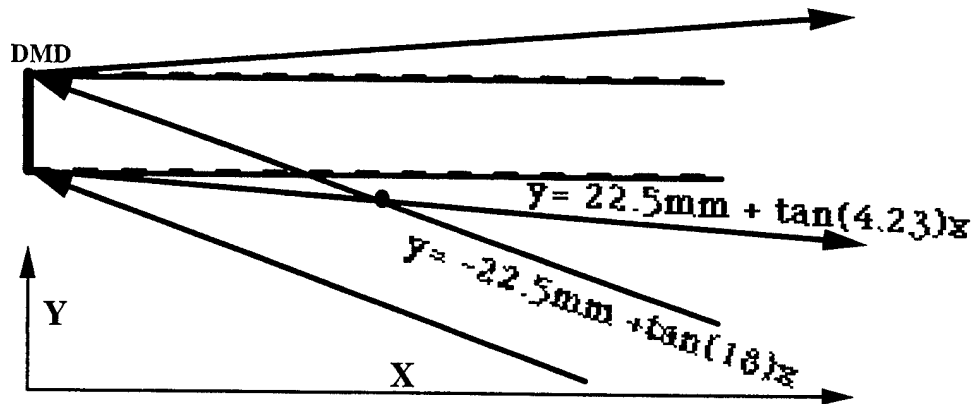


Figure 24. A Re-entrant projection lens.

A well designed system will probably not exceed a 60:1 contrast ratio because the illumination, reflected or back-scattered from lens surfaces, can find its way to the screen. A re-entrant system, particularly one with off-axis illumination, would require a back lens whose aperture would allow both the illumination and projection beams to pass, while an on-axis retro-reflective scheme would use the light from the undeflected and unclamped DMD mirror elements and thus not be able to reject the light from the background structures. We have also developed an illumination method that uses what we refer to as a coupling prism (Fig. 26). There is only one illuminated planar surface of the prism that is also included in the path to the screen. The reflections are thus controllable when the prism is used. The coupling prism approach is thus preferable to that that employs the re-entrant lens.

2.3.3.3 Parallel Light Illumination

A system using parallel illumination is displayed in Fig. 25. The illumination makes an angle with respect to the projection axis, which is twice the DMD mirror tilt angle. A transfer lens of radius y , allowing clearance for the illumination and acceptance of the first diffracted order (as required by imaging theory), is situated two focal lengths away from the DMD. An aperture is located at the focal plane of the lens. This is where the three possible images of the source are formed. Each image of the source is associated with a different DMD mirror orientation (tilt on, undeflected, tilted off). The stop allows only one of these three to pass.



Solution of the two equations is the intersection point of the incoming and outgoing beams. It is the closest lens placement.

$$X(\text{min}) = 179.31\text{mm} = 2f; \quad f = 89.66\text{mm}$$

$$Y(\text{min}) = 1/2 \text{ the lens diam} = 35.76\text{mm}$$

or an $f/1.25$ system.

Figure 25. A simple parallel illumination system.

The required $f\#$ for the transfer lens becomes $x/4y$. The results for different focal length lenses is given below.

Table 6 shows that a parallel illumination system that depends upon the use of a transfer lens requires a fast lens with a long focal length somewhere in the system. This design is unacceptable and was rejected.

Table 6

Positions, radii, and $f\#$ of 1 to 1 transfer lenses in a parallel illumination system.

| x(mm) | y(mm) | f# |
|-------|-------|------|
| 179.3 | 35.8 | 1.25 |
| 200 | 37.3 | 1.34 |
| 400 | 52.1 | 1.92 |
| 800 | 81.7 | 2.45 |
| 1000 | 96.5 | 2.59 |
| 2000 | 170.4 | 2.93 |

2.3.3.4 Use of a Coupling Prism with Parallel Illumination

Next, an alternative shown in Fig. 26 which uses a coupling prism to separate the incoming and outgoing beams was considered. (See Appendix E on color systems for a description of how the prism works.) In this design there are no longer any clearance requirements and thus no transfer lenses. A single 80-mm projection lens would be able to collect the first-order diffracted light even when parallel illumination (collimated to within four degrees) is employed. To eliminate the collection of light specularly reflected from the background structures, a stop is located forward of the lens.

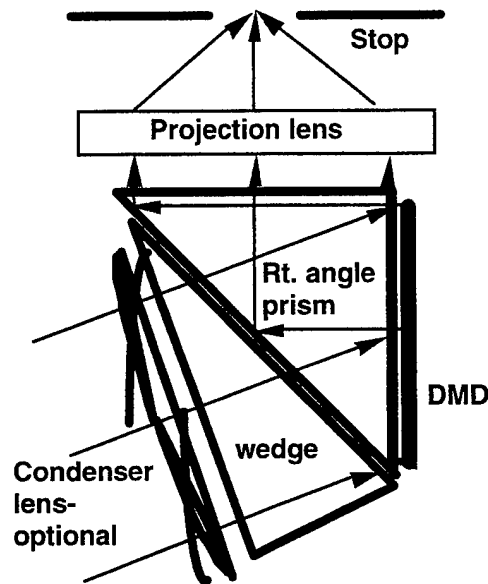


Figure 26. Coupling prism with parallel illumination.

The incoming beam passes through the hypotenuse of the right angle prism while the outgoing beam is totally internally reflected. For converging illumination one adds a condenser as shown.

For parallel illumination, an image of the source is formed in the forward focal plane and is thus the appropriate place for the stop. The arguments presented below for the throughput, contrast ratio, and resolution are valid for this configuration. The analysis that will be presented only require that the stop be located in the image plane of the source.

The discussions above show that there are two practical systems that allow us to illuminate the DMD without interference from the projection lens. The first is the off-axis projection system, and the second is a parallel illumination system that uses a coupling prism to separate the incoming and outgoing beams.

2.3.4 Light valve diffraction effects

In any projection scheme, there will be a plane in which one will find a spatial Fourier transform of the object. Since the pixels are the smallest elements, and the illumination source is

incoherent, the transform is dominated by the pixel structure. Generally one observes a convolution of the source with the diffraction pattern for a pixel. Thus an image of the source will be found at every diffraction spot.

2.3.4.1 Throughput

The Fourier transform of the square aperture function is the diffraction pattern. The throughput T , is the energy contained up to the designated order. It is the fraction of light which the lens passes. The grating structure is ignored, since the coherence length is shorter than a pixel length. Table 7 shows the throughput for a *point source* (an appropriate approximation) as a function of the number of orders retained. Subtracting adjacent columns gives the percentage energy which resides in any given order.

Table 7

Total light in all orders up and including the designated orders and the percentage of the total resident in each order.

| Order | 0 | 1 | 2 | 3 | 4 | 5 | 6 | 7 | 8 | 9 |
|------------|------|------|------|------|------|------|------|------|------|------|
| T (%) | 81.5 | 90.2 | 93.4 | 95.0 | 96.0 | 96.7 | 97.1 | 97.5 | 97.8 | 98.0 |
| Energy (%) | 81.5 | 8.7 | 3.2 | 1.6 | 1.0 | 0.7 | 0.4 | 0.4 | 0.3 | 0.2 |

We can also estimate the throughput from the $f\#$ of the projection lens. As many terms will be collected as satisfy

$$(2f\#)^2 < (1 - \gamma^2) / \gamma^2 = 1 / \tan^2(\Theta_\epsilon) \quad (1)$$

where $\gamma = \delta\lambda / 2x_0$ and Θ_ϵ is the deflection angle for order ϵ ; the dimension of the side of a pixel is x_0 , λ is the wavelength of light, and $\delta - 1$ is a number whose integer part is the highest diffraction order retained. The tangent of the largest angle to pass through the lens is $1 / (2f\#)$. If the $f\# = 4$, then $\gamma = \delta\lambda / 2x_0 < 0.124$, which is only satisfied if $\delta < 3.01$. The intensity minimum is past the second diffraction order. Thus the lens collects more than 93% of the light.

2.3.4.2 Contrast

From the argument that the light structure in the transform plane is a convolution of the diffraction pattern with the image of the light source, we are able to make approximations about the contrast ratio.

There are three diffraction centers: the first associated with the DMD mirrors tilted in the on position, the second associated with structures that are coplanar with the DMD surface (essentially everything that is not the active mirror structure), and the third associated with the DMD elements tilted to the off position. The background illumination is determined by that portion of the diffraction pattern associated with the coplanar structures that pass through the

limiting aperture. The ratio of light obtained with the DMD full on to this unwanted light is an estimate of the contrast.

Two assumptions must be made: first, that the diffraction patterns on all three centers are identical since they all arise from gratings of similar pitch (see Appendix C); and second, that ratio of the coplanar pattern to the “on” pattern intensities, A_ratio , is simply a ratio of areas times the ratio of the surface reflectivity’s of the two surfaces, here taken to be one. The active area for calculation is taken to be 75% of the total.

$$A_ratio = \frac{(\text{Total DMD area} - \text{Active pixel area})}{(\text{Active pixel area})} \quad (2)$$

Furthermore, from Fig. 27 we see that only two of the possible four major diffraction spots overlap the lens aperture for any order higher than the zeroth. This may be considered a vignetting factor. Since the energy in an order, as listed in Table 8, is the total in all four spots, the energy leakage to the screen must be corrected by the vignetting term. An image of the source, is formed at each diffraction order. The amount by which the images, associated with a specific order in the complimentary pattern, overlap with the lens opening (or limiting aperture) will be referred to as the overlap fraction, OF (see Fig. 28).

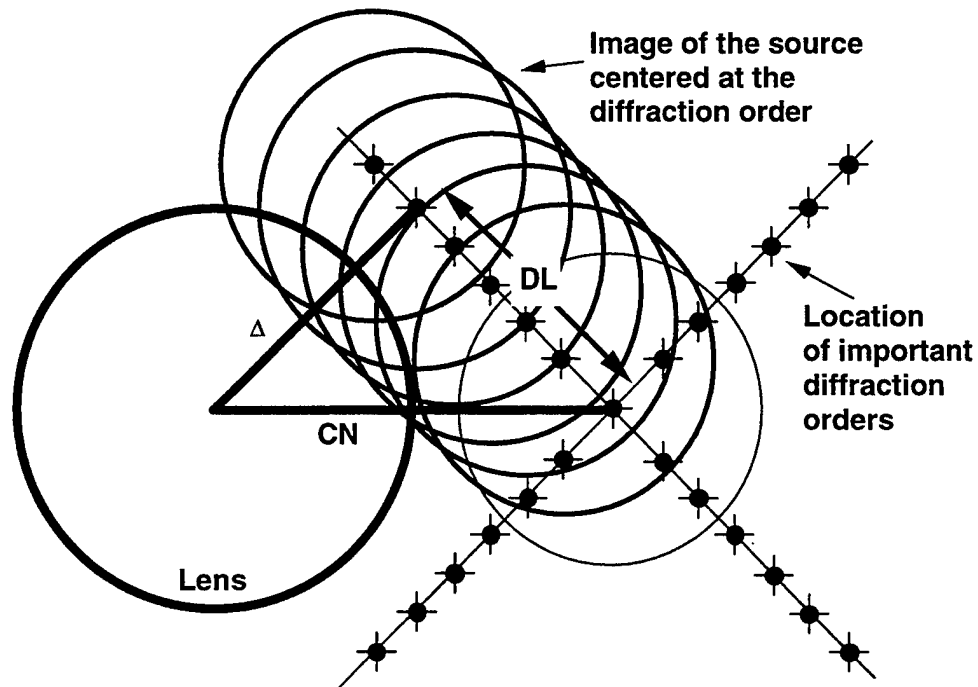


Figure 27. The complimentary pattern nestles about the projection lens as shown. At each diffraction spot location an image of the source is formed.

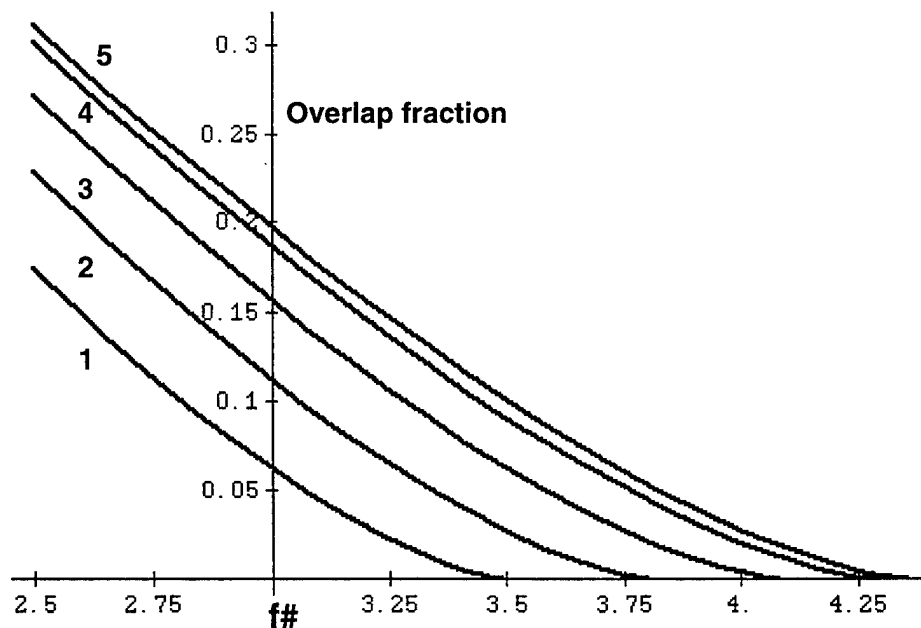


Figure 28. The fraction of overlap as a function of lens $f\#$ for the orders 1-5. The DMD is assumed to have 9-degree mirror tilt.

For an $f/3.1$ lens there is no zero order overlap allowing us to construct Table 8.

Table 8

Complimentary pattern leakage for an $f/3.1$ lens.

| Order | 0 | 1 | 2 | 3 | 4 | 5 | 6 | 7 | 8 | 9 |
|------------|------|------|------|------|------|------|------|------|------|------|
| Energy (%) | 81.5 | 8.7 | 3.2 | 1.6 | 1.0 | 0.7 | 0.4 | 0.4 | 0.3 | 0.2 |
| OF (%) | 0 | 4.46 | 9.26 | 13.6 | 16.7 | 17.7 | 16.4 | | | |
| A_ratio | 0.33 | 0.33 | 0.33 | 0.33 | 0.33 | 0.33 | 0.33 | 0.33 | 0.33 | 0.33 |
| Spots | 1/1 | 2/4 | 2/4 | 2/4 | 2/4 | 2/4 | 2/4 | 2/4 | 2/4 | 2/4 |
| Leak (%) | 0 | .064 | .049 | .036 | .028 | .020 | .011 | | | |

The calculation of the leakage allows us to arrive at an estimator for the ultimate possible contrast ratio. For an $f/3.1$ lens the leakage from the planar, or complimentary pattern, corresponds to a throughput of the order of 0.2%. Since the peak screen illumination corresponds to a throughput of $> 90\%$, this yields an ultimate contrast ratio of almost 500:1. Clearly this is not an achievable number.

It is reasonable to ask what limitations on system performance have been ignored in the estimator for the contrast ratio. To answer this question we must look at the image of the DMD when the light valve is shut. Pictures were taken, and the following observations made: scattering from the holes and mirror edges were of secondary importance. The post and torsion bar structures were

the largest contributors to any unwanted light on the screen. These non-planar structures violate the original assumptions of the calculation. Thus the contrast ratio is not limited by the optics but by the device itself.

Contrast ratio measurements were made. First as to the line arrays. Observations in the sub-pixel regime yielded contrast measurements above 100:1. When light from background structures were included the readings were reduced to 40:1 to 50:1. Readings taken upon the two-dimensional arrays, those that emulate the optical behavior of the fully functional devices, performed better. They yield contrast ratios of better 140:1 and 200:1. It is always clear that most of the unwanted light comes from protrusions and edges. *To improve the performance of the system scattering from the post structures must be minimized.*

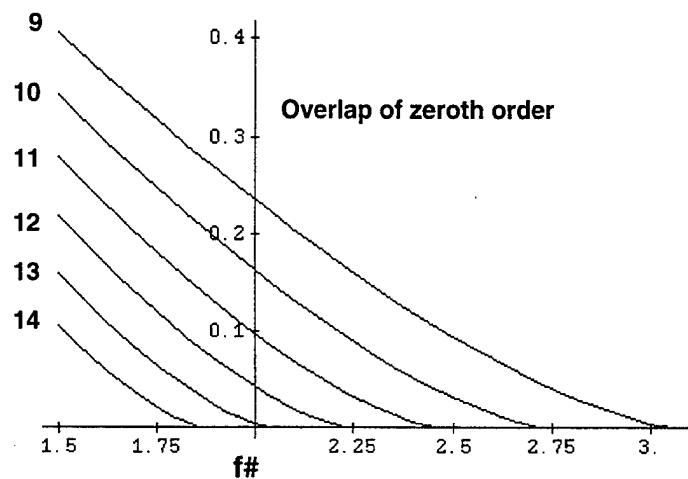


Figure 29. The overlap of the image of the source at the zeroth order location in the complimentary pattern as a function of $f\#$ for DMD mirror tilts of 9 to 14 degrees.

So far it has been assumed that the zero-order component in the complimentary pattern is rejected. Increasing the aperture allows some of this light to pass. Since the complimentary pattern is estimated to be only one third as bright as the projected image, by surface area arguments, a contrast ratio of 100:1 can be retained with an overlap of up to 0.02. Figures 29 and 30 show that the contrast is set by the $f\#$ of the projection lens and the tilt angle of the DMD mirrors. In particular one can see from the graphs that an $f/2$ lens would be usable if the DMD tilt angle were increased about 13° . The faster the lens, the larger the allowed source or the higher the possible collection efficiency. Alternatively, the faster the lens the easier it is to use a metal halide lamp.

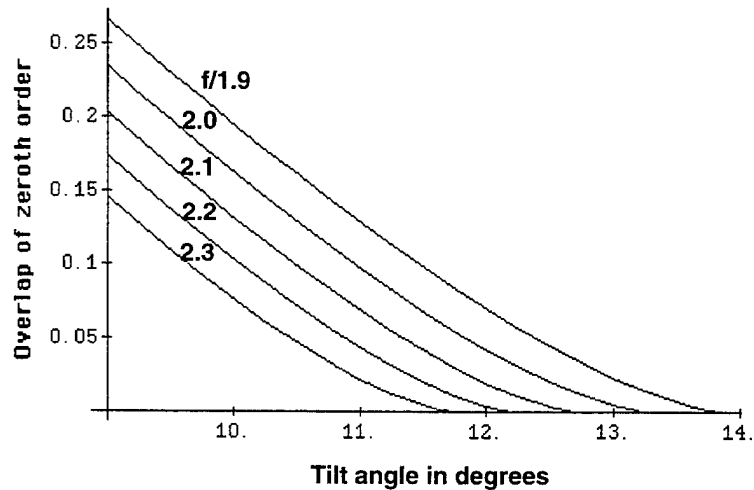
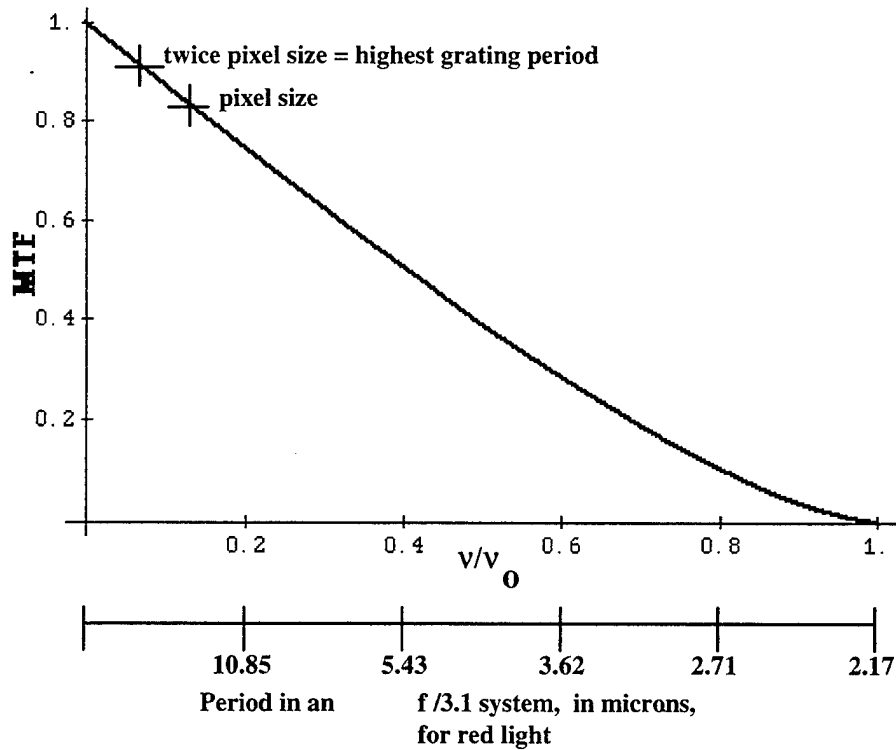


Figure 30. The overlap of the image of the source at the zeroth order location in the coplanar pattern as a function of mirror tilts for projection lens $f\#$ from 1.9 to 2.3.

2.3.4.3 $f\#$ and MTF, a Classical Argument

An estimate of the best modulation transfer function (MTF) obtainable is derived by considering solely the effect of the aperture. The problem then is to determine the optical power (intensity) that passes through the lens aperture, as a function of spatial frequency. The argument is developed in Appendix C. A plot of the MTF vs pixel size demonstrates that the response of the $f/3.1$ system is not aperture limited (see Fig. 31).



MTF for an aberration free system with a circular aperture

$$v_0 = 1 / \lambda f\#$$

After Smith (1990)

Figure 31. The MTF in an aperture limited system.

2.3.4.4 Light Use Efficiency

Parallel and off-axis illumination systems should have close to the same efficiencies. This can be seen by inspection. The $f\#$ of the lens only weakly depends upon how far off-axis we go (for small angles), since the correction involves the proper accounting of vignetting effects. The analysis below shows that the overall efficiency depends upon the $f\#$ of the projection lens. To be more precise, the efficiency will be shown, in Appendix D, to depend upon the ratio of the size limiting aperture to the size of the source's image at the stop's location in the projection lens. The results below are representative of the major design trade-offs.

The simplest configuration that one might consider is a light collection parabola used in conjunction with a condenser lens that focuses the light in the projection lens (Jones 1991). The fraction of the total light that can be extracted from an arc of diameter d , passed through a valve of diagonal V , and thence to the screen, is the collection fraction, CF

$$CF = \{1 + [(\eta^2 - 1) / (\eta^2 + 1)]\} / 2 \quad (3a)$$

where

$$\eta = V / 4df\# \quad (3b)$$

Figures 32a and 32b are families of curves which show how the efficiencies depend upon $f\#$ and arc length in one case and DMD diagonal and arc length in the other. There is a simple physical reason why the collection fraction increases with increasing DMD size for a fixed $f\#$. Since the required magnification of the system drops, the projection lens has a longer focal length, and thus the diameter of its aperture increases. In turn the allowed diameter of the imaged source also increases. Liquid crystal modulators are now made with 75- to 100-mm diagonals. It is a direct consequence of this that large modulators tend to use metal-halide lamps.

We are thus led to the following question: whether it is more appropriate to use a Xenon arc or a metal-halide lamp in the projection system. We can ascertain this by multiplying the collection fractions by the lamp efficiencies and plotting the resulting collection efficiency as a function of the $f\#$ of the projection lens. The Xenon arc lamp has an arc length of approximately 2.3 mm and a lamp efficiency of 28 lm/W, while the metal halide has an arc length of 6 mm and a lamp efficiency of 80 lm/W. Figure 33, a semi-logarithmic plot, shows that the Xenon lamp will outperform the metal-halide lamp, when the DMD diagonal is 37.5 mm, for any projection lens slower than $f/2.8$. For a modulator with a 100-mm diagonal, this crossover point will occur at $f/7.5$.

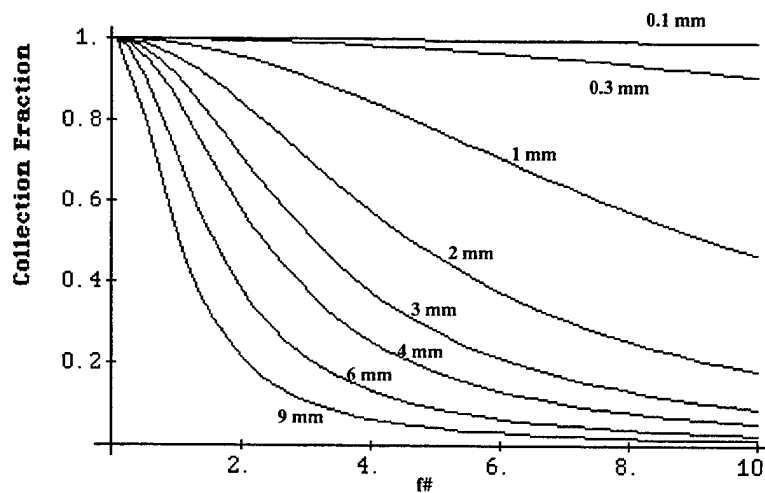


Figure 32a. Collection fraction as a function of $f\#$ for various arc lengths, given a DMD diagonal of 37.5 mm.

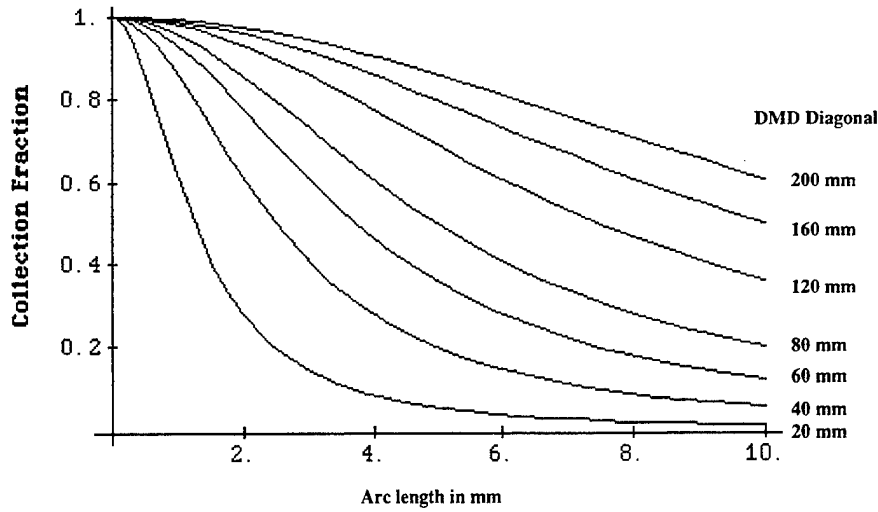


Figure 32b. Collection fraction as a function of arc length for various DMD diagonal sizes, for a f/4 projection lens.

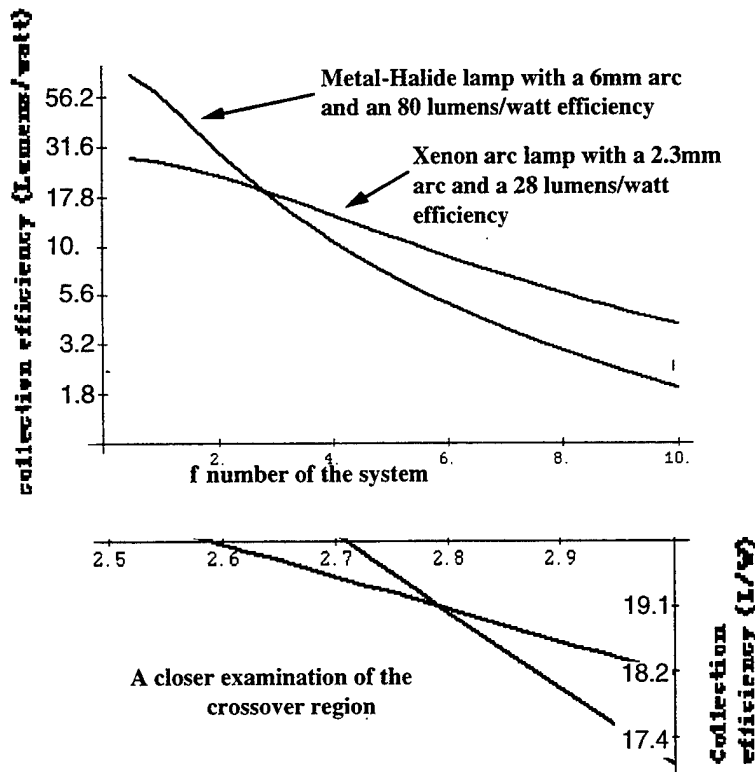


Figure 33. Comparison of the overall efficiencies vs. f# for a 6-mm, 80-lm/W metal-halide lamp and 2.3-mm, 28-lm/W Xenon arc lamp. The calculation assumes parabolic collector.

2.3.5 The prototype

The first phase of the development program was to prove that a projection system could be constructed using the deformable mirror device; using, as much as possible, commercially available parts.

2.3.6 Commercially available parts

Two lenses were chosen that approached the design requirements. Both were medium format enlarging lenses: The Schneider 102-mm $f/5.6$ and the Rodenstock 80-mm $f/4$. While not as fast as $f/3.1$, they did approach the limiting value, and they both had sufficient fields of view to test the off-axis projection scheme. In landscape photography the use of the off-axis imaging scheme is common. It reduces keystoneing. The lenses that allow the configuration are very often referred to as perspective control lenses. In projection systems they are sometimes called anti-keystoneing lenses.

A custom reflector assembly was designed to match the projection lens. We chose to use an ellipse (see Table 9) since it allowed an easy method to fill the shadow region created by the lamp electrodes (though its use does not preclude the use of a parabola in the final design). Reflecting the beam from two conically shaped mirrors as shown in (Fig. 23) translates and tilts the converging beam as shown in Fig. 34. The shadow is filled in both radial and the angular distributions. The uniformity of the fill is then determined by the amount of overlap.

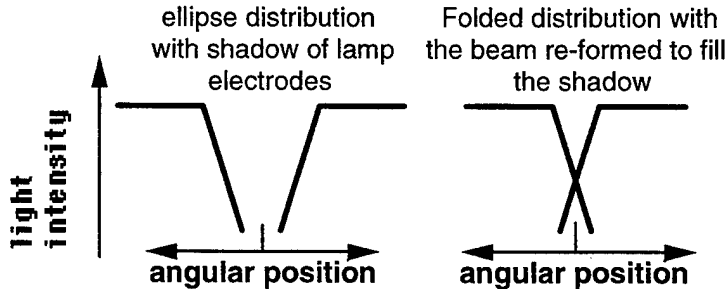


Figure 34. By tilting and shifting the beams from diametrically opposite sides of the ellipse we fill in the central region.

Table 9

Light collection parts specifications for the prototype.

| Part | Shape | Curvature | Diameter |
|------------------|---------|-----------|----------|
| Ellipsoid | 0.394 | 0.2631 | 10.5 in. |
| Truncated Cone | -389.68 | | 6.5 in. |
| Cone Hyperboloid | -94.00 | -10.00 | 2.1 in. |

This scheme was simulated in the ray tracing procedure. Both experiment and calculation indicated that the overlap uniformity was also sensitive to the position of the arc relative to the focus of the ellipse. By allowing a fine adjustment of the position of the lamp in the ellipse, the system could be tuned for maximum smoothness in the light distribution in the center of the image on the screen. A ray trace near the focus of the collection assembly shows the computed spot diameter to be about 12 mm.

2.3.7 Performance

The design presented for Phase I solved many problems while staying within the constraints. We were able to:

- Use a commercially available enlarger lens
- Concentrate on the light collection system

It allowed us to define the problems associated with a commercially viable system. We were able to demonstrate:

- Feasibility of the light collection efficiency criteria
- Optical accessibility to the DMD
- Resolution requirements could be met
- Color capability

The purpose of this section is to discuss the measurements that were made on the various components of the projection system. We developed and confirmed a light budget. The question of light uniformity across the image on the screen is addressed. Procedures for measuring distortion and other aberrations are also discussed.

2.3.7.1 Light Budget

In these tests the light was projected onto a matte-white screen that was assumed to be Lambertian. The light available at different points in the system was measured and compared with expected values. The results are listed in the light budget table (Table 10).

Table 10 - Light budget calculations and measurements.

| | Optimum Expectation | Efficiency in % Theoretical | Efficiency in % Measured | Measured Performance of the Prototype | Expected Performance of the Prototype given Measured Constants |
|-----------------------------------|---------------------|-----------------------------|--------------------------|--|--|
| Light Source | 500 W | | | 436 W | |
| Light Source Efficiency | 28 lm/W | | | | |
| Light at Source | 14000 lm | | | | 11900 lm |
| Ellipse Coll. Eff. | 8100 lm | 58% | | | 6900 lm |
| Ellipse Reflectivity | 7700 lm | 95% | 77% | 5300 lm | 5300 lm |
| Secondary Mirror's Reflectivity. | 6900 lm | 95% each 90% the pair | 90% each 81% the pair | 4300 lm | 4300 lm |
| Hot Mirror Transmittivity | not used | | 88% | | |
| Cold Mirror Reflectivity | 6600 lm. | | 96% | | |
| | Optimum Expectation | Efficiency in % Theoretical | Efficiency in % Measured | Measured Performance of the Prototype | Expected Performance of the Prototype given Measured Constants |
| Light -Post Cold Mirror | 6600 lm | | | 3600 lm | 3600 lm |
| Cond Fresnel Losses | | 0.5% / surf 2% total | 5%/surf 20% total | | |
| DMD/Illum Area Ratio | | 45% | | | |
| Light on DMD | 2900 lm | | | | 1300 lm |
| Proj. Lens Fresnel loss | | 6*1%/lens 94% trans | | | |
| Screen w/ Mirror-100% Active Area | 2700 lm | | | 1400 lm some beam x-sect shaping | 1200 lm |
| Corr. -DMD @ 75% Active Area | 2000 lm | 75% | | | 900 lm |
| Max. Proj. Lens. Diff. Losses | 1900 lm | 93% | | | 837 lm |
| Dichroic Losses | 1500 lm | 80% | | | 753 lm. @90% at color wheel |
| Overall Color System Eff. | | 11% | | | 188 lm. given 25% duty factor for color wheel. |

2.3.7.2 Light Uniformity

The procedure outlined above yielded yet another quantity of interest, the uniformity of the light distribution on the screen. The luminous flux for each square may be displayed. The levels cover a 5:1 range. The levels are close to, but not quite, adequate. It will be the task of Phase II to improve this. In this respect it is hoped that the coupling prism, which moves the DMD closer to the condenser lens, will improve the situation. Table 11 displays the light distribution that was found.

Table 11
Light Distribution.

| | | | | | |
|---|---|---|---|---|---|
| 200 cd/m ² 59 fL 41 lm | 290 cd/m ² 85 fL 59 lm | 400 cd/m ² 117 fL 81 lm | 400 cd/m ² 117 fL 81 lm | 250 cd/m ² 73 fL 50 lm | 150 cd/m ² 44 fL 30 lm |
| 200 cd/m ² 58 fL 41 lm | 480 cd/m ² 140 fL 97 lm | 560 cd/m ² 164 fL 114 lm | 650 cd/m ² 190 fL 132 lm | 420 cd/m ² 123 fL 85 lm | 180 cd/m ² 53 fL 37 lm |
| 190 cd/m ² 56 fL 39 lm | 500 cd/m ² 146 fL 101 lm | 700 cd/m ² 204 fL 142 lm | 800 cd/m ² 234 fL 162 lm | 520 cd/m ² 152 fL 105 lm | 180 cd/m ² 53 fL 37 lm |

2.3.7.3 Distortion and Other Aberrations

The major lens aberrations are: spherical aberration, coma, astigmatism, field curvature, distortion, and chromatic aberration. Since all these aberrations reduce the MTF, measurement of contrast as a function of spatial frequency suffices to characterize the performance. For the highest DMD frequency of 30 cycles/mm (at the object), an observer five feet away from the screen, will see a projected image with 21 line-pairs/degree in the field of view. Campbell and Green (1965) have measured the contrast ratio of an image formed on the retina as a function of the pupil diameter. At 21 cycles/degree pupil diameter changes will cause the contrast ratio to vary from 0.2 to 0.5. A projection lens with an MTF better than 0.4 at the highest spatial frequency will not degrade the perceived image any more than the dilation of the pupil.

Geometric distortion is most easily seen as a change in shape. By measuring the difference in the length of the diagonals and the sides of a rectangular image, pincushion can be ascertained in the off-axis projection scheme. Measurements with the first DMD device indicated that the distortion is < 0.5%.

Chromatic concerns are: lateral color (magnification as a function of wavelength), and MTF as a function of a color. Accurate alignment of three-colored images implies a shift of less than a half a pixel. This means that the lateral color must be less than 0.3mm, with an MTF of better than 0.4 at 0.74 lines/mm (at the image).

2.3.7.4 Optical Tests

There are only a limited number of tests that were required to characterize the system. The first is an MTF measurement as a function of position on the screen. This test can be performed under white light and colored illumination. These measurements may also be done as a function of orientation using radial fans in the test patterns; this separates the tangential and sagittal planes. These measurements can be obtained from the radial fans in the test patterns. If the MTF exceeds 40% at the maximum resolution, the system performance is acceptable.

Distortion measurements involve looking for deviations from a straight line in the borders of the test pattern and mapping out the curvature of any other straight lines in the test pattern. Alternatively, egg-shaped bulls-eye patterns also indicate this type of distortion.

To date no measurable distortion has been seen, being less than 0.5%. Furthermore individual pixels are clearly seen at all points across the screen.

2.3.8 Possible color displays

2.3.8.1 Adaptability to a Color System

Phase I used a field-sequential color system. To achieve this a color wheel was placed at the point labeled reformed light source, in Fig. 23. The impact of a color system, with 180 fields/sec, was observed.

The color wheel did demonstrate that large, high-brightness, field-sequential displays are prone to manifest color field separation, particularly when one moves ones gaze across the display's diagonal. For this reason, the color wheel is not now considered the best choice for a color projection system. The criterion that the system be portable and easily set up seems to point toward a prism color-combining scheme.

There are several possible color systems: a field-sequential single DMD modulator, a three-DMD, three-projector-lens system, and two three-DMD combiner prism schemes. These are discussed below.

2.3.8.2 Color Wheel

The color wheel is an interesting alternative. It ~~has been~~ incorporated in the original black and white design because of its simplicity. The wheel is placed at the location of the reformed light source in Fig. 23, where the beam has its narrowest cross-section. The spot diameter at this point is of the order of a half an inch, both measured and computed.

The color wheel could also be used in a parallel illumination system, except that the wheel must then be located at the limiting aperture in the front focal plane of the projector lens.

The color wheel we designed for Phase I is driven by a synchronous motor rotating at nearly 3600 rpm. Each filter, described in Table 12, occupies a third of the annulus. Unfortunately, at 180 color fields a second there is still some visible color field separation. TI is working this issue of sequential color field "breakup" separate from this program.

Table 12

The color coordinates of the dichroic filters.

| Color | Filter Type | 50% Points (nm) | u | v |
|-------|-------------|-----------------|-------|-------|
| Red | low pass | 590 | 0.507 | 0.349 |
| Green | band pass | 505, 575 | 0.125 | 0.386 |
| Blue | high pass | 515 | 0.136 | 0.145 |

The red and blue coordinates are further out than NTSC color phosphors. The green is slightly closer in. The implication of this is slightly less saturated blue-greens.

2.3.8.3 Triple Projection

Triple projection refers to a system with three projection lenses. As customarily implemented, a separate projector is used for each primary color. The three images are converged on a fixed screen. The system is quite useful for self-contained rear projection units and for fixed display installations.

A three-DMD device color system can be implemented. The illumination source would first be split into three colors, which would eventually be recombined at the screen. The disadvantage of the system is that it uses three projection lenses and thus has convergence problems.

2.3.8.4 Combining Prism

The use of a combining prism reduces the number of required projection lenses to one. Furthermore, the alignment of the DMD light valves (making them optically conjugate) needs be made only once during fabrication of the projector. The projector will be operated in a manner similar to that of an ordinary slide projector. Two prism types are possible, a Phillips type as shown in Fig. E2 (appendix), or a cube as shown in Fig. E3 (appendix). Of the two the cube has the shorter optical path length.

The reflectivity of dichroic films, as a function of wavelength, depends upon the angle that the light makes with the surface normal, while in the film. The reflectivity will be a function of polarization as well. The incident beams are not perpendicular to the films. In order to reduce the beam's angle in the dichroic stack there is a bias to use films of high refractive index embedded in low index media. A comprehensive discussion of the color systems is found in Appendix E.

2.3.9 Summary and Conclusions for Phase I Optics and Illumination System

In Phase I we have demonstrated that a high quality, high efficiency projection system can be built using a DMD. The efficiency is superior to most other commercially available light valve projectors. Image quality of the projector is outstanding, being virtually distortion free and with each pixel being clearly resolvable across the screen. The MTF of the system at 0.8 lines/mm (pixel frequency at the screen) rolled off from 0.7 near the center to 0.26 in the corner. By carefully selecting the dichroics used in the phase sequential system we achieved a color gamut similar to NTSC.

The design considerations dictated the path of development. We have shown that:

- The desired level of resolution can be achieved. Spot sizes in the prototype show that aberrations will be small. The mock-up of the LAC has shown that distortion will be < 1%.
- An efficiency of 3 lm/W is realizable
- The efficiency can be raised by
 - using a more efficient compact arc lamp,
 - increasing the size of the light valve, and
 - increasing the diameter of the projection lens, though to maintain contrast, one would have to increase the deflection angle of the DMD.
- Light uniformity is 5:1 and should be improved in Phase II.
- The magnification of the source by the *collection optics* is controlled by the ratio of two length scales: the object and image distances. For the parabola this is ratio of the condenser lens focal length/parabola focal length. For the ellipse, it is the ratio of the two focal distances. The size limitation of the collector is set by the size of the DMD and the lamp dimensions.
- A three-DMD color system will solve the problem of color field separation that has been observed in a color wheel system.
- A three-projector-lens color system is possible, but requires a fixed setup. This is acceptable for an enclosed rear projection system, but distortion effects in such a system are as yet unknown.
- A three DMD color system is possible using a color combining prism: a cubic structure with crossed dichroics. We have looked a several prism types, and the aforementioned is the only one that yields a short enough back focal length and uses relatively conventional dielectrics to form the interference stack.

2.4 Electronics

In Phase I, it was necessary to develop enough electronics to exercise and test the LAC devices. The objectives and features for these electronics are shown below:

Objectives

- Fully exercise the LAC device for optical testing
- Provide an impressive demonstration
- Offer simple operation

Features

- Simulate proposed address schemes
- Show high resolution gray scale
- Provide fixed pattern animation at 60 field/sec and 3 colors/field
- Offer interactive operation via computer interface
- Have graphical user interface to computer
- Provide computer assisted generation of animated sequences
- Have stand-alone operation mode

A single printed wiring board (PWB) was designed and fabricated to accomplish the above requirements. The block diagram for this electronics showing its interface with both the LAC and a PC was shown earlier in Figure 22.

2.5 LAC Device/System Performance

Figures 35 a-e are a series of photographs showing the various patterns from the LAC projected on to a screen. Although none of the chips were perfect, various patterns could be made to work on different chips. Using a rotating color wheel illumination system, the patterns were projected in color. There were both diagonal row segment defects and "sticking" pixels, but in general the chip was a big success with most of the mirrors functioning correctly.

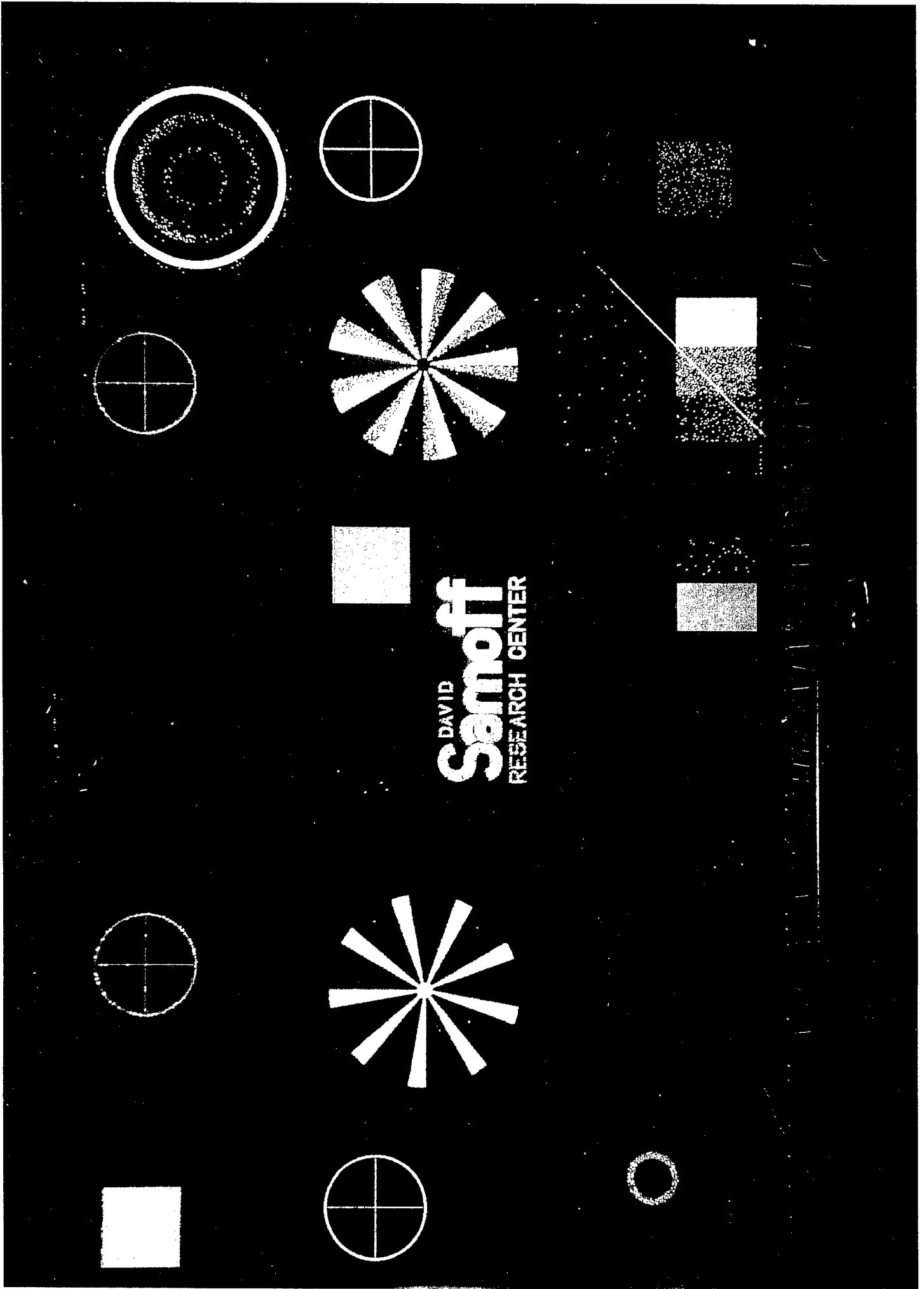


Figure 35a. Pictures from LAC projector.

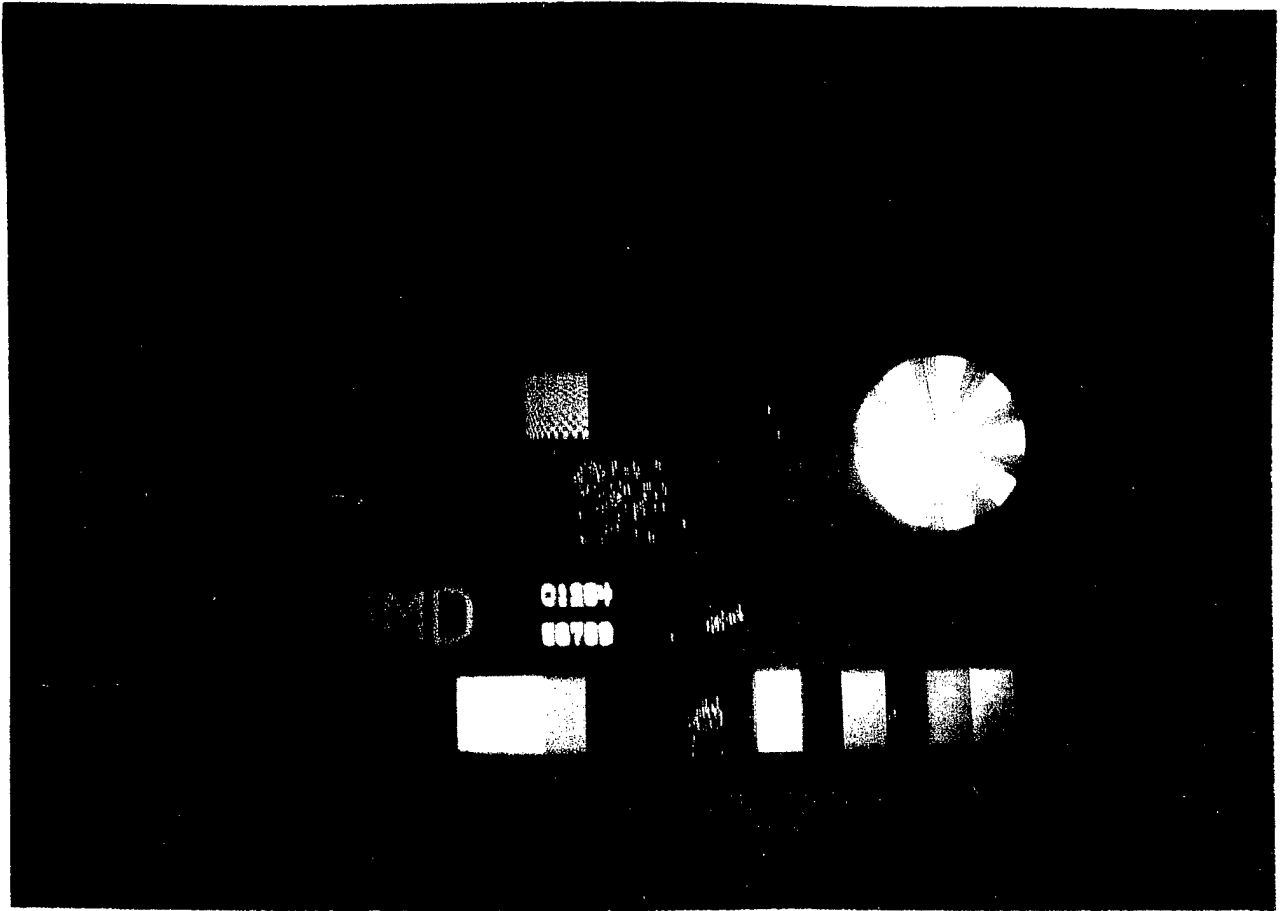


Figure 35b. Pictures form LAC Projector - Con't.

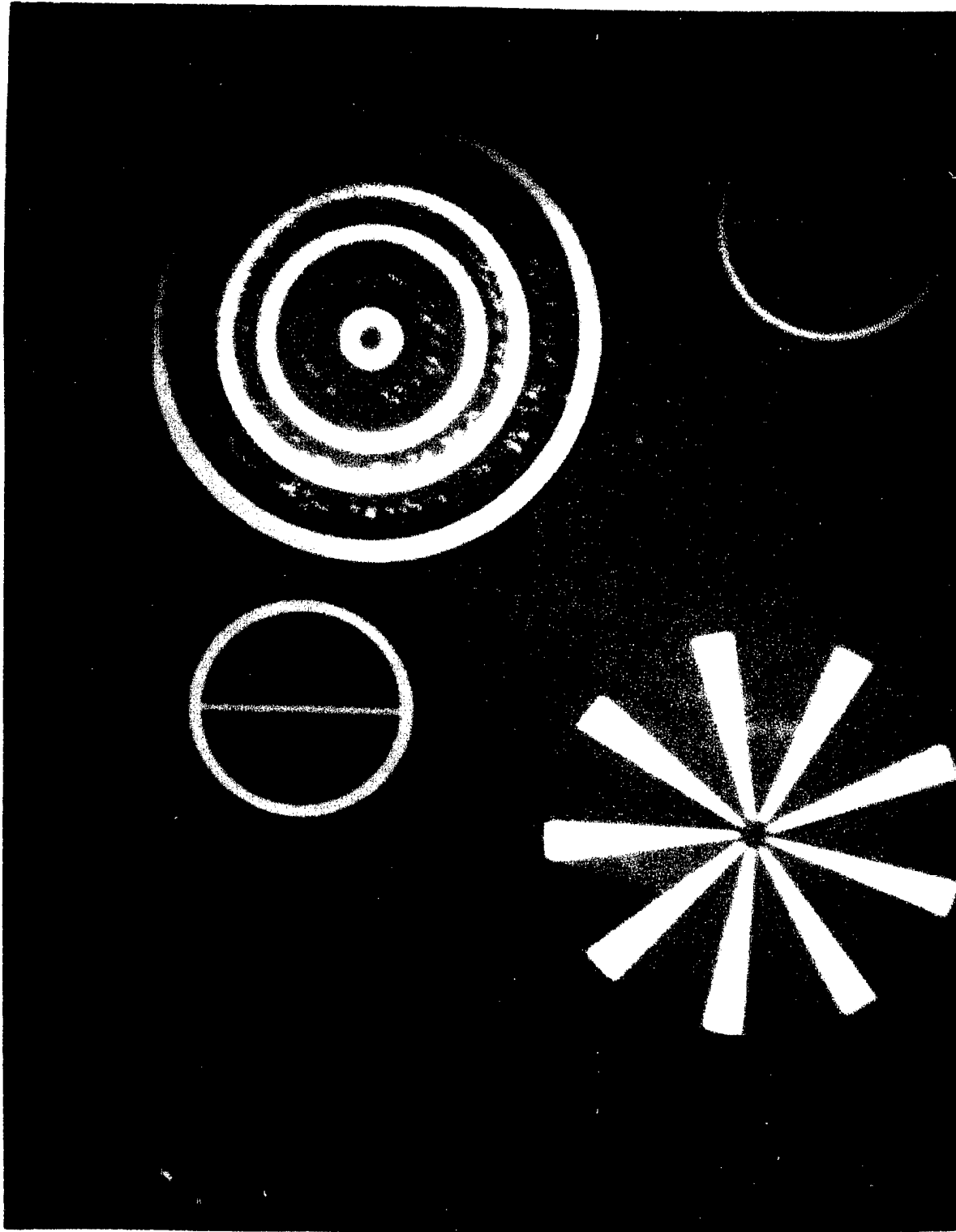


Figure 35c. Pictures form LAC Projector - Con't.

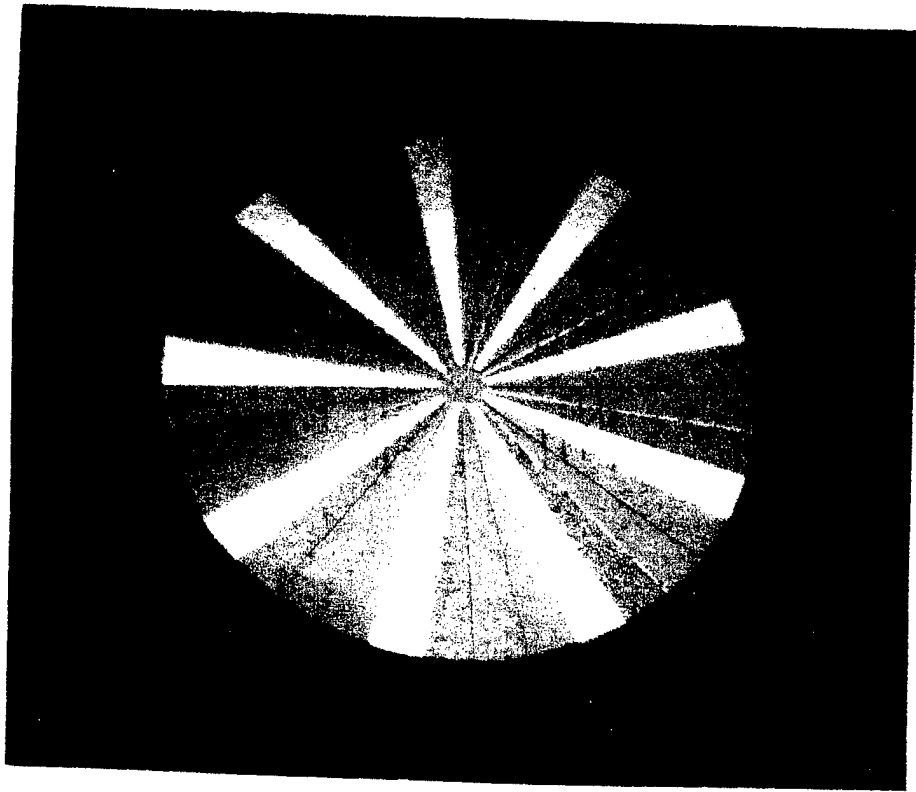


Figure 35d. Pictures form LAC Projector - Con't.

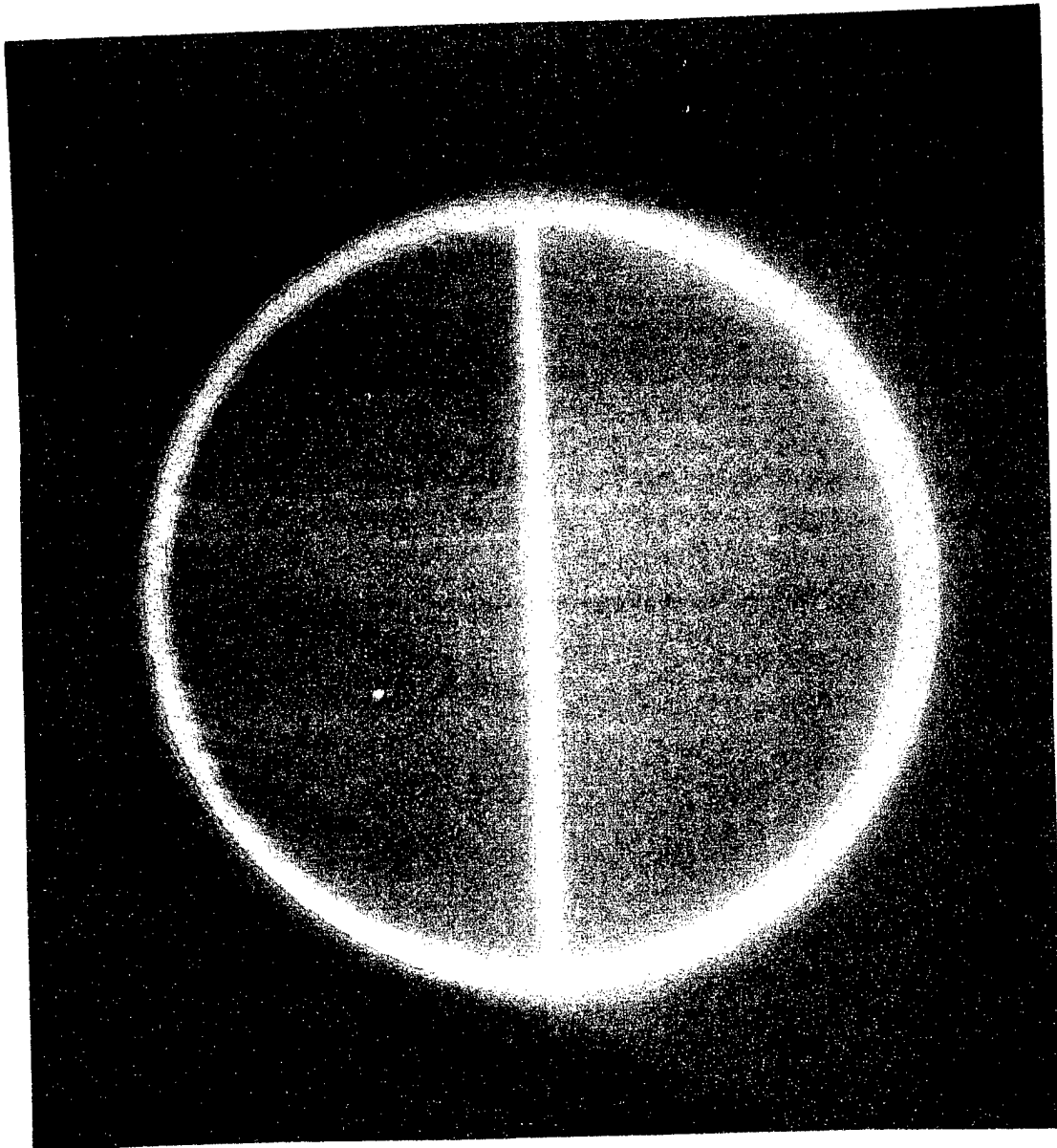


Figure 35e. Pictures form LAC Projector - Con't.

2.6 Phase I Issues/Problems

2.6.1 Photolithography

The biggest problem in Phase I involved photolithography for such a large area semiconductor device as the LAC. The only stepper which could handle the job of writing this 35 x 21mm chip was outdated and had only 1.2 um resolution. Reticle composition was used where the device was written in two halves and then aligned at a vertical center position during fabrication. It was found that a resolution of at least 0.8 um was needed to make this composition seamless. As a result, the performance of these early devices tended to be operator dependent.

TI management committed to purchasing the necessary tools to eliminate this problem in the final HD DMDs. It was also agreed that other more innovative approaches would be considered to handle reticle composition for the HD DMD chip.

2.6.2 Hinge Integrity

This was more a perceived problem than an actual problem. Everybody seemed to question how many cycles the aluminum hinges could take before fatigue caused a failure. At this point in time there was very little known about the materials properties of this single grain, thin film aluminum alloy. However, we knew that life testing of many hinges resulted in essentially no broken hinges. The hinges had been clocked through 100 billion cycles, the equivalent of about 2 years of continuous years operation of a TV, with no problems whatsoever.

With our goal being from 6 to 10 years operation for a TV set, depending on the application, TI was committed to continue a strong efforts in testing, modeling, and basic material science for this alloy and in particular these hinges.

2.6.3 Sticking Mirrors

Another problem which was observed when operating the LAC devices was that of "sticking" mirrors, refer back to Figures 43, a - e. These are pixels (mirrors) stick either +10 degrees "on" (white spots) or -10 degrees "off" (black spots). It was clear that white spots were more objectionable to the observer than were black spots, but neither were desirable. The effect of sticking mirrors seemed to be related to a number of things; i.e., bias voltages, clocking sequences, reset waveforms, packaging contaminants, etc. So as Phase I of the program ended, there were plenty of challenges in this area to be worked.

Fortunately, for this ARPA program, TI dedicated teams to work in several of these critical areas of DMD technology so that throughout the program the program has benefited from the solutions of these problems without having to support them financially.

2.7 Recommendation for HD DMD

Based on Phase I results obtained from testing the DRAM and SRAM 768x576 CMOS memory structures and the 1920x1080 LAC superstructure (mirrors structure), it was decided to go forward with the layout and fabrication of a HD DMD. This device was to consist of a SRAM memory with a minimum of 1920x1080 pixels with the mirror superstructure fabricated over the memory structure. Based on the capability of the new photolithographic tools and techniques, the device would be expanded to 2048x1152 pixels, if possible.

3. PHASE II - NTSC/VGA DMD PROJECTOR FABRICATION

At the time of the proposal, the intent of Phase II was to expand the CMOS array to a full HD 1920 x 1080 and build a mirror superstructure over it. In addition, we would begin working on the final electronics and HD optics/illumination systems designs. However, once we got to this point in the program and had both the 768 x 576 CMOS and mirror structures working, it seemed logical to build an interim PAL format 768 x 576 DMD to further verify that this technology is viable for projection display applications. This approach would also provide us with standard resolution NTSC/VGA/PAL projection capability many months before the final HD projector would be finished. The Government agreed with this interim approach of building a PAL DMD and TI agreed to fund the development of an NTSC/VGA projector around this chip.

3.1 768x576 NTSC/VGA DMD

The following discussions describes the 768x576 DMD chips used in the 640x480 NTSC/VGA projector.

3.1.1 DMD Underlying CMOS Structure

As discussed earlier in section 2.1, both DRAM and SRAM CMOS structures were designed and laid out because of the possibility for marginal operation with the DRAM structure in the presence of very bright illumination conditions.

3.1.1.1 DMD 2T DRAM Memory Structure

The very first area array DMD was fabricated over the 2T DRAM memory structure. The DMD worked, but as the modeling data had predicted, operation was limited to about 9 ft-L of incident light on the device. At higher illumination levels, some of the first data read into the memory during a field would become invalid and render the projected picture unusable. At this point we immediately switched to our backup plan which used the SRAM memory structure.

There will be further discussions in the recommendation section near the end of this report as to what might be done to make the DRAM a viable candidate for the DMD underlying memory structure in the future.

3.1.1.2 DMD 6T SRAM Memory Structure

Next, area array DMDs were fabricated with the mirrors built over the SRAM memory structure. Since the cell consisted basically of a 'flip-flop' and didn't involve the discharge of a capacitor, the light limitation was solved with this approach. In the initial test we were able to illuminate the devices to the 125 ft-L level with no degradation of the picture, but this level was limited only by the amount of available light at the time. So, this 768 x 576 (PAL format) DMD was used to build the world's first NTSC/VGA 640 X 480 DMD projector. Note that with a DMD, pixels which are unused can be addressed off and in this case become a black border around the picture.

3.1.2 DMD Mirror Superstructure

The semiconductor process used in fabricating the DMD mirror superstructure was illustrated in figures 4 and discussed in section 1.5.1. A photo of the conventional PAL DMD mirror structure, known as the "B2" mirror, was shown in Figure 3.

Figure 36 shows a six inch wafer of PAL format DMDs.

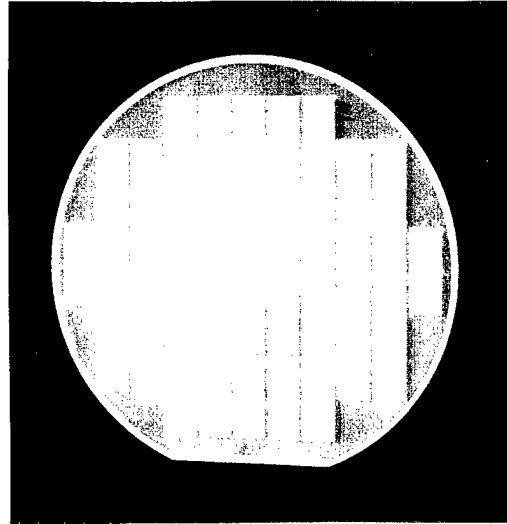


Figure 36. 768x576 DMD Wafer.

3.1.2.1 DMD Mirror Response Time

The response time for a typical mirror is shown in Figure 37 to be < 20 microseconds.

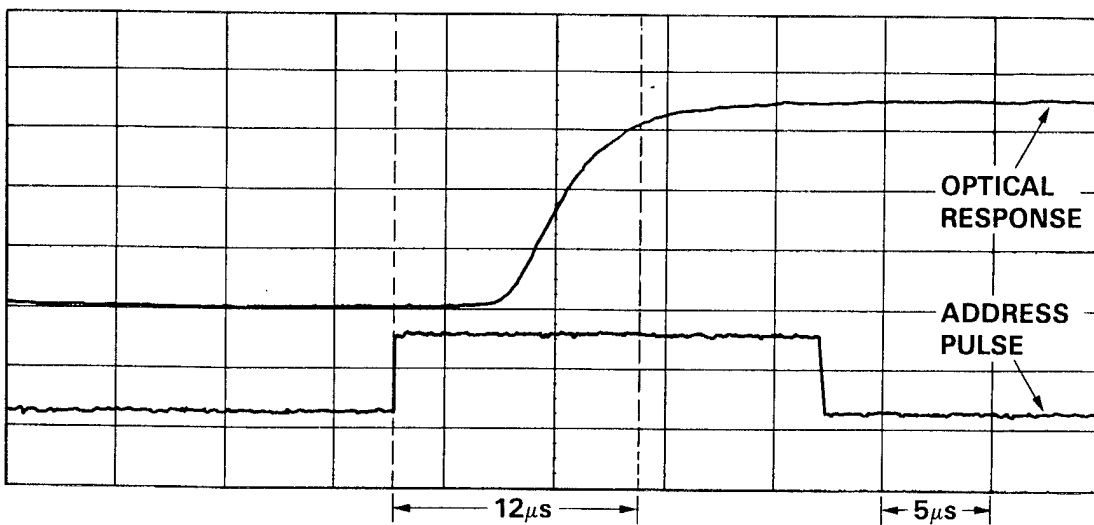


Figure 37. Typical DMD Mirror Response Time.

3.1.2.2 768x576 DMD Simulated Defect Rate

The simulated defect rate for the 768x576 DMD is shown in Figure 38. Here, the reference picture (zero defects) is shown along with simulated results for 10%, 1%, and 0.1% defects. This illustrates that some level of defects may be acceptable for selected applications, although the goal is to product zero defect devices.

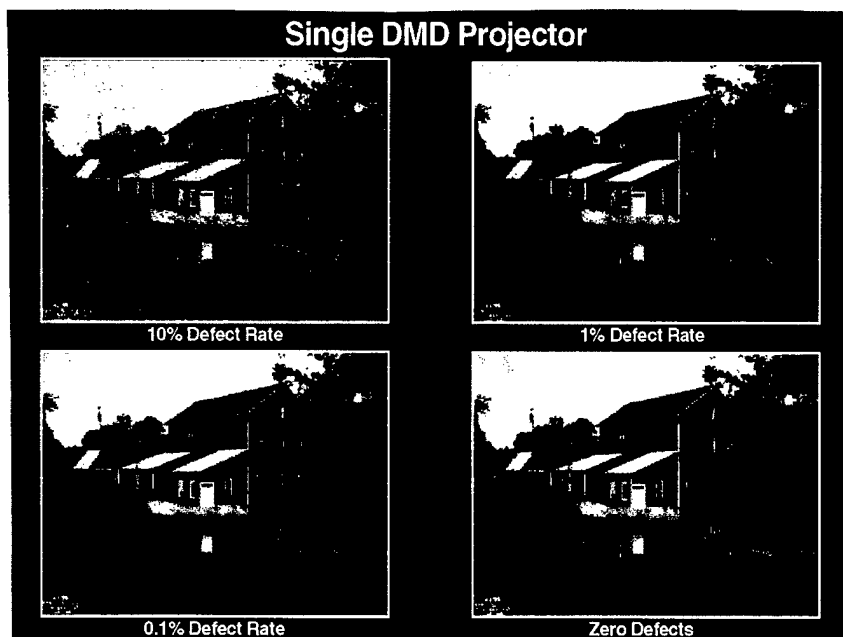


Figure 38. DMD Defect Rate Simulation.

3.2 NTSC/VGA Projector

TI funded an effort to build a 4:3 aspect ratio, NTSC/VGA (640X480 pixel) front projector using a single 768x576 DMD. One of the advantages of the DMD is that unused portions of the device can be addressed off (black) as illustrated in Figure 39. The DMD system operated in the color field sequential mode with a rotating color wheel and dark field optics. The subassemblies making up this projector and it's performance are discussed below.

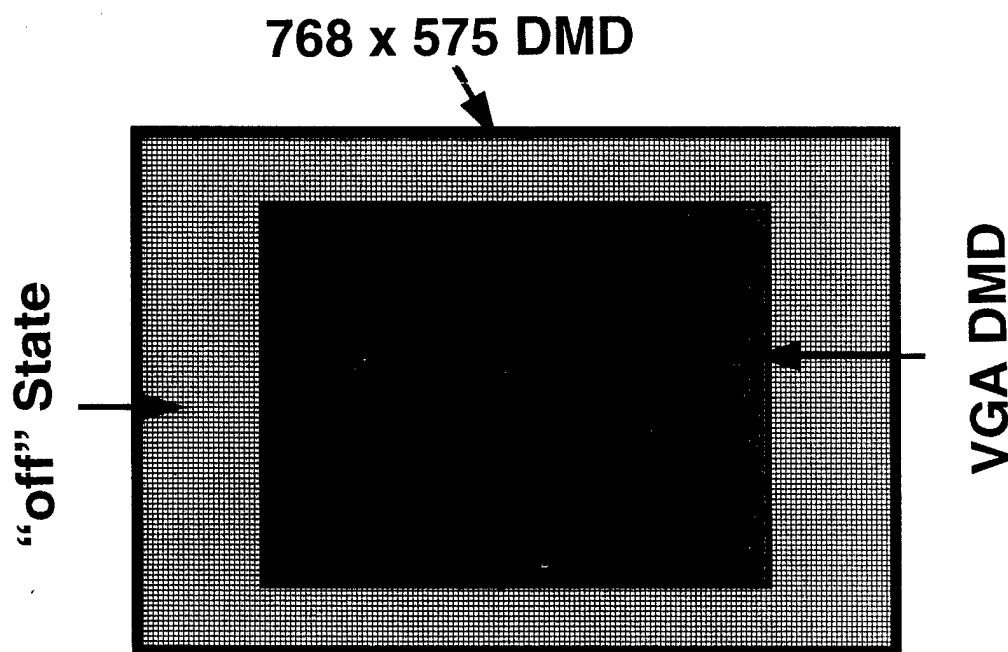


Figure 39. Illustration of 640x480 (NTSC/VGA) using the 768x576 DMD.

3.2.1 640x480 Projector Optics and Illumination System

Figure 9, discussed earlier, shows a block diagram for the dark field optics used in the NTSC/VGA front projector. The initial system used a 1000 watt xeon arc lamp as a primary source of "white light." The beam of light was processed for illuminating the DMD by means of a beam integrator, condensing optics, and a rotating color wheel. A total internal reflective (TIR) prism was used to get the light on-to and off-of the DMD light processor. Finally, a zoom projection lens was used to magnify the image to full screen size.

3.2.2 Color Wheel

The color wheel used in this first projector consisted of a three segment wheel with 120-degree red, green, and blue filters, as shown in Figure 40. Today more sophisticated color wheel arrangements are employed. The wheel rotates at 3600 RPM to provide 180 Hz (color fields per second) operation. The color wheel is synchronized to the system's VSYNC signal generated from the video source and sequences from red to green to blue and in such a way that the transition from blue to red occurs on the rising edge of VSYNC. The display is blanked during the color transitions for short period to prevent any possible display of two colors simultaneously.

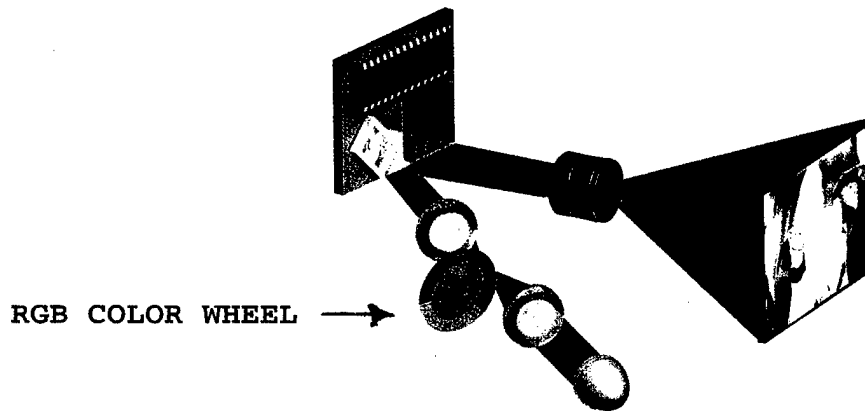


Figure 40. Early Three Segment Color Wheel.

3.3 NTSC/VGA Projector Electronics

The NTSC/VGA projector's electronics assembly consists of a group of boards that implements all of the data processing and storage required for displaying video data with the DMD. The system is composed of 5 boards with the following functions:

- 3 boards A/D converter boards; one each for red, green, and blue video inputs.
- 1 board System controller/reformatter breadboard containing all of the clock generation, gamma correction, data reformatting, and system control circuitry.
- 1 board DMD/VRAM module containing the DMD, data memory, and associated data, address, and control buffers.

3.3.1 Grayscale Using Pulse Width Modulation (PWM)

Grayscale in this digital system is accomplished with a technique known as pulse width modulation. The projector offers 8-bits grayscale or 256 shades per color. This corresponds to 16.7 million color combinations. The basic timing for PWB is shown in Figure 41 (example shown for 7-bit system for simplicity). In principle, the picture's most significant bit plane is loaded into the DMD's memory and the mirrors are set accordingly and left in this state for 1/2 the frame time. Then the 2nd most significant bit is loaded and the mirrors are set and left for 1/4 the frame time. This process continues until the least significant bit is loaded and the mirrors are set for 1/128 the frame time (for this example, actually 1/256 frame time in projector). In practice, a much more complicated sequence is used with some of the lower order bit data being inserted into the longer periods of the higher order bits. However, the overall integrated effect of this optimized bit ordering will always be equivalent to the generalized case shown in the figure.

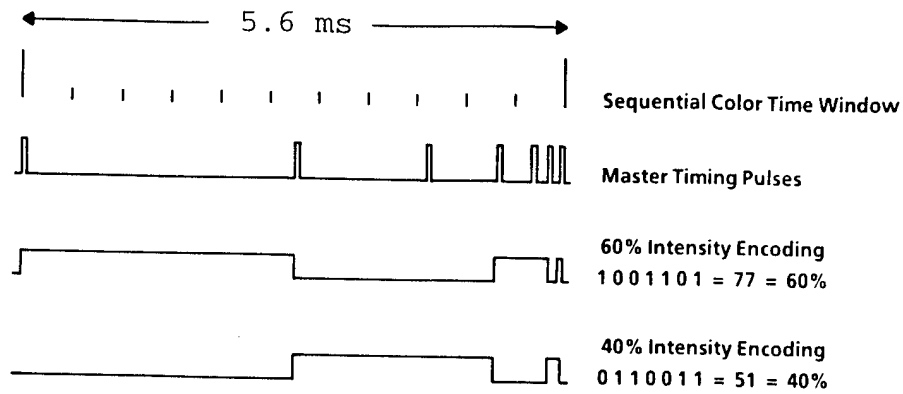


Figure 41. Pulse Width Modulation Timing Shown for 7-bits.

The effect of PWM operation was discussed earlier in Figure 7 and shown by the level of brightness of the dots. The mirrors are shown in the "on" (bright) state for various propositions of the frame time.

3.4 Projector Mechanical System

Figure 42 shows a concept sketch for the first NTSC/VGA single DMD projector. This package contains all the optical components mentioned above, the lamp, and the DMD drive electronics board. The remaining electronics boards, lamp power supply and video source equipment is contained in a separate relay type equipment rack.

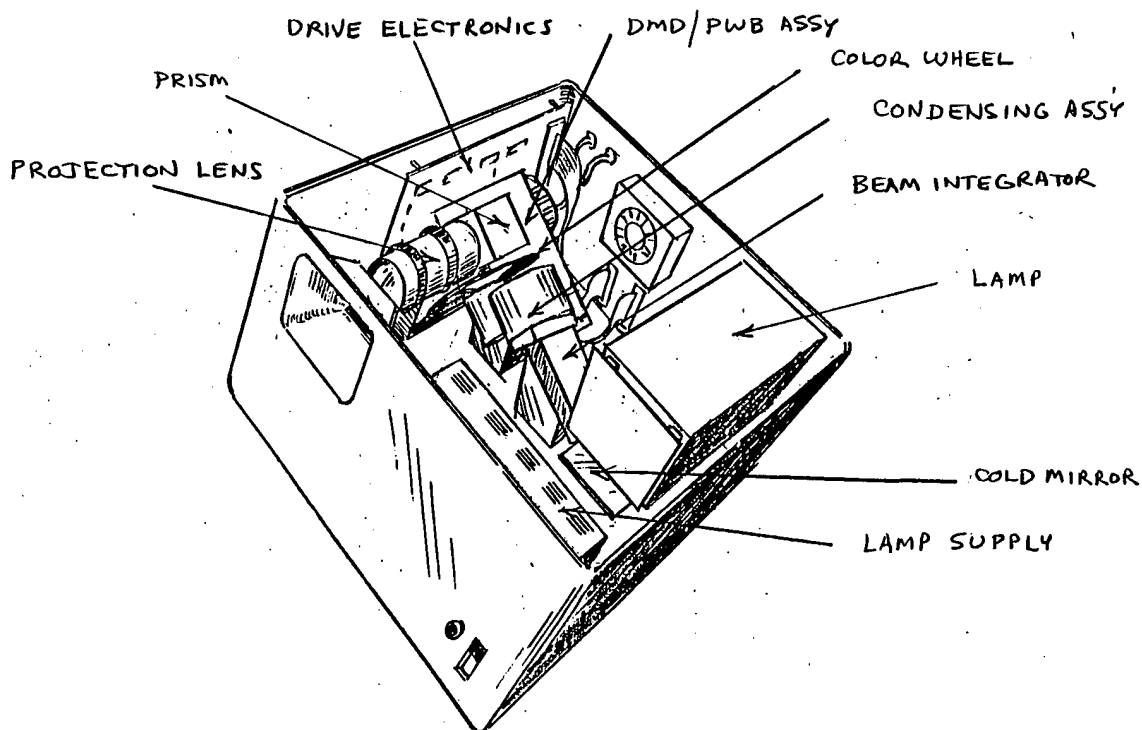


Figure 42. NTSC/VGA Projector Concept Sketch.

3.4.1 System Block Diagram

Figure 43 shows a block diagram for the single-DMD NTSC/VGA projector system.

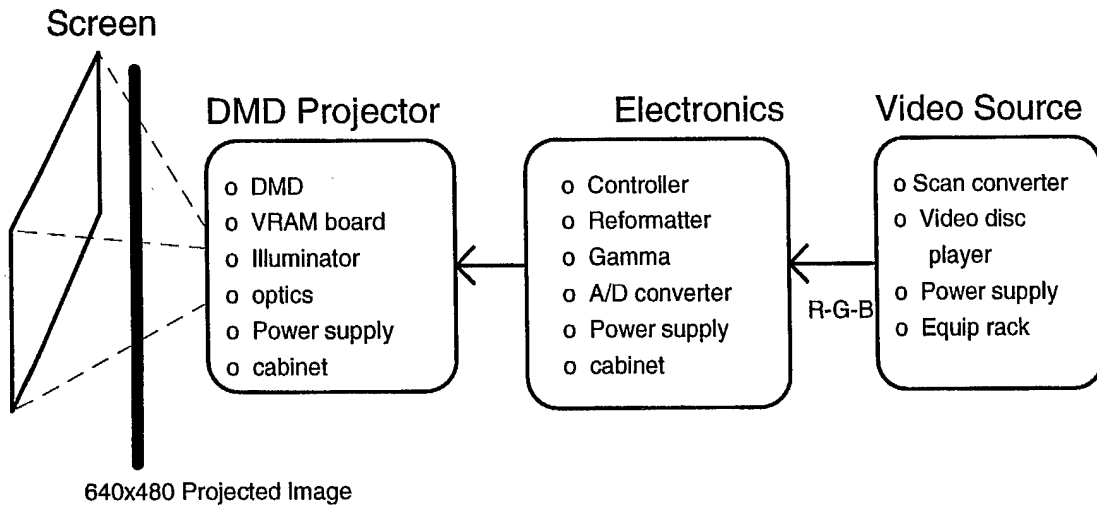
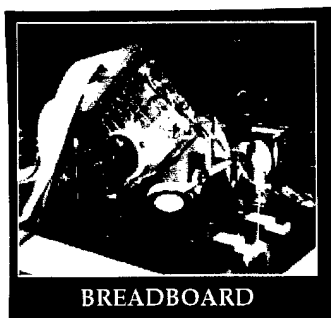
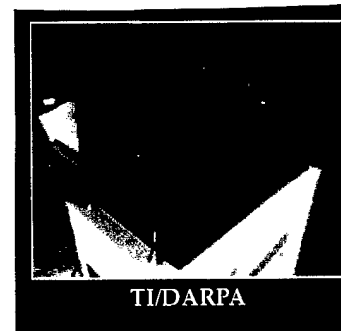


Figure 43. Block Diagram for Single-DMD Projector System.

Actual pictures of the projector with the cover off and on are shown in Figures 44a and 44b, respectively.



(a) Cover Removed



(b) Completed Projector

Figure 44. NTSC/VGA DMD Projector.

3.5 Projector Performance/Results

The first picture shown with the projector was of a “red millhouse” and although there were 1000s of pixel defects and some line defects, the results were exciting. A copy of this first picture is shown in Figure 45.

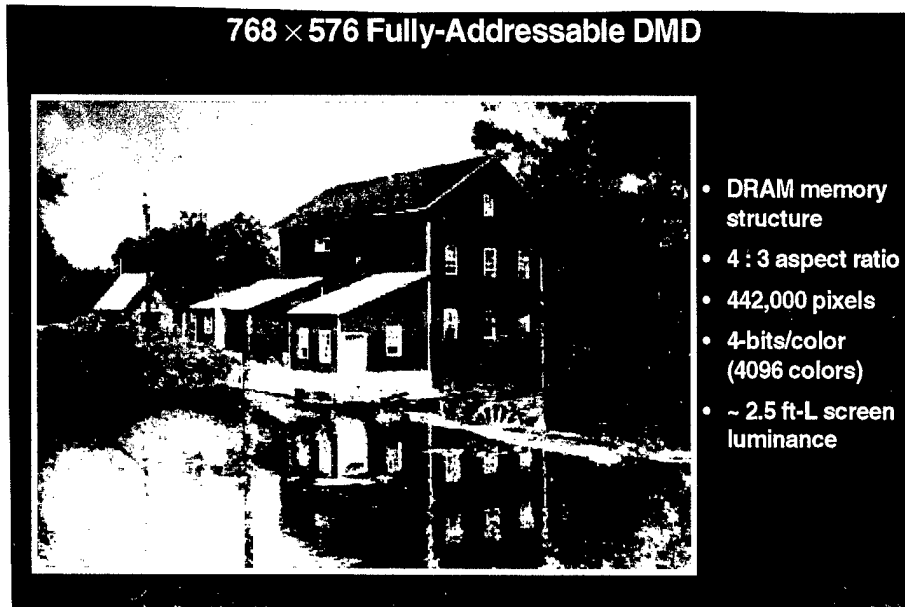


Figure 45. First Picture from 640x480 DMD Projector.

3.5.1 Performance of DMD 640X480 NTSC/VGA Projector

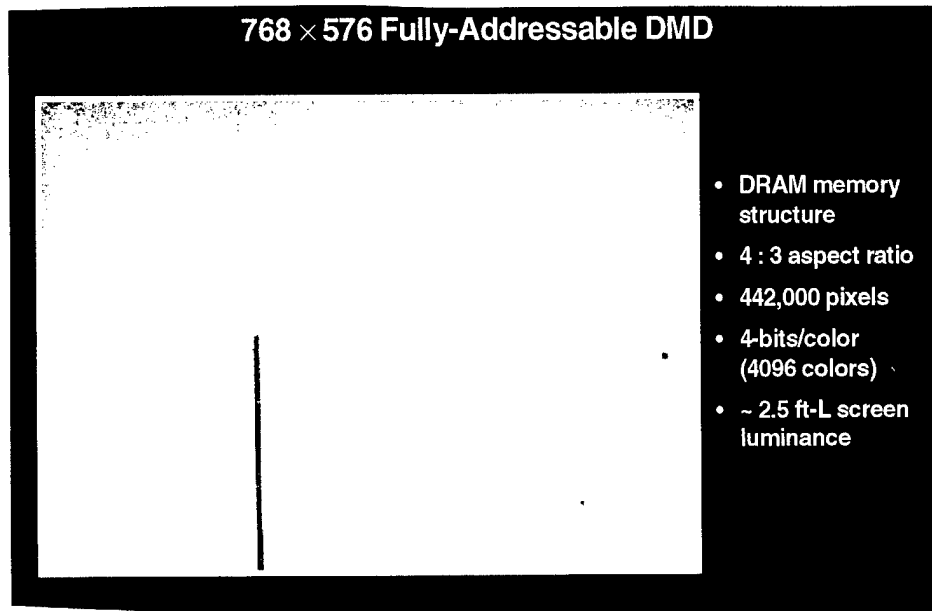
The performance characteristics for the first NTSC/VGA projector are shown below:

Performance Characteristics for NTSC/VGA DMD Projector

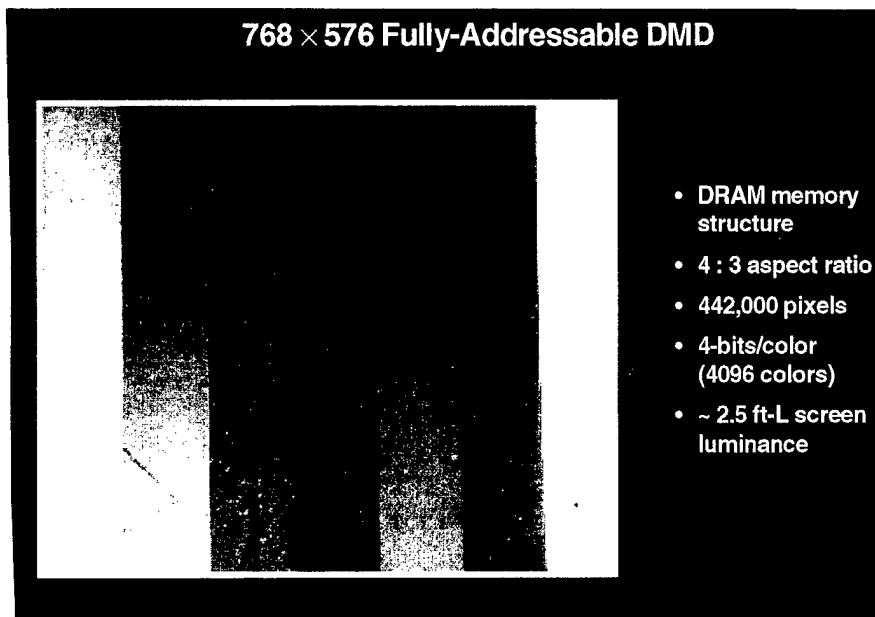
| | |
|---------------------------|---|
| • Number of DMD Pixels | 768 x 576 |
| • Number of Active Pixels | 640 x 480 x (1 DMD) |
| • Mirror Size | 16 microns, square |
| • Pixel Spacing (pitch) | 17 microns |
| • Contrast Ratio | 55:1 |
| • Screen Size | >52 inches |
| • Aspect Ratio | 4:3 |
| • Screen Brightness | 120 ft-L @ 21-inch diagonal 22 ft-L @ 52-inch diagonal |
| • Light Source | 1000 Watt xenon |
| • Number of Gray Levels | 256 per color |
| • Pixel Convergence | Self Aligned |

3.5.2 Other Projected Results

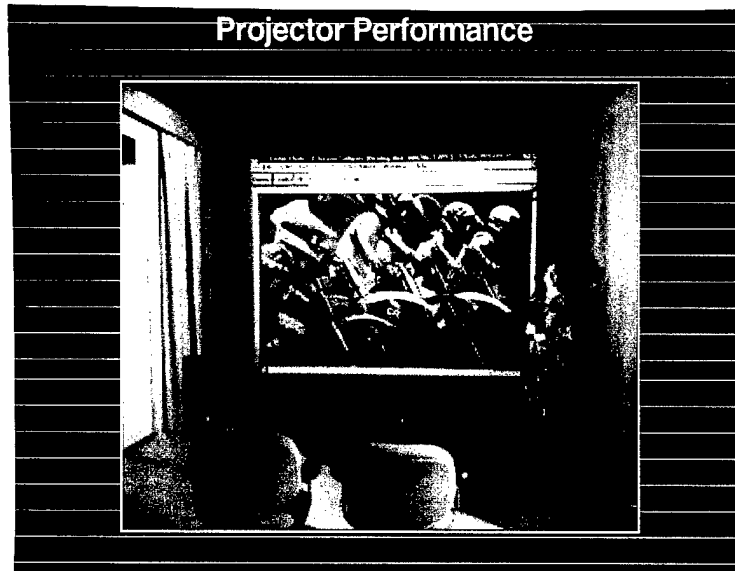
Additional pictures taken from the screen illustrating the performance of the NTSC/VGA projector are shown in Figure 46 a - c, two show the early devices with defect and one (c) with near perfect DMD.



(a) Defects on White Background Shown in First DMDs.



(b) Color Bars Taken From Projector With First DMDs.



(c) Later VGA picture with near perfect DMD, shown on 15-foot diagonal screen.

Figure 46. Pictures Taken from DMD NTSC/VGA Projector.

3.6 Lamp Failure

The DMD NTSC/VGA projector was delivered to Wright Laboratory in Dayton, Ohio in April, 1994. Sometime later during normal operation of the projector at WL the xenon lamp exploded. TI performed a failure analysis and traced the problem to the metal-to-ceramic seal in the lamp. Analysis of other similar lamp revealed a problem with this interface. TI worked with the lamp vendor to resolve the problem. Appendix G provides failure analysis data and corrective action.

The projector was repaired by installing a new improved lamp and installing additional protective (safety) shielding in the projector such that the lamp is fully contained. Safety procedures for handling of this class of lamps was also instituted at this time and are included in Appendix G.

The goal for future projection display products will be to use lower wattage, lower pressure lamps. But regardless of the lamp type, it is recommended that safety procedures be followed when handling, removing or installing, the lamps.

4. PHASE III - FULL HDD DMD PROJECTOR

The ARPA HD Display represents the first all digital HDTV projection system from source through display. The system is built around the electrical input, optical output digital micromirror device (DMD). This high definition DMD consists of a 2048 x 1152 array of aluminum micromechanical mirrors arranged in a square grid and mechanically attached to the underlying silicon. Each mirror can be individually deflected according to the contents of the DMD's memory and address circuitry to reflect (or not reflect) light into the system's optical path.

The design goal of the ARPA HD System was to operate with US HDTV standard(s) as the input source and still be able to operate in a "US HDTV" mode when that hardware is not readily available. This goal was accomplished by designing the input of the ARPA HD System to be compatible with a digital version of the SMPTE 240 standard interface which became known as the SMPTE 260 standard interface. This approach has several advantages. First, since US HDTV standards vary and are based on rectangular pixels, HDTV specific hardware should be functionally separate from the ARPA HD System. Second, a commercially available SMPTE 260 digital recorder can be used when a US HDTV source is not available. Third, analog HD sources (i.e. HRV Workstation) can be fed into the HD recorder and output to the ARPA HD System as SMPTE 260.

A diagram showing the relationship of the sources to the ARPA HD System is illustrated in the Figure 47.

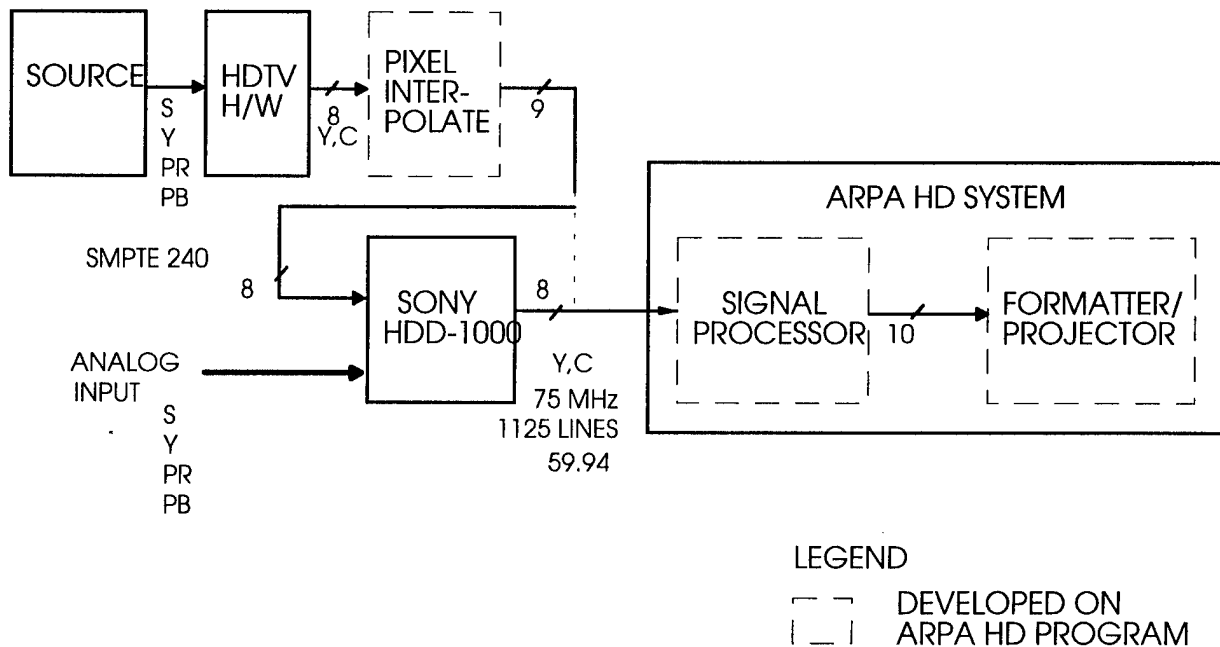


Figure 47. ARPA HD System/Source Block Diagram.

The hardware developed on the ARPA HD Program is shown in dashed boxes in Figure 47. The pixel interpolate hardware takes 8-bit interlaced digital data (1248 x 960 rectangular pixels), transfers the data to 1716 x 960 for square pixels, and formats the data inside the 1920 x 1035 SMPTE 260 format. This hardware also creates the necessary timing and sync signals for the standard. The signal processor receives the standard interface data as Y, PR, PB data and converts the data to an RGB format. The interlaced data is then divided into 4 channels of red, green, and blue and output to the Formatter/Projector as Real Data. The Signal Processor has also been designed to allow a progressive scan upgrade to provide non-interlaced data to the Formatter/Projector. The computed lines are output to the Formatter/Projector as Derived Data. The Formatter/Projector receives the data from the Signal Processor, seams the 4 channels of data, formats the data into bit planes, and sends the data to the DMD. The Formatter/Projector also houses the optical system. The light is sourced from a lamp contained in the Projector, split into red, blue, and green components, reflected off of the respective DMD, recombined in the prism, and output through a projection lens onto a viewing screen.

The ARPA HD System and support hardware is packaged as shown in Figure 48. The Pixel Interpolate and Signal Processor Functions are physically housed in one 9U x 340 subrack. The Formatter Function is housed in a separate subrack. These subracks are housed with the electronics power supplies, fans, and an audio delay unit in a single electronics rack. The Projector sits on top of the electronics rack and contains the Projector Electronics, the optical system including the lamp, and the lamp power supply. The HD Recorder is housed in a separate rack.

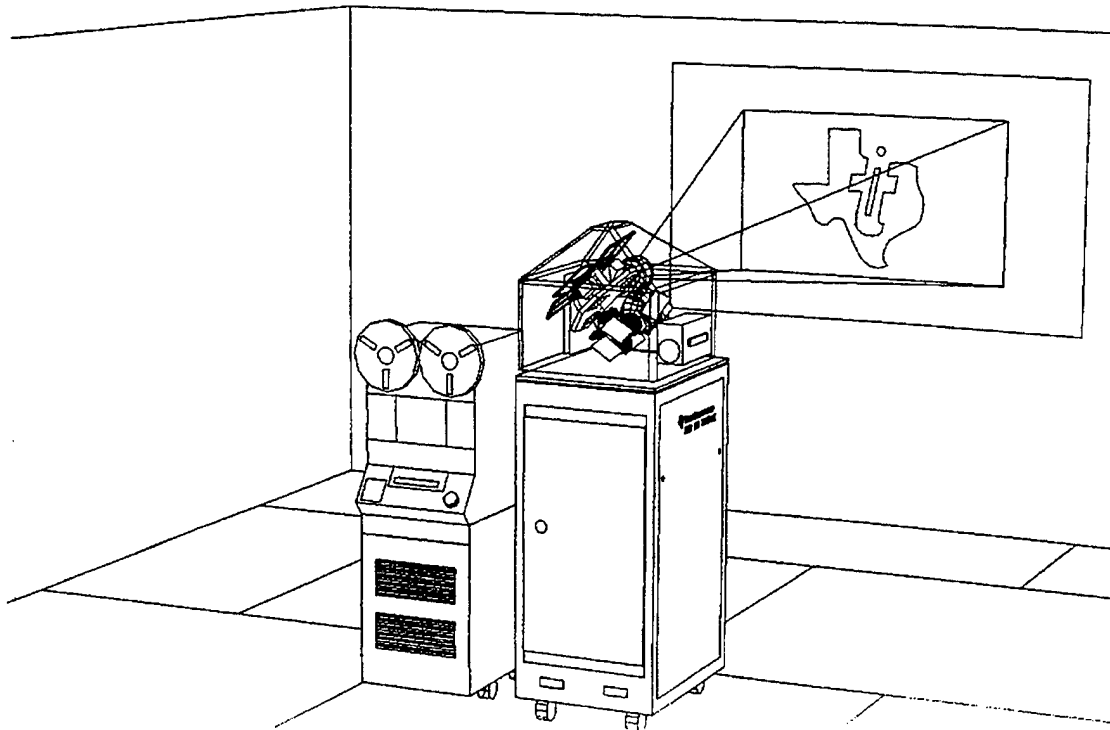


Figure 48. ARPA HD System.

4.1 2048x1152 HD DMD

The HD DMD uses the same 16 micron pixel cell as the conventional B2 PAL/NTSC DMD chip but has a larger array of 2048 pixels per row and 1152 rows. If the PAL and HD images were to be viewed on comparable size screens, there would be five (5) HD pixels for each of the pixels on the NTSC chip. Figure 49 illustrates this by showing the impact of simulated pixel defects between the two.

**Defect Simulation
For 3-DMD Projector with Random Defect Color**



NTSC Resolution
Defect density = 1 per 16 pixels
View from distance of approximately 6 feet

HDTV/ATV (1280x1024) Resolution

Figure 49. Comparison of NTSC and HDTV Resolution.

4.1.1 HD DMD Layout

The architecture for the 2048 x 1152 HD DMD is shown in Figure 50. As for the case of the PAL chip each input will handle 16 columns of data, so there are 128 input pads for both the upper and lower portions of the DMD device. Also, along the left side of the chip are two 10-bit row decoders, one for the top half and one for the bottom half of the chip. The HD DMD chip is 37 x 22 mm which presented somewhat of a challenge for the photolithography requirements.

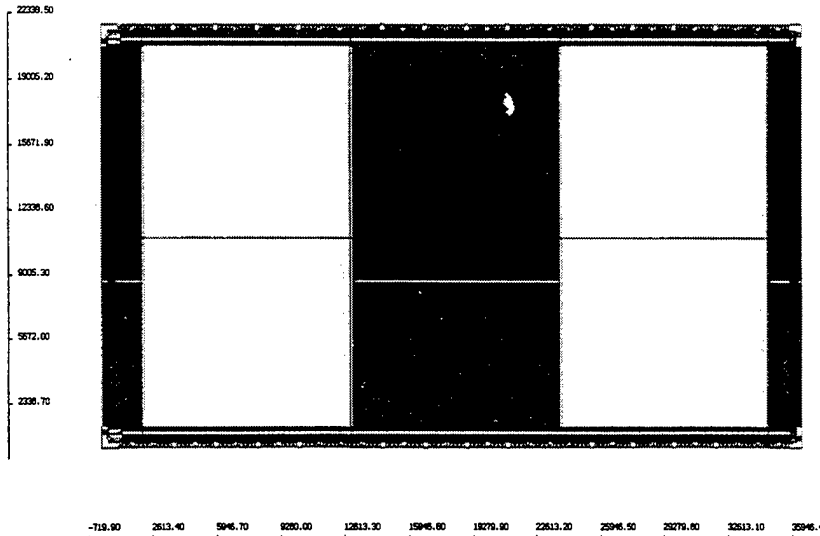


Figure 50. Chip Architecture for the 2048 x 1152 HD DMD.

4.1.2 HD DMD Photolithography

In 1992 there were only a few available steppers that could write patterns using standard 5x photomasks over such a large field of view and with the high resolution required for this HD DMD chip. Therefore, the HD chip uses reticle composition in which the patterns are written in sections and spliced together to provide a virtually “seamless” large-area DMD chip.

The technique used to write the patterns is called “cut-and-repeat” and consists of reticles, illustrated in Figure 51, with a left end (L), center (C), and right end (R) portions of the circuitry.

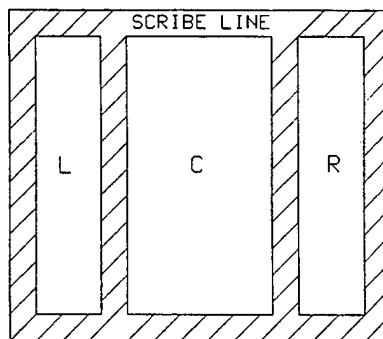


Figure 51. HD 2048 X 1152 DMD Reticle.

The sequence for writing the patterns on a wafer are shown in Figure 52. As shown, first the left end cap is written, then the center section is written five (5) times, and finally the right end cap is written. As shown in the figure, each reticle section (example L) is repeated at each of the eleven (11) chip locations on a 6-inch wafer and then the next section (example C) is written, and so on.

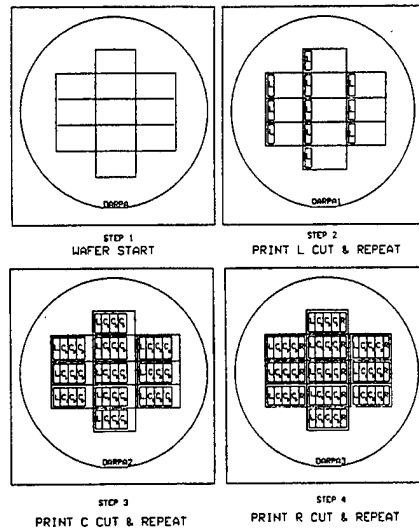


Figure 52. Cut-and-Repeat Reticle Composition Technique used for 2048 x 1152 DMD.

4.1.3 HD DMD Package

A custom ceramic package was developed for the 2048 x 1152 DMD. The contacts are in the form of a pin-grid on the back side of the package. Contacts between these pins and the corresponding pads on the printed circuit board is made with an elastomer (pressure sensitive) connection as illustrated in Figure 53. A mechanical clamping mechanism is used to apply the necessary amount of pressure to assure good electrical contact at the package pins.

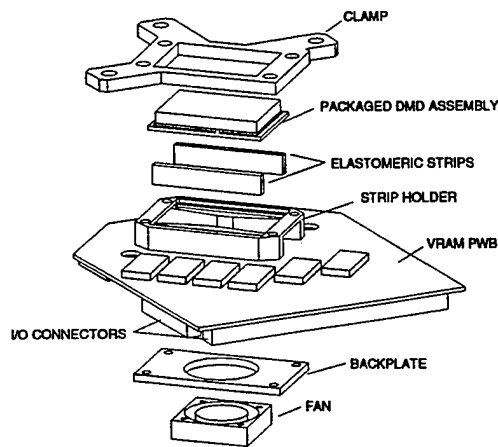


Figure 53. DMD Ceramic Package.

4.1.4 DMD Testing

The high volume electro-optical test of B2 DMD PAL devices poses a major challenge, especially when the issues and the requirements are changing as the DMD technology progresses. The purpose of this section is to provide a succinct account of the current state (Nov. 1992) of the Electro-optic test as being conducted in the probe area; and use it as the platform for identifying where and how test throughput and test accuracy can be enhanced. A practical approach will consist of phased implementations whose scope at each phase will be closely coupled with the test environment and requirements associated with the applicable state of art in DMD technology.

All test data shown below were taken several years ago on the very first HD DMDs built on the DARPA program. It should be pointed out that problems illustrated in this data have long since been worked out for the DMDs used in current display products.

4.1.4.1 Electrical Testing

4.1.4.2 Current State of the Electro-optical Test

The purpose of the testing is to give electro-optic characterization results to the physicists and process engineers; and to function as a filter to pick out "high quality" devices for packaging. The screening criteria sits on an upward sliding scale, in which each improvement sets the bottom limit for the subsequent lots. Every functional DMD device is thoroughly tweaked and fine-tuned at probe to enhance the chance for packaging. All functional devices are tested in detail regardless of row, column, and/or slant defects in order to obtain superstructure statistics.

4.1.4.3 Current Test Procedure

DMD testing consists of the following phases:

- a.) Physical handling of the device, alignment, and landing the probe card.
- b.) Stimulating the device under test (DUT) with data patterns and reset/bias signals. fine tune device by adjusting reset/bias levels and sometimes frequency to optimize functionality. The process is done manually through eye-hand coordination.
- c.) Observe/record artifacts and gross/static defects such as column/row failures, slant lines, and damaged areas.
- d.) Mentally divide the device into 9 segments. Assess fine defects per 1000 mirrors which are representative in each of the nine areas.
- e.) Erase pattern to minimize undesirable metal-memory effect.
- f.) Post test handling.

4.1.4.4 Artifacts and Defects

Common imperfections can be categorized as follows:

- a.) Artifacts such as mottling (reflection non-uniformity), line pairing, streaks across the superstructure.
- b.) Static defects such as column and row failures; and slow/twinkling pixels.

- c.) Operational damage where mirrors were blown away; small damaged areas are normally due to electrical short. Large damaged areas caused by either reset of the combination of reset and bias signal. depending on suuperstructure integrity, the catastrophic failures may occur at reasonably low levels with no forewarning, or as a result of intentional over-stressing in an attempt to enhance performance. Slant line failures may be due to mirrors being blown away, collapsed towards on direction or unidirectional.
- d.) Randomly scattered errors can be categorized in Table 13:

Table 13. Categorized Mirror Defects

| Type of failure modes | Expected mirror state as driven by electrical signal | | |
|---|--|----------|----------|
| | +1 state | 0 state | -1 state |
| non-working pixel (CMOS cell or superstructure failure) | 0 | 0 | 0 |
| uni-directional pixel | +1 or 0 | 0 or 0 | 0 or -1 |
| collapsed pixel (address margin or physical failure) | +1 or -1 | +1 or -1 | +1 or -1 |

4.1.4.5 Device Tracking, Documentation, and Test Results

While operating in chip mode, extra precautions are needed to track the device, since there are no identification on individual chips. Contents for each box of devices and their locations are clearly marked on the box covers. However, there is the danger of mismatching the top and bottom half of each box when several boxes are opened at the same time. By placing miniature labels into the bottom half of the box this potential cause for confusion is eliminated. The documentation associated with device testing is as follows:

- a.) Input log-in and label bottom half of device-carrier-box.
- b.) fill in data sheet for each device. Selective video recording of representative and special devices.
- c.) Single line entry into the Chronological test log
- d.) Key-results filled in on four different Summary-wafer maps immediately after completing a device. These plots provide information for making decisions. Test result summary are keyed into a data base on the network, made available to the project.

4.1.4.6 Areas for Test Automation and Improvements

This section reviews the major test steps in section 4.1.4.3 for automation and improvements.

4.1.4.6.1 Device Handling

Adding more device receptacles onto the chucktop will enhance loading efficiency and purchasing an "individual-die-auto-alignment" program will reduce alignment time and required operator dexterity. However, the ultimate solution for streamlining device handling lies in wafer mode operation.

4.1.4.6.2 Optimizing Device Functionality

DMD devices in their current state require intensive human intelligence to bring forth optimum functionality. It is a delicate decision in determining how far to push the Vbias and Vreset to enhance device functionality without damaging the device. As the device technology advances, a point will be reached where a standard set of procedures can be universally applied to all devices, and the variations in signal levels will fall within a narrow window.

4.1.4.6.3 Artifacts/Static Defects/Gross Defects

The human vision system is remarkably effective in recognizing complicated visual patterns such as mottling, pairing, and streaks, etc.. It readily recognizes column and row failures. It does not get confused by twinkling and slow pixels. This is an area where a human in the loop will actually enhance throughput. However, to improve documentation and communicating device problem, a camera at the microscope should be incorporated to take color pictures for the area of interest.

4.1.5 Conventional B2 HD DMD Characterization Summary

Table 14 shows the results of the characterization study done to determine the limiting factors for the contrast ratio of the B2 HD DMD Display. In general, the HD devices tested had an average tilt angle of 8.4 degrees, an active area of 69%, and good die registration in the package. Pulse width modulation efficiency was calculated at 84%. The overall efficiency was modeled using measured and theoretical parameters and found to be about 46%. The measured number on the benchtop reflectivity setup was somewhat higher, but within the measurement of error. The measurements are detailed below:

Table 14.

Characterization Study to Determine the Limiting Factors for the Contrast Ratio of the B2 HD DMD Display

| SUMMARY CHART | | | | | |
|----------------|------------|-----------|--------------------------------|-------------------|----------------|
| DEVICE # | TILT ANGLE | OP COND* | REFLECTIVITY ** f2.8 / f4.5 | PIXEL ACTIVE AREA | PWM EFFICIENCY |
| 2571130-3 | 7.7 | 5.5,10,20 | 49.0%, 44.2% | | |
| 2671005-23-8 | 8.3 | 5.5,10,20 | 50.2%, 45.7% | | |
| 2800001-17-02 | 8.26 | 5.5,10,20 | | | |
| 2800000-12-3 | 9.06 | 5.5,10,20 | | | |
| 2800000-12-8 | 9.07 | 5.5,10,20 | | | |
| 8530004-6-2 | 8.27 | 5.5,10,20 | | | |
| 85300003-20-10 | 8.02 | 5.5,10,20 | | | |
| 2323060-7 | 8.52 | 5.5,12,29 | | | |
| 2671000-9-1 | | | | 68.5% +2% | |
| CALCULATED | | | 46.3% | | 84% |
| AVERAGE | 8.4 | | 49.6%, 45.0% | 68.5% | |
| | | | | | |
| | | | | | |

*OP COND = (Vaddr, Vbias, Vreset)

** Pulse width modulation efficiency used in this measurement was 96%

4.1.5.1 Tilt Angle Characterization

Average of Centroid method (~100k mirrors), HD SSG

Full sweep = +1 to -1 direction/2

Table 15 shows the results of tilt angle characterization of some of the very first HDD DMDs. An HD Static Scene Generator (HDSSG) was used to generate a black and then a white image to cause the mirrors to tilt in the +1 and -1 direction. The temperature of the devices was observed to change considerably by internal heating caused by device shorts. Temperature greatly affects angle by "sagging" the Aluminum hinges on the order of .02 angular degrees per degree Celsius. Since the devices temperatures were not monitored the measurement of error is ± 0.25 degrees. Also, line pairing problems could not be measured because of image problems.

Table 15

Tilt Angle Characterization Data for 1st HD DMDs

| DATE | DEVICE | FULL SWEEP/2 | COMMENTS |
|---------|---------------|--------------|--|
| 4/8/94 | 2571130-3 | 7.7 degrees | Reflections from the +1 direction show significant separation that is indicative of the odd/even row differences as seen in PAL devices. Overall angle significantly less than 10 degree target. |
| 4/8/94 | 2671005-23-8 | 8.3 degrees | This chip had a steeper angle but still far short of the 10 degree target. The angle was also observed to decrease with time, probably because the high current draw of this device began heating the device and inducing hinge sag. No major indication of significant line pairing, although odd/even image patterns would be needed to verify this. |
| 4/20/94 | 2323060-7 | 8.52 degrees | has a minimal current draw of 140 mA |
| 4/20/94 | Other devices | | Most had high current draw on the order of 1-1.5 Amps, and thus became very hot |

4.1.5.2 Reflectivity Data

Collimated white light source measurement angle optimized for individual device tilt angle. Measure in operation with HDSSG using a single bit plane sequence which has a calculated PWM efficiency of 96%.

Device # 2571130-3
 f = 2.8 r = 48.97%
 f = 4.5 r = 44.2 %

Device # 267005-23 #8
 f = 2.8 r = 50.2 %
 f = 4.5 r = 45.7 %

Measurement of Error: +5%
 Deposited Aluminum
 Post Passivation Al dep reflectivity 89%
 This is comparable to past measurements.

4.1.5.3 Pixel Active Area

A photomicrograph was taken and the active reflective area was measured off of the photo. Grid analysis of photo concluded that the active area was 68.5% with $\pm 2\%$ measurement error.

4.1.5.4 Window Transmission

Transmission was measured with a white light source semi-collimated and a UDT power meter. The window was measured at 20 degrees incident into the window and at normal incidence out of

the window and compared to the detector reading without the window in the optical path. The measurement error is approximately $\pm 1\%$ because of lamp fluctuations

20 degrees in: 97.1%
0 degrees out: 98.3%

4.1.5.5 Die Registration In Package

The flatness between mirrors was measured using a Zygo Interferometer. The peak to valley mirror difference along hinge axis averaged 0.02 microns and the peak to valley mirror difference perpendicular to hinge averaged 0.15 microns. The overall flatness of the die in package was less than 40.6 microns as measured with the Browne & Sharpe tool. The small difference in flatness was thought to cause minimal effects in overall reflectance.

4.1.5.6 Pulse Width Modulation (PWM) Efficiency

The PWM efficiency was calculated and not measured. The current PWM uses 8 bit planes with a 40 Mhz load time which calculates to 92% efficiency. However, prior to May the load time was only 20 Mhz which calculated to 84% efficiency. This worse case value was used in calculating the total device performance.

4.1.5.7 Modeled Device Performance

Modeled performance numbers:

| | |
|------|-----------------------------------|
| .89 | Aluminum reflectivity |
| .685 | Active area |
| .84 | PWM efficiency |
| .95 | Diffraction Coef. (Gale/Florence) |
| .97 | Window transmissivity (IN) |
| .98 | Window transmissivity (OUT) |

46.3% Total Device Efficiency (1992 data)

4.2 1920x1080 Projector Optics and Illumination System (Sarnoff)

4.2.1 System Performance.

4.2.1.1 Brightness, contrast, uniformity.

Simulations, using proprietary software, were carried out to predict screen brightness and uniformity of screen illumination. Rays, in the plane perpendicular to the direction of the discharge, were weighted according to the brightness map of the arc; whereas, the weighting in directions out of the plane was assumed to follow a Lambertian fall off.

4.2.1.2 Collection region

The calculations indicate that the area of best collection efficiency is located in a 4 mm wide, 5 mm high region that is shown as a rectangle in Figures 54 through 58. The lamps made by Hamamatsu appears to have the most compact arcs, with the 5 mm 575 Watt lamp being about 1.5 times as bright as the equivalent 7 mm lamp.

4.2.1.3 Light distribution in the stop of the projection lens

The calculations allow us to estimate the collection efficiency of the optics, the light distribution on the screen and the light distribution in the stop of the projection lens. The distribution of light in the stop of the lens is an indicator of the ultimate contrast ratio that can be achieved as explained below. Figure 59 is a plot of such a distribution. Note that almost all the light traced through the system resides in the circle that defines the $f/2.8$ cone.

Each of the three possible orientations of the micro-mirrors has an $f/2.8$ circle of light associated with it. They line up along a line oriented at 45 degrees; a representation of this line and the three circles is shown above the scatter plot of figure 59. Thus points that lie outside the circle are only a problem if they lie along the 45 degree line. There are virtually no events in this set. The reason derives from the anamorphic illumination scheme; it is restricted to be about $f/2.8$ along the narrow dimension of the DMD, but is slower in the perpendicular direction. This allows the light in the critical direction to be better collimated.

4.2.1.4 Screen uniformity

Carrying the ray trace to the screen allows one to estimate the light distribution in the image plane. The results for a 5 mm arc gap are present in three different forms: Figure 61 is a 3-D plot of the brightness, the equivalent contour plot is presented in Figure 62, while Table 16 gives a numerical enumeration.

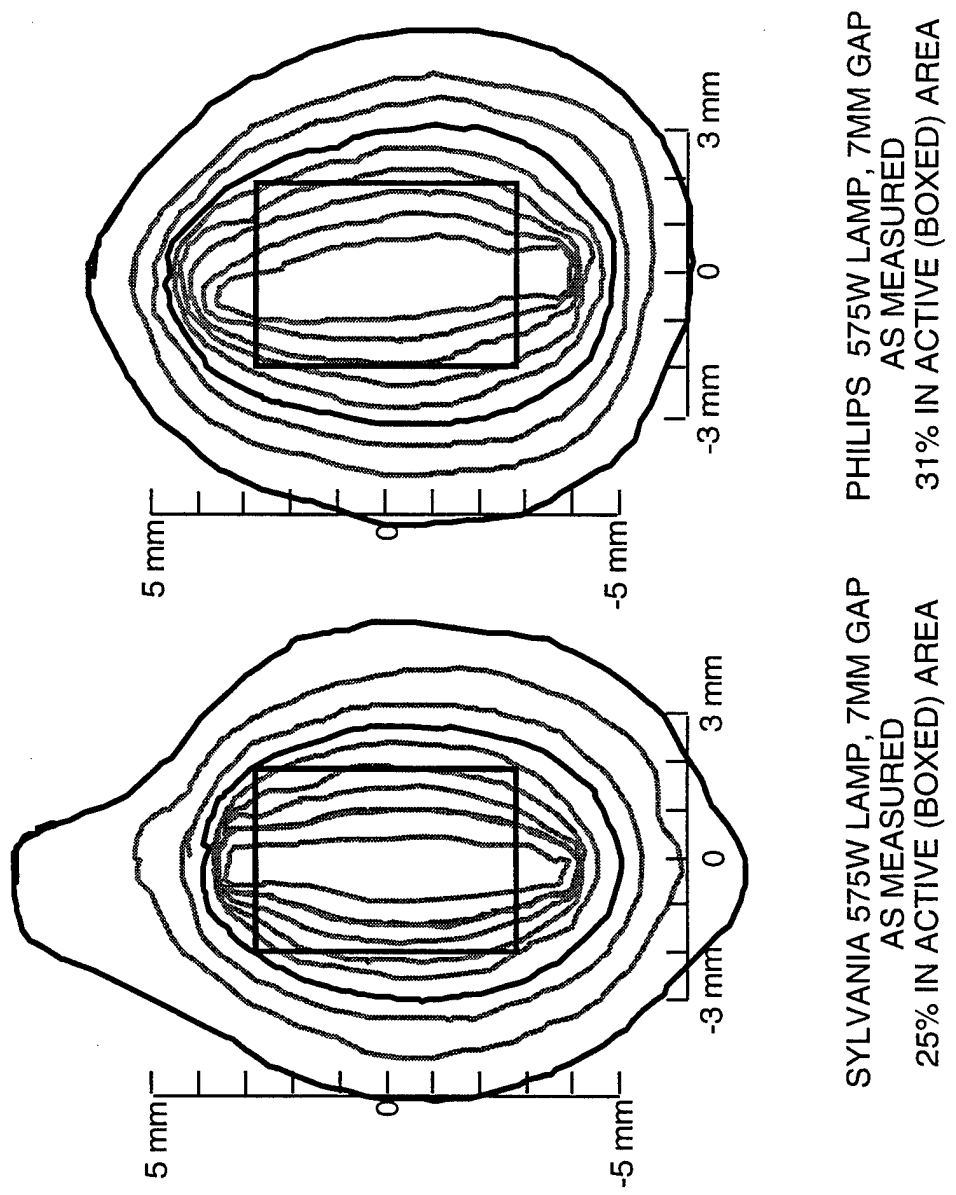
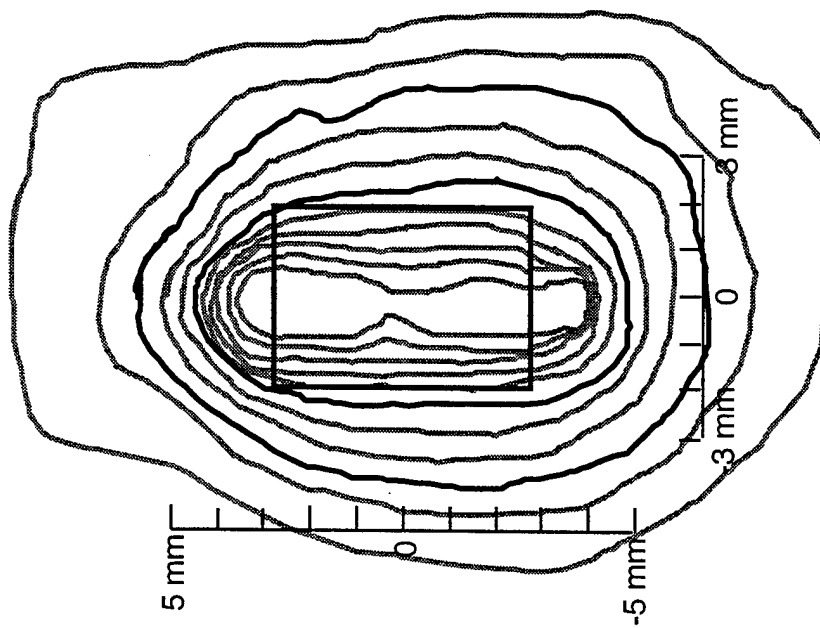
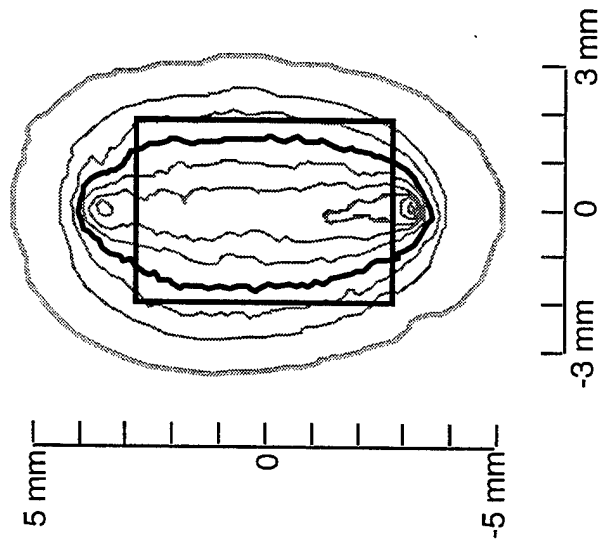


Figure 54. The Sylvania and Philips 575 W, 7mm gap metal-halide lamps. The black lines are 50% and 25% isophots. The rectangle is the 4 by 5 mm collection region.



HAMAMATSU 575W LAMP, 7MM GAP
AS MEASURED
42% IN ACTIVE (BOXED) AREA



HAMAMATSU 575W LAMP, 7MM GAP
HAMAMATSU SPECIFICATION
(HATCHED LINE IS NOT DATA-
IT IS GIVEN ONLY AS A GUIDE TO
THE READER)

Figure 55. Measured arc distribution for the 7mm gap metal-halide lamp vs. the specification of Hamamatsu for the same lamp. The measured lamp is less compact than specifications. As before the black lines denote the 50% and 25% isophots. Since Hamamatsu stops supplying data at the 30% point, a hatched line is provided as a guide to the reader.

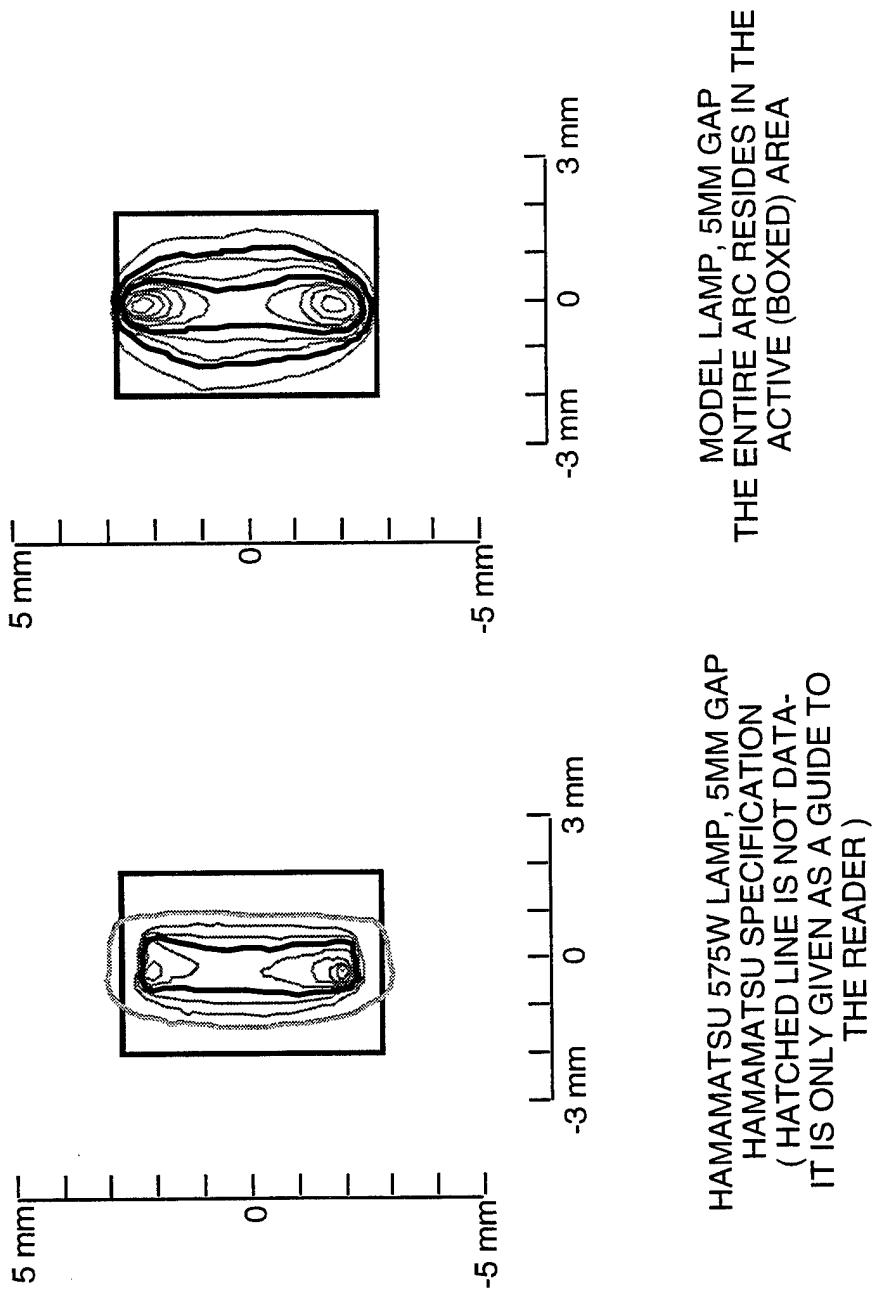


Figure 56. A comparison of the specifications for the Hamamatsu 575W metal-halide lamp with the 5mm gap and the model that was used in the initial design of the projector. The black line as given to denote to 50% and 25% isophots. Since Hamamatsu's data does not go below the 30% point a hatched line is provided as a guide to the reader.

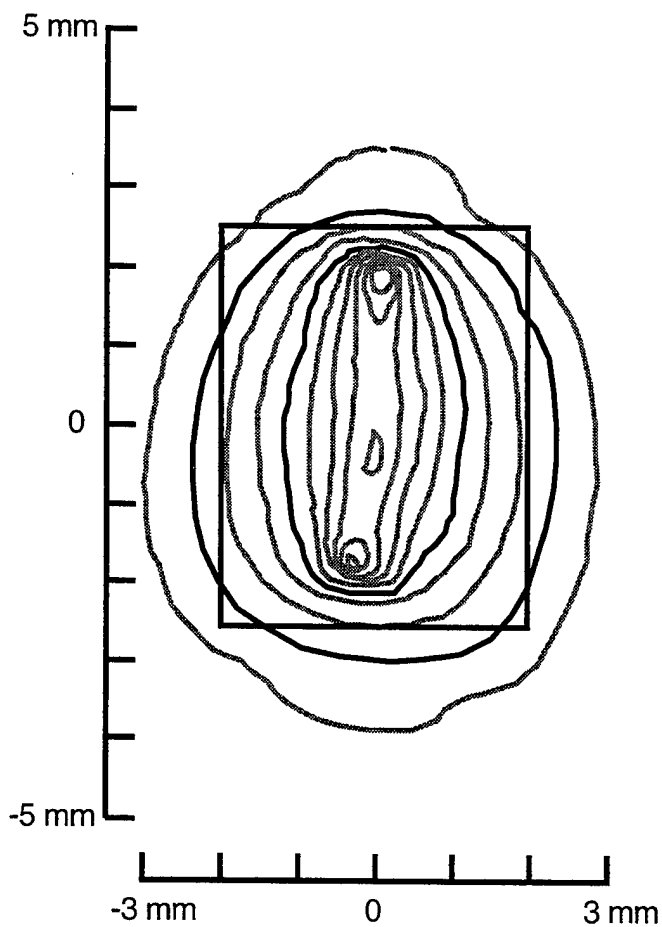


Figure 57. The Hamamatsu 575W metal-halide lamp with the 5mm gap as measured. The black line as given to denote to 50% and 25% isophots. The arc is larger than the manufacturer's specifications, a little over 60% of the light resides in the effective collection region.

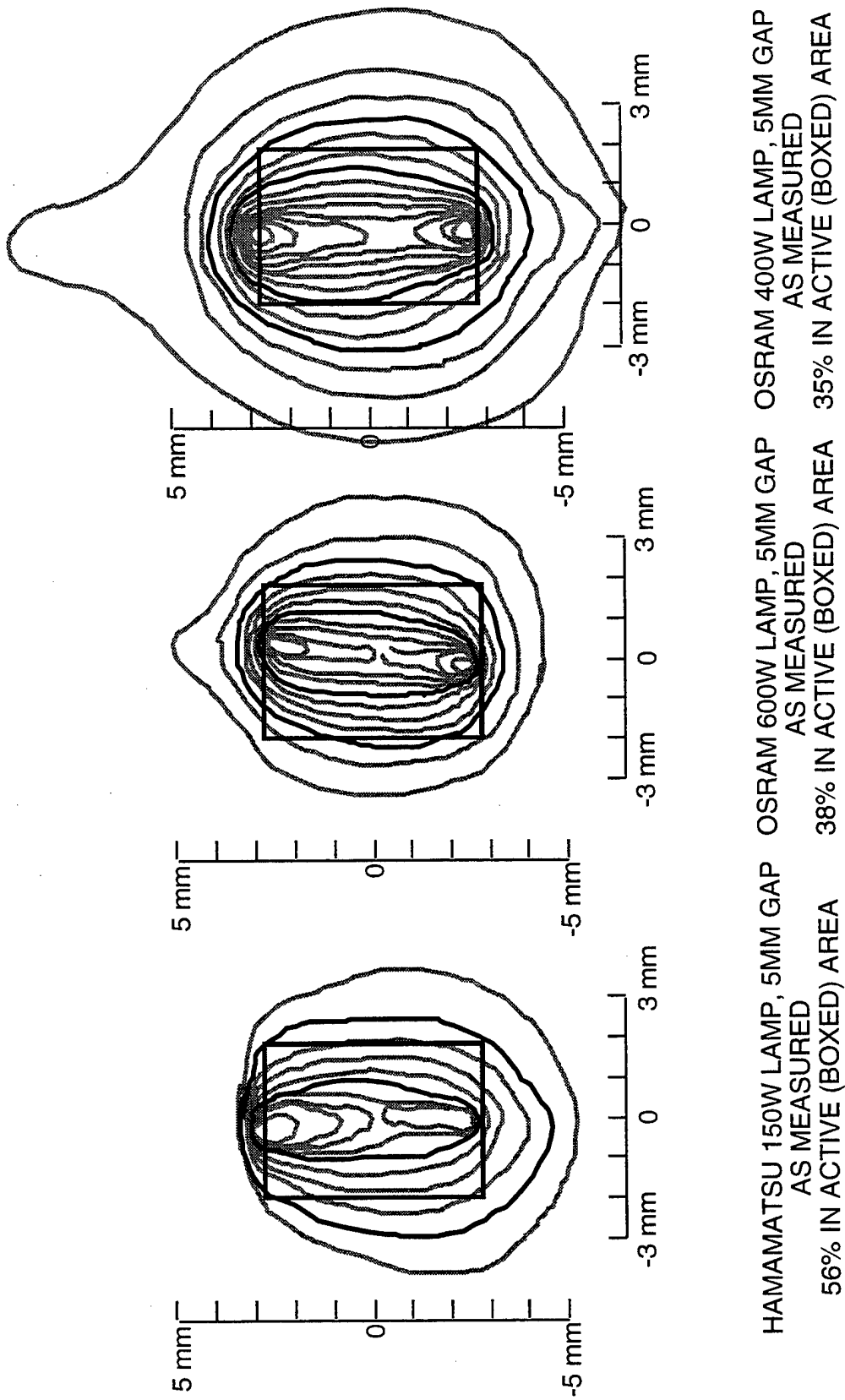


Figure 58. Profiles of various 5mm gap metal-halide lamps.

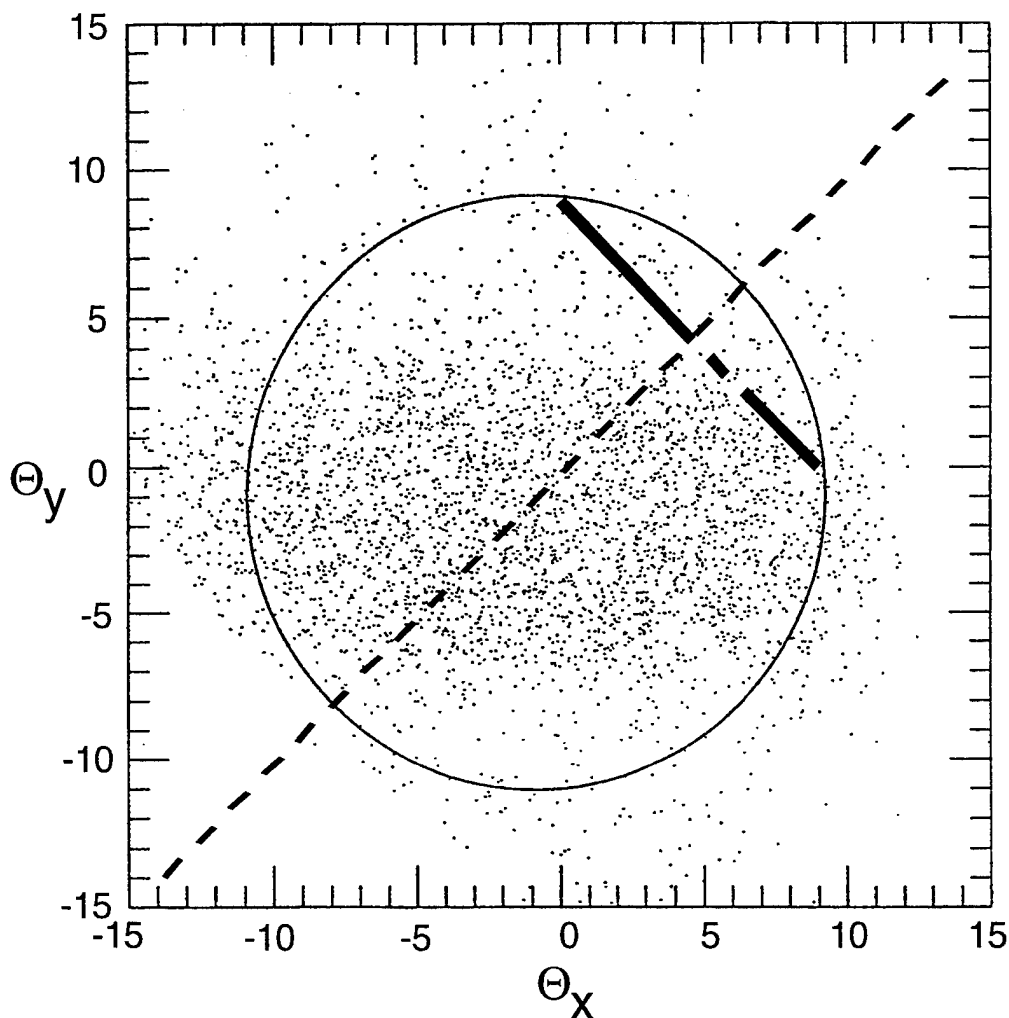
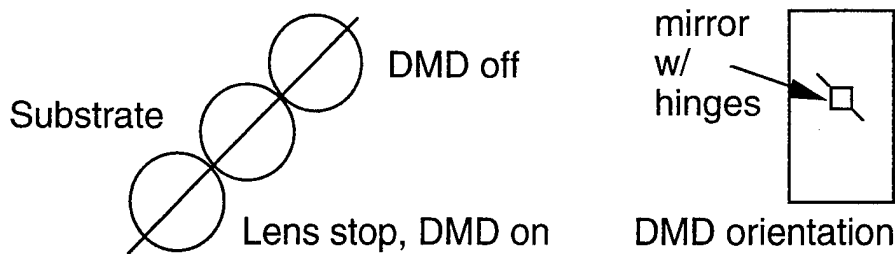


Figure 59. The ray distribution in the projection lens' stop for a 7 mm gap arc lamp. The circle shows the limit of the $f/2.8$ stop. The dashed line gives the orientation of three notable regions. Each region is $f/2.8$. They are the regions where the light goes: if the DMD is on (mirror tilts in the one position), if the mirrors are undeflected, and if the DMD mirrors are off. The three circles lie along a 45 degree line, and are tangent to their neighbors. Note very few rays spill into adjacent circles. This means that the contrast will be high. Contrast can be increased with very little loss of light by leaving a crescent shaped web in the aperture as shown by the dot-dashed line.

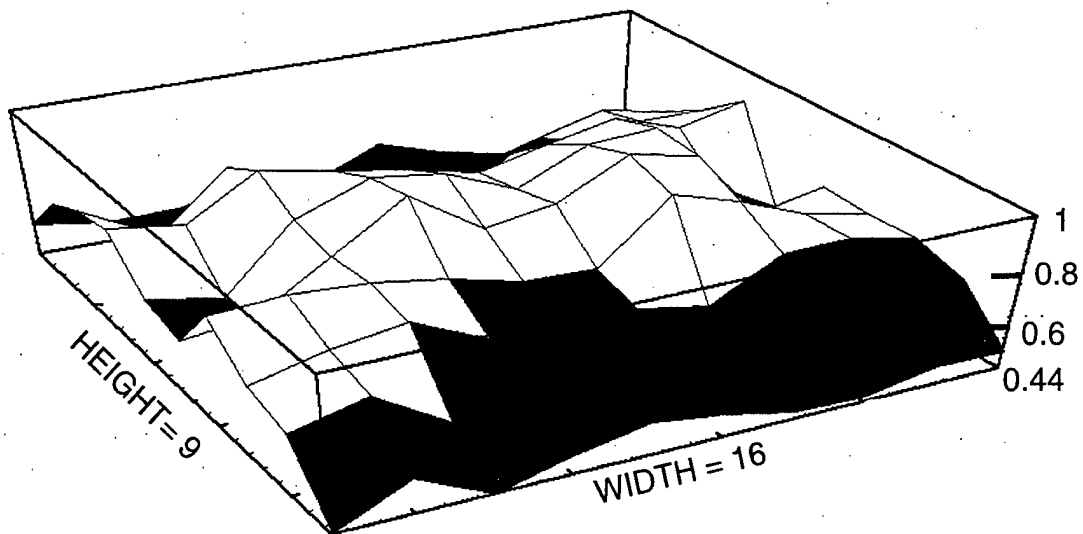


Figure 61. Surface plot of calculated screen brightness as a function of position. The lamp is assumed to have a 5mm gap.

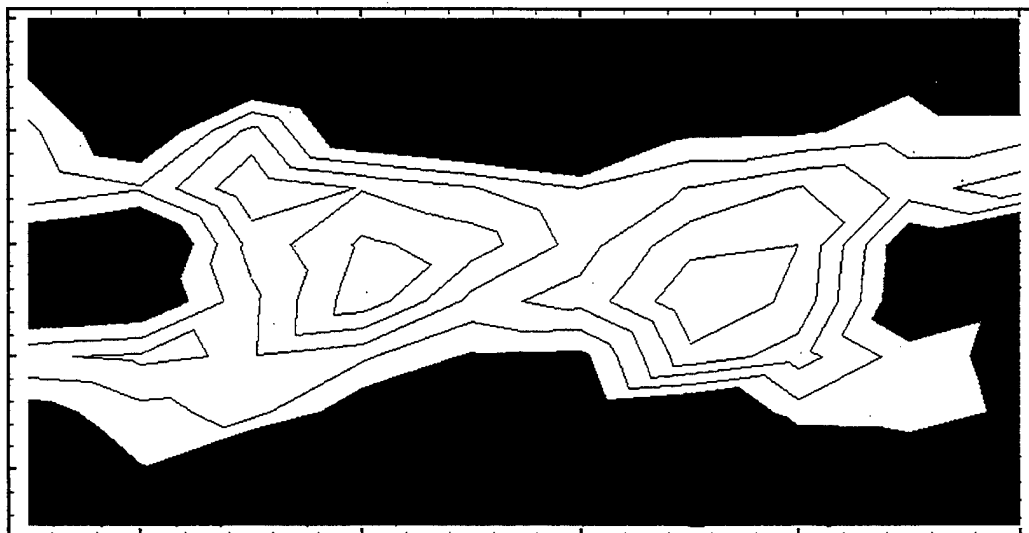


Figure 62. Contour plot of calculated screen brightness as a function of position. The lamp is assumed to have a 5mm gap.

Table 16

The calculated screen brightness as a function of position.
The lamp is assumed to have a 5mm gap.

| | | | | | | | | | |
|-------|-------|-------|-------|-------|-------|-------|-------|-------|-------|
| 0.445 | 0.569 | 0.433 | 0.509 | 0.563 | 0.527 | 0.471 | 0.457 | 0.511 | 0.502 |
| 0.669 | 0.738 | 0.575 | 0.579 | 0.567 | 0.569 | 0.464 | 0.634 | 0.671 | 0.677 |
| 0.714 | 0.779 | 0.816 | 0.696 | 0.515 | 0.683 | 0.636 | 0.773 | 0.781 | 0.727 |
| 0.844 | 0.862 | 0.844 | 0.805 | 0.734 | 0.727 | 0.946 | 0.872 | 0.771 | 0.719 |
| 0.643 | 0.670 | 0.839 | 0.999 | 0.833 | 0.871 | 1.000 | 0.947 | 0.678 | 0.728 |
| 0.683 | 0.628 | 0.870 | 0.969 | 0.935 | 0.829 | 0.944 | 0.959 | 0.689 | 0.556 |
| 0.845 | 0.804 | 0.952 | 0.901 | 0.854 | 0.798 | 0.854 | 0.910 | 0.827 | 0.885 |
| 0.810 | 0.669 | 0.869 | 0.658 | 0.604 | 0.543 | 0.731 | 0.735 | 0.768 | 0.769 |
| 0.738 | 0.594 | 0.647 | 0.577 | 0.534 | 0.546 | 0.558 | 0.662 | 0.730 | 0.678 |
| 0.563 | 0.521 | 0.521 | 0.581 | 0.531 | 0.641 | 0.559 | 0.501 | 0.575 | 0.573 |

The following experimental data for both luminance and small area contrast measurements were taken for the projector using a 7 mm Hamamatsu lamp and mock DMDs. The mock devices, consisting of mirror strips that are alternately tilted at +10 and -10 degrees represent tilted mirror arrays which simulate the DMD structure. Figures 63 and 64 show the experimental results for luminance uniformity while Table 17 shows the normalized screen brightness.

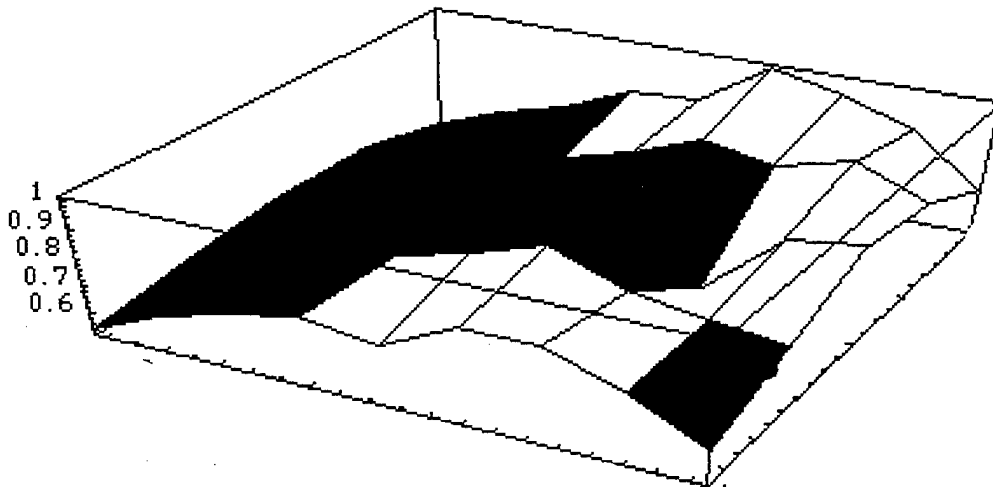


Figure 63. Surface plot of measured screen brightness as a function of position.

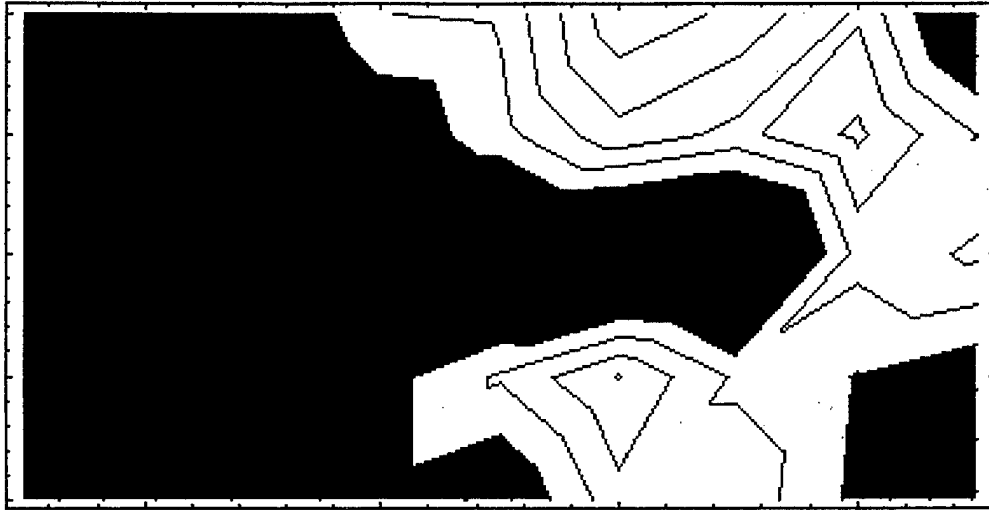


Figure 64. Contour plot of the measured screen brightness as a function of position. Each contour is a 5% change in brightness.

Table 17

A map of the normalized brightness on the screen.

| | | | | | | | | |
|-----|-----|-----|-----|-----|------|-----|-----|-----|
| .56 | .65 | .72 | .83 | .84 | 1.00 | .95 | .87 | .69 |
| .65 | .62 | .67 | .67 | .82 | .91 | .86 | .93 | .83 |
| .64 | .60 | .65 | .65 | .65 | .63 | .61 | .85 | .88 |
| .59 | .62 | .72 | .77 | .84 | .92 | .82 | .62 | .75 |
| .53 | .65 | .72 | .77 | .73 | .86 | .86 | .78 | .65 |

4.2.1.5 Contrast

This same tilted mirror array was used to simulate the DMD structure in a series of contrast ratio measurements.

Table 18 shows a map of the screen broken into 45 regions. Each region is represented by a pair of numbers that indicate the "on" and "off" luminance in foot-Lamberts while Table 19 shows the contrast ratio calculated from the data. The 9X16 image covered an area of 11.22 square feet so that the total light on the screen is the equivalent of 1088 lumens.

Table 18

A map of the light output from the projector as measured on a Lambertian screen. A coarse blazed mirror was used instead of an actual DMD. The pairs of numbers correspond to white and black levels. Their ratio may be taken as the contrast ratio.

| | | | | | | | | |
|-----------|-----------|-----------|------------|------------|------------|------------|------------|------------|
| 69 1.1 | 84 1.2 | 93 1.4 | 100 1.6 | 95 1.4 | 112 1.7 | 112 1.7 | 101 1.6 | 84 1.5 |
| 77 1.2 | 80 1.5 | 94 1.5 | 100 1.6 | 109 1.9 | 120 1.9 | 107 1.9 | 102 1.9 | 98 1.8 |
| 83 1.3 | 78 1.6 | 84 1.6 | 84 1.7 | 84 1.7 | 82 1.8 | 80 1.9 | 110 2.1 | 115 1.8 |
| 84 1.3 | 80 1.6 | 87 1.6 | 87 1.8 | 106 2.0 | 118 2.0 | 112 2.1 | 121 2.0 | 108 1.9 |
| 73 1.2 | 85 1.3 | 94 1.4 | 108 1.6 | 109 1.8 | 130 2.0 | 124 1.8 | 113 1.5 | 90 1.2 |

Table 19

A map of contrast ratio. The ratio of the pairs numbers that correspond to white and black levels are taken and a contrast ratio calculated.

| | | | | | | | | |
|----|----|----|----|----|----|----|----|----|
| 63 | 70 | 66 | 62 | 68 | 66 | 66 | 63 | 56 |
| 64 | 53 | 63 | 62 | 57 | 63 | 56 | 54 | 54 |
| 64 | 49 | 52 | 49 | 49 | 46 | 42 | 52 | 64 |
| 65 | 50 | 54 | 48 | 53 | 59 | 53 | 60 | 57 |
| 61 | 65 | 67 | 67 | 61 | 65 | 69 | 75 | 75 |

4.2.1.6 Lamp life

Figure 65 is a comparison of the lamp lives of a metal-halide lamp and of a relatively safe xenon arc lamp. The curve indicates that the particular metal-halide lamp has a slower degradation in its light output as a function of time than the xenon lamp. The usable life for the metal-halide lamp is given to be approximately 2 to 3 times longer than that of the xenon lamp. It is expected that further development will continue to improve the lifetimes of metal-halide lamps (the metal salts allow the use of a halogen cycle).

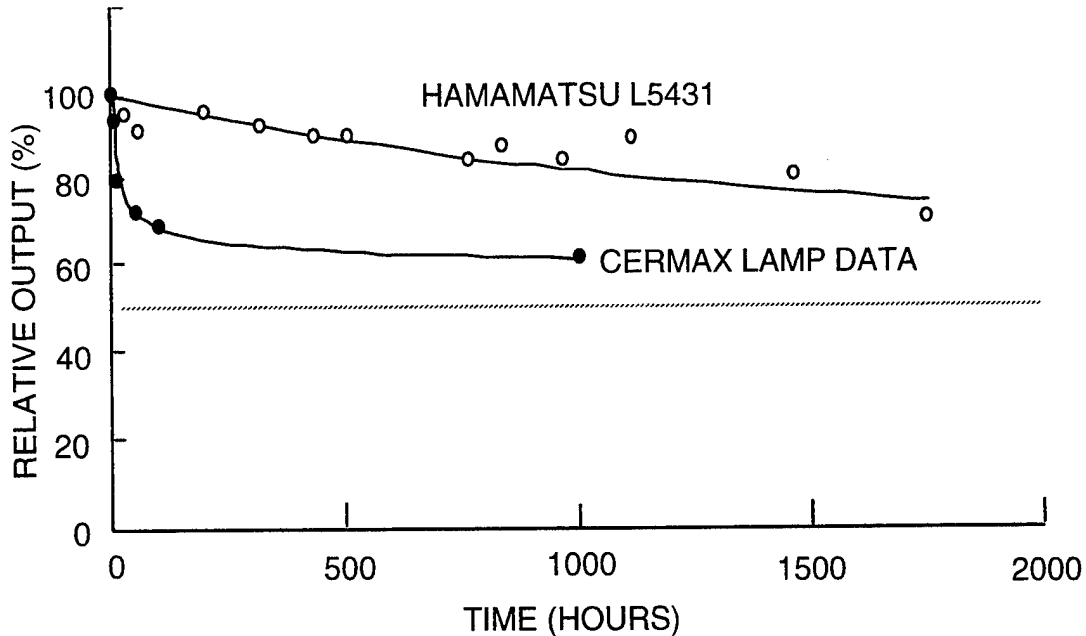


Figure 65. Manufacturers lifetime data for two lamp types.

4.2.1.7 Colorimetry

The colorimetry of the projection system depends on the bandpass of the filter set. The color coordinates of the lamp are very close to $x=0.33$, $y=0.33$. However, the Hg yellow line presents a problem; it contains a significant amount of energy, and if it is included in either the red or green light paths, it will cause the primary color locations to migrate a significant distance away from the prescribed NTSC points. The yellow line must be excised to obtain a color gamut that meets or exceeds that of commercially available color picture tubes.

Figure 66 is a stylized representation of the band edge filters and their effect on the effective throughput of the optical system. The color coordinates that are derived from the calculations are given in Table 20. Figure 67 illustrates the spectrum of the Hamamatsu 575W metal-halide lamp and the suppression of the Hg yellow line through the use of the filter set.

Figure 68 shows a map of color temperatures as a function of arc position a 575 Watt Hamamatsu metal-halide lamp with 7mm arc size. Figure 69 gives the X-Y color coordinates as a function of arc position for the same lamp. Figure 70 shows a CIE 1933 color diagram with this data superimposed on it.

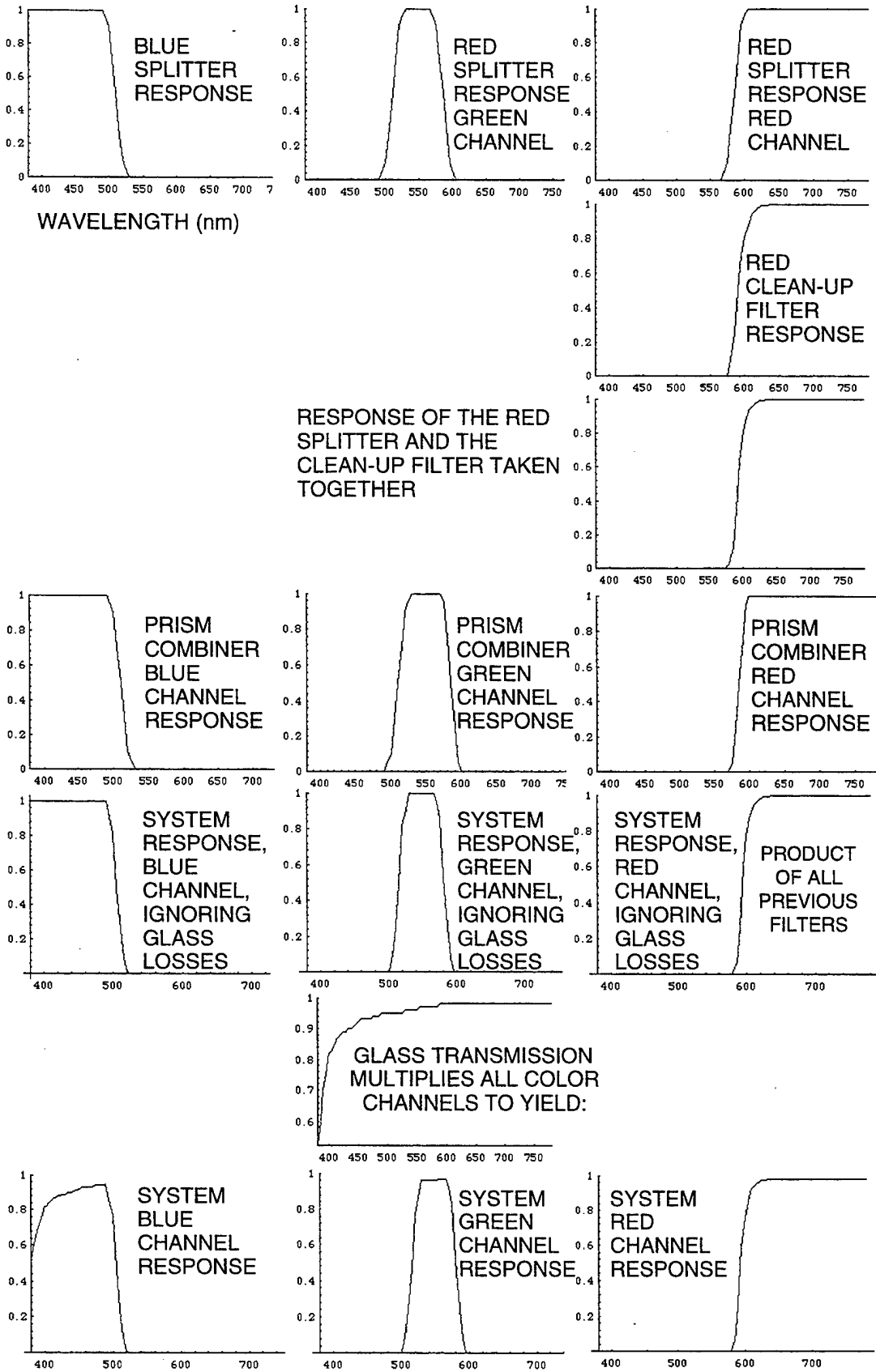


Figure 66. The response of a lossless filter set.

Table 20

The color coordinates for the primary colors and white, for three designs. Sarnoff-1 and the NRC design use only the color separating and combining plates, Sarnoff-2 uses an extra red filter in the illumination path.

| Design | red | | green | | blue | | white | |
|------------|-------|-------|-------|-------|-------|-------|-------|-------|
| | x | y | x | y | x | y | x | y |
| Sarnoff-1 | 0.654 | 0.345 | 0.33 | 0.65 | 0.138 | 0.071 | 0.322 | 0.327 |
| Sarnoff -2 | 0.666 | 0.333 | 0.33 | 0.65 | 0.138 | 0.071 | 0.312 | 0.324 |
| NRC | 0.652 | 0.347 | 0.269 | 0.703 | 0.137 | 0.074 | 0.309 | 0.310 |

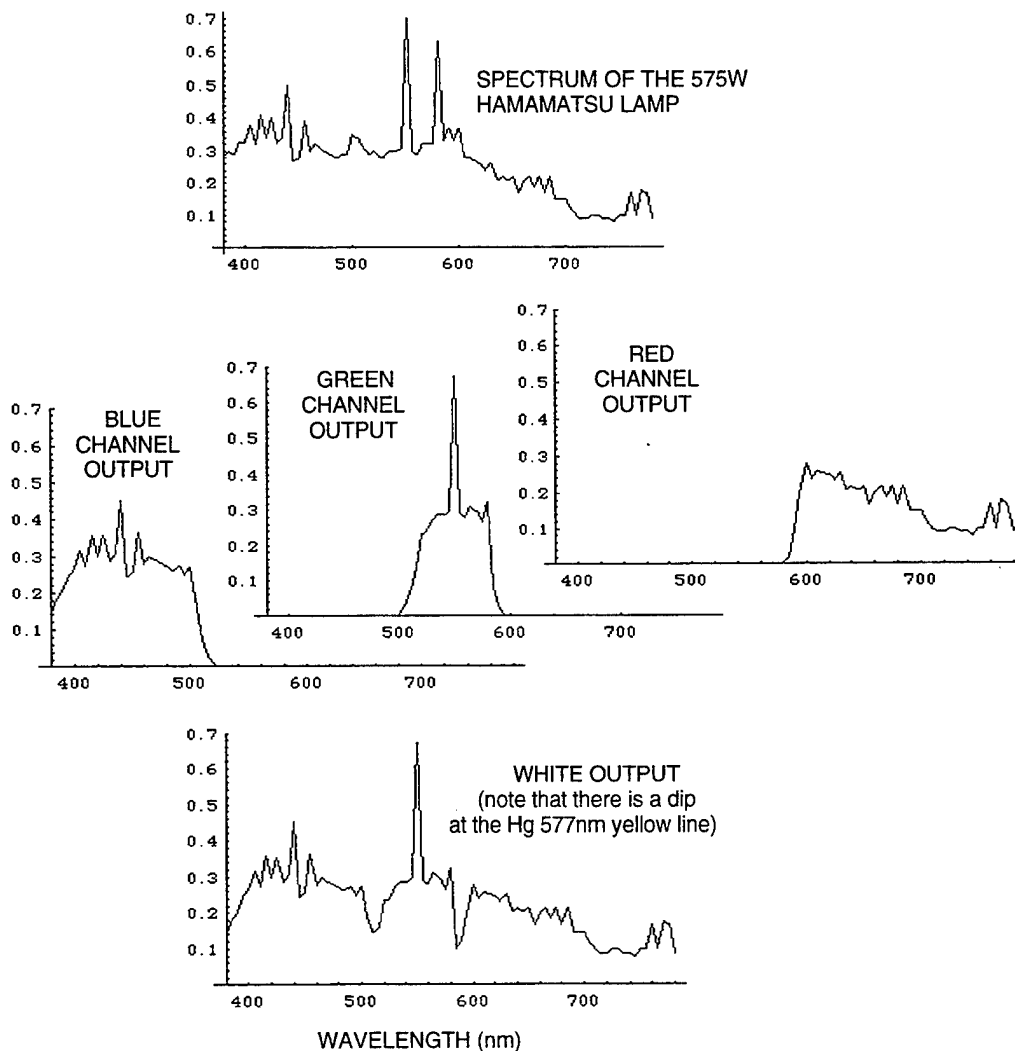


Figure 67. The spectrum of the Hamamatsu 575W metal-halide lamp and the suppression of the Hg yellow line through the use of the filter set.

| | A | B | C | D | E | F | G | H | I | J | K | L | M |
|----|---|---|------|------|------|-----------|---|---|---|---|---|---|---|
| 1 | | | | | | electrode | | | | | | | |
| 2 | | | | | | | | | | | | | |
| 3 | | | 5521 | 5341 | 8785 | 6676 | | | | | | | |
| 4 | | | | | | 6869 | | | | | | | |
| 5 | | | | 7112 | 8914 | 7071 | | | | | | | |
| 6 | | | | | | 7348 | | | | | | | |
| 7 | | | | 7449 | 9209 | 7695 | | | | | | | |
| 8 | | | | | | 7746 | | | | | | | |
| 9 | | | 5397 | 7611 | 9283 | 7775 | | | | | | | |
| 10 | | | | | | 7731 | | | | | | | |
| 11 | | | | 7410 | 8791 | 7532 | | | | | | | |
| 12 | | | | | | 7306 | | | | | | | |
| 13 | | | | 6858 | 8036 | 7051 | | | | | | | |
| 14 | | | | | | 6778 | | | | | | | |
| 15 | | | | 6043 | 7150 | 6418 | | | | | | | |
| 16 | | | | | | 6191 | | | | | | | |
| 17 | | | | | | electrode | | | | | | | |

Color temperature (°K) vs. position in the arc

Figure 68. A map of color temperature as a function of position in the arc of the 575W Hamamatsu metal-halide lamp. The electrode to electrode spacing is 7mm.

| | A | B | C | D | E | F | G | H | I | J | K | L | M |
|----|---|---|--------------|--------------|--------------|--------------|--------------|--------------|---|---|---|---|---|
| 1 | | | | | | electrode | | | | | | | |
| 2 | | | | | | | | | | | | | |
| 3 | | | .332 .345 | .336 .351 | .285 .306 | .306 .349 | | | | | | | |
| 4 | | | | | | .304 .318 | .283 .307 | .301 .337 | | | | | |
| 5 | | | | | | | | .297 .331 | | | | | |
| 6 | | | | .300 .314 | .282 .303 | .294 .324 | | | | | | | |
| 7 | | | | | | .293 .322 | | | | | | | |
| 8 | | | .335 .348 | .298 .312 | .281 .301 | .293 .321 | | | | | | | |
| 9 | | | | | | .294 .322 | | | | | | | |
| 10 | | | | .300 .315 | .286 .304 | .296 .324 | | | | | | | |
| 11 | | | | | | .299 .327 | | | | | | | |
| 12 | | | | .308 .322 | .292 .313 | .302 .332 | | | | | | | |
| 13 | | | | | | .306 .337 | | | | | | | |
| 14 | | | | .321 .336 | .302 .325 | .312 .343 | | | | | | | |
| 15 | | | | | | .317 .344 | | | | | | | |
| 16 | | | | | | electrode | | | | | | | |
| 17 | | | | | | | | | | | | | |

X-Y color co-ordinates vs
position in the arc

Figure 69. A map of X-Y color coordinates as a function of position in the arc of the 575W Hamamatsu metal-halide lamp. These coordinates are map onto the CIE color diagram. The electrode to electrode spacing is 7mm.

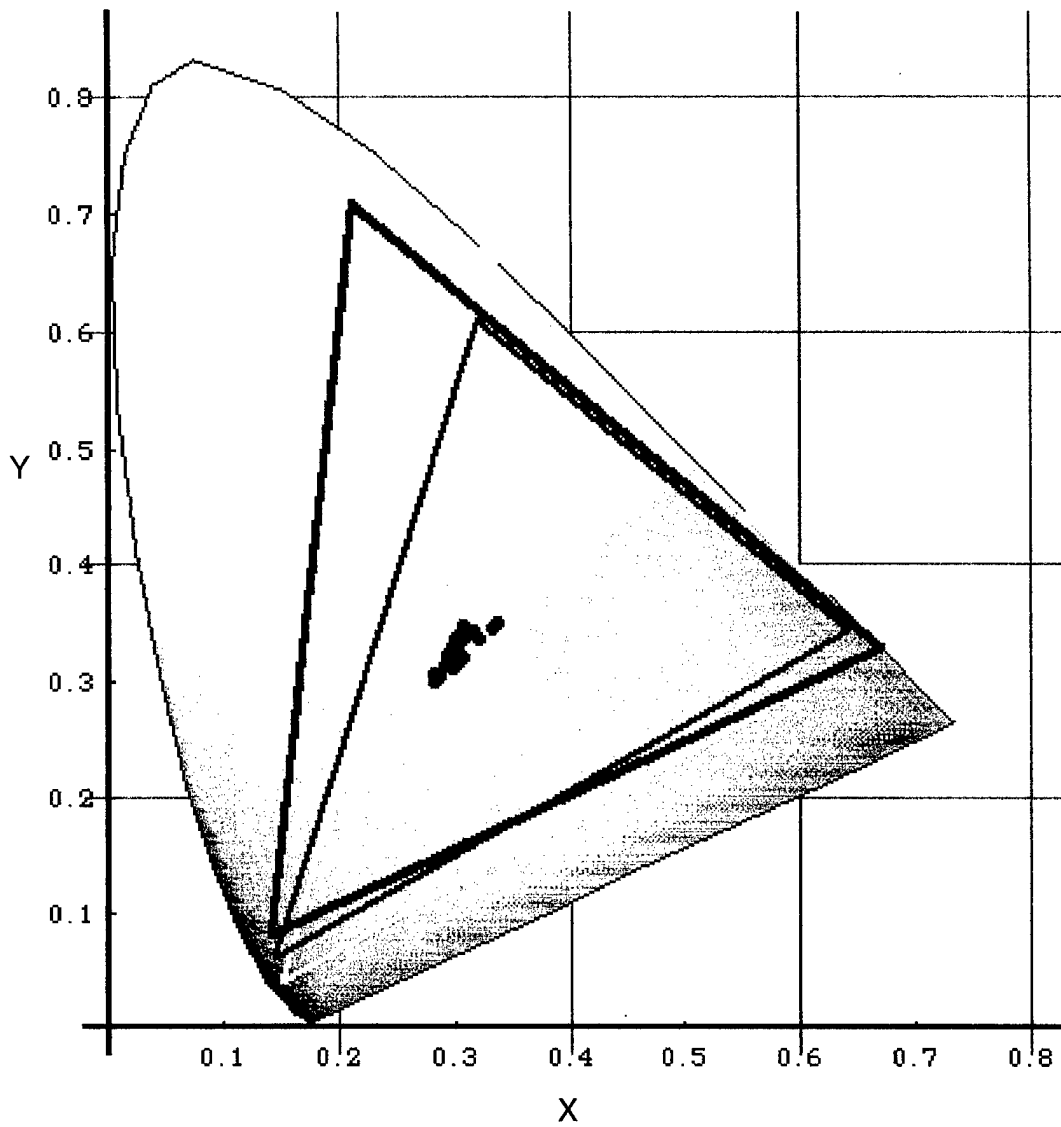


Figure 70. CIE 1933 color diagram. The large black triangle is the NTSC standard, the small black triangle shows the color gamut for current commercial CRTs, and the white triangle denotes the gamut that is possible with the Hamamatsu 575W lamp and the Sarnoff-2 dichroic filter set. The black dots show the color coordinates at several locations in the image of the arc lamp.

4.2.2 Light Budget

A current accounting of the efficiency of the existing projector and an estimate of the best possible eventual performance is given in Table 21. A 575W metal-halide lamp with a 5 mm gap is the light source. The 5 mm lamp's arc is close in shape to that of the model. Any significant differences between current and estimated performance lies in the efficiencies of the DMD and the dichroics. The National Research Council of Canada (NRC) is supplying new filters; their designs, using Ta₂O₅ and Al₂O₃, approach the original Sarnoff filter simulations and are estimated to be 70% efficient. The dichroics in the projector at the time of measurement were 85% rather than 90% or 95% reflective and thus the filter set is only 45% efficient.

Table 21

A light budget for currently existing projector, and with improved elements.

| | Part efficiency (%) | With "new" Dichroics and Current DMD | March '94 System |
|--|---------------------|--------------------------------------|------------------|
| Light source | 560 W | 560 W | 560 W |
| Light source efficiency | 80 lm/W | 80 lm/W | 80 lm/W |
| Light at source | 44800 lm | 44800 lm | 44800 lm |
| Arc shape correction | 60% | 60% | 60% |
| Ellipse collection efficiency, including DMD aperture | 25% | 25% | 25% |
| Ellipse reflectivity | 94% | 94% | 94% |
| White light mirror | 98% | 98% | 98% |
| Shott glass | 99% | 99% | 99% |
| Condenser lens | 96% | 96% | 96% |
| Fresnel losses | | | |
| Coupling prism | 80% | 80% | 80% |
| Dichroic efficiency, including color correction (upper/lower) bounds | 70%/57% | 70%/57% | 45% |
| DMD activity including timing and reflectivity losses | 60% | 40% | 40% |
| Projection lens losses | 95% | 95% | 95% |
| Efficiency (%) | 4.2%/3.4% | 2.7/2.2% | 1.8% |
| Screen lumens | 1875 /1530 lm | 1250/1019 lm | 812 lm |
| Efficiency | 3.3 / 2.7 lm/W | 2.2/1.8 lm/W | 1.4 lm/W |

4.2.3 Conclusion

Our objective of designing a highly efficient projector using three DMDs and a metal-halide lamp has been achieved. The projector is easily assembled and aligned. Using a metal-halide lamp results in a projector that is significantly safer to service than one based upon xenon lamps; and since the lamps have longer life, requires less maintenance.

We estimate that the light efficiency for the projector can be a world leading 3 lumens per Watt when the new dichroics and a 60% reflective DMD are used. This performance is achievable even though the DMD is relatively small for a system using an arc gap as large as 5 mm. The light efficiency with the current dichroics and a 40% reflective DMD, is still a very respectable, 1.4 lumens per Watt. An overall filter efficiency of between 57% and 70% is maintained while preserving saturation and delivering a color gamut that is better than that of a CRT. These characteristics have been retained under these difficult circumstances by designing filters without overlap of the bandpass regions and with steep stable band edges. These performance standards are attained even though color requirements force a notch in the spectral response to be placed at the mercury yellow line. Colorimetry thus requires a 13% penalty in filter efficiency, accounting for nearly half the filter losses.

To achieve our goals we went beyond what is currently taken as the state-of-the-art. Two items were of particular concern. The 575 Watt 5 mm arc lamp has been only recently become available. We have found that its arc is not as compact as the manufacturer claims, a situation that has occurred in almost all the lamps that were examined. The other was the manufacture of the dichroic filters. The need for wide angular tolerance, polarization insensitivity, and steep band edges leads to a filter design that, to produce reliably, requires good monitoring equipment. The filters are clearly realizable, as has been demonstrated by the National Research Council of Canada, but are not in the current inventory of designs supplied by commercial vendors.

4.3 HDD DMD Projector System Electronics

The functional block diagram for the electronics portion of the Formatter/Projector is shown in Figure 71 and consists of a computer interface, a Data Formatter, and the Projector Electronics as shown in the Figure below. The Computer Control provides the flexibility and user control. The Data Formatter receives the RGB real and derived data and converts the data into the bit plane format for display to the DMDs. The Projector Electronics stores the data in frame buffer memory for transfer to the DMDs. Each of these is described in the following sections.

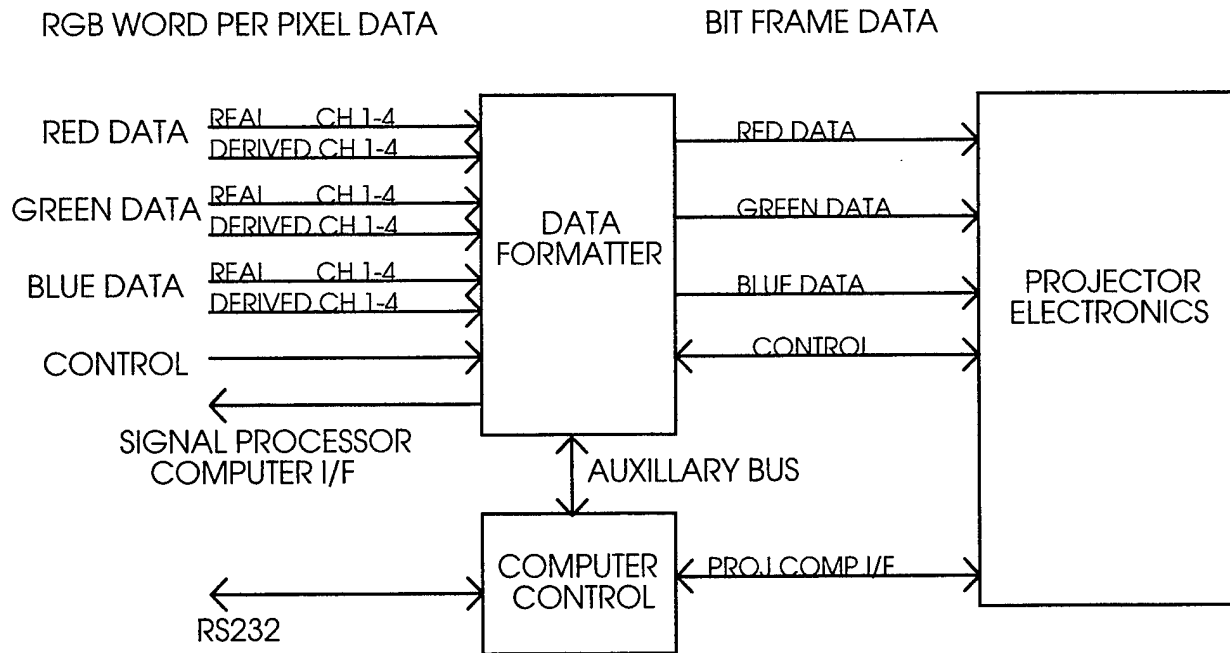


Figure 71. Formatter/Projector Electronics.

4.3.1 Computer Control

The Computer Control function provides the capability to write and read registers, memories, and programmable parts in order to initialize, control, test, and reconfigure the Data Formatter and Projector Electronics.

4.3.2 Data Formatter

The Data Formatter receives the digital RGB video data, seams the data, converts the data to Bit Plane format, and sends the data to the Projector Electronics where the data is stored in frame buffers for presentation to the DMD devices. A functional block diagram of the Data Formatter is shown in Figure 72.

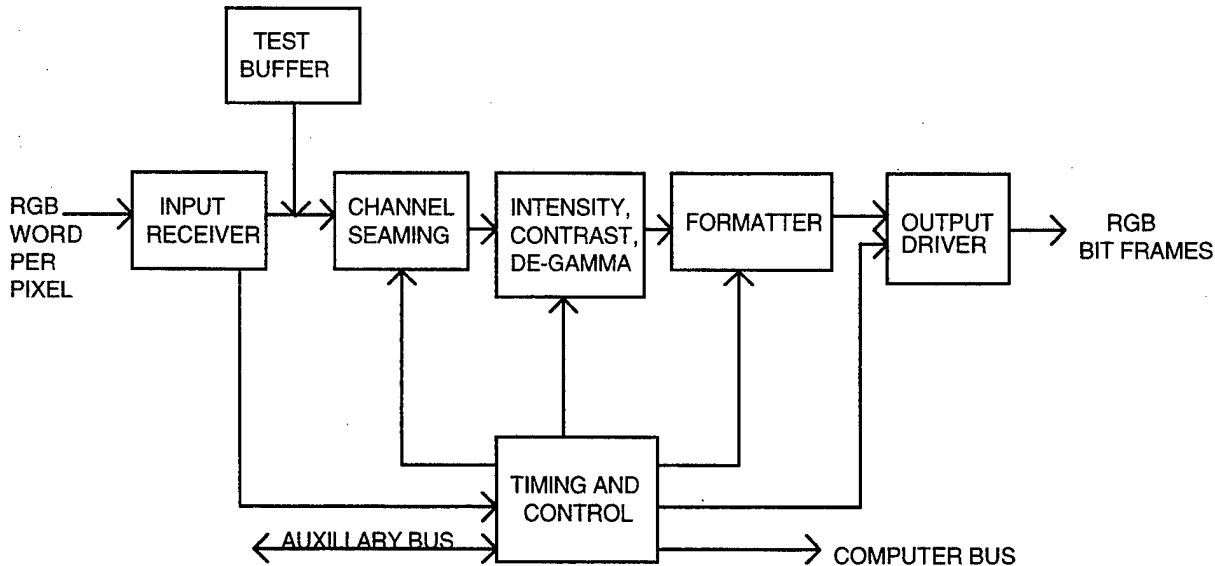


Figure 72. Data Formatter Block Diagram.

4.3.2.1 Input Receiver

The Input Receiver terminates the differential ECL RGB video data/control and translates the signal levels to TTL logic levels. The output of this functional block will be single-ended TTL.

4.3.2.2 Test Buffer.

The Test Buffer provides a full frame of data that will provide both a test and static scene capability through the Formatter/Projector.

4.3.2.3 Channel Seaming

The data from the Input Receiver block is buffered in a line deep FIFO to allow seaming of various data formats into the 512 pixel wide channels (1/4 line of the DMD array). In the ARPA system, the data is originally sourced from a SMPTE standard which is 1920 pixels wide (horizontal). The 1716 active pixels of the HDTV source are centered inside the 1920 wide format (outer pixels are zero or black). The ARPA Signal Processor then sends the data to the Formatter/Projector in the proper format (RGB/4 channels per color/ real and derived lines). The data format is described in detail in Section 4.1. Data is sent in continuous fields of 550 pixels for each channel (the first 140 of channel 1 and last 140 of channel 4 are invalid data). The data is then seamed to center the 1920 in the 2048. Horizontal electronic alignment can then be performed by changing the seaming of a particular color. Figure 73 illustrates the relationship of the input data, the seamed data, and the display.

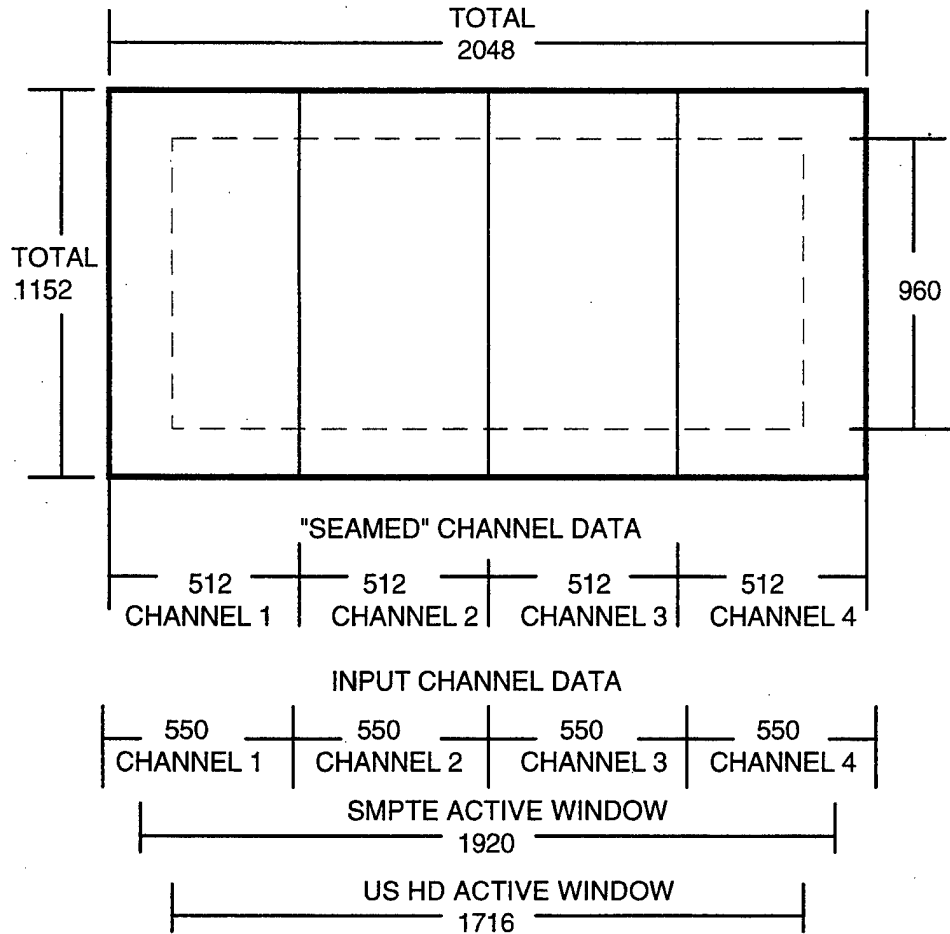


Figure 73. Input/Seamer/Display Relationship.

4.3.2.4 Data Intensity, Contrast, and De-Gamma Function

The video data output of the seaming function will be used to address a look-up table whose output will become the new video data stream. The look-up table(s) will support up to 10-bits on both the input and output. The look-up table(s) will be RAM based and loadable via the Computer Auxiliary Bus.

This block will provide several data manipulation functions including Gamma compensation, Intensity compensation, and Contrast compensation. Each function will be user selectable based on the characteristics of the video data source.

Two banks of look-up tables will be used so that one bank can be loaded from the Computer Auxiliary Bus while the other is used in the video data stream. This will allow the look-up table contents to be updated without interrupting the video data stream and corrupting the display.

4.3.2.5 Formatter

The Formatter separates the "seamed" word per pixel RGB video data into individual bit planes for presentation to the DMD. It utilizes a double buffer topology with one formatter bank receiving data and the second bank supplying data to the DMD. The Formatter consists of 24 identical formatter blocks or cells to support three color streams of four channels (3 colors x 4 channels/color x 2 banks). The formatter output data will be sent to the frame buffer in bit plane order. The bit planes can then be sequentially loaded to the DMD resulting in the proper spatial display order.

4.3.2.6 Output Driver

The Output Driver function translates the TTL data to ECL data for transmission to the Projector Electronics. This function also receives ECL control signals from the Projector Electronics and converts them to TTL levels.

4.3.2.7 Timing and Control

The timing and control function provides clocks to all the other functions in the data pipeline and can be programmed via the auxiliary bus to handle various modes of operation.

4.3.3 Projector Electronics

The Projector Electronics receives the bit plane ordered video data from the Data Formatter, buffers two frames (or three fields) of video data, and loads the DMD in the time modulated sequence required for each DMD (red, green, and blue). The Projector Electronics functional block diagram is shown in Figure 74.

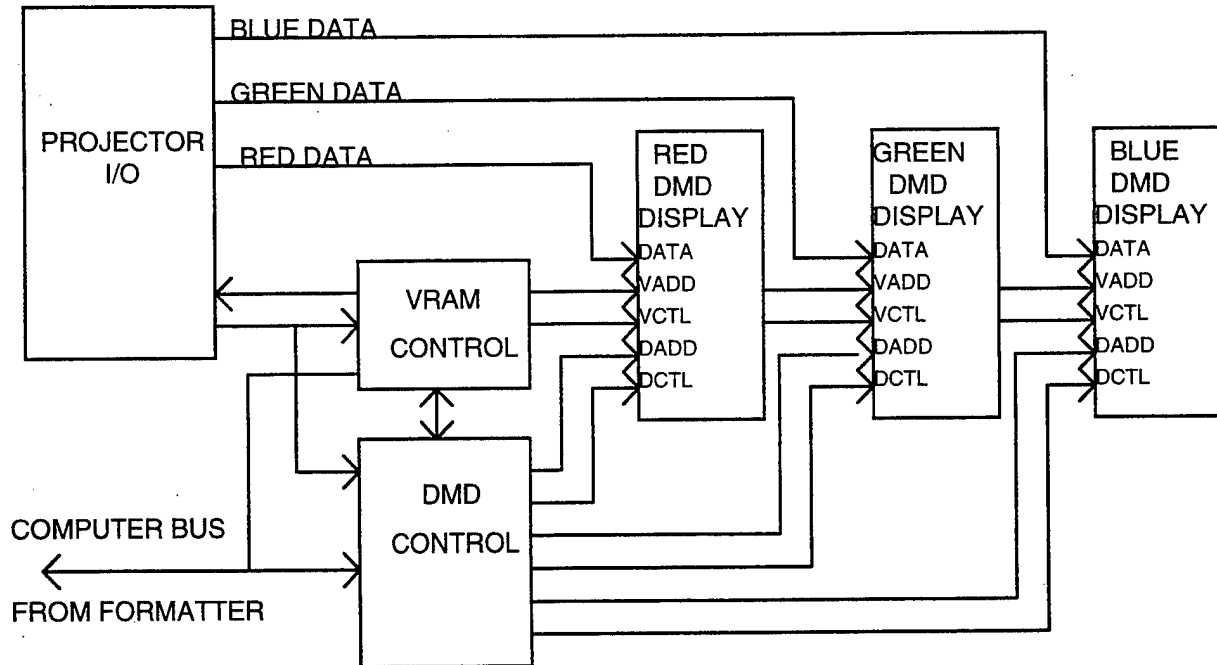


Figure 74. Projector Electronics Block Diagram.

4.3.3.1 Projector I/O

The Projector I/O function primarily translates the ECL level RGB bit plane data and translates the data to TTL levels. The Projector I/O also translates TTL control signals to ECL levels for transmission to the Data Formatter.

4.3.3.2 VRAM Control

The VRAM Controller will generate the address and DRAM timing required to write the bit plane ordered data into the VRAM frame buffer. Counters in this block will keep track of pixel position and line number for the incoming video data. All counters and control logic will be reset by the VSYNC signal to prevent system lock up if the incoming video is momentarily corrupted.

The video data presented to the Data Projector will be field corrected progressive scan ordered for all modes of operation of the Display Subsystem.

The VRAM Controller will arbitrate access to the frame buffer between the DMD Controller serial transfer requests, the incoming data writes, and DRAM refresh cycles.

4.3.3.3 DMD Controller

The DMD Controller will generate the address and DMD timing required to write the bit plane ordered data from the VRAM frame buffer to the DMD. The loading, setting and clearing sequence for each DMD (red, green, and blue) will be independent to accommodate temporal

differences in the gray shade generation of each color. The sequence information will be stored in an easily re-programmable media.

4.3.3.4 Red, Green, and Blue DMD Display

The DMD Display function for each color provides the VRAM frame buffer which stores the bit frame data before transfer to the DMD, the 2048x1152 DMD, and the associated DMD Bias/Reset control circuitry. The VRAM frame buffer can hold two complete frames of video data which can accommodate all modes of operation.

4.3.4 Proscan Motion Adaptive Algorithm (Sarnoff)

4.3.4.1 Purpose

This section describes the functional parameters and operability of the DMD Proscan additions to the DMD Source Electronics System that is to be used by Texas Instruments and ARPA. The DMD Proscan additions are boards that are added to the present DMD Source Electronics. The first section of this document discusses the current setup of the DMD Source Electronics; the report then discusses how the new Proscan sub-system architecture is implemented in the design. It presents a description of the motion signal derivation algorithm as well as the averaging algorithm that creates the additional pixels. It shows detailed block diagrams of all boards implemented in the design as well as block diagrams of all custom PLDs.

4.3.4.2 System Background (Interlaced Mode)

The Digital Micro-mirror Device (DMD) is being developed under an ARPA contract, MDA 972 90C 0008, as an HDTV capable high brightness projection display. Any interlaced HDTV video signal can be easily supplied via the standard SMPTE 240M interface (the digital interface is clearly defined by the SONY Corporation). Initially, the input will be supplied via interface electronics from the Advanced Digital HDTV, AD/HDTV, hardware system. However a new HDTV system is currently being proposed for FCC acceptance by the Grand Alliance Consortium. The David Sarnoff Research Center is one member of the Grand Alliance Consortium. The Digital Micro-mirror Device chip and drive electronics are being designed and fabricated at Texas Instrument, Inc. The AD/HDTV interface will have the capability of directly interfacing to the AD/HDTV hardware or to a commercial digital video tape recorder, VTR, so that pre-recorded digital output from the AD/HDTV decoder system may be displayed on the DMD system when the AD/HDTV hardware is not available for direct interface. Interface through the digital VTR electronics of live video from an HDTV video camera will also be possible when a suitable camera is available. All signals and interfaces will be handled directly in digital form with no intermediate conversions to and from an analog format. A high-level block diagram of the system is presented in Figure 75.

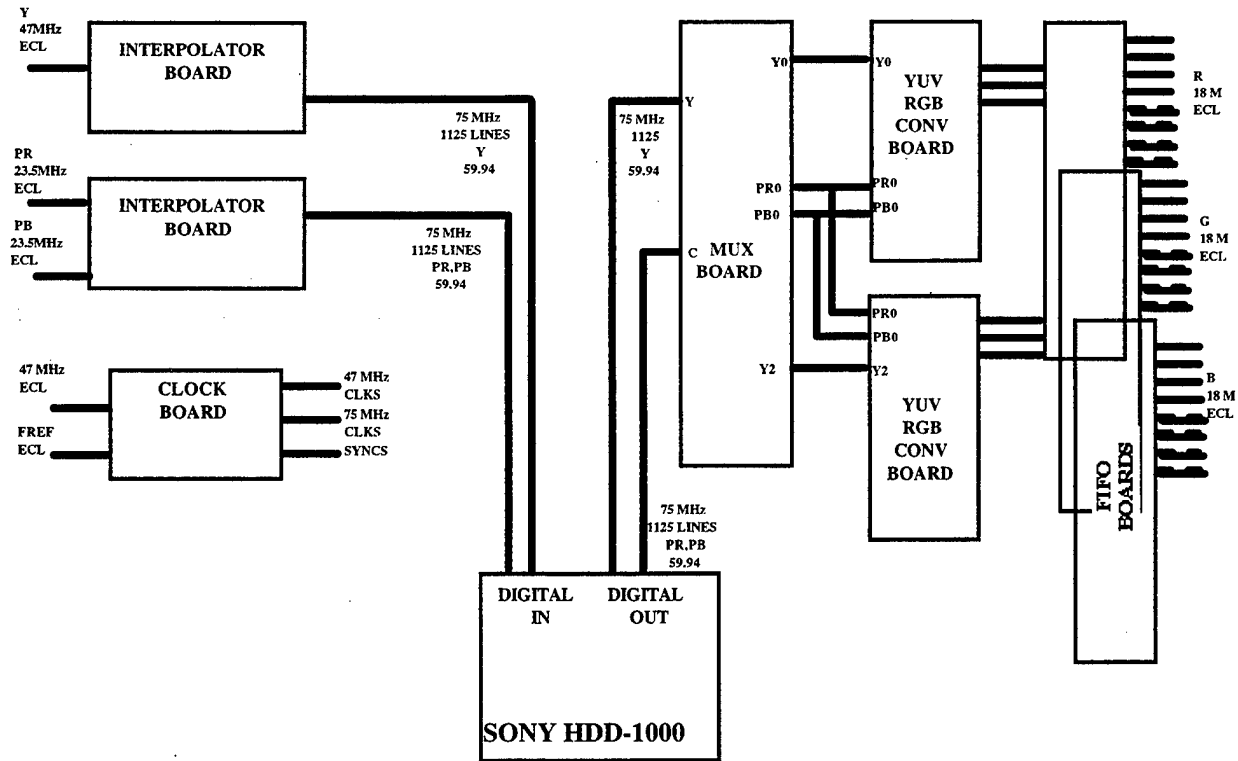


Figure 75. DMD Overall System Diagram.

4.3.4.3 System Description

The DMD system is divided into two subsystems: one subsystem presents digital video information to the HDD 1000 digital tape recorder (the pre-HDD1000 subsystem), the other subsystem takes information from the HDD 1000 digital tape recorder (the post-HDD1000 subsystem). There are three boards that present information to the recorder, namely the luma interpolation/filter board, the chroma interpolation/filter board and the clock generation card. Six boards comprise the post HDD1000 subsystem, namely the sync/demux card, two color matrix cards, and three FIFO cards. All of these boards are presented in Figure 75.

4.3.4.4 Nest Configuration

All boards designed for the DMD project are located in a 9 mu 20 slot Eurocard nest. In the back of the nest is a panel with six connectors that interface to a variety of sources and destinations. Figure 76 shows how external devices are attached to the DMD electronics.

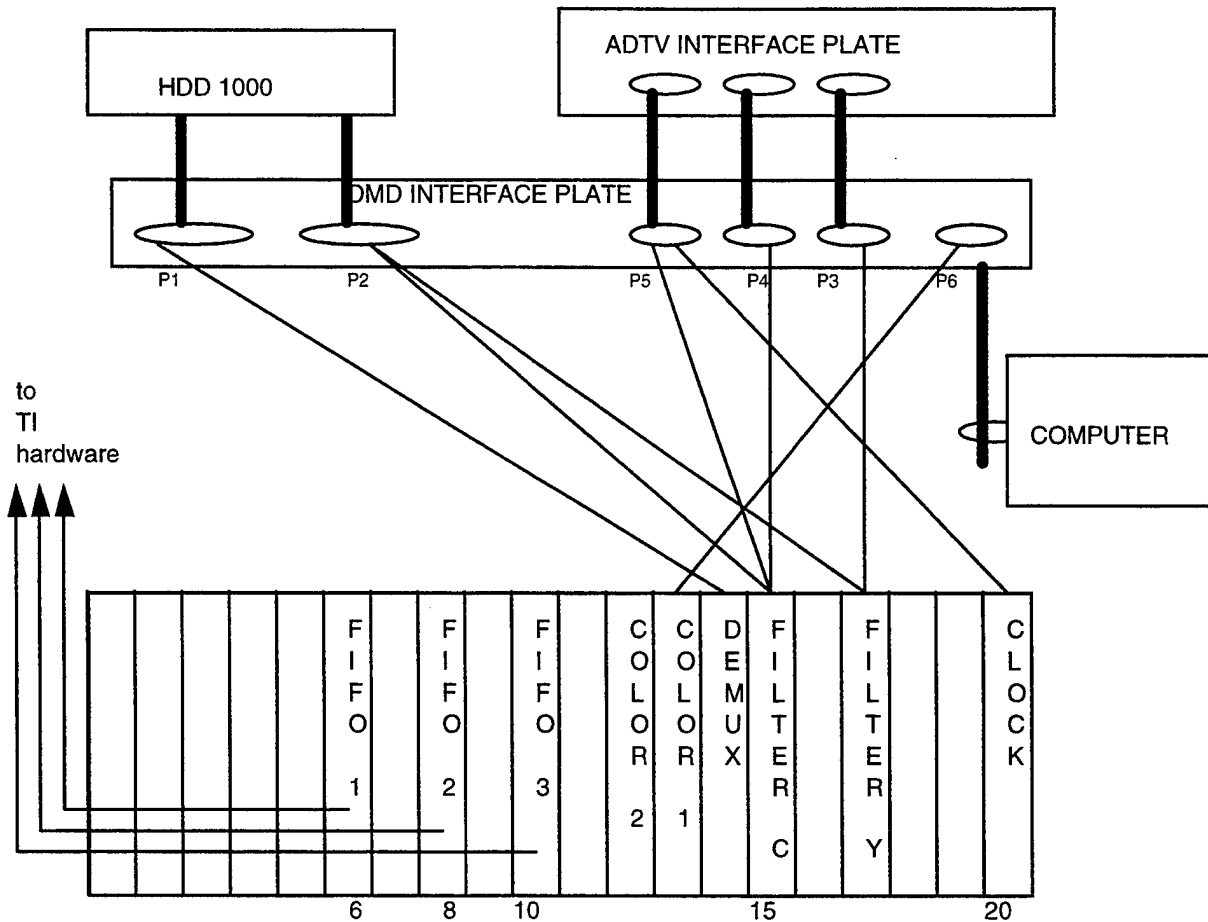


Figure 76. Nest Cabling Diagram.

The nest is driven by three power supplies for the present configuration, one +5 Volt 40 Amp power supply, one -5 Volt 40 Amp supply and one +/- 15 Volt 3 Amp dual power supply.

4.3.4.5 Reference Documents

Documents shown in Table 22 constitute provisions of this specification. Wherever this specification and the referenced documentation differ, this specification shall take precedence.

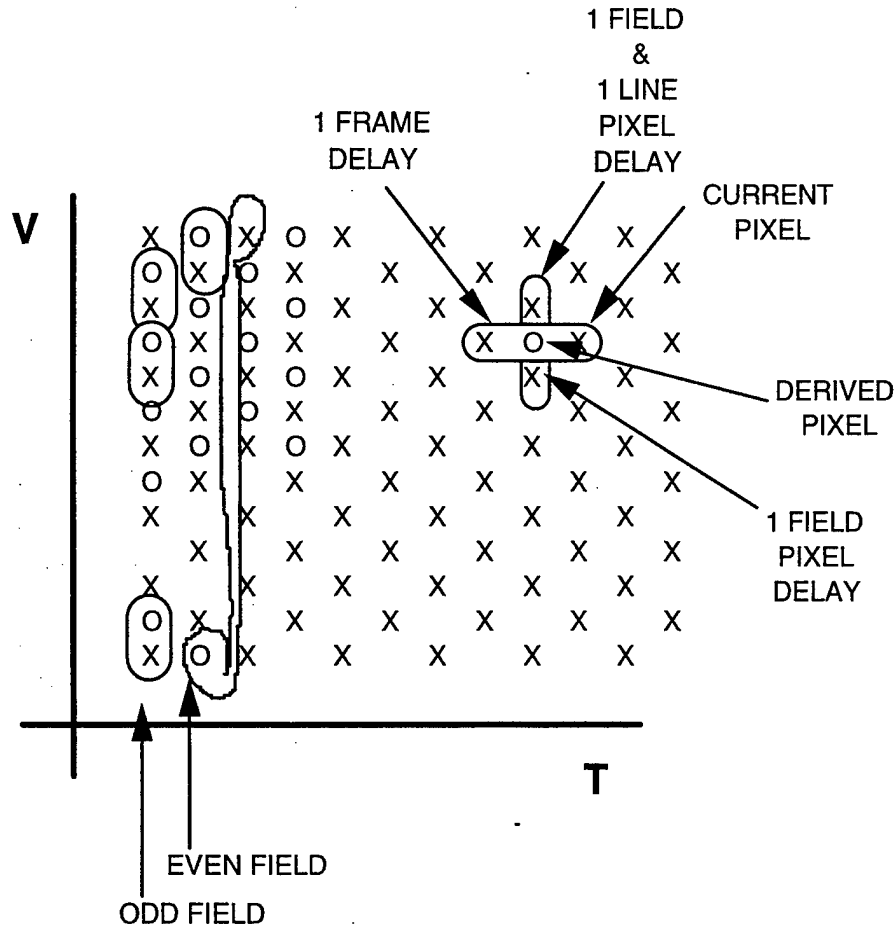
Table 22 - Reference Documents

| Document Title | Date |
|--|--------------|
| SMPTE Standard for Television-Digital Representation & Bit Parallel Interface-1125 High Definition Production System | June 15,1992 |
| Interface Control Specification ARPA High Definition Display Program | June 24,1993 |
| DMD Project Documentation | August 1993 |

4.3.5 PROSCAN Theory of Operation

4.3.5.1 PROSCAN Definition

The objective of the Proscan algorithm is to generate a new line of video information for every real line of video information. The derived line is generated by looking at four pixels located in both the temporal and spatial direction. Figure 77 shows a Vertical/Temporal (VT) diagram indicating the pixels to be used in the Proscan algorithm.



NOTE: ODD FIELD 563 LINES OF REAL DATA AND 562 LINES OF IMAGINARY DATA
 EVEN FIELD 562 LINES OF REAL DATA AND 563 LINES OF IMAGINARY DATA

Figure 77. VT Diagram Describing Proscan Algorithm.

The X pixels in the VT diagram represent real pixels that come from some source, namely the HDD 1000. The O pixels represent the derived pixels that are created using the Proscan generation algorithm. The algorithm looks at pixels a field ahead and behind the pixel being derived, as well as pixels a line ahead and behind of the pixel being derived; it then averages the four pixels dependent on the intensity of the motion signal. The motion signal is derived from

the amount of motion from the green channel, the value is created by performing a frame difference on the pixels one field ahead of and one field behind the pixel being synthesized. The VT diagram also shows that an even number of derived lines exist in every odd field and an odd number of derived lines exist in every even field. Therefore, in order to satisfy the TI specification requirement of eight 18 MHz data channels, the last line of real data from the odd field has to be sent to the TI electronics at the same time as the first line of derived data of the even field.

4.3.5.2 PROSCAN Algorithm

Figure 78 shows the Proscan algorithm to be used in the creation of the derived pixels. Values of the input byte stream that are a frame apart are added together creating a temporal average signal. In addition, values that are a line apart are added together creating a line average. The average temporal value is subtracted from the average spatial value and compared to a motion signal. The minimum of these two values is then compared to the inverted motion vector. The maximum of the two values is added to the temporal average of the four original pixels to create the derived pixel.

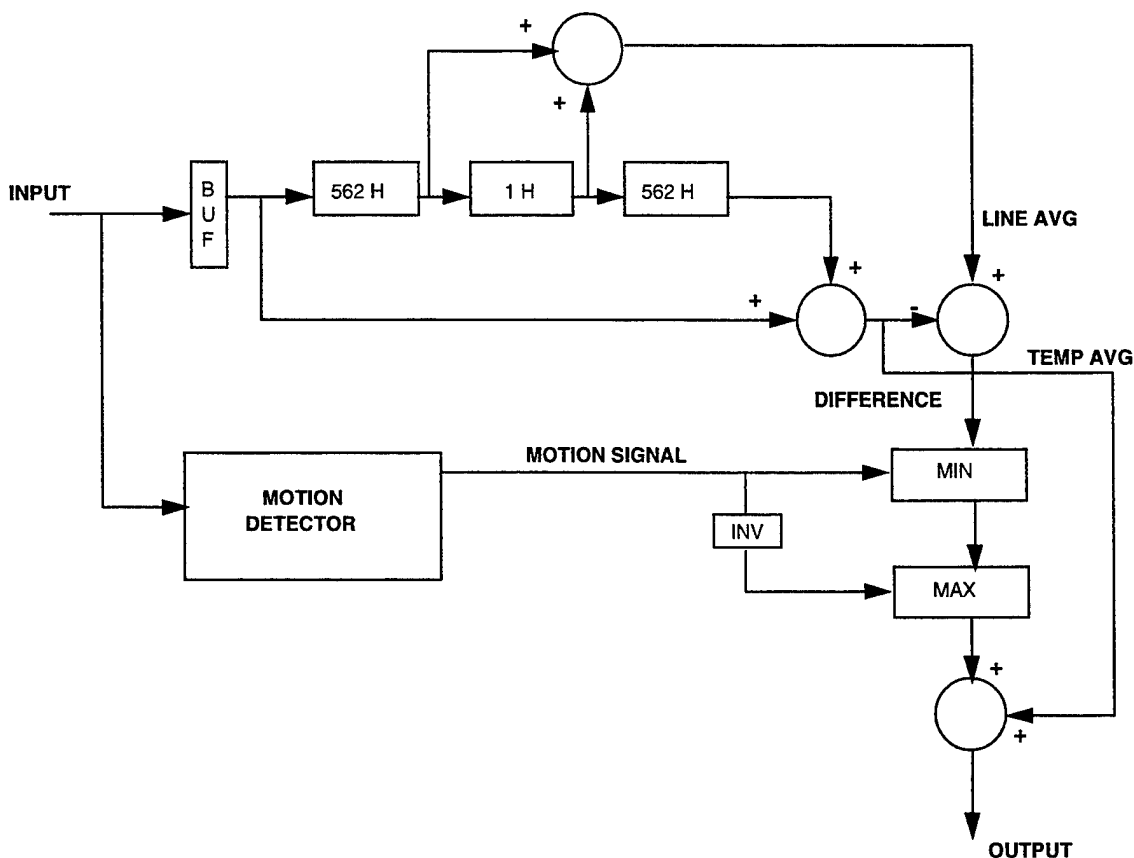


Figure 78. Proscan Generation Algorithm based on a Thompson Patent.

The soft switch function implemented by the MIN, MAX, INV and adder functions are fundamentally limiters that compare the motion signal value to the difference signal. The difference signal is selected as long as it does not exceed the motion signal, if it exceeds the motion signal the output is clamped to the motion signal value. Figure 79a shows the operation of the circuit when the motion signal exceeds the difference signal.

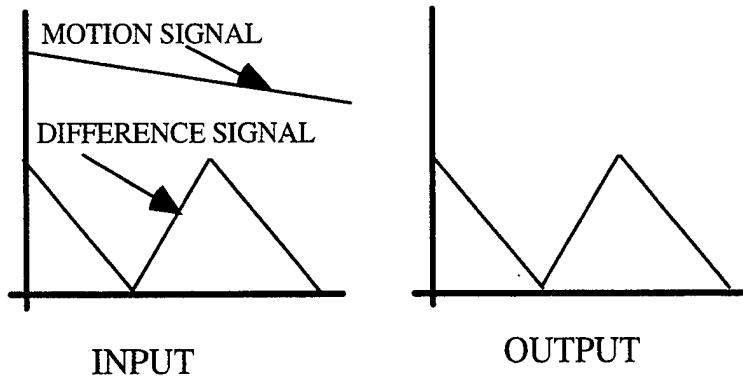


Figure 79a: Motion signal exceeding Difference signal.

Figure 79b shows the operation of the circuit when the difference circuit exceeds the motion signal.

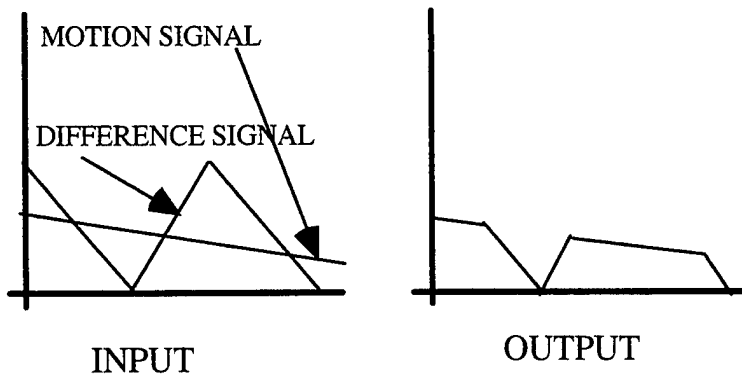


Figure 79b. Difference signal exceeding Motion signal.

The INV and MAX functions perform the exact same function except for negative values. The negative motion vector will be compared to a negative difference value. If the difference value is more negative than the motion value then the motion signal prevails, if not the difference signal prevails. The equation the logic executes is shown below.

$$\text{output} = [\text{limit}(\text{line average} - \text{temporal average})] + \text{temporal average}$$

(where limit is based on the motion signal)

The equation clearly shows that when the motion signal is very high, signifying a significant amount of activity, the output is based completely on the line average. When there is no activity on the motion signal then the output is completely composed of the temporal component.

4.3.5.3 Motion Detector Description

Figure 80 shows the motion detector block diagram that is implemented in the algorithm. There is an IIR filter in the loop that spreads the motion signal beyond a frame as well as vertical spreading with the MIN detector. The source of information for the motion detector architecture will be the green channel. The information is stored in a frame store so that a frame difference signal can be generated. Since the important information to extract at this point is if any motion occurred, the absolute value of the frame difference signal is then taken. The horizontal spreader will use the highest motion signal that has occurred within nine horizontal pixels, four pixels in either direction of the current pixel. Therefore, if the current frame difference signal was large, it would make eight additional signals have a high degree of motion.

At this point there is a horizontal sub sampling of the information, namely, that the frame difference will be used for two adjacent pixels. The sub sampling will reduce the amount of hardware needed in the design.

The MAX function immediately following the horizontal spreader will pick between the current frame difference signal or a percentage of the one that occurred one frame ago. Once a frame difference signal is of significant value it will take a number of frames in order for its effects to disappear. This effect is accomplished with only one frame store where other algorithms use multiple frame stores.

The final MAX function will pick the largest frame difference signal between the current value, a proportionate value of frame difference signal a frame old, or the frame difference signal one line before or after the current reference point. The MIN function eliminates any possible oscillations. The frame delay that holds the frame difference signal is half the size of a full HDTV frame due to the sub sampling.

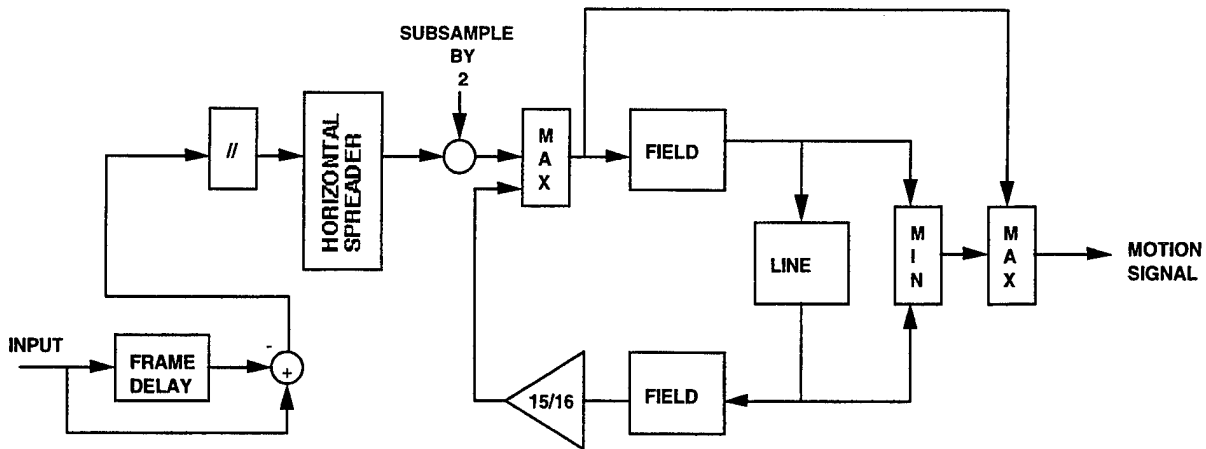


Figure 80. Motion Detector Block Diagram.

4.3.6 Board Level Implementation

The Proscan part of the DMD source electronics is designed to operate with four boards. There are two different boards that have to be designed. One board is the Motion Signal Board (MSB) that derives the motion signals. The other board, the Proscan Processing Board (PPB), generates the derived pixels from the real pixels.

4.3.6.1 System Level Implementation of Proscan

A block diagram signifying how these boards are interconnected is shown in Figure 81. The MSB takes the two 38 MHz input channels that represents the green channel and generates an identical motion signal for each one of the PPB boards. The motion signal is calculated at the pixel data rate then sub sampled by a factor of two. Each PPB operate on one color, therefore there are three boards for an RGB system. The PPB has four 38 MHz data inputs and four 38 MHz data outputs. Two of the input busses are for the real data that is sourced by the HDD 1000 and the other two are the motion signal inputs. Two of the output busses are delay compensated real pixel information, and the other two busses are derived data or the generated lines of information. Control information is not shown in Figure 81.

Each bus is defined as containing either an even pixel or an odd pixel. This bus format allows 74.2 MHz data to be reliably processed by the hardware.

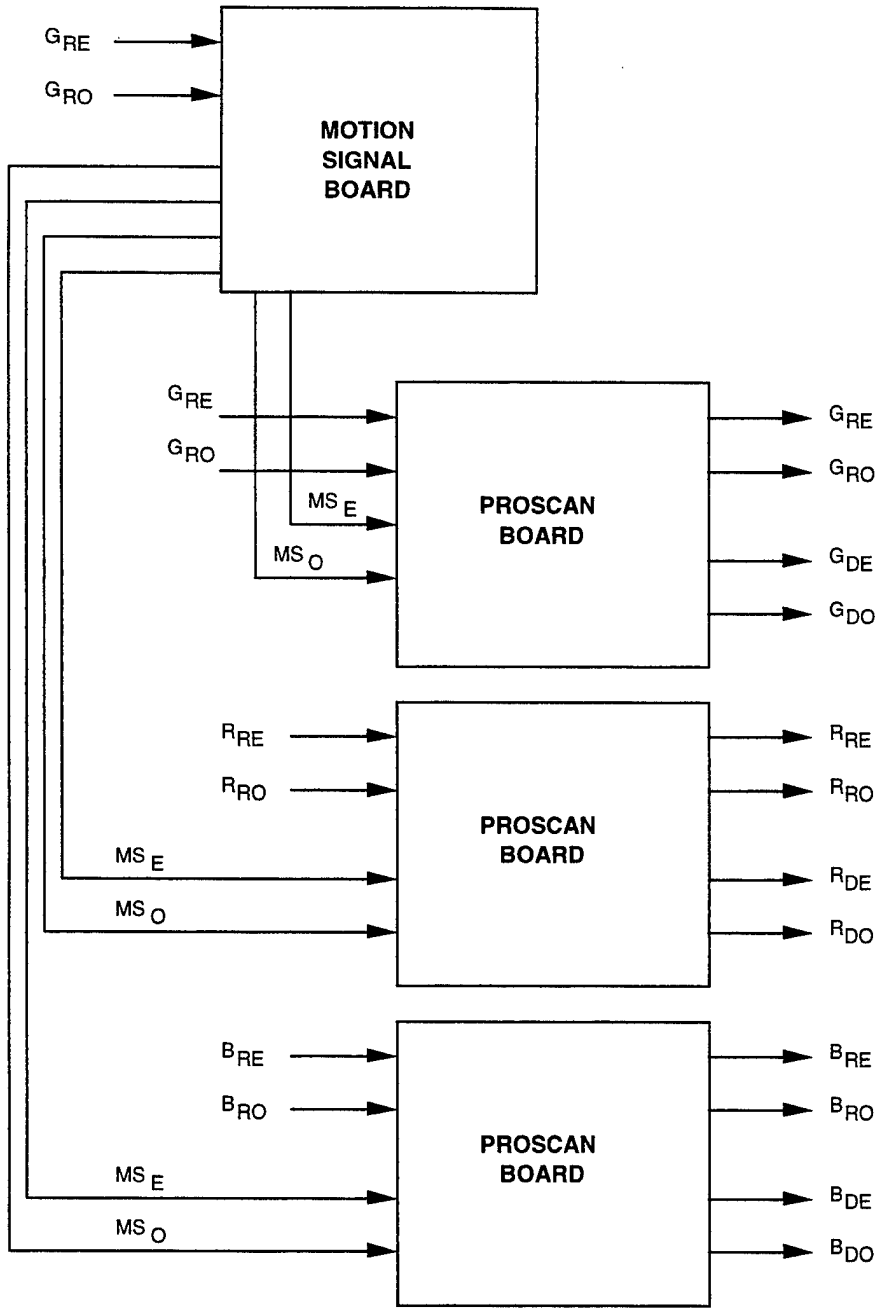


Figure 81. Proscan Board Level Interconnect.

4.3.6.2 Board Orientation with Proscan

A block diagram signifying how the proscan boards fit into the overall DMD source electronics system is shown in Figure 82. The complete system with proscan contains 10 printed circuit boards.

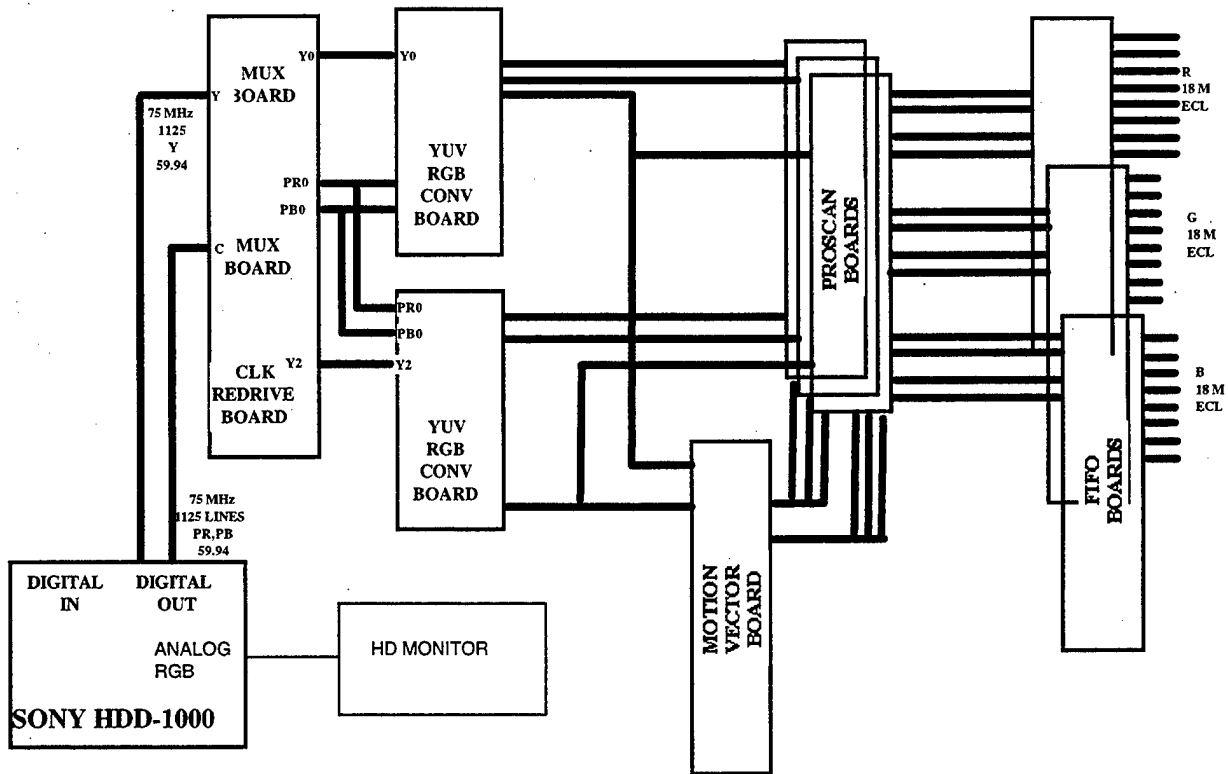


Figure 82. System Block Diagram With Proscan.

The three PPB interface to the two Color Matrix Boards and the three FIFO boards. Each PPB takes one even pixel 38 MHz bus from a Color Matrix Board and a second odd pixel 38 MHz bus from the other Color Matrix Board. The outputs of the PPB supply four 38 MHz busses to a FIFO board. The MSB accepts data from the green channel to determine the motion signals for the PPB, it then supplies each PPB with identical motion signals on two 38 MHz busses. Each of the aforementioned busses are ten bits wide.

4.3.6.3 NEST CONFIGURATION WITH PROSCAN

A diagram signifying where the boards are located in the card cage is shown in Figure 83. This configuration is significantly different then the system without the proscan sub-system. The three FIFO boards have moved to slot numbered 1, 2 and 3. The three PPB have been placed in the old FIFO locations namely, slot numbered 6, 8, and 10. The MSB is placed in slot number 11. The green channel FIFO board is defined in slot number one, and the green channel PPB is defined in slot number 6. The rest of the system has remained unchanged in terms of slot assignment.

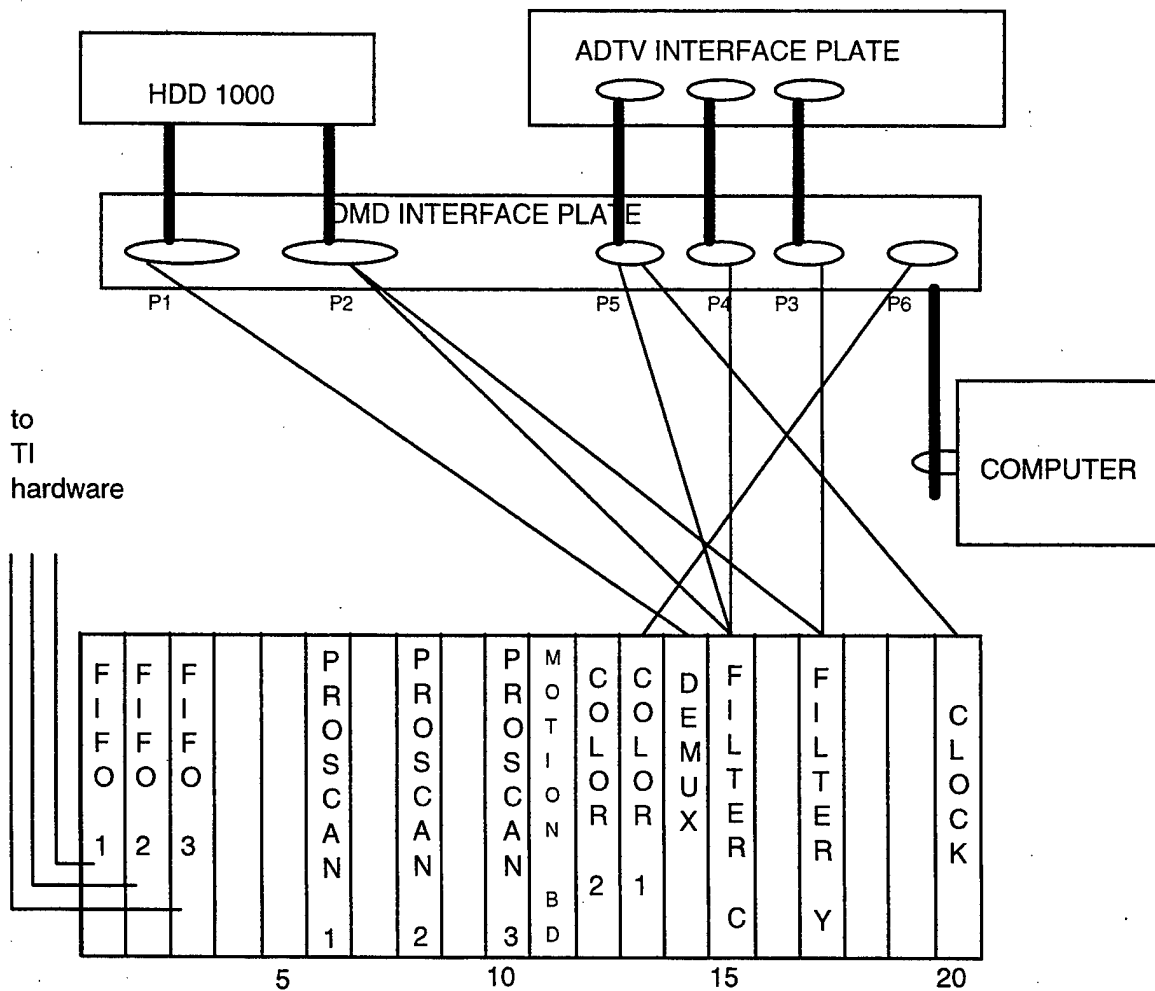


Figure 83. Nest Definition With Proscan.

4.3.7 Board Level Definition

The entire DMD source electronics system has nine boards within the system. The proscan algorithm will add an additional four boards making a total of thirteen boards for the system with proscan. This section will describe in detail the two different type of boards that comprise the proscan option of the design.

4.3.7.1 Input/Output Definitions

This section will describe how data enters and leaves both of the proscan boards.

4.3.7.1.1 Input Clocking Specification

The input data rate of the Proscan Processing boards and the Motions Signal board is 38 MHz. Therefore, each channel or color has an even and odd sub-channel. Each sub-channel is latched

into an Altera chip using the 38 MHz system clock (optionally delayed) that is sent from the Sync Drive Board. The Altera chip multiplexes the incoming data into two additional sub-channels for each 38 MHz input creating an A and a B data path. The chip creates two signals from the 38 MHz clock and the horizontal blanking signal that is supplied to the board. The timing diagram in Figure 84 shows how the incoming 38 MHz data path is broken into two 18 MHz data paths. Signals PHASE1 and PHASE2 are locked to the horizontal signals and the 38 MHz clock in order to guarantee the phase relationship to be identical every time the board is activated. HB DLYD is used to create the signal PULSE which in turn create PHASE1 and PHASE2. These signals are then used to enable every other pixel that comes into the integrated circuit, thereby creating two separate busses each containing every other pixel from the incoming data stream. The diagram shows how the even sub-channel input is distributed to create even sub-channel A DLYED and even sub-channel B. Sub-channel A contains all the even numbered pixels, 0, 2, ..., and sub-channel B contains all the odd numbered pixels, 1,3,....

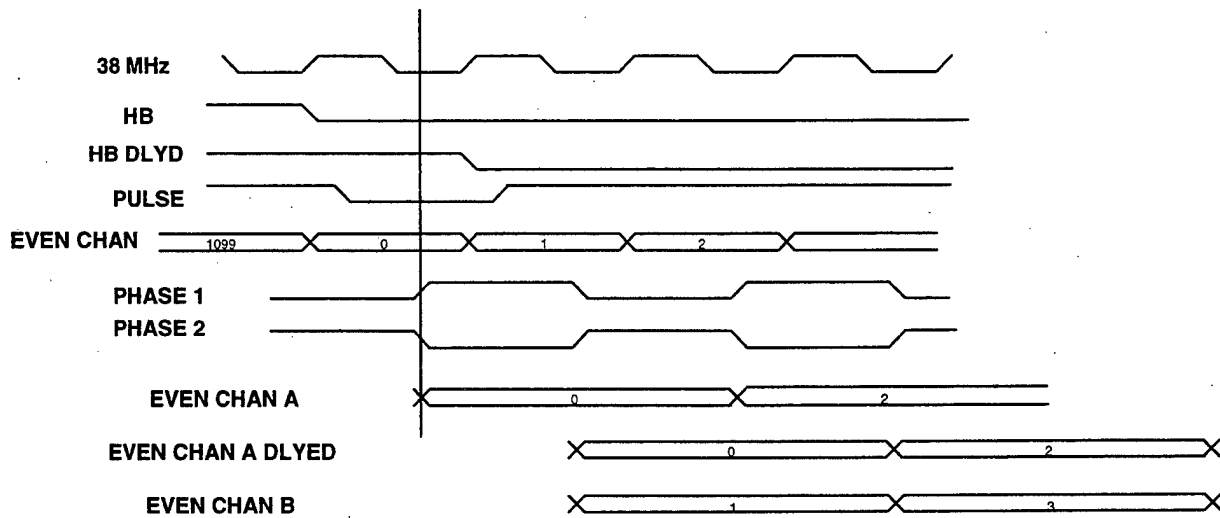


Figure 84. Input Timing.

4.3.7.1.2 Input Definitions

4.3.7.1.2.1 Input Signals to the Proscan Processor

38MHz_CLK: A continuous square wave timing signal, with a nominal frequency of $74.18/2$ MHz and with a duty cycle of $50 \pm 10\%$.

EVEN_DATA: A ten bit wide data bus, stable at the rising edge transition of timing reference $74.18/2$ MHz_CLK that carries the even channel of the data. The even channel is defined to be all pixels with an even index number starting from a reference point, namely the horizontal sync signal.

ODD_DATA: A ten bit wide data bus, stable at the rising edge transition of timing reference $74.18/2$ MHz_CLK that carries the odd channel of the data. The odd channel is defined to

be all pixels with an odd index number starting from a reference point, namely the horizontal sync signal.

HB: A one bit designator which is asserted logic high for the blanking period of the video line.

VB: A one bit wide data signal, stable at the rising edge transition of timing reference 74.18/2 MHz_CLK that carries the active vertical pixel information. A LO on the signal represents active information.

F: A one bit wide data signal, stable at the rising edge transition of timing reference 74.18/2 MHz_CLK that carries even and odd field information.

EVEN_MS: A ten bit wide data bus, stable at the rising edge transition of timing reference 74.18/2 MHz_CLK that carries the even motion signal value.

ODD_MS: A ten bit wide data bus, stable at the rising edge transition of timing reference 74.18/2 MHz_CLK that carries the odd motion signal value.

4.3.7.1.2.2 INPUT SIGNALS TO THE MOTION SIGNAL GENERATOR

38MHz_CLK: A continuous square wave timing signal, with a nominal frequency of 74.18/2 MHz and with a duty cycle of $50 \pm 10\%$.

EVEN_DATA: A ten bit wide data bus, stable at the rising edge transition of timing reference 74.18/2 MHz_CLK that carries the even channel of the data. The even channel is defined to be all pixels with an even index number starting from a reference point, namely the horizontal sync signal.

ODD_DATA: A ten bit wide data bus, stable at the rising edge transition of timing reference 74.18/2 MHz_CLK that carries the odd channel of the data. The odd channel is defined to be all pixels with an odd index number starting from a reference point, namely the horizontal sync signal.

HB: A one bit designator which is asserted logic high for the blanking period of the video line.

VB: A one bit wide data signal, stable at the rising edge transition of timing reference 74.18/2 MHz_CLK that carries the active vertical pixel information. A LO on the signal represents active information.

F: A one bit wide data signal, stable at the rising edge transition of timing reference 74.18/2 MHz_CLK that carries even and odd field information.

4.3.7.1.3 Output Clocking Specification

The output section of the Proscan Processing boards and the Motion Signal board will accept the 18 MHz data paths and clocks and combine the A and B signals together to form one 74.18/2 MHz data path. The 18 MHz clock will be delayed 10 ns so that it will trail the 74.18/2 MHz clock by approximately 4 ns. This will allow the 38 MHz data flow plenty of set up and hold time as it leaves the boards being clocked by the 38 MHz clock. Figure 85 shows how the two 18MHz data is combined into one 38 MHz data path.

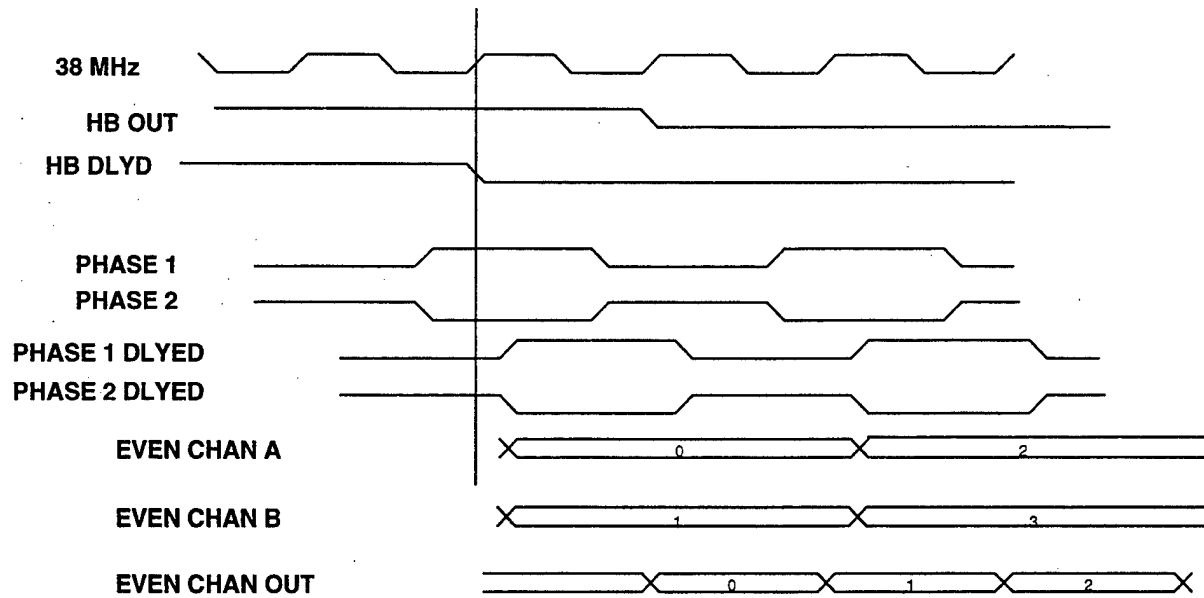


Figure 85. Output Timing.

4.3.7.1.4 Output Definitions

4.3.7.1.4.1 Output Signals from the Proscan Processor

REAL_EVEN_DATA: A ten bit wide data bus, stable at the rising edge transition of timing reference 38MHz_CLK that carries the even channel of the data.

REAL_ODD_DATA: A ten bit wide data bus, stable at the rising edge transition of timing reference 38MHz_CLK that carries the odd channel of the data.

DERIVED_EVEN_DATA: A ten bit wide data bus, stable at the rising edge transition of timing reference 38MHz_CLK that carries the even channel of the data.

DERIVED_ODD_DATA: A ten bit wide data bus, stable at the rising edge transition of timing reference 38MHz_CLK that carries the odd channel of the data.

HB: A one bit designator which is asserted logic high for the blanking period of the video line.

VB: A one bit wide data signal, stable at the rising edge transition of timing reference 74.18/2 MHz_CLK that carries the active vertical pixel information. A LO on the signal represents active information.

F: A one bit wide data signal, stable at the rising edge transition of timing reference 74.18/2 MHz_CLK that carries even and odd field information.

4.3.7.1.4.2 Output Signals from the Motion Signal Generator

EVEN_MS: A ten bit wide data bus, stable at the rising edge transition of timing reference 74.18/2 MHz_CLK that carries the even channel of the data.

ODD_MS: A ten bit wide data bus, stable at the rising edge transition of timing reference 74.18/2 MHz_CLK that carries the odd channel of the data.

4.3.7.2 Motion Signal Board

The Motion Signal Board generates the motion signals for all three channels in the system, the input channel to the MSB is the green channel. It uses the HB signal to generate its 74.18/4 MHz clock from the incoming 74.18/2 MHz clock.

The MSB has eight (8) PLD parts that are used in the motion signal generation process. The eight chips on the board are CLOCK, CNTRB and CNTRC, VECGEN, VECEXP1 and VECEXP3, VECSIG, and TEST. The CLOCK chip accepts two 38 MHz data paths as inputs and generates four 18 MHz data paths. The COUNTERS chips have four internal counters in it so that the appropriately spaced reset signals to each individual line and field delay chips can be generated independently. VECGEN performs the frame difference and absolute value function for the MSB. The VECEXP takes the maximum value of nine horizontal adjacent pixels, this procedure effectively horizontal spreads the motion signal. VECSIG performs an evaluation of four pixels in order to determine the correct motion signal. The TEST chip will be used to generate different values so that the operation of each board can be independently verified.

4.3.7.2.1 Motion Signal Board with More Detail

A diagram showing the detailed design of the MSB is shown in Figure 86. Within the diagram are a number of symbols that represent certain components that are presently defined: an F/2 symbol represents a field delay chip, an L symbol represents a line delay chip, an A symbol represents an Altera chip, an R symbol represents a register, an E symbol represents a 10125 ECL to TTL translator, and a T symbol represents a 10124 TTL to ECL translator chip.

The MSB has an input section, four identical processing sections and two identical output sections. The board accepts two 20 bit ECL busses representing two 10 bit TTL data busses. It also has a clock and a horizontal sync signal supplied by the Color Matrix board and the Sync board. The two data busses enter the CLOCK Altera integrated circuit where it is split into four separate data paths, each data path processes a horizontal pixel. The TEST Altera allows a variety of test patterns to stimulate the board.

The four processing units accept and process data at the 74.17/4 MHz rate. Each section has a frame store within its architecture that can hold one quarter of an HDTV image. The VECGEN Altera IC generates an absolute value frame difference signal to the output section's VECEXP Altera IC.

The VECEXP chips processes all four horizontal pixels at the same time and performs a motion signal spreading function. Specifically, it will place into the current pixel sample the highest value frame difference signal selected from the four adjacent pixel locations on either side of the currently referenced pixel. Since the frame difference signal or motion signal can be sub-sampled by a factor of two, there are only two output sections needed for this design.

The frame difference signal is further processed by the VECSIG Altera chip. This PLD will examine four different signals; namely the current pixel, a field delayed value, a field plus a line delayed value, and a frame delayed value in order to determine which signal has the highest

motion value. The chip will select the highest value from these four values as the current motion signal. This operation allows motion signals to last many frames beyond its origination frame. The motion signal will have to be delayed by the appropriate values in order to get the aforementioned reference pixels.

The CNTRB Altera integrated circuit controls the amount of delays for the processing section delay chips. The total delay for one section of one frame is 1125 lines of 550 pixels, where 2200 pixels is divided into four groups. The CNTRC altera chip controls the amount of delay for the output section delay chips. The output delay is distributed differently so the counters have to sent different signals so that the appropriate tapped reference points are correctly acquired. Also, since this path is in a feedback loop, pixel delays have to be compensated thereby making the counter values different from other values.

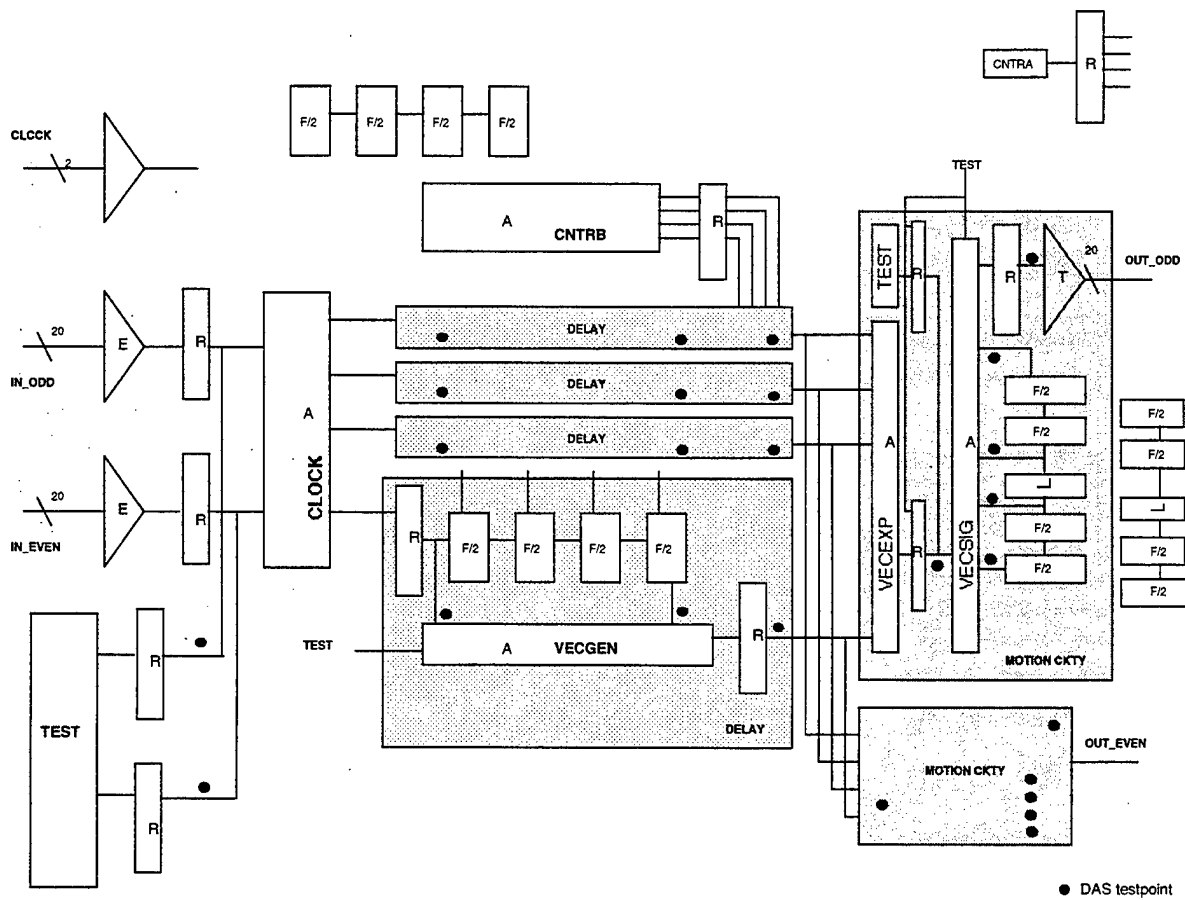


Figure 86. Detailed Motion Signal Board Block Diagram.

The data leaves the MSB at the 74.17/4 MHz effective rate but is actually sampled by the 74.17/2 MHz clock.

4.3.7.2.2 Motion Signal Board Delays

It takes nineteen (19) 18MHz clock cycles to pass through the MSB.

4.3.7.3 Proscan Board

The Proscan Processing Board (PPB) is used by each color to generate the derived pixels. It accepts two motion signals from the Motion Signal Board (MSB), an even motion signal and an odd motion signal. The motion signals have an effective throughput rate of approximately 18 MHz as previously mentioned. The design of the PPB is essentially embedded within a number of PLD integrated circuits.

The PSB has seven (7) separate PLD's in the design. The seven different chips are called CLOCKV2, CLOCK, CNTRA, ADDERS, SWITCHV2, OUTPUTGN, and TEST. The CLOCK, and TEST designs are identical to the ones used in the MSB, with CLOCKV2 being a slightly modified version of the one previously used. The CNTRA chip has the same structure as the other counter chips but with different parameters. The ADDERS design generates spatial and temporal averages; it also generates the difference signal between these averages. SWITCHV2 is a design that implements a soft switch between the spatial and temporal averages. OUTPUTGN is a design that takes two input channels operating at 18 MHz and outputs them in one 38 MHz data channel.

4.3.7.3.1 Proscan Board with More Detail

A diagram showing the detailed design of the PPB is shown in Figure 87. The same symbols used on the previous design are used on this design, they are: an F is a field delay chip, an L is a line delay chip, an A is an Altera chip, an R is a register, an E is a 10125 ECL to TTL translator, and a T is a 10124 TTL to ECL translator chip.

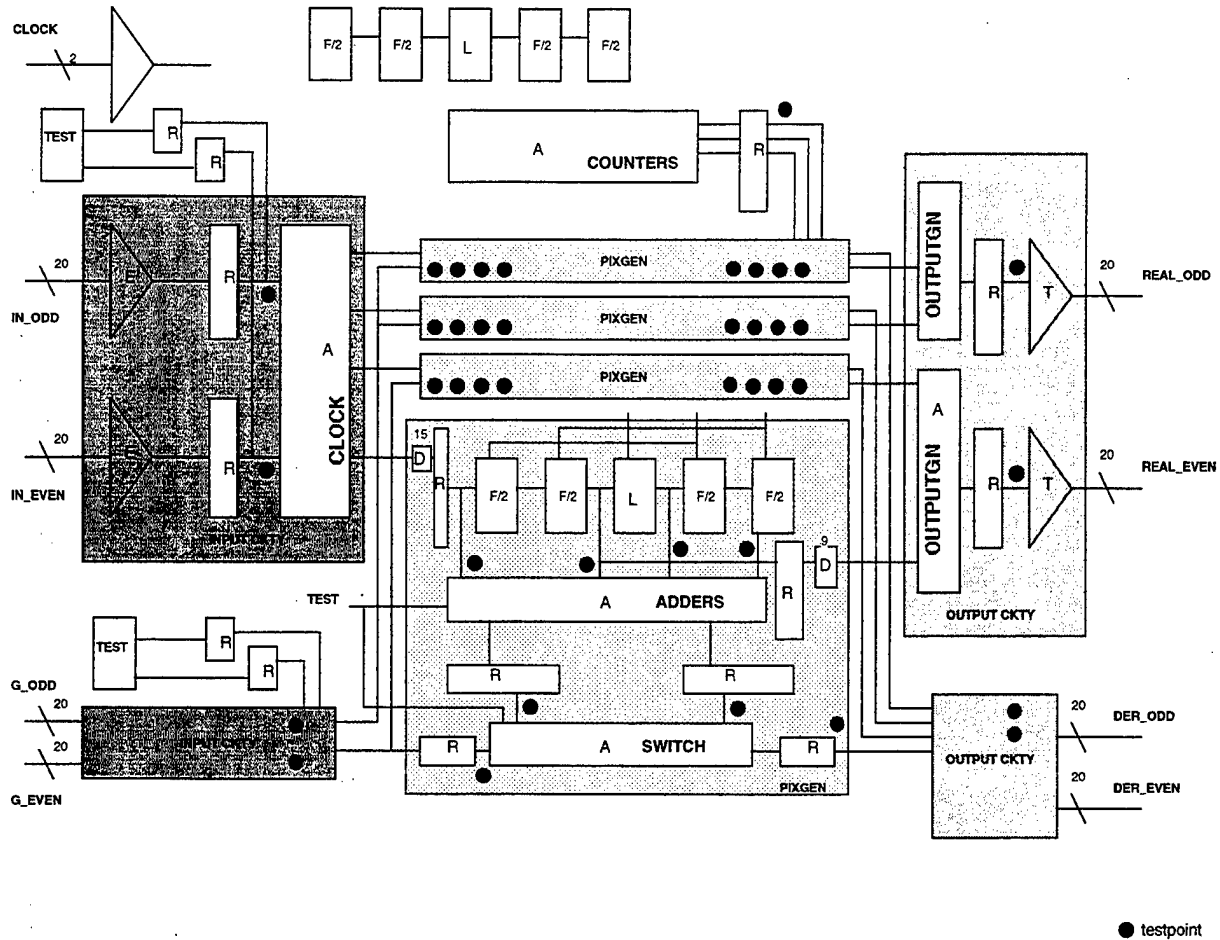


Figure 87. Detailed Proscan Processing Board Block Diagram.

The design has three separate sub-sections: the input section, the processing section and the output section. This design is slightly more complicated than the MSB because it has more processing capability. Also, since there is no horizontal processing implemented on the design, each processing channel operates independently.

The PPB has four input busses, two of the busses are the even and odd motion signals that have been generated by the MSB. The other two signals are the even and odd data signals generated by the Color Matrix boards. All inputs can be bypassed by selecting the TEST Altera PLD that supplies known patterns to all data busses. The CLOCKV2 Altera will create four data paths that operate on adjacent pixels exactly as the MSB operated thereby creating four 74.17/4 MHz data paths.

The four processing paths are identical, each processing path operates on a different horizontal pixel. The processing blocks contain elements that generate three delayed points that are separated by a field, 563 lines, and a frame. These delay lines are controlled by the CNTRA Altera that generates the control signals to the field and line delay chips. Figure 88 shows the relationship between the delayed pixels on the block diagram using field and line delay parts, these delay points are also shown on the VT diagram.

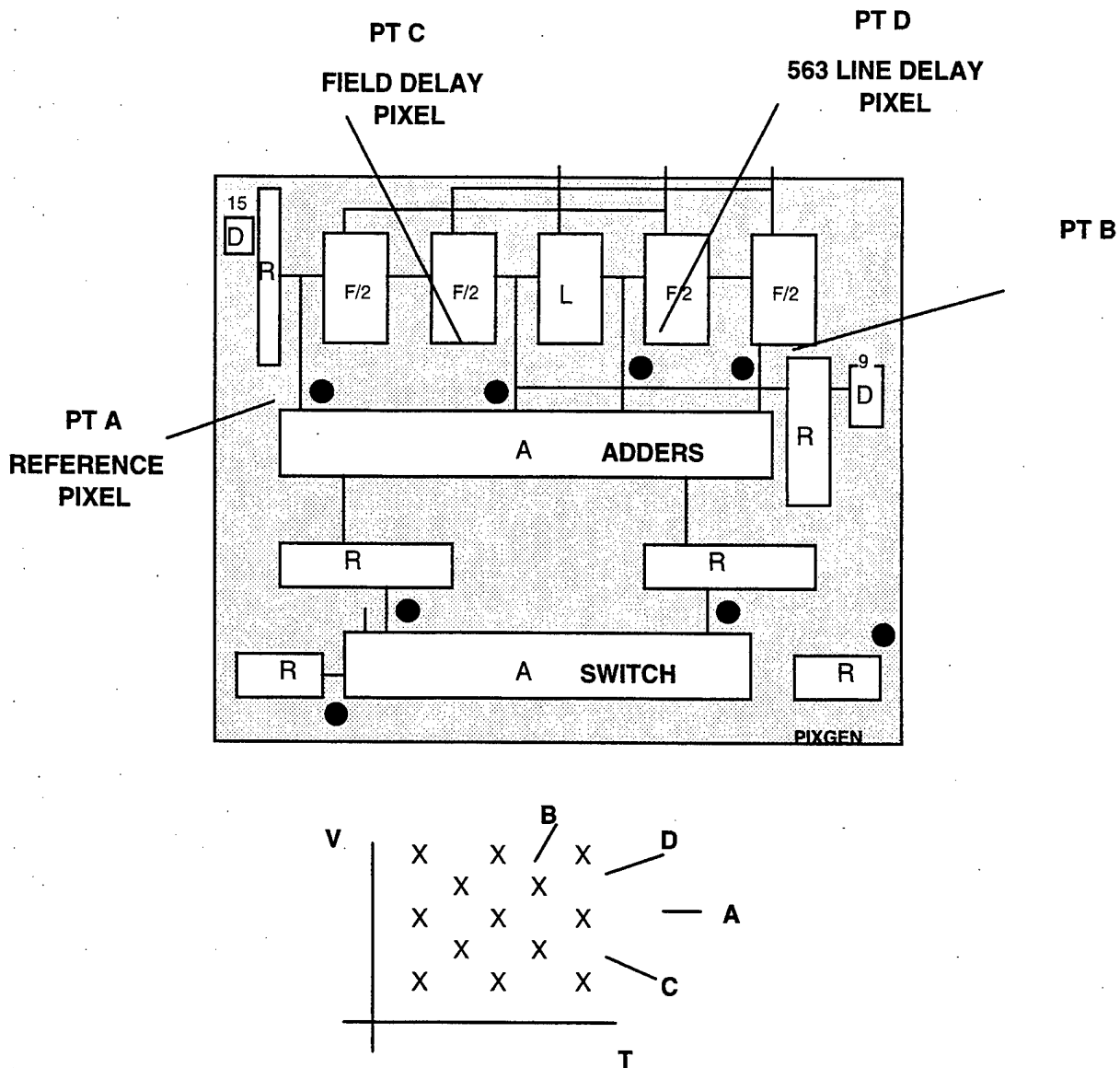


Figure 88. Relationship between pixels on the PPB.

The ADDERS Altera performs the spatial and temporal averaging operations for the algorithm. It also takes the difference between these two signals and supplies it to SWITCHV2 Altera PLD. The SWITCHV2 Altera will execute the soft switch operation discussed earlier in this document. It accepts the motion signal as well as the difference and temporal signals previously generated by the ADDERS PLD. The even motion signal operates on pixel values X0 and X1 while the odd motion signal operates on values X2 and X3. The diagram below shows how the motion signal as well as the data signals are distributed to the four processing logic blocks.

| | | | |
|-----------------|----------------|---------|--------------------|
| | | BLOCK A | X0 X4 X8 Y0 Y2 |
| EVEN INPUT | X0 X2 X4 X6 X8 | | |
| ODD INPUT | X1 X3 X5 X7 | BLOCK B | X1 X5 X9 Y0 Y2 |
| | | | |
| EVEN MOTION SIG | Y0 Y2 Y4 Y6 Y8 | BLOCK C | X2 X6 X10 Y1 Y3 |
| ODD MOTION SIG | Y1 Y3 Y5 Y7 | | |
| | | BLOCK D | X3 X7 X11 Y1 Y3 |

The processing blocks have to align the incoming data to the motion signal information, therefore additional pixel delay elements have been placed into the data path. The processing block also supplies compensated real data information to an output section. The real data is identical to the incoming data with the exception that it has been aligned in time to the derived data so they exit the board in the format previously mentioned in this document. The delay is obtained by adding a number of pixels elements to the field delay tapped value.

The two output sections of the design use an OUTPUTGN Altera integrated circuit. The chip accepts two data busses at the processing block rate and multiplexes them together to obtain a single bus at twice the clock rate.

4.3.7.3.2 Proscan Board Delays

It takes fourteen(14) 18MHz clock cycles to pass through the PPB. The delay to match the data with the motion signal is at twelve (12) 18 MHz clock cycles. To match the real data to the derived data it takes nine (9) 18 MHz clock cycles. The H,V, and F signals need eleven (11) 18 MHz clock cycles to be matched with the data path signals.

4.4 Projector Performance

Measured performance of the DARPA HDD Projector are shown in Table 23.

Table 23

Final HDD DMD Projector Results

| | |
|-----------------------|-----------------|
| • Screen Illuminance | 1056 Lumens |
| • Lamp Power | 575 Watts |
| • DMD Pixels | 2048x1152 |
| • HD Projector Pixels | 1920x1080 |
| • Pixel Spacing | 17-microns, x&y |
| • # DMDs | 3 |
| • Aspect Ratio | 16:9 |
| • Contrast Ratio | 30:1 +* |
| • Field Rate | 60 Hz Proscan |
| • Gray Levels | 8-bits/color |
| • Source | SMPTE260 |

+ Current B2 DMD mirrors have only 8 degree (design goal 10 degrees) tilt angle

* New "hidden hinge" DMD mirror superstructure achieved: 110:1 Checker Board

180:1 Full On-off

5. HDD PROGRAM RESULTS

The following summarizes the DMD HDD Projector development program in viewgraph form as taken from the Final Program Review.

5.1 Summary

5.1.1 Objective

- ✓ To develop a prototype high-definition projection display using the Texas Instruments Digital Micromirror Device (DMD)
 - With 1920x1080 pixels
 - With screen size of 60-inches or greater
 - With screen brightness of 1000 Lumens.

5.1.2 Approach

- ✓ Develop DMD chips for projection display applications:
 - Fixed pattern test array with 1920x1080 mirrors (pixels)
 - CMOS DMD address array >256x256 pixels (768x576)
 - Full-up 2048x1152 HD DMD array
- ✓ Build a 640x480 (NTSC/VGA) pixel projector using 768x576 DMD
- ✓ Develop projection optics for DMD projectors (Sarnoff)
- ✓ Develop peripheral address circuitry for DMD interface
- ✓ Develop system interface to source of HD video (Sarnoff)
- ✓ Develop HD DMD motion adaptive interlace-to-proscan algorithm (Sarnoff)
- ✓ Demonstrate DMD HD projector to Government at final program review.
- ✓ Deliver the HDD projector to Wright Laboratory

5.1.3 Status

- ✓ Completed 768x576 CMOS array
- ✓ Completed 768x576 fully-addressable DMD
- ✓ Completed 640x480 NTSC/VGA 1-DMD front-screen projector
- ✓ Completed 2048x1024 CMOS array
- ✓ Completed 2048x1152 HD DMD chips
- ✓ Completed 3-DMD illumination and optics subassembly
- ✓ Completed HD DMD electronics
- ✓ Completed HD video source (front-end) electronics
- ✓ Completed motion adaptive interlace-to-proscan algorithm and electronics
- ✓ Completed 1920x1080 HD 3-DMD front-screen projector
- ✓ Demonstrated HDD projector DARPA technology showcase in Washington, D.C.
- ✓ Demonstrated HD DMD projector at program final review
- ✓ Delivered HD DMD projector to the Government
- ✓ Completed Final Report.

5.1.4 Schedule/Tasks

| | |
|--|-------|
| ✓ Program start | 03/90 |
| ✓ 1-DMD test optics (Sarnoff) | 05/91 |
| ✓ 768x576 DRAM CMOS | 08/91 |
| ✓ 1920X1080 limited addressability chip (mirrors only) | 09/91 |
| ✓ 768x576 SRAM CMOS | 01/92 |
| ✓ 768X576 fully addressable PAL DMD | 04/92 |
| ✓ 640x480 NTSC/VGA 1-DMD projector using 768x576 DMD | 05/92 |
| ✓ 2048x1152 SRAM CMOS | 10/93 |
| ✓ 2048X1152 HD DMD | 11/93 |
| ✓ DMD HD electronics | 11/93 |
| ✓ 3-DMD HD optics (Sarnoff) | 01/94 |
| ✓ 1920x1080 HD 3-DMD projector | 01/94 |
| ✓ Motion adaptive progressive scan algorithm/electronics | 06/94 |
| ✓ Demo DMD HD projector at final program review | 02/95 |
| ✓ Deliver HD projector to the Government | 03/96 |
| ✓ Complete Final Report | 08/96 |

5.2 Performance vs. Goals

Table 24 gives a comparison of the original HDD projector's performance goals vs. the actual measured results.

Table 24

Performance - Actual vs. Goals for DMD Based HDD Projector

| <u>PARAMETER</u> | <u>GOALS</u> | <u>ACTUAL</u> |
|-----------------------|-----------------|-----------------|
| ✓ Screen illuminance | 1000 lumens | 1056 lumens |
| ✓ Lamp power | 500 Watts | 575 Watts |
| ✓ DMD pixels | 1920x1080 | 2048x1152 |
| ✓ HD projector pixels | 1920x1080 | 1920x1080 |
| ✓ Pixel spacing | 17-microns, x&y | 17-microns, x&y |
| ✓ # DMDs | 3 | 3 |
| ✓ Aspect ratio | 16:9 | 16:9 |
| ● Contrast ratio | 150:1 | ** 30:1 |
| ✓ Field rate | 60Hz proscan | 60 Hz proscan |
| ✓ Gray levels | 7-bits/color | 8-bits/color |
| ✓ Source | ----- | SMPTE260 |

** New "hidden hinge" mirror contrast ratio measured at 180:1 for full on-off fields with NTSC DMD

5.3 Recommendations

Based on the results of the ARPA DMD based HDD projector and the known improvements in both the DMD device and system technology, the following recommendations are made for any future work in this high definition area.

5.3.1 New “Hidden Hinge (HH3)” HD DMD

To be competitive with traditional CRT based projection television systems and emerging LCD projectors, the DMD projection system needs a contrast ratio exceeding 100:1 while maintaining optical efficiency. The original B2 HD DMD can only deliver a contrast ratio in the neighborhood of 50:1 due to light diffracting off edges and flat surfaces and getting into the lens aperture. This effect is shown in Figure 89 where some reflected light can be seen coming from the hinges, hinge posts, and mirror edges even in the case where the mirrors are in the “off” state. The most significant source of contrast ratio degradation in the conventional superstructure is stray light diffracted from the hinges, hinge support posts, and the nonorthogonal mirror edges at the landing tip.

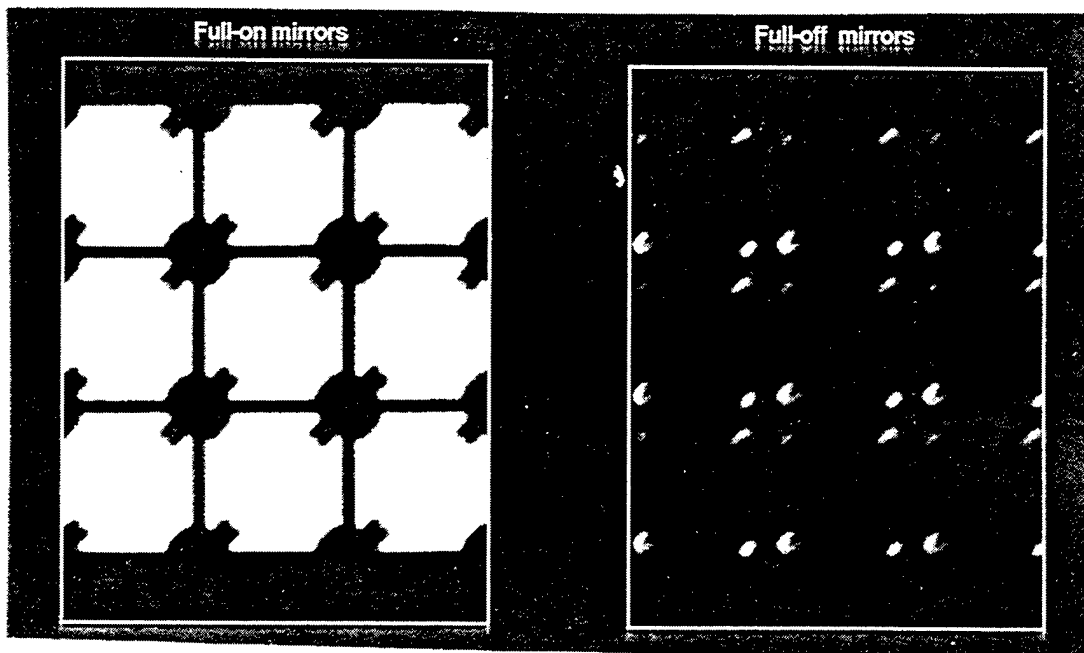


Figure 89. Light Reflected from the B2 Mirror Structure for both the “on” and “off” States.

To overcome this contrast loss and to provide higher mirror active area (higher aperture ratio), TI has developed a new mirror superstructure called “hidden hinge (HH3)”, shown in Figure 90, to provide more square mirrors for the same size array. The hinges and hinge support posts are hidden under the mirror. The mirror is connected by a mirror support post to an underlying yoke. The yoke in turn is connected by torsion hinges to hinge support posts. The address electrodes and landing electrodes are coplanar with the hinge. There are two air gaps, one between the mirror and the underlying hinges and address electrodes, and a second between the coplanar address electrodes and hinge and an underlying third level of metal of the CMOS SRAM structure. Since the hinges and support posts are hidden under the mirror, they cannot diffract light and; therefore, do not degrade the contrast ratio. Also, the mirror edges at the landing tip

are orthogonal, less light is diffracted, resulting in a better contrast ratio. The greater mirror area leads to greater optical efficiency. System contrast ratios of 110:1 have been measured, meeting the contrast ratio requirements of > 100:1 with improved optical efficiency. All future DMDs will use this significantly improved superstructure.

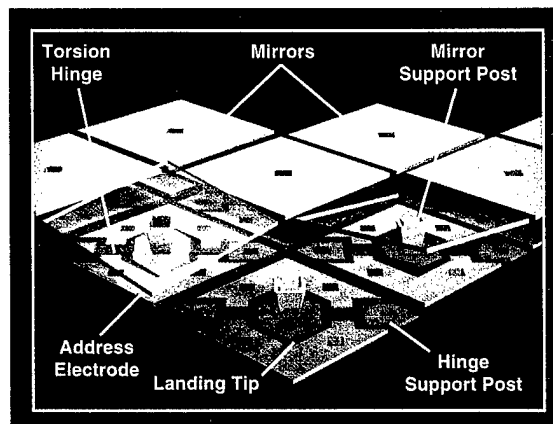


Figure 90. "Hidden Hinge" DMD Superstructure.

5.3.2 DRAM CMOS Structure

The first CMOS structure tried under the DMD mirrors consisted of an array of 2-transistor (2T) dynamic random access memory (DRAM) cells. The structure worked at low light levels, but when operated under high brightness conditions the cell 'hold time' decreased to the point where data valid could not be assured, allowing the picture to degrade before the next field of data could be presented. This quickly led to changing the CMOS cell to a static random access memory (SRAM) structure which had 'built-in' memory (flip-flop) to overcome this problem.

However, today semiconductor technology has advanced to the point where it should be possible to develop a DRAM memory structure underlying the DMD mirrors. Also, with the "hidden hinge" mirror shading the underlying CMOS and with now know additional ways to shield the incoming light, a DRAM CMOS structure looks promising and it is recommended that such an approach be pursued as soon as possible. The 2T vs. 6T cell could have significant impact on CMOS yield resulting in lower cost and higher reliability DMDs. The less densely populated cells also opens up possibilities for redundancy or possibly small pixel sizes.

5.4 QRA

Significant progress has been made in verifying the reliability of the DMD. We achieved a DMD design baseline including the SRAM CMOS, hidden hinge superstructure, and hermetic weld seal package. Since baseline, we have made dramatic improvements in yields, resulting in production of the first zero-defect packaged and burned-in DMDs in November, 1994. By January 1995 we were only packaging DMDs with five or less single point defects. A year earlier we were packaging devices with up to 500 defects. This trend is expected to continue very low defect, high performance as products are qualified for production.

TI continues Reliability Assessment Testing and has eliminated most of the known risks areas by successfully passing the tests shown in Table 25 (data as of February 1995). This was achieved by selecting a hermetic package to eliminate package integrity concerns, by changing the CMOS design to provide electro-static discharge (ESD) protection to the 2000-volt level, and by changing the hinge materials and processes to eliminate hinge memory effects.

Table 25
DMD Qualification Data
February 1995

864 X 576 DMD Assessment Test Results

| TEST TYPE | TEST DESCRIPTION | MIL-STD-883D REFERENCE | RESULTS |
|---------------------|---|---------------------------|---------|
| Thermal Shock | 15 cycles, -25°C to +100°C | Method 1011, Condition B | Passed |
| Temperature Cycling | 100 cycles, -25°C to +100°C | Method 1010, Condition A | Passed |
| Moisture Resistance | 10 days, T-cycles, RH to 100% | Method 1004 | Passed |
| Seal Integrity | Fine and Gross Leak | Method 1014, Condition B1 | Passed |
| Altitude | | | |
| Operating | Sea Level to 12,000 Feet | Method 1001, Condition A | Passed |
| Non-operating | Sea Level to 20,000 Feet | | Passed |
| ESD Susceptibility | 3 +/- 2000-Volt Pulses on Each Pin Combination | Method 3015, Class 1 | Passed |
| Mechanical Shock | 5 Shock Pulses, 6 Axis, 1500 G Peak, 0.5 Msec Pulse | Method 2002, Condition B | Passed |
| Vibration | 20 G Peak, 20-2000 Hz, 3 Axis, 48 Minutes Total | Method 2007, Condition A | Passed |
| Acceleration | 10,000 G, Y Axis, 1 Minute | Method 2002, Condition B | Passed |
| Bond Strength | | Method 2011, Condition B | Passed |
| Die Attach | | Method 2027 | Passed |

Table 25-Con't
DMD Qualification Data
February 1995

| TEST TYPE | TEST DESCRIPTION | RESULTS | COMMENTS |
|-------------------------------------|---|-------------|--|
| Hinge Fatigue Accelerated Life Test | 60.5-billion mirror cycles | Passed | No evidence of hinge fatigue. |
| Hinge Memory Characterization | 1000-hour test samples at 65°C, 100/0 duty cycle | Passed | 2-volt bias shift in 1000 hours acceptable. Isolated pixel failures are remaining challenge. |
| Reliability Life Test | 1000-hour test samples at: 25, 45, and 65°C, and 50/50 duty cycle | In Progress | Completed 850 hours at 45, 65, and 85°C. 5 units shorted due to particle problems. 38 new pixel failures on 27 units (1.4 pixels / unit). Average increase goal = 1.0 pixel / unit. |
| | 1000-hour test samples at: 25, 45, and 65°C, and 95/5 duty cycle | In Progress | 95/5 duty cycle test samples started. |
| Optical Performance | Defect mapping, tilt angle | Complete | |
| | Uniformity, reflectivity, and contrast ratio | In Work | Sample capability 3/95. |

5.5 Manufacturing

The worldwide display market in year 2000 is estimated to be > \$20B. Driven by the opportunity that such a potential market offers, Texas Instruments' commitment to bring DMD display technology to market with highly compelling, affordable, and reliable display products is one of the largest for any single technology in the history of the company. Manufacturing facilities are in place in Dallas, Texas to carry DMD technology to the end of this decade and plans are in place for future expansion well into the next millennium.

5.6 Dual-use Display Products

Based on marketing data and projections, we expect that affordable and reliable DMD display products will be available that can satisfy a large portion of the military and Government display requirements. As a result, our goal is to achieve a robust commercial base from which the military can order “off-the-shelf” display products. In addition, we would expect to make available through TI and/or other OEMs, more military “hardened” digital display products. Table 26 lists some of the dual-use application that DMD displays are expected to support.

**Table 26
Dual-use Applications of DMD-based Displays**

| Military | Commercial/Consumer |
|--------------------------------------|----------------------------|
| Shipboard displays | Consumer television |
| Command control displays | High-definition television |
| Training/simulation displays | Conference room displays |
| Digital mapping | Professional displays |
| Multimedia (video/computer) displays | Cinema projectors |
| Air traffic control displays | Home theater displays |
| Workstation displays | Workstation displays |
| Monitors | Video games |
| Helmet-mounted displays | Virtual reality |
| Heads-up displays (HUD) | Automotive HUD |
| Large situation awareness displays | Personal displays |

More specifically, we recently worked with outside consultants in an attempt to understand the size of the military display market. The results of this evaluation are shown in Figure 27. The accuracy of this data is uncertain at this time, especially with all the changes taking place within the Government, but it is clear that there is a need for these products that results in a sizable market.

5.7 Benefits to Society

DMD display products offer safe, compelling digital display performance. There is no high voltage radiation from these projector products and the stability and sharpness of the picture is “easy on the eye”. The displays should be ideal for workstation applications where operators sit all day staring at their screen.

A goal of Texas Instruments is to make sure that DMD technology is made available use in many "dual use" military applications in the future.

5.9 Acknowledgments

Texas Instruments would like to take this opportunity to thank the following organizations for their strong support throughout the DARPA HDD program at TI:

1. To DARPA (ARPA) for their willingness to get behind DMD technology at a time when it seemed like a "far out" approach to HD displays. The \$10M-plus which DARPA funded this effort, over a five year period, coupled with TI R&D and other funding from a TI partner allowed DMD technology to gain enough momentum in the research labs to allow this development effort to gain corporate venture status within TI. In particular, thanks to Dr. Lance Glasser, Dr. Marko Slusarczuk, Dr. David Slododin, and Dr. Mark Hartney for their strong support over the continued length of the program.
2. To Wright Laboratory for their support, direction, and attention to the program on an almost daily basis. Also, for the contract support and scheduling of reviews. A special thanks to Dr. Darrell Hopper and Capt. Robert Blanton.
3. To the David Sarnoff Research Center (Sarnoff) for the expertise they brought to the program as a partner with responsibility in the area of optics and front-end electronics. Thanks especially to Dr. Phil Heyman, Dr. Herschel Burstyn, and Mr. Nicola Fedele.

Appendix A

DISPLAY SYSTEMS

A. SELF LUMINESCENT

1. CRT

The color CRT display has a long history, and has shown itself to be adaptable to the demands of large high-definition displays. Recent developments in the field have pushed resolutions to 2048 by 2048 with a brightness approaching 30 fL. There is usually a tradeoff between resolution and brightness; and thus tubes at commercial broadcast standards can be as bright as 80 fL (Masterman et al., 1990, 1991). A 43-in.-diagonal high-definition screen would have a light output of 193 lm. The efficiency of a CRT display is also high, in the range of 5 to 20 lm/W (Goede, 1991).

CRTs are also used in projection displays. Currently available units with resolutions of 1000 to 2400 lines have light outputs of between 500 and 1620 lm, with 1000 lm being typical (Matthies and Heyman, 1991). The typical efficiency of a projection TV may only be of the order of 2.7 lm/W, based upon a phosphor efficiency for white-D (NTSC standard white) of 11 lm/W. Overall efficiency will drop if the energy requirements for beam deflection are included. Clearly, the light utilization is not as great as for direct-view systems. The reduction in efficiency is mainly due to the difficulty in collecting the light being emitted by the phosphor screen, a Lambertian source (Stroemer, 1989).

2. Electroluminescent

Electroluminescent displays use phosphors that are excited via the application of an electric field. They have been made in arrays as large as 1000 x 1000, not quite at high-definition display (HDD) standards. Brightnesses are in the 5- to 30-fL range, depending upon manufacturer and color. Typical efficiencies, for the most efficient color in a display, lie in the 0.8- to 30-lm/W region (Goede, 1991).

3. Plasma

The pixel count for some versions of these displays approach HDD standards. Efficiencies of 1.5 lm/W have been demonstrated. However, there remain problems in developing a full-color display for lack of suitable materials (Goede, 1991). Some of these problems may be overcome through the use of phosphors. The gas is made to radiate in the UV, and it is this radiation that excites the phosphors.

4. Light Valves

a. Oil-film modulators

There are two main suppliers of oil-film light-valve projectors: GE (Telaria) and Gretag (Eidophor). These projectors, in effect, write diffraction gratings on the oil film. The efficiency of the Telaria system is of the order of 0.5 lm/W (Good, 1971). Oil-film displays are usually expensive but exhibit a large amount of light on the screen, from between 4000 to 56000 lm (Matthies, 1991). The high light levels make these projectors ideal for theater-size displays, even though their efficiencies may be low.

b. Liquid crystals

Two schemes are employed to modulate the light in LCDs: polarization rotation through a twisted nematic (TN) medium, and scattering by polymer-dispersed liquid crystal (PDLC).

It is well known that only a large change in optical properties over the scale of the wavelength of light will give rise to reflection or scattering. Thus, if the directrix, the axis of polarizability, of a liquid crystal slowly rotates by 90°, efficient coupling can be made between two crossed polarizers: the TN crystal in the on-state is optically active. When an external electric field is applied, so as to align the cells' polarization vectors along the direction of light propagation, no polarization rotation is possible, and thus the valve is turned off. In PDLC scattering can take place if dispersed particles in the cell differ in index from the surrounding medium. Since the polymer used can have an index tensor, orientation of the "particle" by an external field can effectively give rise to index matching between the solute and solvent in a specific direction of propagation. The operation leads to transparency (Bruce, 1991), (Scheuble, 1991).

The highest efficiencies that have been reported to date are for liquid crystal light valves of the dispersive type. In particular a Nematic Curvalinear Aligned Phase (NCAP) modulator placed in a Sharp projection system was shown to have an efficiency of 4.4 lm/W with a contrast ratio of about 40:1. Since these devices are scatterers, and since the lens aperture both collects the desired light and rejects the scattered light, the contrast and efficiency are correlated quantities (Jones, 1991).

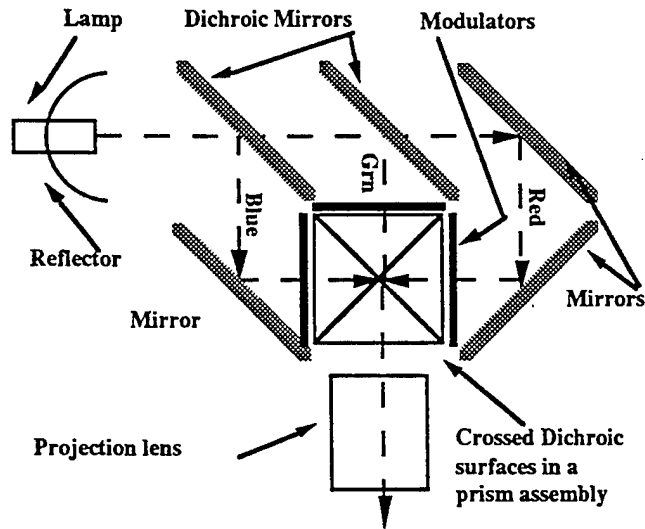


Figure A1. *A color projector using transmissive liquid crystal light valves. The geometry is similar to that used in the Kodak and Hughes systems (Miyasaka,1989).*

Given the basic physics of operation, there are various drive, addressing, and illumination schemes that are possible. Many of these are covered in Bruce (1991) and Scheuble (1991). Some classic designs for transmissive liquid crystal modulators can be found in Miyasaki (1989). These are shown in Figs. A1 and A2.

Some novel methods are possible if one uses reflective liquid crystal light modulators. One, used in conjunction with a laser-addressed light valve, used a re-entrant lens system (Mori, 1988). A full discussion of the system, and one that can be configured for use with the DMD, will be discussed in a later section.

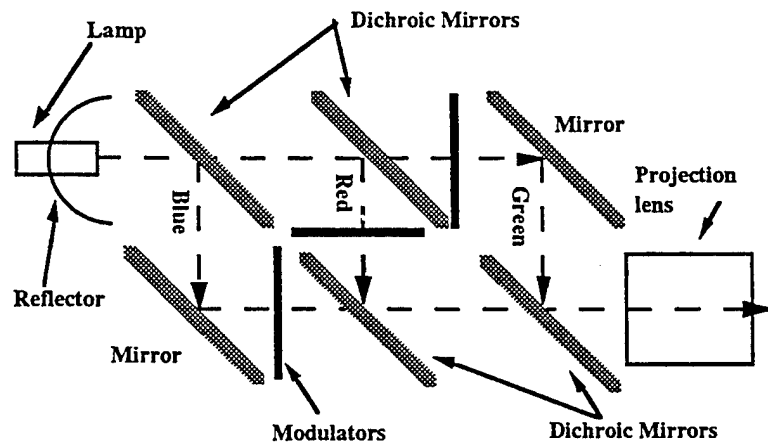


Figure A2. *A color projector using transmissive liquid crystal light valves. The geometry is similar to that used in the Epson and Sharp systems. The former uses a halogen lamp, while the latter uses a metal-halide arc lamp (Miyasaka, 1989).*

c. Deformable Mirror Device (DMD)

The deformable mirror device is an array of mirrors on torsion bars. The mirrors are driven by electrostatic couples. The devices that are discussed in this paper have picture elements (pixels) that are taken to be $17\ \mu$ on a side. The device diagonal is taken to be 37.5 mm, and the aspect ratio as 16:9. The diffraction pattern associated with a square aperture influences throughput and contrast.

Appendix B

SYSTEM REQUIREMENTS

A. ASPECT RATIO

As we pointed out earlier, a minimum requirement was a 3:5 aspect ratio but that the industry was clearly moving to the 9:16 aspect ratio. The 1080 x1920 pixels contained in the TI light valve express the latter standard.

B. RESOLUTION

The pixels are on a 17- μ pitch; thus a resolution of 30 lines/mm in the projection system is the minimum standard requirement. If we wish to resolve the square pixels on the screen, a higher resolution will be required. There is much debate as to whether or not a better picture is obtained if one can resolve the pixels. From the point of view of design, if one has the spatial frequency response to resolve pixels, it is an easy matter to reduce the Modulation Transfer function (MTF) by defocusing. Since defocusing acts like a low pass filter, the pixels will be smoothed out. Maintaining resolution of the pixels puts constraints on the apertures in the projection system. The optical resolution criteria can be restated as the collection of sufficient orders, or Fourier components, of the diffracted optical field.

C. SCREEN BRIGHTNESS

We need a screen brightness that, at the very least, is comparable to that of the large-screen CRTs. This implies something in excess of 30 fL. For design purposes, a screen image diagonal of at least 60 in. is assumed. Given a 9 x 16 aspect ratio, this diagonal implies an area of 10.7 sq ft. Since the total amount of light on the screen is the brightness times the area, we find that we require a minimum of 320 screen lm. For comparison, the SHARP projection television is specified as having a peak screen brightness of 55 fL. By assuming that the illumination is uniform over the 40-in.-diagonal picture and a 3 x4 aspect ratio, we calculate 290 screen lm. (Note that the 290 lm are obtained via a 150-W metal-halide lamp, yielding an overall efficiency of 1.9 lm/W. Assuming a factor of 0.8 for the efficiency of the color splitters and combiners, we arrive at a 2.4 lm/W efficiency for an equivalent black and white system.) Typically the SHARP liquid crystal projector is run with an 80-in.-diagonal, yielding a screen brightness of a little less than 14 fL.

If the prototype system is to allow the use of a color wheel, the amount of light budgeted must be increased by approximately a factor of four, thus compensating for the serial display of the three separate color fields plus the blanking times between fields. The equivalent black and white projection system must be able to deliver about 1400 lm to the screen. By replacing the color wheel system with a three-modulator display, we should be able to increase the average brightness of the projection system to about 110 fL. (See Table 8). A screen brightness of better than 50 fL is suggested by (Schlam, 1991).

D. CONTRAST

The accepted contrast criteria currently appears to be a moving target. It was considered, once, that a contrast ratio of better than 10:1 was good enough (Schlam, 1991). However, current displays are expected to perform at ratios as high as 50:1, 100:1, or better (Ando et al., 1989), (Stroemer, 1989). There are at least two reasons for this. First, the 10:1 contrast ratio must be maintained under ambient light conditions, which will reduce the apparent contrast. Second, the demands made by such fields as medical imagery and surveillance are pushing the state of the art. Operators in these fields use criteria that are based upon their experiences in viewing film negatives.

E. DYNAMIC RANGE

Since high-definition display systems will have to replace film in fields where the analysis criteria depends upon the properties of photographic medium, luminance and color dynamic range are important. Scales that range from 8 to 12 bits/color are discussed (Demos, 1989). Clearly not only does the number of bits/color set the greyscale, but it also sets the number of colors and their saturation as well.

F. EFFICIENCY

The question of efficiency can be phrased with respect to three criteria:

- screen brightness relative to line power input,
- screen brightness referenced to the optical power available from the light source, and
- the optical efficiency of the light source.

From a systems' viewpoint the first criterion is paramount, the others being steps along the way. The review of current display indicates that an efficiency near 3 lm/W, from lamp electrical input to the screen, is very competitive.

Appendix C

DIFFRACTION

A. THE LIGHT VALVE STRUCTURE

As was stated in the main text, the effects of diffraction from the DMD elements determine the optical behavior of the device in a projection system.

The relative importance of diffraction effects for various devices can be ascertained in the following manner. The image size is taken to be 5 ft at a 10-ft distance. A typical liquid crystal modulator may be 100 mm on the diagonal. Taking the resolution to be 500 x 500 pixels, each pixel will be approximately 140 μ . Red light is 0.7 μ . Thus the second zero occurs at an angle of 0.6°. For a 17- μ pixel, as one finds on the DMD, the second zero occurs at 4.7°. Thus, diffraction effects are nearly an order of magnitude larger in a DMD light valve than in a typical liquid crystal display. This must be taken into account when matching the collector to the projection lens.

B. DIFFRACTION FROM RECTANGULAR LIGHT VALVE ELEMENTS

Both liquid crystals and the DMD use discrete pixels. One can assume that each element is a rectangular aperture with dimensions $2x_0$ by $2y_0$ through which light is diffracted. The diffraction pattern is described by, t , the Fourier transform of the transmittance function. The transmittance function is unity within the aperture and zero elsewhere. Thus for a rectangular aperture

$$t = \{ \sin(2\pi u x_0) / \pi u \} \{ \sin(2\pi v y_0) / \pi v \} \quad (C1 a)$$

where

$$u = \alpha - \alpha' / \lambda, \quad \text{and} \quad v = \beta - \beta' / \lambda. \quad (C1 b)$$

Here α and β are direction cosines. The difference between the unprimed, incoming direction, and the primed outgoing beam, is a measure of the scattering angle (Klein, 1970). The zeroes in the diffraction pattern, in the x direction, occur when the angle of diffraction, ϕ , is

$$\phi = \sin^{-1}(m\lambda / 2x_0) \quad (C2)$$

and m is an integer that defines the diffraction order.

A good imaging system will pass the zeroth, first, and possibly the second diffraction orders. The statement is justified by Fourier analysis.

The Abbe theory of image formation states that any imaging system possesses a plane with a Fourier transform of the object. Light propagation from the transform plane will reconstruct the image by appropriately summing over the Fourier components in the image plane. If the limiting aperture is placed in the transform plane, then only low spatial frequency Fourier components will be allowed to pass. In other words the limiting pupil acts as a low pass spatial filter. Since the zeroth order just carries brightness information, the aperture must be made large enough to pass the first diffraction order associated with the highest desired spatial frequency. Thus we have an estimate for the minimum stop size in the system. This is the aperture that rejects the undesired beam deflected by the light valve.

Throughput

In any projection scheme, an image plane for the source will exist. What will be observed is a convolution of the source image with the diffraction pattern for a pixel. Initially the source image will be ignored. The act of focusing the source superposes the diffraction patterns of the pixels (each pixel element has an identical pattern at infinity, and it is this pattern that the lens brings from infinity to the focal plane). The incoherent light source implies no mixing terms in the intensity. The diffraction pattern is formed far away from the grating and thus the Fraunhofer theory is valid. These simplifications allow the effect of the limiting aperture to be calculated. The electric field is proportional to the Fourier transform of the transmittance function. The intensity in the transform plane, I , is then simply i^2 . Thus for a point light source

$$I \propto \{ \sin^2(\tau)/\tau^2 \} \{ \sin^2(\omega)/\omega^2 \} \\ = j_0^2(\tau) j_0^2(\omega) = \text{sinc}^2(\tau) \text{sinc}^2(\omega). \tag{C3}$$

All three expressions are identical, by definition, $j_0(\tau)$ is the spherical Bessel function, and $\text{sinc}(x) = \sin(x)/x$. The variables τ and ω are placeholders for $2\pi u x_0$ and $2\pi v y_0$, respectively. The Bessel function maxima occur at τ or $\omega = 0, 1.430\pi, 2.459\pi$, etc.

Since the maximum throughput is unity, a normalization is defined

$$N = \text{normalization} = \int_0^\infty \frac{\sin^2 \tau}{\tau^2} d\tau = \frac{\pi}{2} \tag{C4}$$

and thus throughput, T , becomes

$$T = \text{throughput} = \frac{\int_0^{\tau_0} \frac{\sin^2 \tau}{\tau^2} d\tau \int_0^{\omega_0} \frac{\sin^2 \omega}{\omega^2} d\omega}{\left(\frac{\pi}{2}\right)^2} \quad (C5)$$

The equation is a simplification since the projection lens, or limiting opening, is actually a circular aperture, not square, and the image of the light source has finite size. The results, however, are valid as a lower limit estimate of the throughput because the brightest elements in the diffraction pattern are ostensibly on a vertically oriented cross. The intensity maxima that are off the cross are ignorable as can be seen in the following table where p,q denotes the order pair for the maximum (adapted from Born and Wolf, 1975).

TABLE C1

The Location and Relative Strengths of the Intensity Maxima for a Square Aperture

| | q = 0 | q = 1 | q = 2 |
|-------|---------|---------|---------|
| p = 0 | 1 | 0.04718 | 0.01694 |
| p = 1 | 0.04718 | 0.00226 | 0.00080 |
| p = 2 | 0.01694 | 0.00080 | 0.00029 |

If only the zeroth order maxima is to be retained, we put the aperture edge at the first minima, then τ_0 and ω_0 are taken to be $m\pi$, and $n\pi$, respectively; with $m = 1$. For the retention of the first order maxima it is sufficient to take $m = n = 2$. Collection of higher-order terms are equivalent to taking higher values of m and n . Table 5 shows the throughput, for a *point source*, as a function of the number of orders retained. Throughput increases very slowly after the retention of the second order.

The model can be made more complete by assuming that an image of the source is formed at each point of the diffraction pattern, a convolution of the two effects. The weighting associated with each point can be taken as the ratios of the peak intensities in the diffraction pattern. Because of the finite size of the source, some light from the higher orders can pass through the projection lens. The finite source size can simultaneously increase the light throughput, yield a gentler roll-off on the MTF (rather than what would be considered a brick-wall filter), and decrease the contrast ratio.

To consider the question of throughput, start by considering a projection lens with a given focal length. The problem is actually one of angles, not distances, and thus it is possible to measure all quantities relative to focal length of the lens. Define $\gamma = \delta\lambda/2x_0$, as before. Maxima occur when $\delta = 0, 1.43, 2.459, 3.470, 4.479, 5.482, 6.484$, etc. There are two circles in the problem, the aperture of the projection lens and the image of the source. The radii of the two circles can be taken to be r_1 and r_2 , respectively (see Fig. C1). The image size relative to the aperture may be defined as M . Let us call the diffraction angle for any given order, Θ_ϵ . Clearly the zeroth order is in the center of the lens. Thus the sides of the triangle connecting the center of the projection lens, the center of the diffraction order, and an intersection point of the two circles, are defined by the following set of equations:

$$\tan(\Theta_\epsilon) = \gamma / \sqrt{1 - \gamma^2}, \quad (C6 a)$$

$$r_1 = 1/(2 f\#), \quad (C6 b)$$

$$r_2 = M r_1, \quad (C6 c)$$

and

$$\Delta = \tan(\Theta_\epsilon). \quad (C6 d)$$

The area of the quadrilateral, Quad, formed by two such triangles can be derived from:

$$\text{Quad} = 2 [s(s-r_1)(s-r_2)(s-\Delta)]^{1/2} \quad (C7 a)$$

with

$$s = (r_1 + r_2 + \Delta). \quad (C7 b)$$

It is now possible to apply the law of cosines to find the base angles, A and B, of the triangle:

$$\cos(A) = (r_1^2 - r_2^2 + \Delta^2)/(2\Delta r_1) \quad (C8 a)$$

$$\cos(B) = (r_2^2 - r_1^2 + \Delta^2)/(2\Delta r_2). \quad (C8 b)$$

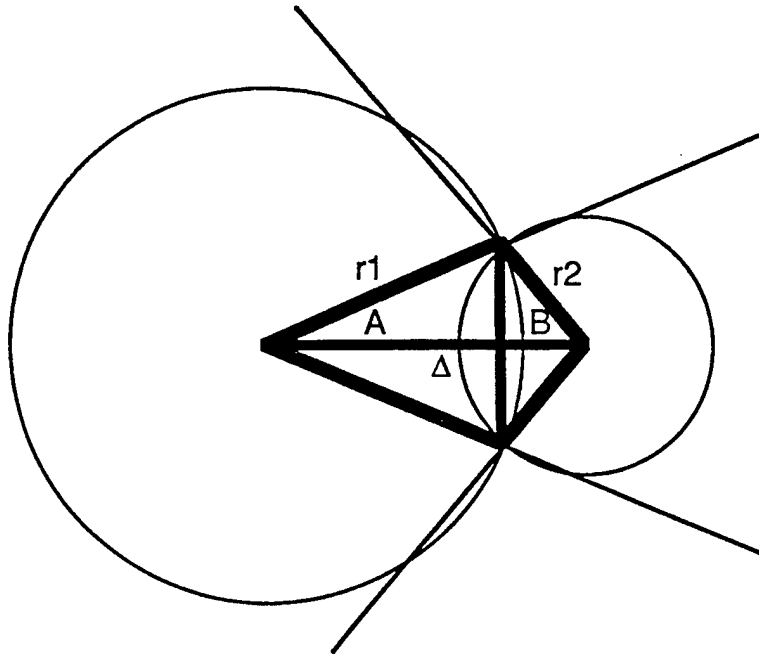


Figure C1. *The image of the source with a radius, r_2 , overlaps the limiting aperture of radius, r_1 .*

The sectors of the circles involved at the intersection of the circles are therefore:

$$S_1 = A r_1^2 \quad (\text{C9 a})$$

and

$$S_2 = B r_2^2. \quad (\text{C9 b})$$

Giving the area of the intersection, I , as

$$I = A r_1^2 + B r_2^2 - \text{Quad.} \quad (\text{C10})$$

To find what fraction of the order, OF , makes its way through the projection lens, the overlap area must be divided by the area of the image of the source or

$$OF = I / (\pi r_2^2). \quad (\text{C11})$$

Figures C2a and C2b show OF as a function of M for $f/4$ and $f/3.1$ projection lenses. M is the ratio of the size of the source image size to that of the limiting aperture.

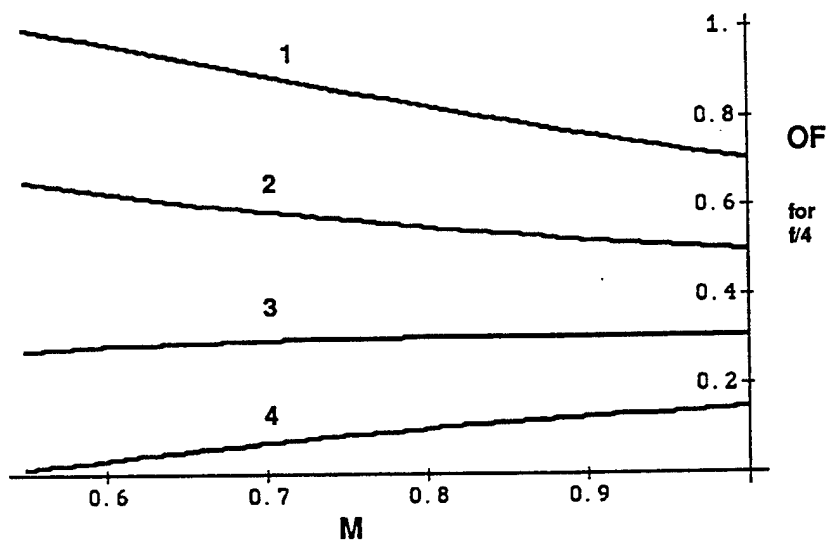


Figure C2a. The overlap vs M for orders 1-4 in an $f/4$ system.

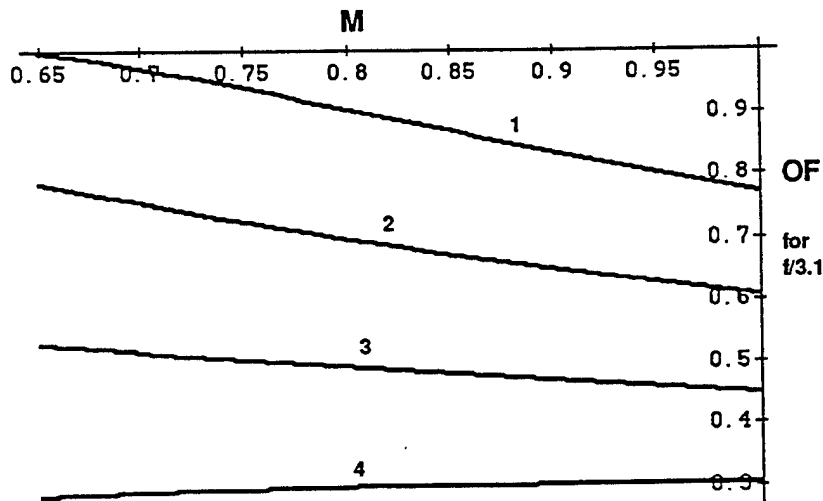


Figure C2b. The overlap vs M for orders 1-4 in an $f/3.1$ system.

Multiplying OF by the appropriate entries from Table 5, gives the amount of energy in each order, and thus a reasonable estimate of the lens throughput. For the $f/4$ lens and $M = 0.9$ we find a throughput of 90.3%, while an $f/3.1$ lens will allow 92% of the light pass. These are small corrections to the estimates derived by assuming a point source (see Table 5).

C. PROJECTION LENS $f\#$

Since it has been shown that the light collection efficiency depends upon the $f\#$ of the projection lens, it is important to see how fast a lens we are allowed to use. The DMD device will throw out three beams: one that corresponds to the specular reflection from structures parallel to the DMD surface, and two more, one each for the mirror elements flipped into the "on" and "off" positions, respectively. If the mirror tilt angle is α then each of beam directions are spaced by 2α . The collection system images the light source to fill the projection lens. This image will also be found in the other beam directions. A good choice is one where the $f\#$ of the projection lens is such that the aperture is equal to the spacing between beam centers. Thus

$$f\# = \cotan(2\alpha). \quad (C12)$$

TABLE C2
A Simple Estimate of Allowed Project Lens $f\#$ as a
Function of Mirror Tilt Angle

| | | | | |
|--------------------|-----|-----|-----|-----|
| α (degrees) | 9 | 10 | 11 | 12 |
| $f\#$ | 3.1 | 2.8 | 2.5 | 2.3 |

Corrections for diffraction may be made. The situation can be modeled by stating that at each diffraction spot an image of the source will be formed. In essence, the image of the source has been convoluted with the diffraction pattern.

Contrast ratio

Here we solve for the contrast ratio using the argument that the light structure in the projection lens is a convolution of the diffraction pattern with the image of the light source. The geometry is as in Fig. 5 (in the main text) and Fig. C3. Draw a line, CN, connecting the center of the lens with the center of the complimentary pattern. In units of the projection lens focal length

$$CN = \tan(2 \text{ Tilt}) \quad (C13)$$

where tilt is the mirror's mechanical deflection angle in radians. The position of the diffraction spot location relative to the center of the complimentary pattern is DL, which in analogy with Eq. C6 is

$$DL = \tan(\Theta_E). \quad (C14)$$

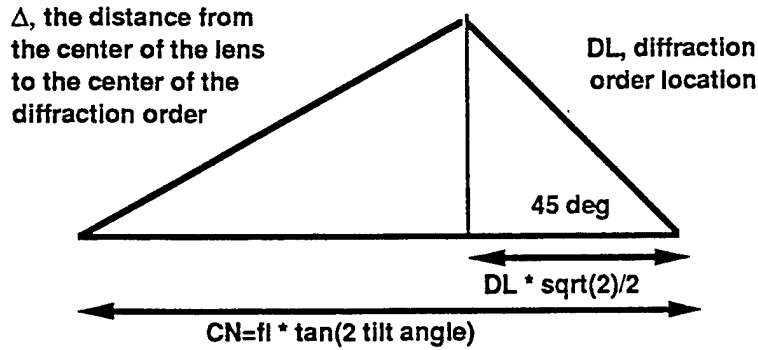


Figure C3. A closer look at the triangle of interest.

The angle included between the lines CN and DL is 45° , since the DMD mirrors have torsion bars on their corners. Note, we are primarily interested in the light diffracted along the two principle axes in the problem, and have ignored the off-axis contributions. From the triangle a relation can be found for Δ

$$\Delta = \sqrt{CN^2 + DL^2 - \sqrt{2} CN DL}. \quad (C15)$$

From the above we arrive at a definition for the overlap fraction, OF. The overlap fraction as a function of projection lens $f\#$, for various diffraction orders, is shown in Fig. 6. The mirror's deflection is taken to be 9° , and the size of the image of the source is taken to be equal to the lens aperture ($M = 1$).

The overlap fraction as a function of $f\#$ is plotted in Fig. 6, for various orders. The values for an $f/3.1$ lens are read from the plot and Table 6 constructed.

One can open up the size of the lens beyond $f/3.1$ and look at the amount of light that passes through to the screen from the zeroth order of the coplaner pattern. The analysis is similar to that presented above, and the results are plotted in Figs. 7 and 8.

D. MTF, IN A DIFFRACTION LIMITED SYSTEM

By considering solely the effect of the aperture, an estimate of the best possible modulation transfer function (MTF) is obtained. The problem is to determine the intensity throughput as a function of spatial frequency. (Goodman, 1968) (Born and Wolf, 1975).

Here begins an outline of the formal argument that leads to our previous intuitive approach. One must recognize that an imaging system, using incoherent illumination, is linear in intensity, the square of the electric field. The intensity at the image is then a convolution of the object intensity with the square of the electric field transmission function of the system. This square is the impulse response. The Fourier transform of the intensity at the image is then the product of the frequency content of the source multiplied by the intensity frequency response of the system. The electric field transfer function, however, for a point source, can be thought of as having three parts: an outgoing spherical wave to the aperture (also known as a propagator), a pupil function (in the simplest case a hole in a screen) and a converging spherical wave from the aperture. In the far field, the spherical wave propagators behave as plane waves and, therefore, the electric field transmission function takes on the form of the Fourier transform of the pupil function. Since the incoherent system has an impulse response that is the square of the magnitude of the electric field transmission function, the frequency response must again be a transform, the autocorrelation of the pupil function. For real quantities, there is no distinction between the operations of autocorrelation and convolution. Thus, when no aberrations are present, the frequency response of an incoherent system is simply a convolution of the pupil function with itself. But this is just the overlap of the aperture and the aperture shifted.

Having justified the intuitive procedure, we may now apply it to the problem of MTF estimation. First consider a sinusoidal intensity pattern with a period, μ . In particular

$$I = \sin^2(2\pi x/[2\mu]) = \{1 - \cos(2\pi x/\mu)\}/2 . \quad (C16)$$

This equation leads to a small digression. We are interested in the intensity spectrum that can be defined as the autocorrelation integral of the spectrum of the electric field. The spatial spectrum of the electric field, for the sinusoidal grating, consists of two delta functions shifted by equal amounts above and below the carrier, while the transform of the intensity has three delta functions, one at the carrier frequency, one above, and one below. The shift in the intensity spectrum is twice that of the electric field. In other words, the electric field "beats" against itself, yielding sum and difference signals. [Note: this is the basis of heterodyne spectroscopy.] It also exemplifies the difference in the calculation of the frequency responses of coherent and incoherent systems. The former, is an autocorrelation of products [the electric field's frequency content times the pupil function], while the latter is a product of the autocorrelation functions, that of the source field and that of the pupil function, respectively.

From the grating equation it is known that maxima will occur at

$$\sin[\theta] = 0, \quad \lambda/\mu, \quad -\lambda/\mu \quad (C17)$$

Because we are dealing with a sinusoid, these are the only locations. The aperture will attenuate the side lobes. The condenser system re-images the source in the plane the projector lens at the locations specified by the grating equation. The amount of light in the side lobes that is passed is

dependent upon how much overlap exists between the image of the source, when shifted by in angle θ , and the lens aperture. If the image of the source is the same diameter as the lens aperture, the procedure recovers the definition of the MTF for an aberration free system. In particular the procedure yields

$$I(\text{at the image}) = \{1 - \rho \cos(2\pi x/\mu)\}/2 \quad (\text{C18 a})$$

where

$$\rho = \text{Overlapping area/aperture area.} \quad (\text{C18 b})$$

The modulation depth ρ , can be found by finding the contrast at the image

$$\rho = [I(\text{max}) - I(\text{min})] / [I(\text{max}) + I(\text{min})]. \quad (\text{C18 c})$$

Given that the image of the source matches the size of the lens aperture, a particularly simple expression for the normalized area of overlap, ρ , may be obtained (Smith, 1990)

$$\text{MTF}(v) = \rho(v) = (2/\pi) (\chi - \cos\chi \sin\chi) \quad (\text{C19 a})$$

where

$$\chi = \text{Arc cos} (\lambda f\#/\mu) \text{ and } v = 1/\mu. \quad (\text{C19 b})$$

The cutoff frequency is defined as that point at which the MTF approaches zero. This condition is satisfied when $\chi = 0$, or $\mu = \lambda f\#$.

For an $f/3.1$ system and a wavelength of 0.7μ (red), this corresponds to a period of 2.17μ . Figure 9 is a plot of the MTF for an ideal system.

E. MTF REQUIREMENTS

We need not construct a projection system that is significantly better than the image forming capabilities of the eye. The MTF is a contrast ratio as a function of spatial frequency. We need to examine the contrast ratio of an image falling on the retina of the eye. The MTF falls below that of a diffraction limited system due aberrations in the eye lens.

We may assume that we have a 60-in.-diagonal image on the screen formed from a projector at ten feet. We further assume an observer at five feet. There are about 1100 line pairs along the diagonal. This leads to 21 line pairs per degree in the field of view. The contrast ratio on the retina falls to between 0.2 and 0.5 depending upon the pupil diameter that ranges between 5.8 mm and 2 mm. (OSA handbook section 12-8). An MTF of 0.4 at the highest spatial frequency

(30 lines/mm at the DMD) will yield changes that are comparable to those induced by variations in pupil size. Thus we take an MTF of 0.5 at 30 lines/mm (1 line/mm at the screen), to be sufficient. The argument depends upon the fact that MTFs of optical systems, separated by diffusing elements, are multiplicative.

Appendix D

COLLECTION EFFICIENCY CALCULATIONS

A. PARABOLIC COLLECTOR

An easily analyzed projection system consists of a light collection parabola used in conjunction with a condenser lens to focus the light in the projection lens. Since the light valve is reflective we unfold the system and place the DMD between the condenser and projection lenses. The condenser lens has a focal length that is m times longer than the projection lens and is at the same time m times further away from the projection lens than the light valve. Thus the condenser still focuses the light source in the projection lens. We are now able to modify the development of Jones (1991).

Following Fig. D1, we assume a source of diameter, d , at the focal point of the parabola. The distance from the vertex to the focus, which is at $z = 0$, is f .

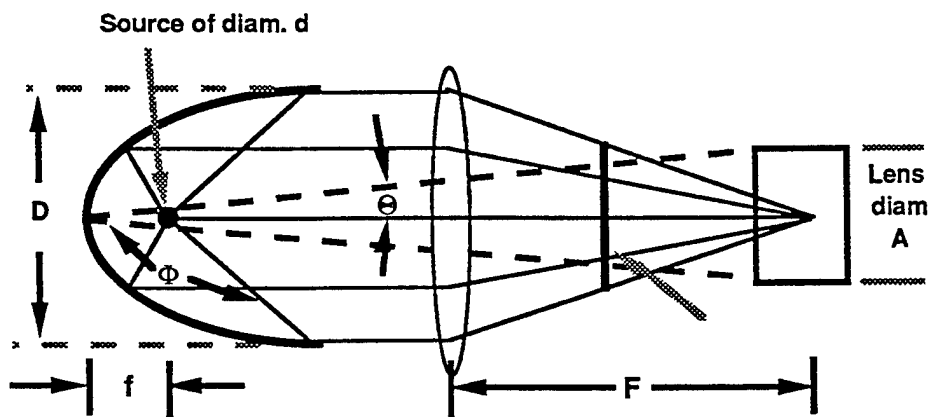


Figure D1. *The equivalent of a DMD illumination scheme.*

The equation for the reflector is thus

$$z+f = r^2/4f \tag{D1}$$

The half angle of the light acceptance cone is ϕ , and with

$$\tan \phi = r/z = D/2 / [\{ (D/2)^2/4f \} - f] \tag{D2 a}$$

$$= D/2f [\{ D^2/16f^2 \} - 1]. \tag{D2 b}$$

Here D is the diameter of the parabola that is m times the diagonal of the film gate. The fraction of the light collected is CF where

$$CF = [1 - \cos \phi]/2. \quad (D3)$$

The half-angle θ , in Fig. D1, is that subtended by the source, with diameter d , as viewed by an observer located at the reflector. It is largest for an observer near the vertex. For light reflected near the vertex of the parabola, the worst case, the angular deviation will be given by $\tan \theta = d/2f$. It is very easy to determine the size of the spot formed by focusing the light from the parabola with a condenser lens of focal length F . We note that a parallel bundle of rays will always focus in the focal plane. If the bundle is tilted with respect to the optical axis by an angle, θ , the point of focus will be a distance F away from the lens but along the tilted line. The focal point for the tilted bundle of rays is thus, $A/2$, the spot image radius, off the optical axis with

$$A/2F = \tan \theta = d/2f. \quad (D4)$$

The argument above is effectively a derivation of the Helmholtz equation for infinite conjugates (Longhurst, 1964).

This gives us yet another way to look at the situation. We note that the magnification of the source is the ratio of the focal length of the condenser F , to the source-reflector distance. The source-reflector distance is a minimum at the vertex. Thus calculations about the vertex will yield a worst case estimate.

Substituting for f we find

$$\tan \phi = D/(2Fd/A) [\{D^2/16(Fd/A)^2\} - 1]. \quad (D5 a)$$

Furthermore we note that the diagonal of the DMD, V is D/m while the focal length of the projection lens P , is F/m . Since these quantities appear in the equation only as ratios, the scaling factor m never explicitly appears. As a consequence

$$\tan \phi = V/(2Pd/A) [\{V^2/16(Pd/A)^2\} - 1]. \quad (D5 b)$$

With A/P as the $f\#$ of the projection lens and $\eta = V/4df\#$ we obtain $\tan \phi = 2\eta/(\eta^2 - 1)$ and thus find the collection fraction to be

$$CF = \{1 + [(\eta^2 - 1)/(\eta^2 + 1)]\}/2. \quad (3a)$$

Since the arguments above depend upon the examination of an imaging system in terms of the optical invariant, the results do not depend upon the particulars of the components. The results reflect the efficiencies obtainable from any light source with any reflector.

Collection Fraction of an $f/4$ system as a function of arc length and light valve diagonal

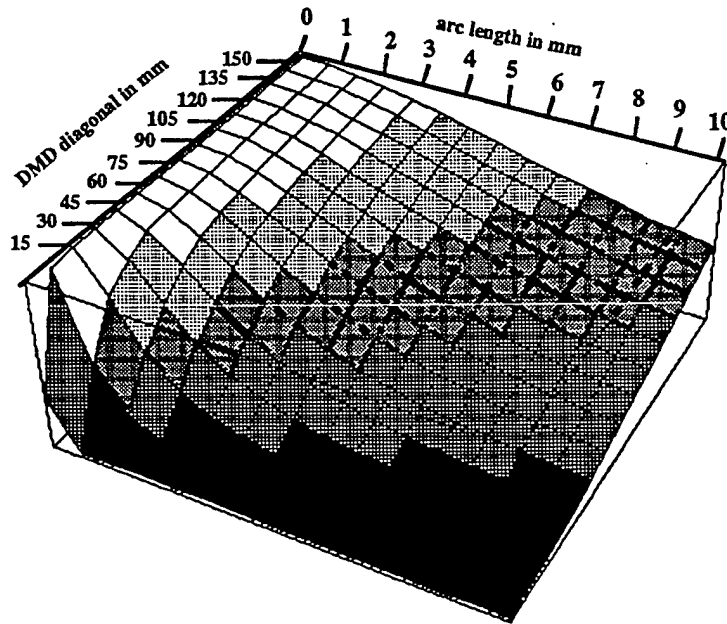


Figure D2a. The collection fraction surface vs arc length and DMD diagonal size, for an $f/4$ projection system.

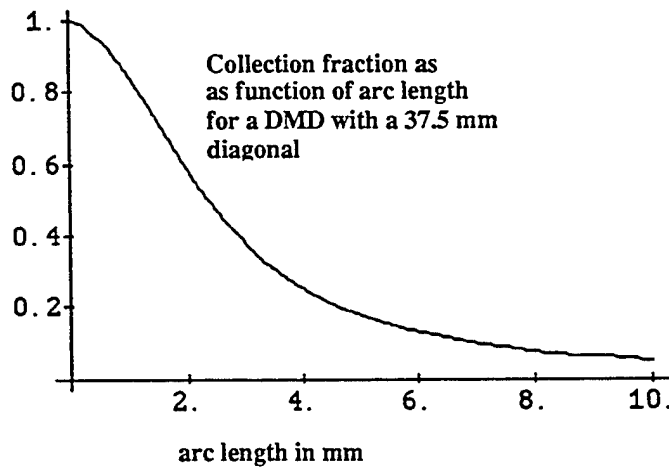


Figure D2b. Collection Fraction vs arc length for an $f/4$ system.

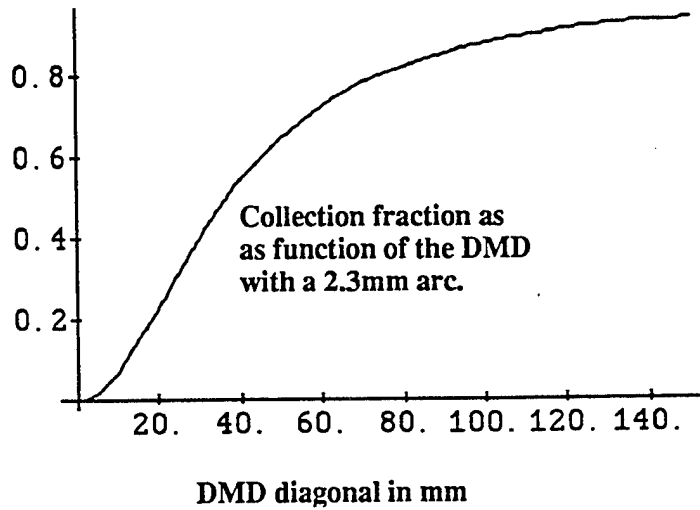


Figure D2c. *Collection Fraction vs DMD diagonal size for an f/4 system.*

Figure D2 a shows the two-dimensional surface that defines the collection fraction as a function of both arc length and DMD diagonal for an $f/4$ system. Figures D2b and c show cuts through the surface for a constant 37.5-mm diagonal and 2.3-mm arc, respectively.

Figures 10a and 10b, in the main text, show how the efficiencies depend upon f number and arc length and DMD diagonal. Figure 11 includes the efficiency of the lamp in the calculation.

B. ELLIPTICAL REFLECTOR

As was stated earlier, the behavior of the optical system should be independent of the details of the reflector shape. The arguments follow as a consequence of the optical or Lagrange invariant; which is effectively the product of the linear and angular magnification of an imaging system. This can be demonstrated by following through the collection efficiency arguments for the ellipse.

There are two foci that describe the elliptical surface, f_1 and f_2 , which are measured from the vertex of the collector. They are associated with the major and minor semi-axes a and b , which are measured from the center of the ellipse. The following analysis uses the equation for the ellipse based upon the centered coordinate system:

$$(z/a)^2 + (r/b)^2 = 1. \quad (D6)$$

It will be found that there is one less equation than variables. However, the length scale is as yet undefined. We are thus free to measure all lengths in units of the focal length of the projection

lens. Thus the real scale of the problem will not be set until we define the projection lens, or, in effect, the size of the image on the screen. An alternate way of stating the situation, is that angles are the important factors in the problem.

The relationship between the semi-axes, a and b , and the focal distances are well known. One can also define the distance between the foci as $2c$. Thus

$$a = (f_1 + f_2)/2 \quad (D7 a)$$

$$c = (f_1 - f_2)/2 \quad (D7 b)$$

$$a^2 = b^2 + c^2 \quad (D7 c)$$

so
$$b^2 = f_1 f_2 \quad (D7 d)$$

The magnification, m , of the arc is simply the ratio of the image to object distances

$$m = f_2/f_1 = A/d. \quad (D8)$$

We denote d and A as the diameters of of the arc and its image, respectively. If the system is matched, the diameter A is also the diameter of the projection lens. The lens diameter in units of the focal length is simply

$$A = 1/f\#. \quad (D9)$$

For the purposes of calculation one may consider the device of diagonal, v , to be a transparency placed a distance, x , away from ellipse center. Since the screen is effectively very far away it is possible to take the DMD to projector lens distance to be the focal length, which is unity in the scaled units. This leads to the equation

$$x + c = 1. \quad (D10)$$

The device is set at $z = x$ and at that point $y = v/2$. This, among other things, fixes the light cone that projects out to the screen. The half angle of the light acceptance cone is again ϕ , and

$$\tan(\phi) = (v/2)/(x - c). \quad (D11)$$

Again we define the collection fraction as

$$CF = [1 - \cos \phi]/2. \tag{D3}$$

which is the fraction of a sphere that is intercepted in the collection cone. We can also find the collection efficacy by multiplying the result by the lamp efficiency in lm/W. By assuming a projector lens of 82 mm, a device diagonal of 37.5-mm, a Xenon lamp with a 2.3-mm arc length and an efficiency of 28 lm/W, and a metal-halide lamp with a 6-mm arc and an efficiency of 80 lm/W; a plot of efficacy as a function of projection lens $f\#$ may be obtained. This is shown in Fig. D3. It is seen that the metal halide lamp does not outperform the Xenon lamp until the projection lens becomes faster than $f/2.7$. This is virtually the same result obtained using the parabolic reflector. The results are clearly reflector-type independent, as was surmised from imaging arguments.

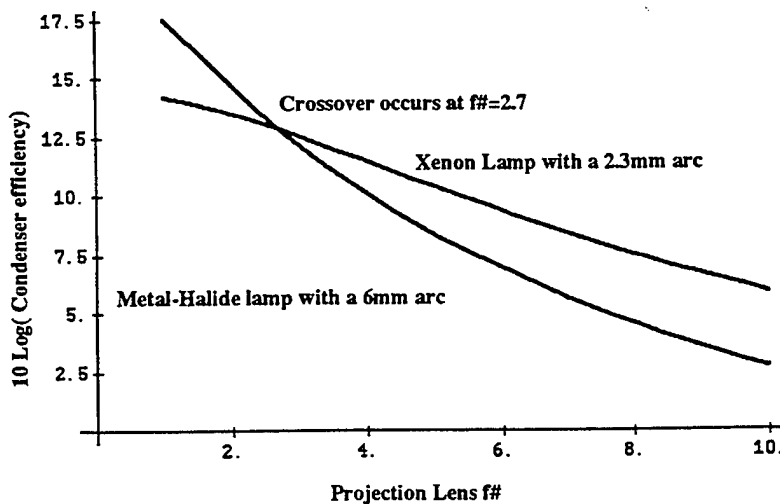


Figure D3. *Collection efficacy of an ellipse as a function of projection lens $f\#$ for a Xenon arc lamp and a metal-halide lamp, given a DMD with a 37.5-mm diagonal.*

From the above discussion it should be clear that any of the following will increase the efficiency of the projection system:

- *Increase the size of the device (to increase the focal length of the projection lens and thus allow a larger image of the source)*
- *Increase the mirror deflection angles (to allow the use of a faster projection lens)*
- *Minimize the size of the arc in the lamp*
- *Maximize the lamp efficiency (consistent with the arc size)*
- *Increase the size of the pixels (to reduce diffraction effects)*

Appendix E

COLOR DESIGNS

A. COMBINING PRISM

In any configuration that uses dichroics one must be concerned about the efficiency of the dichroics as a function of incidence angle in both the color separation and combination stages. This is particularly true if the beam intersecting the dichroic surface is not collimated.

B. A PRISM-COUPLED DMD DISPLAY FOR COLOR PROJECTION: A FIRST APPROXIMATION

A prototypical color projection system was examined. The design criteria call for minimization of color shifts across the screen, and sufficient magnification to form a 60-in.-diagonal image at ten feet.

The required magnification calls for a lens with a focal length in the neighborhood of 80 mm. The back focal lengths of the medium format Rodenstock and Schneider lenses are shorter than the effective focal length. The back focal length may be increased, indeed, even made longer than the effective focal length, by employing a reverse telephoto (or retrofocus) lens (Smith, 1990). Basically, a retrofocus lens can be thought of as a diverging achromat placed in front of (toward the screen) a good standard lens. A custom design would use the strong negative lens not only to increase the back focal length but as a corrector for the Petzval curvature as well. This is the basis of many wide angle fast designs. We thus know that it is possible to design a lens that will meet the requirement of a long back focal length.

The next item of interest is the color combining assembly. The most compact approach will use some kind of prism system. The most compact version uses two crossed dichroic layers. Such a prism may be found in Fig. A1. A possible disadvantage is that the geometry may be very susceptible to color shifts as a function of incidence angle. An interference filter's passband depends upon angle, this dependence for small angles goes as

$$\lambda_{\theta} = (\lambda_0/n) (n^2 - \sin^2(\theta))^{0.5}.$$

The effective index of the dielectric layer is n . The expression fails for large angles because there is a polarization dependence as well. Ignoring this for a moment and taking the derivative of this expression yields

$$d(\lambda_{\theta})/d\theta = -(\lambda_0/n) \sin(2\theta) / [2 (n^2 - \sin^2(\theta))^{0.5}].$$

This clearly shows a maximum sensitivity about the 45° angle of incidence, exactly the angle used in the crossed dichroics.

The sensitivity can be reduced if we operate at a lower angle or increase the effective index of the dielectric stack. These questions were addressed by de Lang and Bouwhuis (1963).

A simple bandpass filter can be made by constructing a quarterwave stack. A stack is comprised of alternate high and low index layers. By making the high index layer three-quarters of a wave (or any odd multiple of a quarter wave) the effective index is raised. The procedure, however, causes the red filter to have a reflectivity in the blue as shown in Fig. E1. Thus, the red-green combiner must precede the blue reflective dichroic layer. The eye is more sensitive to the red-green fields than the blue field, and therefore one would like to minimize the angle of incidence with respect to the red reflective dichroic, even at the expense of the blue reflective film. The prism assembly shown in Fig. E2 allows the angle between the red film's normal and the optical axis to be reduced to 11.25° , while limiting the angle with respect to the blue film to 22.5° . The variation of the band edges for the two colored films, for a 9° variance about the nominal beam direction is 30 nm. Figure E1 demonstrates that there is also a difference in behavior for the transverse magnetic and electric polarizations. The prism shown has a longer path length than the crossed dichroic layers.

A design that shortened the path between the DMD and the color combining cube and that further separated the illumination and projection directions further was sought. The solution lay in the use of a right angle prism. The prism, which was shown, in Fig. 4, makes use of the fact the tilt of the mirrors in the DMD will redirect the outgoing light of interest so as to experience total internal reflection (TIR), off the hypotenuse. The illumination beam enters via the hypotenuse. The DMD is mounted on one of the legs, while the outgoing light exits via the other leg.

A preliminary examination has been carried out for the design of a projection system using crossed dichroics in the combiner and coupling prisms to gain access to the DMD. Increasing the effective index of the films, relative to the medium in which they are embedded, decreases the angular and polarization dependence of the dielectric stack. The highest index films are TiO_2 , (at 2.7) and ZnS (at 2.35). The latter is difficult to produce. Thus the highest practical index is 2.35. Embedding crossed dichroic plates in air will work better than if they are encased in glass, but the air equivalent distance between the lens and the DMD will increase. Achieving a good compromise design is the task of Phase II. Figure E3 shows what a projector using the above described methods would look like.

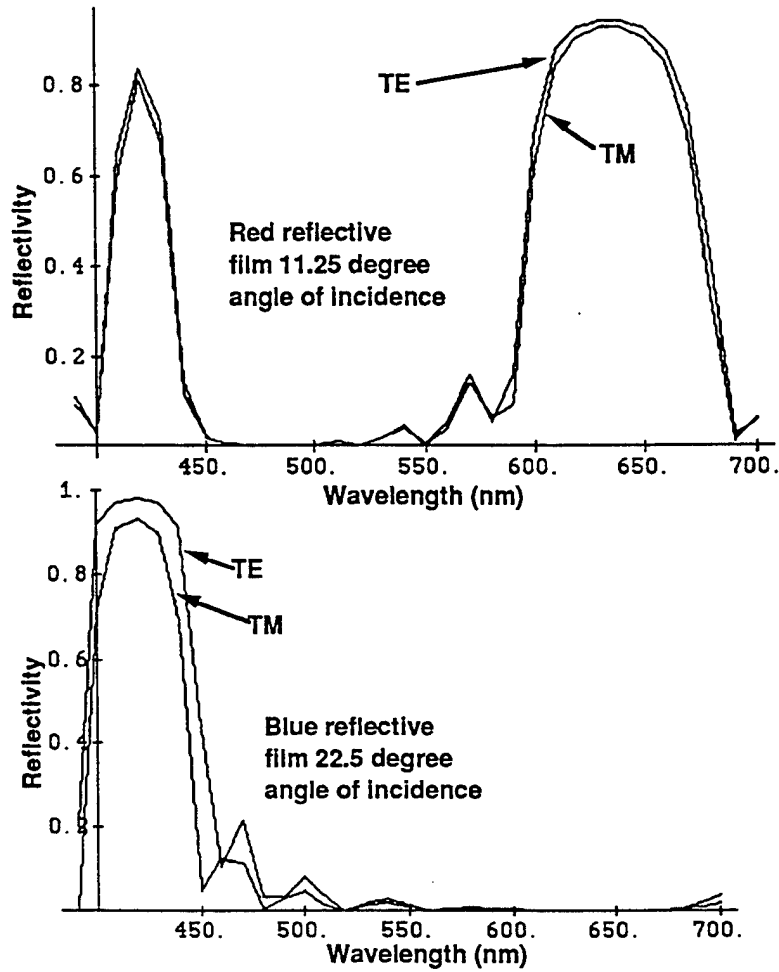


Figure E1. *The behavior of a 1/4 - 3/4 wave stack of films of index 1.75 and 2.35 on a between media of index 1.78.*

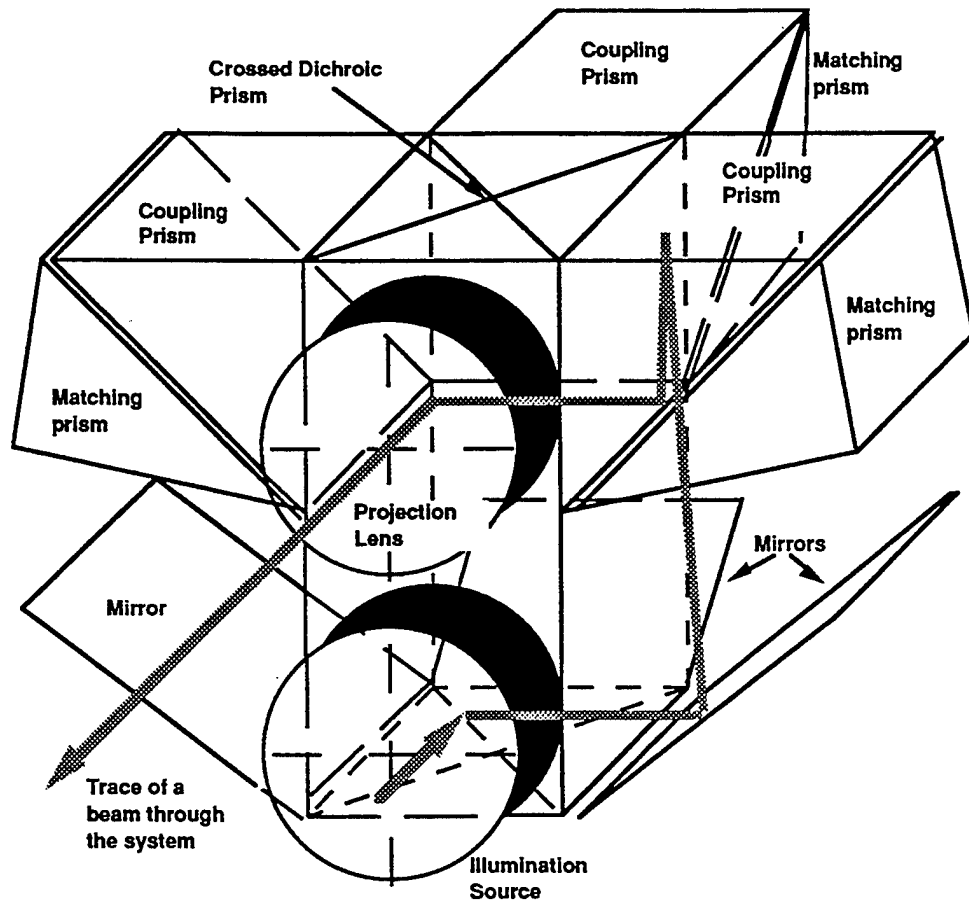


Figure E3. *A design using parallel illumination and a crossed dichroic color combining prism. A stop forward of the projection lens eliminates the unwanted images and sets the effective $f\#$ of the system.*

Appendix F

SCREENS

The function of a screen is to present a surface on which to form the image. It also must redistribute the illumination in an evenly amongst the viewers. This function may be achieved through the use of lenses and mirrors, or by employing scattering centers. The various methods may be found in both front and rear projection screens.

A basic understanding of the screen starts by assuming that it is a mirror or window. These structures do virtually nothing to the light distribution. Thus in the simplest model, the light from the screen propagates as if its screen was specular (or mirror like), by definition. Consequently, structures on the screen can only modify the specular behavior.

As a first approximation to an understanding of the problem let us assume that we have a collection of particles that are scattering centers. These particles will redirect the light *relative* to the specular direction (the grating equation actually gives the direction of the outgoing wave relative to the incident direction). If the light interacts with only one scattering center (single scattering), a memory of the incident direction exists and a distribution about the specular direction is created.

The simplest sort of scatterer is the driven dipole. In a uniform medium there is no scattering because, by random phase arguments, one can show that the electric field will vanish in all directions, except the forward direction. Non-uniformity destroys the symmetry, and thus a contribution arises. If the medium is isotropic one finds two contributions to the radiated field: a specular component and a dipole radiation pattern centered about the specular direction. A single dipole has a radiation pattern that follows a cosine-squared law, where the angle is relative to the incident direction. An ensemble of dipoles a various sizes may differ slightly from this pattern. Models exist that build up a scattering function given a Gaussian distribution of particle sizes. They ostensibly yield the Ornstein-Zernike result for fluctuating media (Stanley, 1971); the radiation pattern becomes the Fourier transform of the two point correlation function, which in this case is a Lorentzian.

$$I(q) = \text{Const}(1/[1 + q^2\xi^2]) \quad (\text{F1 a})$$

where

$$q = 2k\sin(\theta/2) . \quad (\text{F1 b})$$

Here q , is the momentum change of light elastically scattered by a soundwave (Bragg Scattering), k , the wave vector of the light, and ξ , the characteristic size of an inhomogeneity in the medium. The angle is the scattering direction relative to the incident beam.

By the half angle formula, and a Taylor expansion of the denominator we find two components:

$$I(\theta) = C1[1 + C2 \cos(\theta)] , \quad (F1 c)$$

one specular, and the other a Lambertian distributed about the specular direction.

A diffuse scatterer may be considered to be composed of many single scatterers operating in series. The problem is known as multiple scattering. If carried far enough, any memory of the incident direction is lost. In such a situation one expects to find something that behaves as a true Lambertian source, with the distribution centered about the normal to the surface.

A. FRONT PROJECTION

Now we must ask ourselves, what a matte white screen does to the incident radiation. The surface must be represented as a collection of mirrors with an orientational distribution. In the case of a white screen, for normally incident light, this distribution is adjusted to form approximately a Lambertian, or cosine, distribution about the perpendicular to the screen's surface. Given the above arguments, the most reasonable assumption would be that the reflected light, in general, would follow a Lambertian-like distribution centered about the specular direction. We have measured the distributions from both a matte white screen and an aluminized lenticular screen. Light was projected onto the four corners that correspond to the limits of the off-axis projection scheme. The geometry is shown in Fig. F1. The vertical and horizontal radiation patterns for the matte white screen may be found in Figs. F2 through F9. They behave in the expected manner.

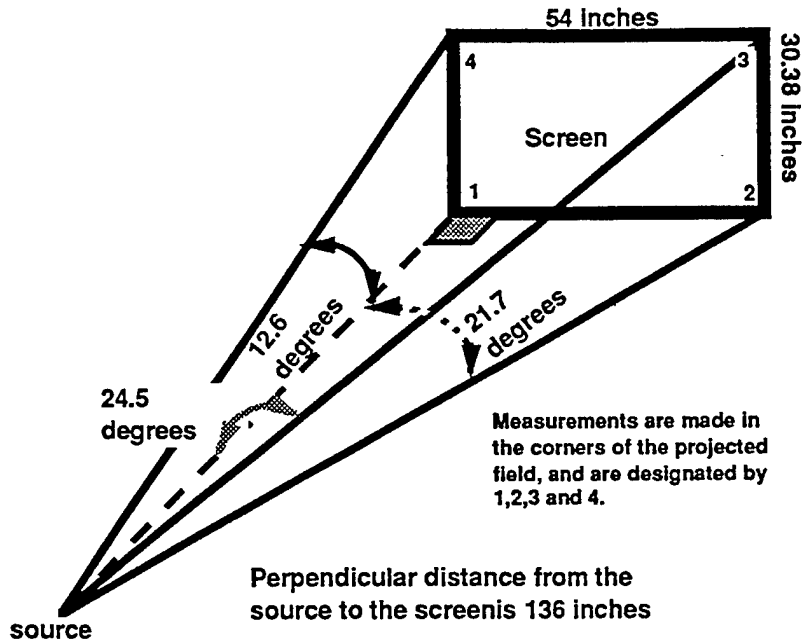


Figure F1. The geometry used for characterizing the screens.

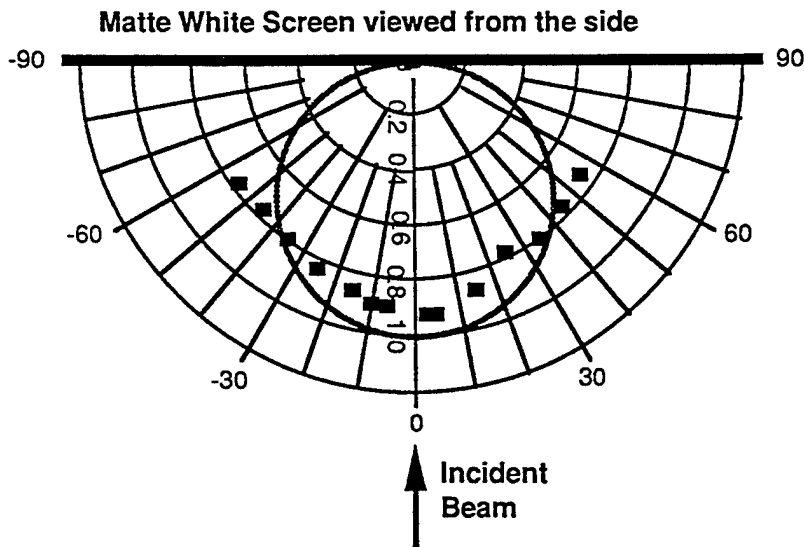


Figure F2. Brightness (luminance) of a matte white screen with normal illumination at position 1. Data are taken along a cut in the vertical direction. The curve represents the distribution from a Lambertian source.

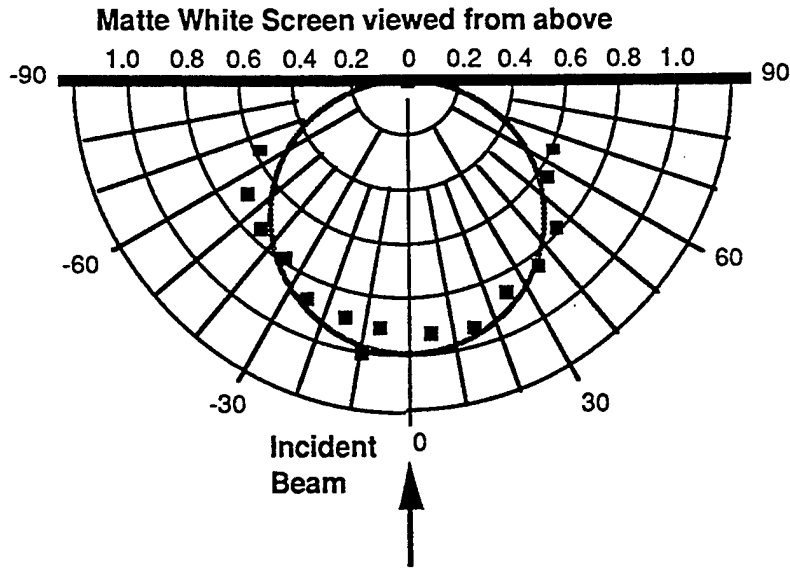


Figure F3. *Brightness (luminance) of a matte white screen with normal illumination at position 1. Data are taken along a cut in the horizontal direction. The curve represents the distribution from a Lambertian source.*

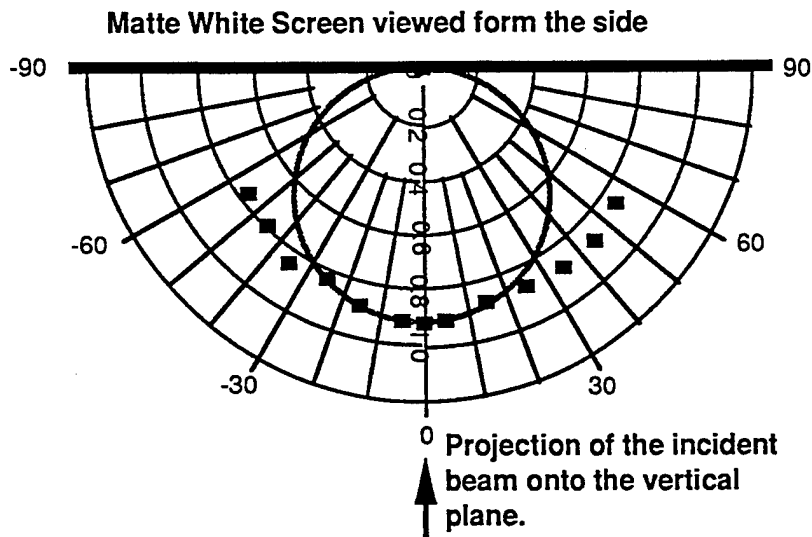


Figure F4. *Brightness (luminance) of a matte white screen with non-normal illumination at position 2. Data are taken along a cut in the vertical direction. The curve represents the distribution from a Lambertian source.*

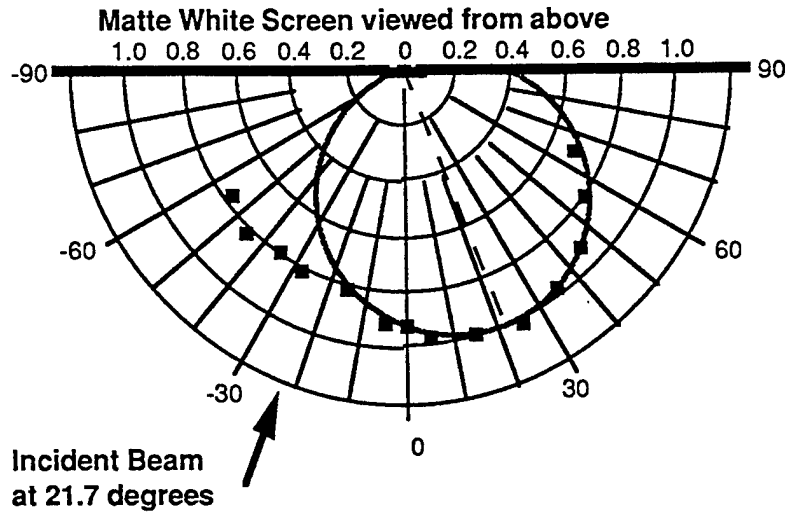


Figure F5. *Brightness (luminance) of a matte white screen with non-normal illumination at position 2. Data are taken along a cut in the horizontal direction. The curve represents the distribution from a Lambertian source.*

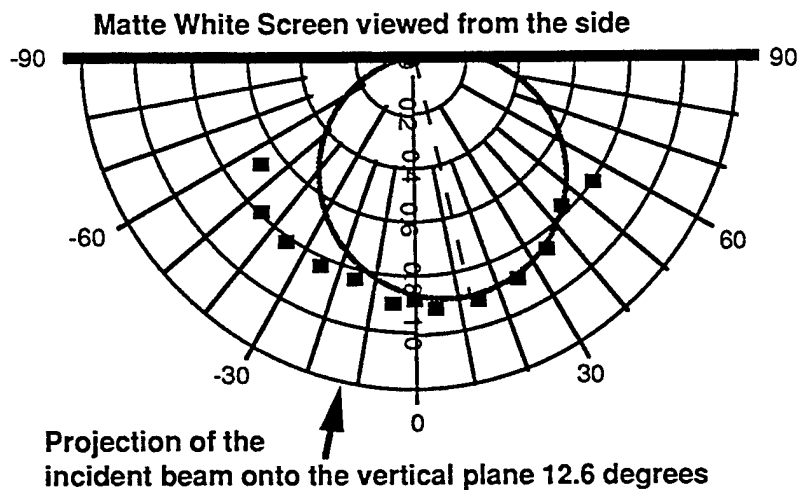


Figure F6. *Brightness (luminance) of a matte white screen with non-normal illumination at position 3. Data are taken along a cut in the vertical direction. The curve represents the distribution from a Lambertian source.*

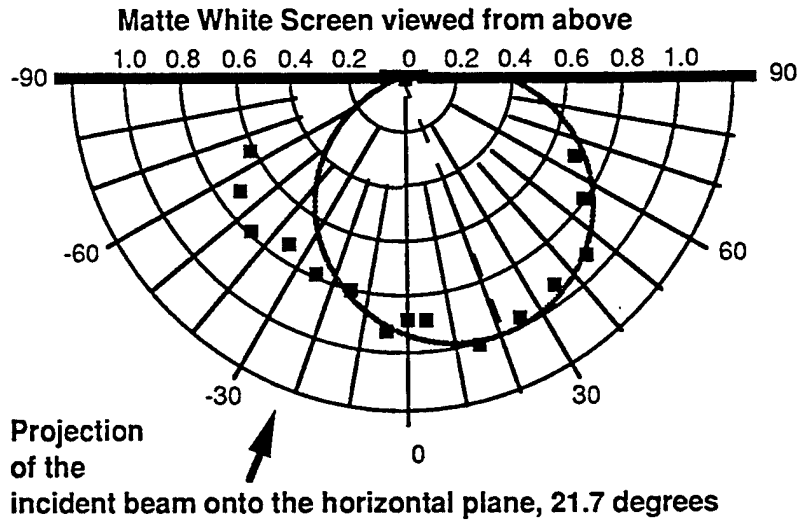


Figure F7. *Brightness (luminance) of a matte white screen with non-normal illumination at position 3. Data are taken along a cut in the horizontal direction. The curve represents the distribution from a Lambertian source.*

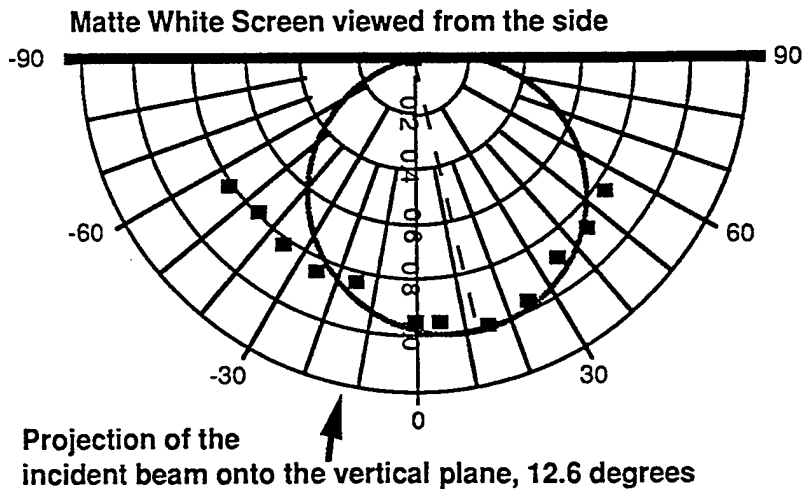


Figure F8. *Brightness (luminance) of a matte white screen with non-normal illumination at position 4. Data are taken along a cut in the vertical direction. The curve represents the distribution from a Lambertian source.*

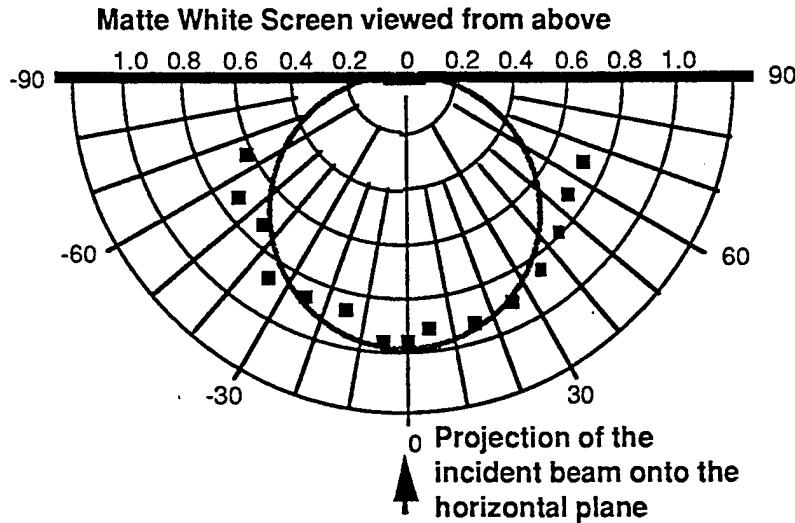


Figure F9. *Brightness (luminance) of a matte white screen with non-normal illumination at position 4. Data are taken along a cut in the horizontal direction. The curve represents the distribution from a Lambertian source.*

Lenticular screens are designed to give a wide horizontal distribution, and a narrow vertical one. Commercial units assume near normal incidence. As a result they do not work well with the off-axis projection system that we are currently using. However, they may be tailored to such a scheme, in much the same manner rear projection screens have been tailored to triple projection systems.

A commercial aluminized lenticular screen was also examined using various illumination directions. The radiation patterns are shown in Figs. F10 through F17. The screen is not tailored for the off-axis projection scheme that we have used in the prototype. It is better suited for an on-axis projection scheme.

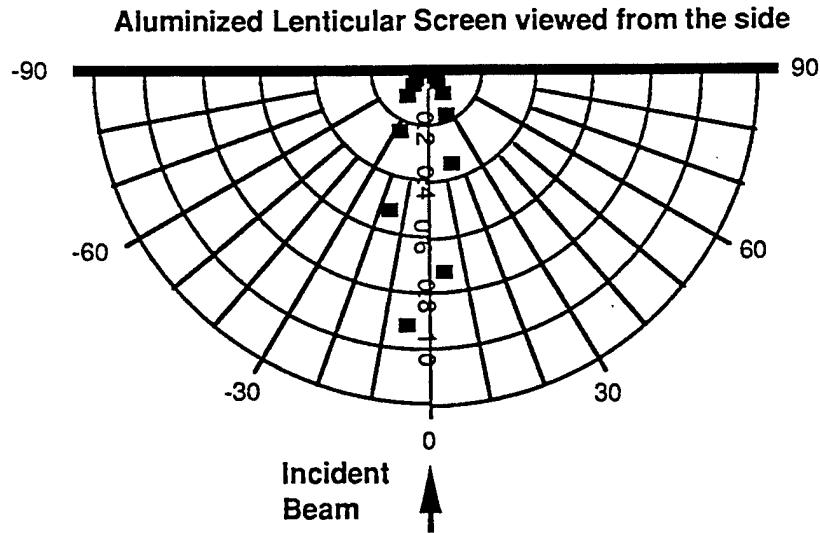


Figure F10. *Brightness (luminance) as a function of angle for an aluminized lenticular screen at position 1. The scan is in the vertical plane, normal to the screen's surface. The vertical plane and the screen plane intersect along a line that is parallel with the axes of the lenticules.*

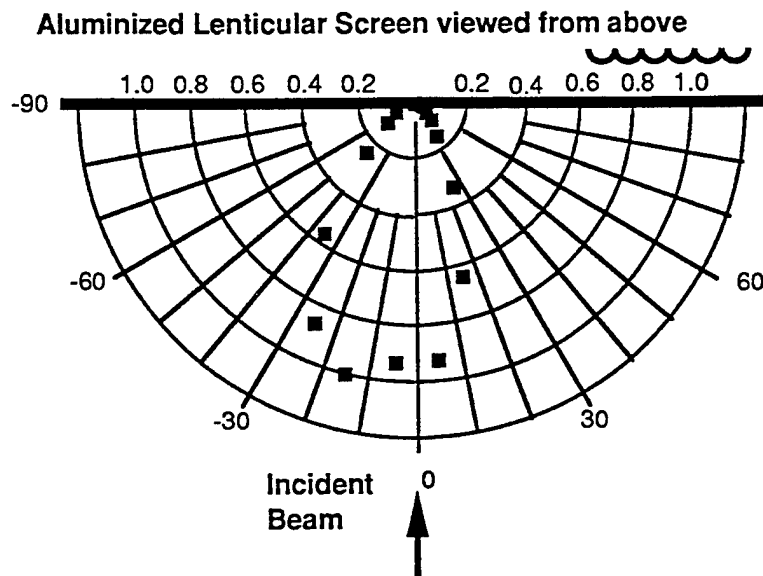


Figure F11. *Brightness (luminance) as a function of angle for an aluminized lenticular screen at position 1. The scan is in the horizontal plane, and thus perpendicular to the axes of the lenticules in the screen. Here we have a near normal incident beam.*

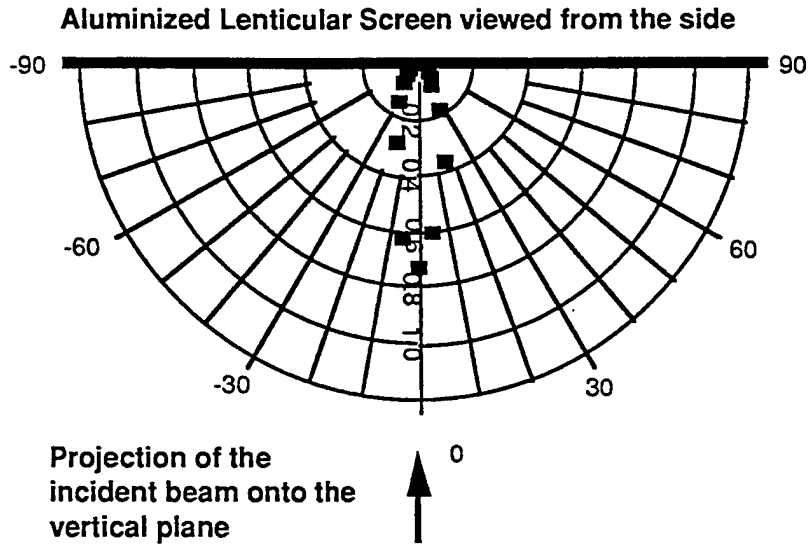


Figure F12. *Brightness (luminance) as a function of angle for an aluminized lenticular screen at position 2. The scan is in the vertical plane, normal to the screen's surface. The vertical plane and the screen plane intersect along a line that is parallel with the axes of the lenticules.*

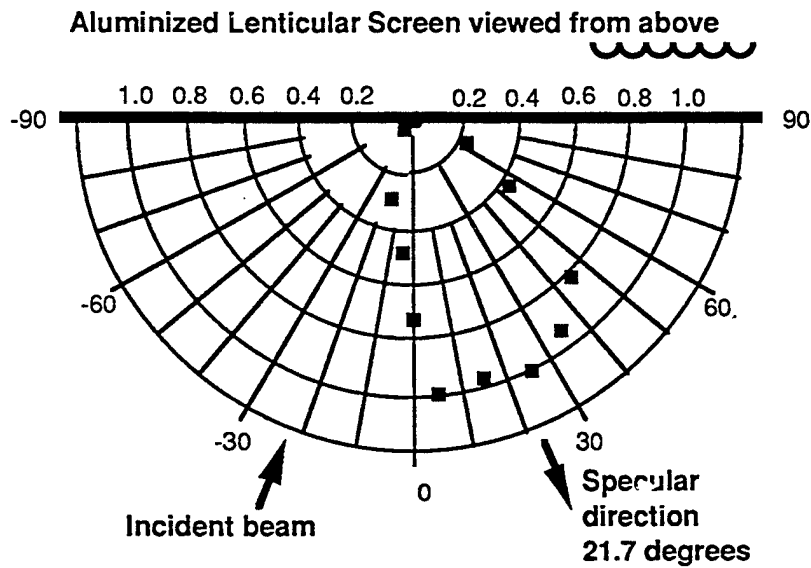


Figure F13. *Brightness (luminance) as a function of angle for an aluminized lenticular screen at position 2. The scan is in the horizontal plane, and thus perpendicular to the axes of the lenticules in the screen.*

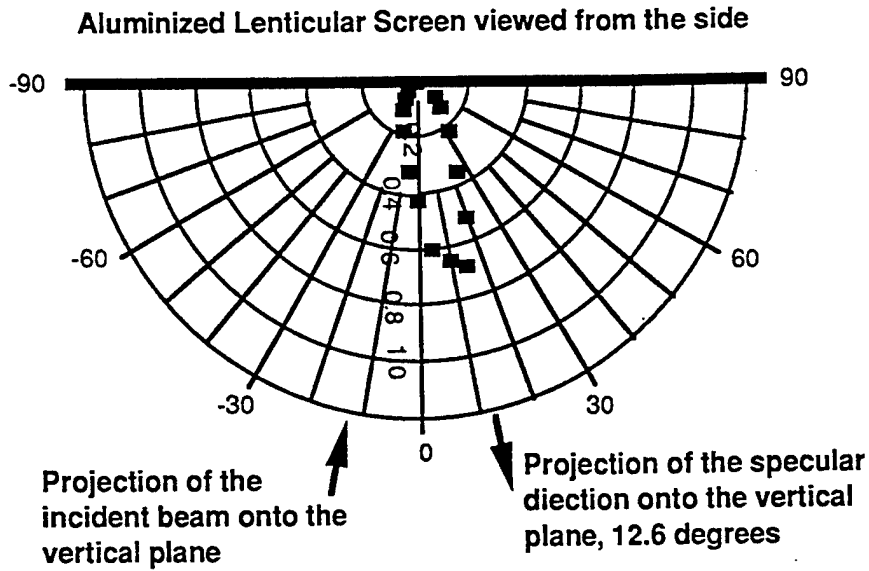


Figure F14. *Brightness (luminance) as a function of angle for an aluminized lenticular screen at position 3. The scan is in the vertical plane, normal to the screen's surface. The vertical plane and the screen plane intersect along a line that is parallel with the axes of the lenticules.*

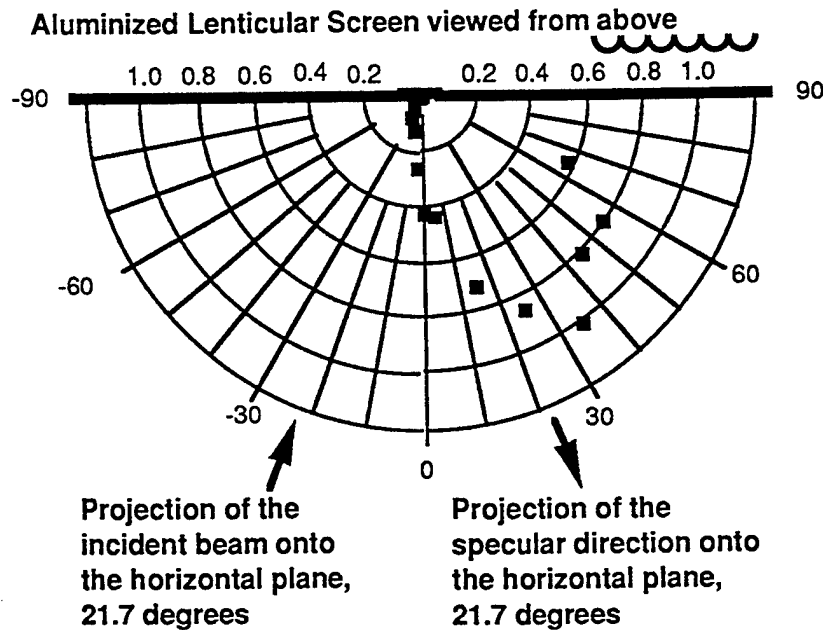


Figure F15. *Brightness (luminance) as a function of angle for an aluminized lenticular screen at position 3. The scan is in the horizontal plane, and thus perpendicular to the axes of the lenticules in the screen.*

B. REAR PROJECTION

Rear projection screens can be of two types: scattering, or diffusive, and lens-like. The latter type controls the directions of the emitted light better, and is thus the screen of choice when one uses *triple projection*. (By triple projection we mean three independent projectors, one for each color. The final picture is formed by supposing the three colored images at the screen.)

The diffusive screen may have particles embedded in it, or a rough surface deposited over it. Unless it is truly Lambertian, directional information about the incident light direction will not be effaced. As a result the color balance, in a triple projection system, may vary as the viewer moves about in angle. Also, since multiple scattering is being employed, some light must be scattered in the rearward direction. Thus a diffusive screen is the less efficient of the two alternatives.

Lenslet rear projection screens used in triple projection consist of at least four active layers: the first being a Fresnel lens to collimate the light from the three sources, the second layer makes the collimated colored beams parallel to each other. The remaining two layers disperse the light horizontally and vertically. The fields of view in each direction about the centerline are usually taken to be ± 45 and ± 10 , respectively. These rear projection systems have an advantage over front projection in environments where ambient light levels are high because the light effectively emanates from slits at the front surface. A black matrix mask is applied to reduce reflected ambient light. Since the light from the projector is focused through the slits, no loss of throughput is experienced. Thus the effective contrast ratio is improved.

Rear projection screens can be adapted to off-axis projection systems by selecting the correct segment of the Fresnel Lens, as shown in Fig. F18.

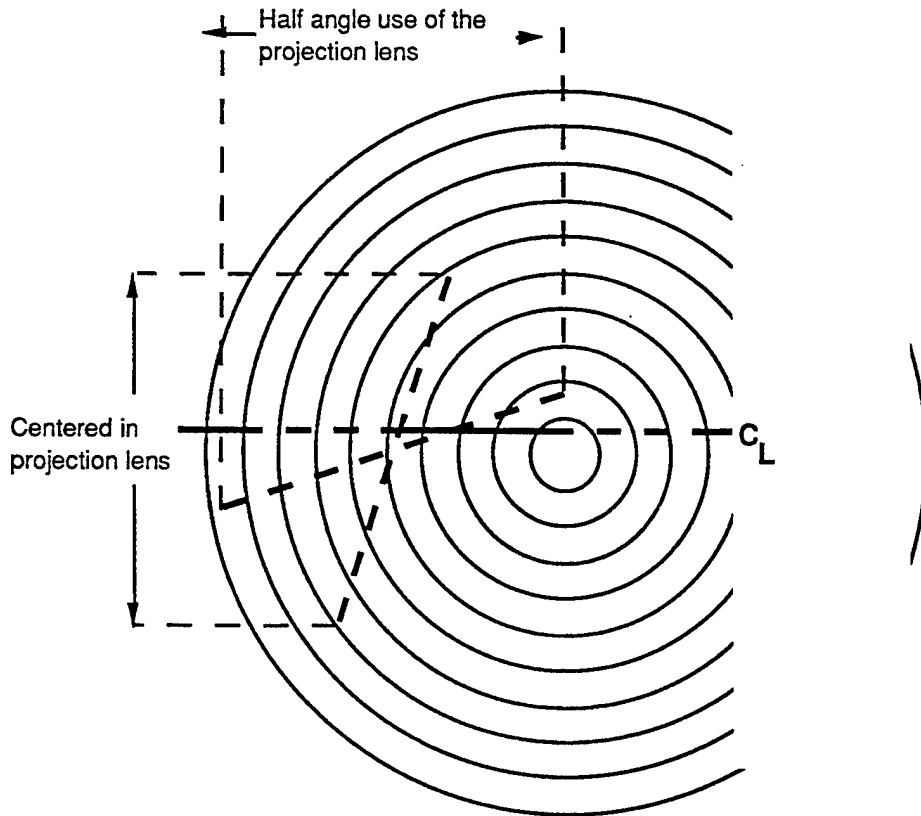


Figure F18. *For a rear projection system the screen must first collimate the light before dispersing it. A Fresnel lens is always used for this. For the off-axis projection we need to chose an off center segment of the Fresnel.*

Appendix G

- 1) Failure Analysis of ILC Lamps
- 2) Lamp Safety Operating Instructions



FAILURE ANALYSIS OF ILC LAMPS

- WHEN INVESTIGATION STARTED
- REASONS FOR THE INVESTIGATION
- DEVELOPMENT OF THE ACOUSTIC MICROSCOPE CAPABILITY
- LIST OF LAMPS ANALYZED
- MANUFACTURING PROCESS ISSUE
- ARPA PROJECTOR LAMP EXPLODED AT ASD

PLANS

- MEET WITH ILC QUALITY MANAGER JOHN REILLY AND MANUFACTURING MANAGER
- DISCUSS THE FINDINGS
- REQUEST A CORRECTIVE ACTION PLAN BY ILC
- MONITOR THE CORRECTIVE ACTION PROCESS AND RESULTS



FAILURE ANALYSIS OF ILC LAMPS

WHEN INVESTIGATION STARTED

- THE INVESTIGATION STARTED IN JANUARY OF 1994 WITH THE EXPLOSION OF ONE LAMP IN LION PROJECTOR AT TI
- THE EXPLODED LAMP WAS 1000 WATT SER #3EQ-4476
- THE LAMP HAD LESS THAN 100 HOURS OF OPERATION
- INFORMED BY LION THAT LAMPS ALSO EXPLODED AT THEIR FACILITY
- THE LAMP WAS SENT TO ILC FOR FAILURE ANALYSIS
- FAILURE ANALYSIS FROM ILC STATES OVERHEATING OF THE LAMP AS A CAUSE OF THE EXPLOSION
- THE CORRECTIVE ACTION INCREASED THE BRAZE MATERIAL AT THE NECK REGION OF THE ANODE
- WE ALSO RETURNED ANOTHER LAMP WITH LOW LUMENS AND BLACK REFLECTOR
- THE FAILURE ANALYSIS INDICATED THAT THE CONTAMINANTS WERE SPONGY AND THEY CAME FROM THE PALCO BRAZING MATERIAL



FAILURE ANALYSIS OF ILC LAMPS

REASON FOR THE INVESTIGATION

- EARLY MORTALITY OF LAMPS
- MY DOUBTS OF THE ILC FAILURE ANALYSIS
- THE ACOUSTIC MICROSCOPE WAS DEVELOPED BY DR. TOM MOORE (CRL) TO DISCOVER CRACKS IN SEMICONDUCTOR CERAMIC AND PLASTIC PACKAGES
- DR. MOORE DESIGNED A SPECIAL ROTATIONAL FIXTURE THAT CAN HOLD AND ROTATE THE LAMPS
- THE FIRST RESULTS WERE OBTAINED THE 6th OF JULY

LIST OF LAMPS ANALYZED

- TWELVE LAMPS WERE ANALYZED
- THE RESULTS INDICATE A LARGE NUMBER OF BRAZING VOIDS IN THE CERAMIC TO METAL AND METAL TO GLASS
- DR. TOM MOORE'S MEMO



FAILURE ANALYSIS OF ILC LAMPS

MANUFACTURING PROCESS ISSUE

- BRAZING MATERIAL PURITY
- BRAZING THICKNESS AND TEMPERATURE
- METRICS OF PARTS WELDED TOGETHER

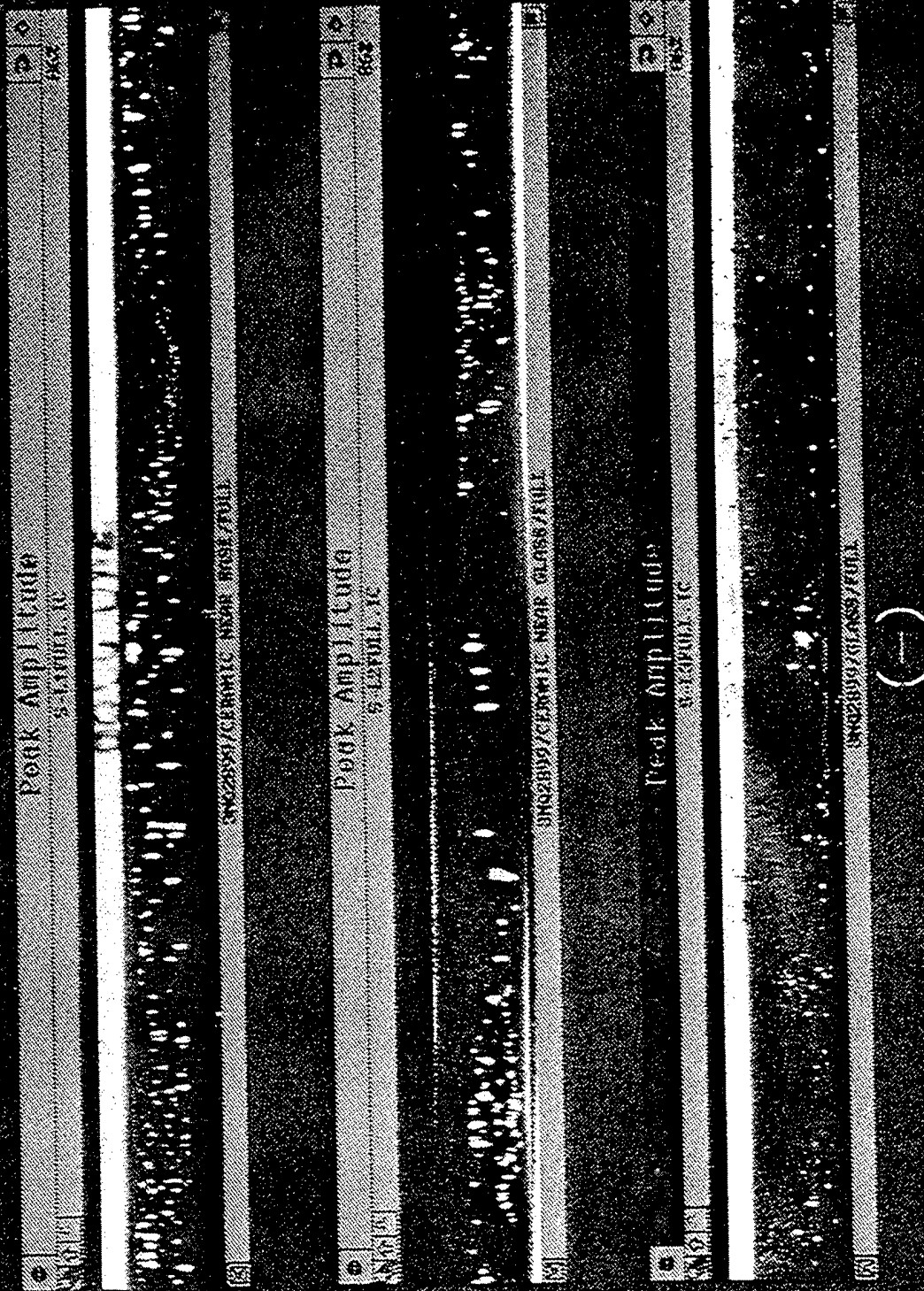
ARPA PROJECTOR LAMP EXPLODED AT ASD

- PRELIMINARY PHOTOS
- EXHIBIT THE LAMP ITSELF
- VOID VISIBLE AT THE GLASS BRAZING AREA
- NEED TO PROVIDE FAILURE ANALYSIS AND CORRECTIVE ACTION TO THE AIRFORCE (ASD)

PLANS

- MEET WITH ILC QUALITY MANAGER JOHN REILLY AND MANUFACTURING MANAGER
- PRESENT THE INFORMATION THAT I PRESENTED TO YOU
- DISCUSS ALL THE FINDINGS
- REQUEST A CORRECTIVE ACTION PLAN BY ILC
- MONITOR THE CORRECTIVE ACTION PROCESS AND RESULTS

1 LX1000c-f Ser# 3MQ2899 Date Code 9352 130Hrs Dim Light Ref Black



The Negative marking on the lamp is the center of the photos

4 LX300F Ser#3-11 38AA4477 Date Code8310 550 Dim Light

Peak Amplitude
7.330E+10

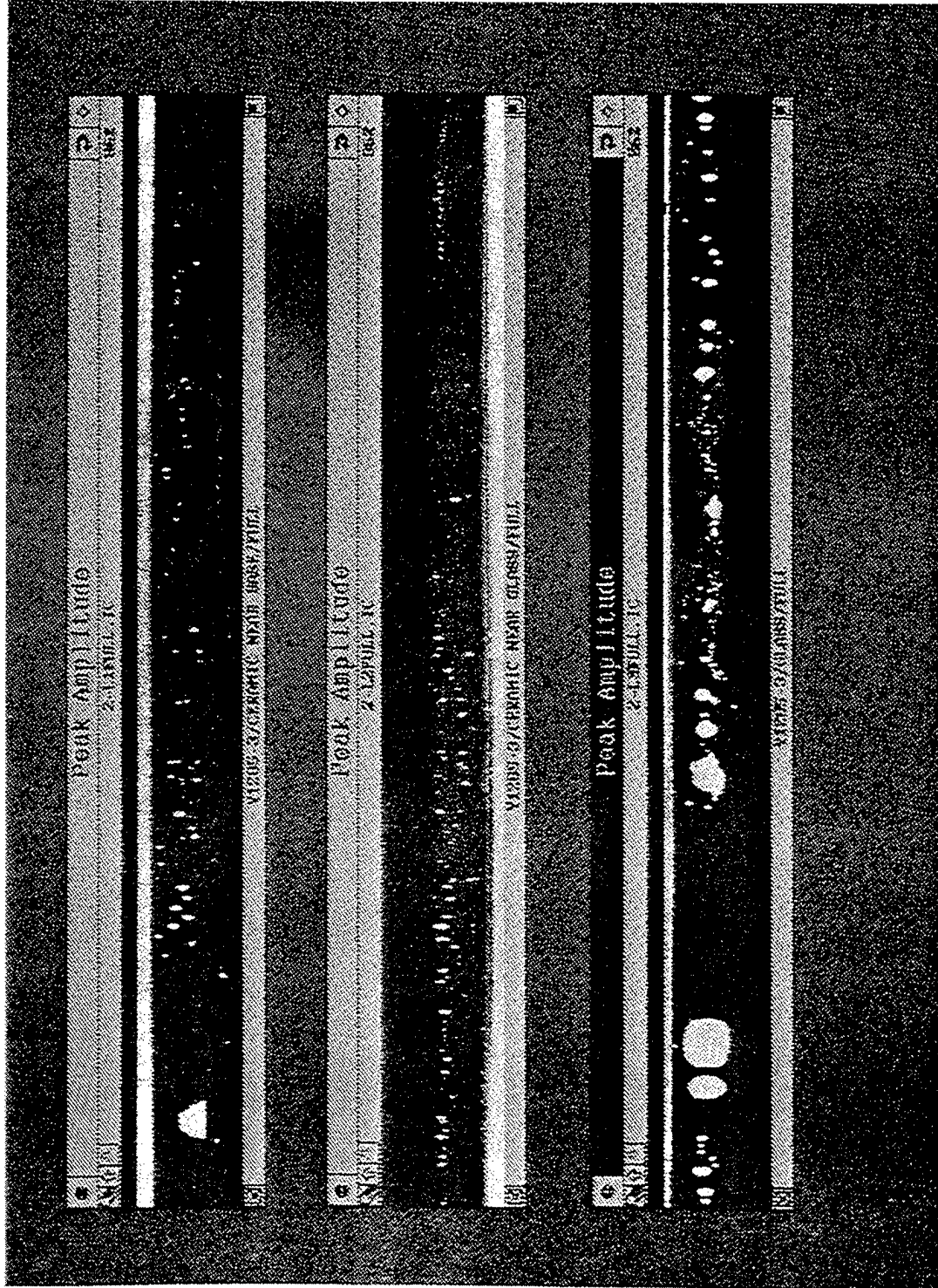
62777 11.8

3-11 3000 6477/CERAMIC NEAR ROSE/FUEL

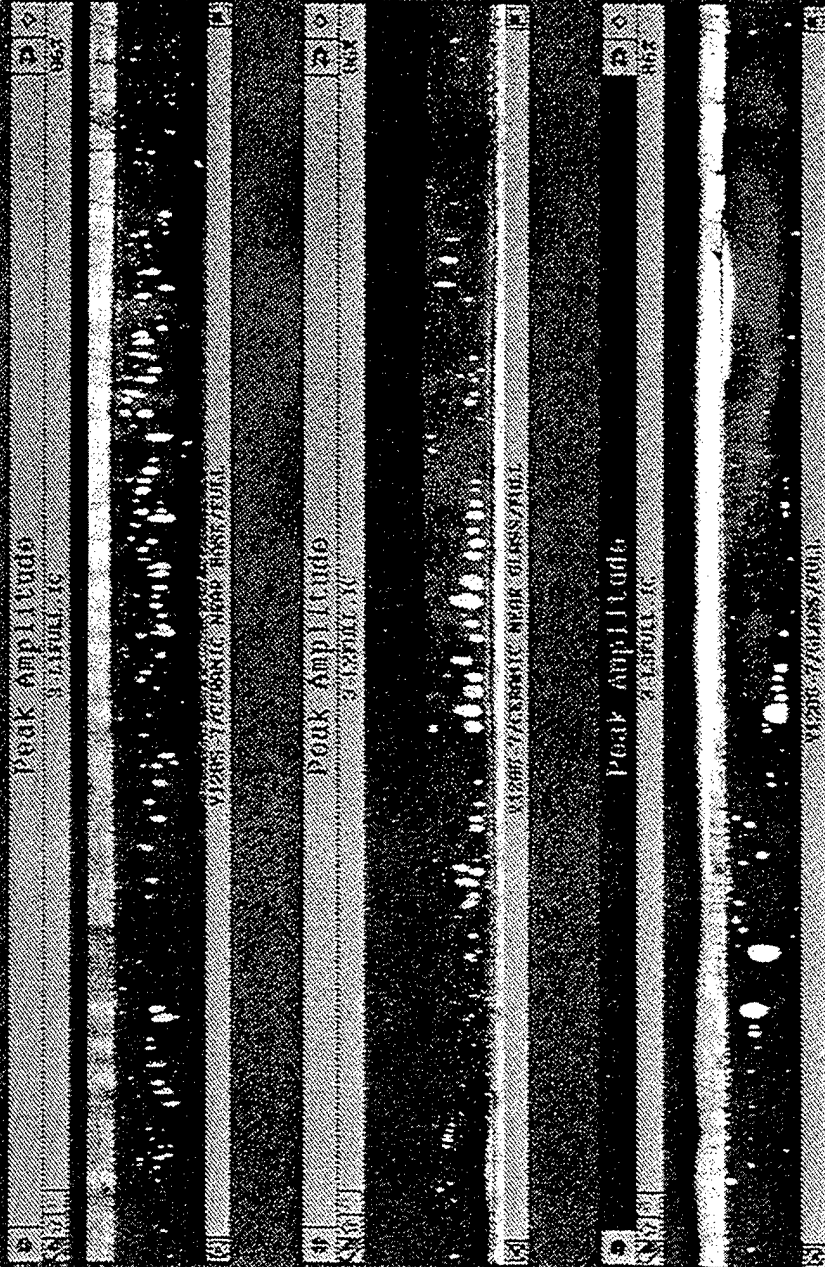
Peak Amplitude
7.325E+10

3-11 3000 6477/CERAMIC NEAR GLASS/FUEL

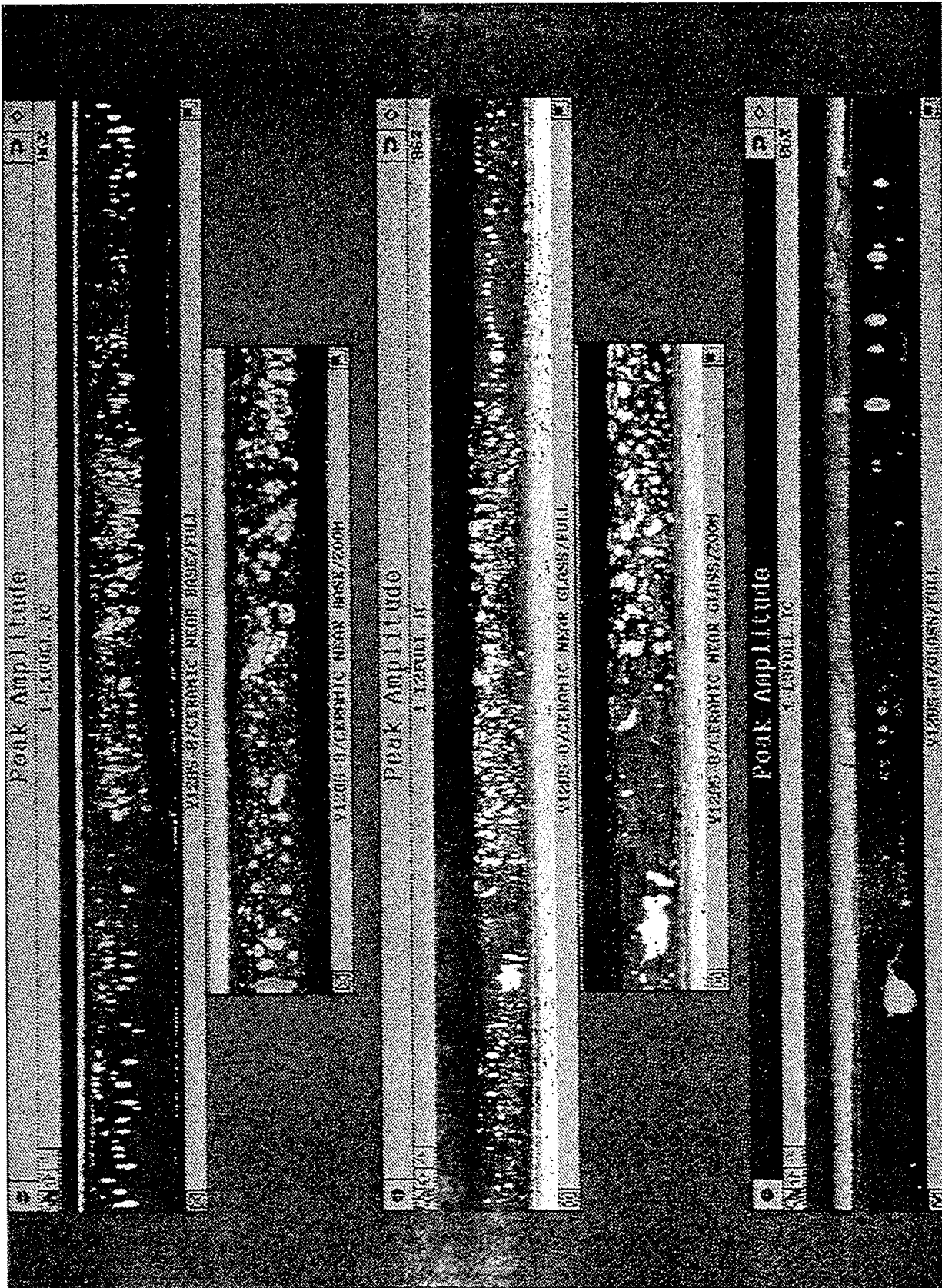
#5 Y1285 Ser#Y1285-3 Date Code 9344 2Hrs Reflector Turned Brown Same as #6



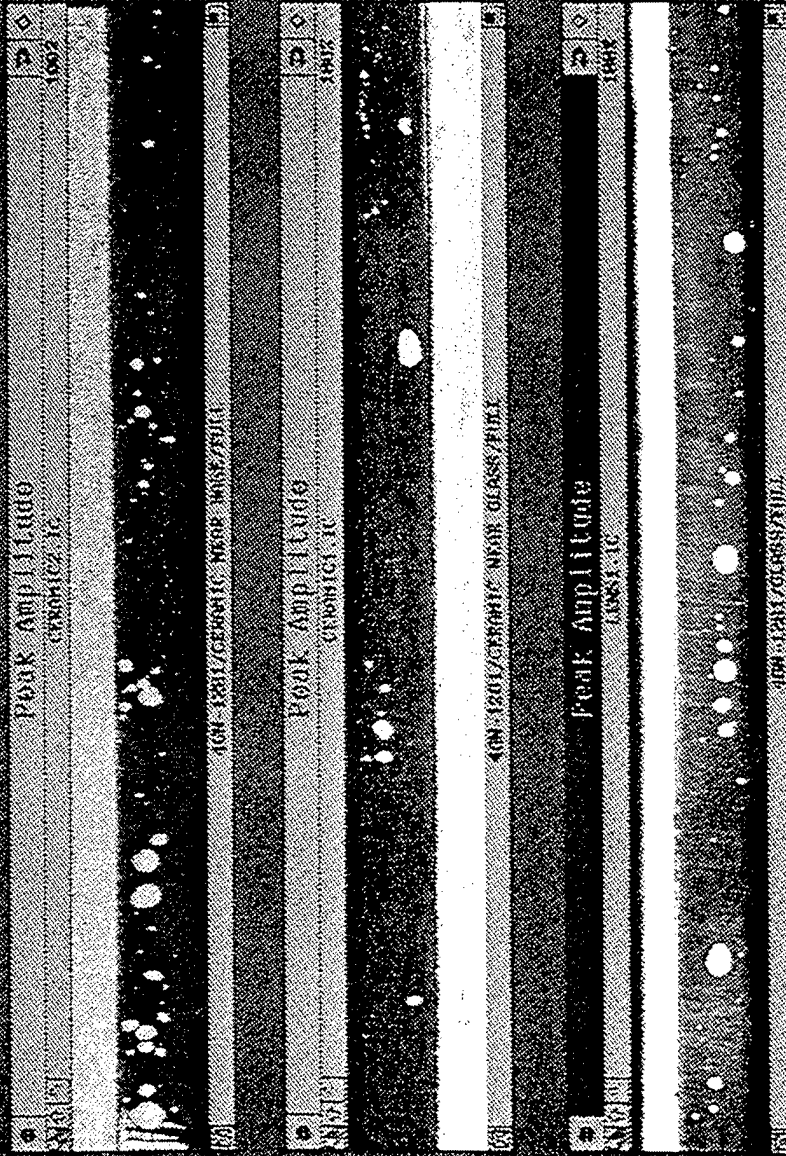
6 Y1285-7 Date Code 9344 36Hours Repl.Cracked & Brown (SID)



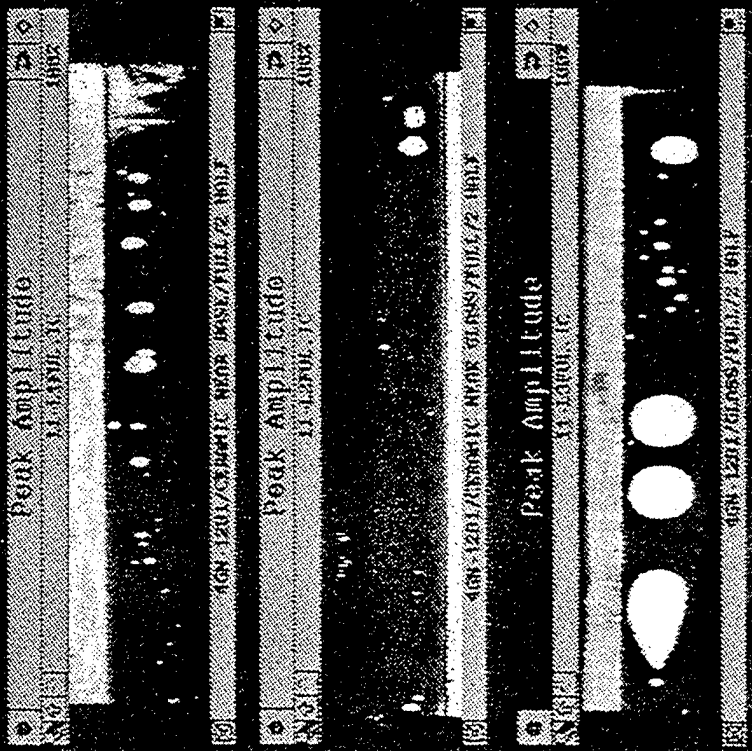
#7 Y1285-8 Ser# Y1285-8 Date Code 9344 90Hrs Dim Light Reflector Black



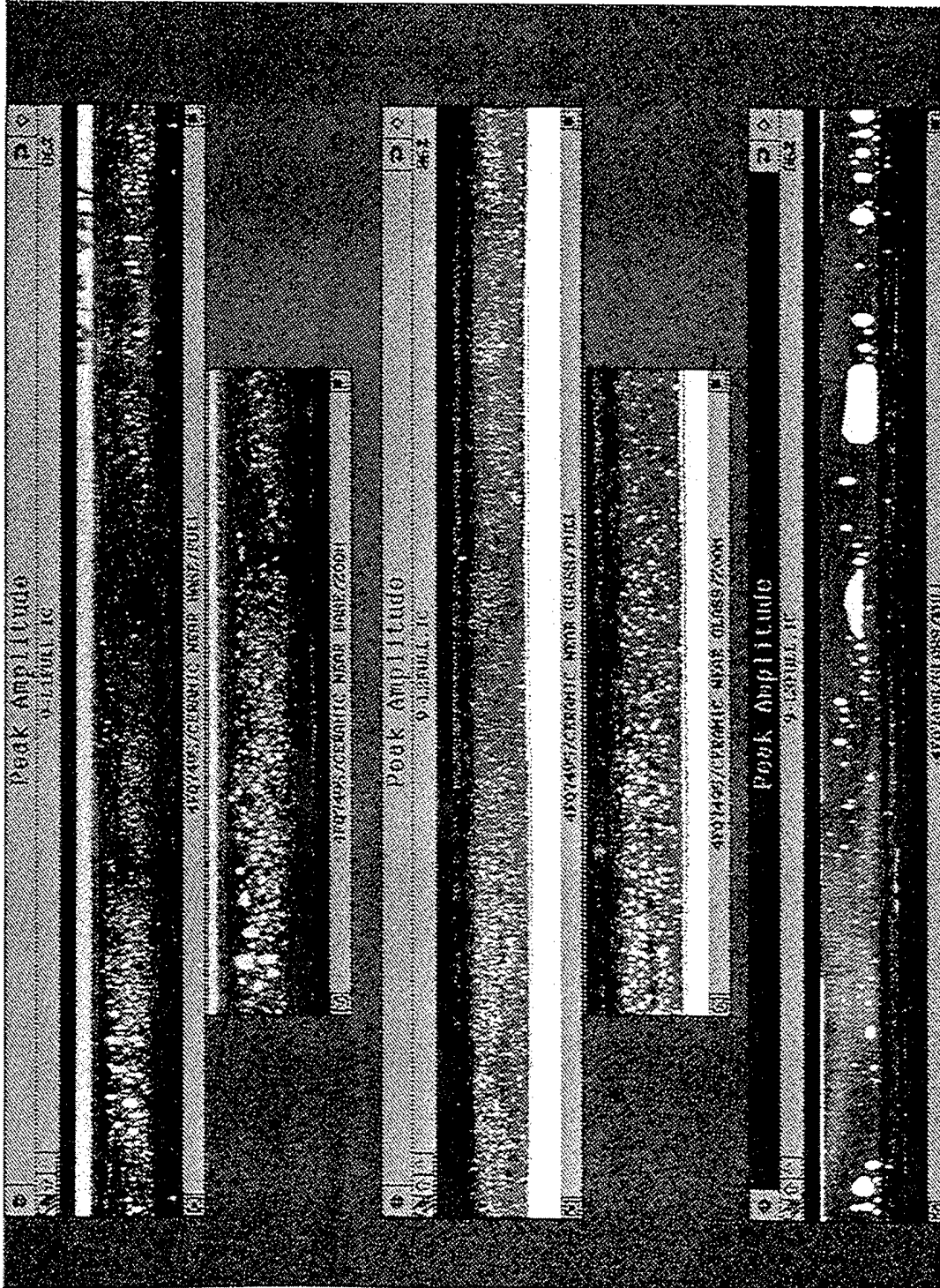
8 Y1285 4GN-1281 Date 3/9/94 Zero Hours Lamp Dissected First Half



8A Y1285 Ser#4GN-1281 Date 3/9/94 Zero Hrs Dissected 2nd Half

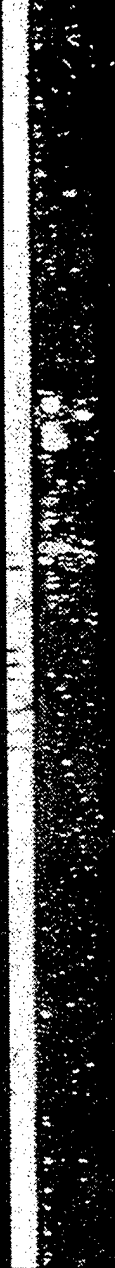


#9 LX1000c-f Ser# 4FQ7495 Date Code 9426 Zero Hrs Last lamp in stock



10 LX1000c-f Ser# 3LQ1494 Date Code 9348 40Hrs Refl.Total Black

Peak Amplitude
16.410031e



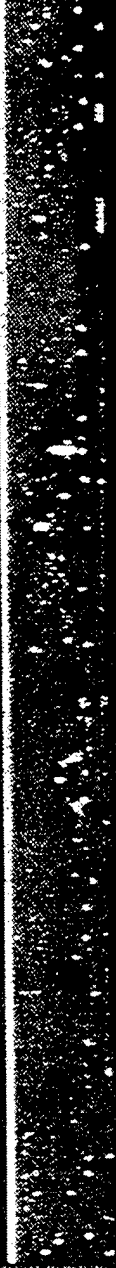
16.410031e 16.410031e

Peak Amplitude
16.410031e



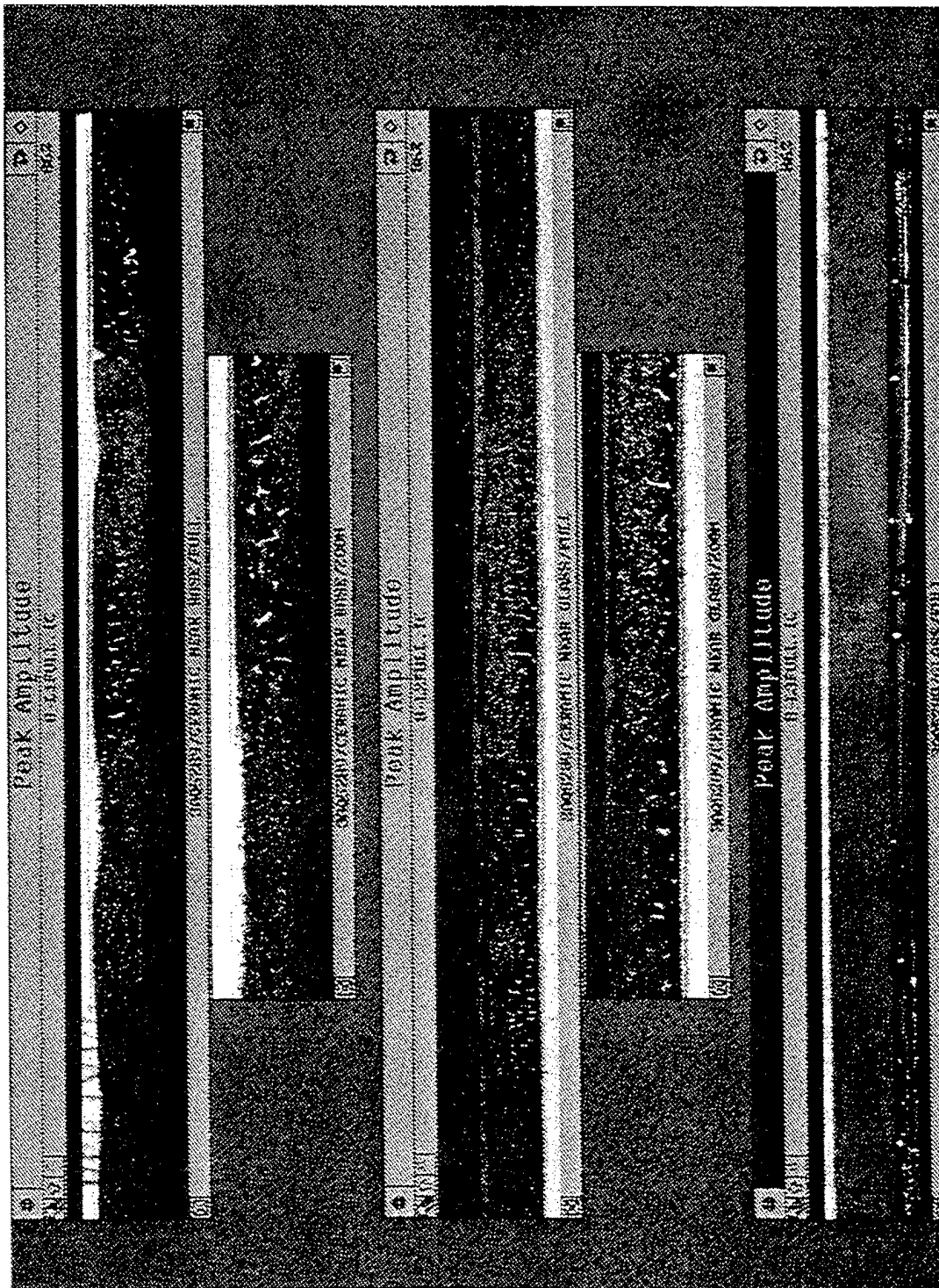
16.410031e 16.410031e

Peak Amplitude
16.410031e

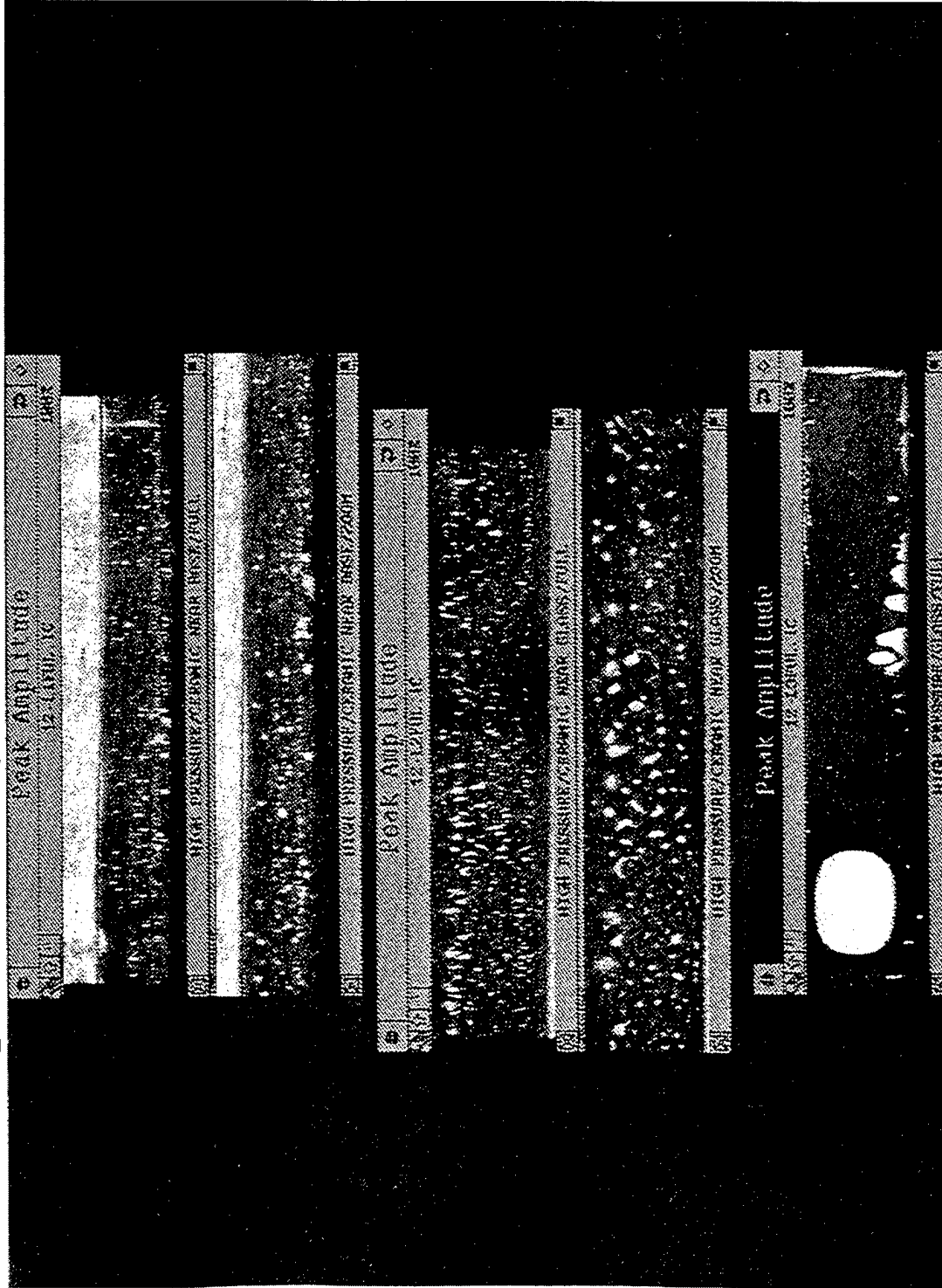


16.410031e 16.410031e

11 LX1000c-f Ser#3AQ5289 Date Code 9306 92Hrs Dim Light



12 LION High Pressure Lamp Date Code N/A Hrs N/A



Digital Imaging Venture Project Safety Operating Instructions

| Title | Date Issued | OI Number |
|--|-------------|-----------|
| Generation, Control, and Distribution of Safety Operating Instructions | | SOI001 |

1.0 Scope

These Safety Operating Instructions are generated for the Digital Imaging Venture Project (DIVP) to provide specific operating policies and procedures for areas not covered by Texas Instruments Safety Practices and which cannot effectively be covered by individual DIVP work area safety practices.

2.0 Functions Affected

This procedure applies to the Digital Imaging Venture Project of the Corporate Venture Projects of Texas Instruments Incorporated.

3.0 Policy

It is the policy of the Digital Imaging Venture Project to document the policies and procedures which affect the safety and health of people and the safety of equipment and facilities with Safety Operating Instructions.

4.0 Generation of Operating Instructions

Any member of the Digital Imaging Venture Project may generate a Safety Operating Instruction.

5.0 Review and Approval of Operating Instructions

Safety Operating Instructions are reviewed by the safety unit manager and designees from:

- Display
- Hardcopy
- DMD Development
- Quality and Reliability
- Administration
- Manufacturing

Safety Operating Instructions are approved by the Digital Imaging Manager.

Digital Imaging Venture Project Safety Operating Instructions

| Title | Date Issued | OI Number |
|--|-------------|-----------|
| Generation, Control, and Distribution of Safety Operating Instructions | | SOI001 |

6.0 Distribution of Safety Operating Instructions

- Safety Operating Instructions are available to all members of the Digital Imaging Venture Project by accessing the CVP Information System files at:
`\\DNBSO1\CVPINFO\SONRELEASED\SOIXXX.DOC`
- Copies of the Safety Operating Instructions are not to be routinely printed.
- When new Safety Operating Instructions are issued, each member of the department will be informed of the addition.
- New Safety Operating Instructions (SOI's) will be explained to the employees at department or work group meetings.
- New employees in Digital Imaging will have the SOI system explained to them upon joining the department and will have each Safety Operating Instruction explained by the supervisor as part of orientation.

7.0 Control of Safety Operating Instructions

- The DIVP Safety Coordinator is responsible for the control of Safety Operating Instructions.
- The DIVP Safety Coordinator will have each Operating Instruction audited annually and will make changes and corrections as appropriate.
- The approved copy of each Operating Instruction will be stored in the Digital Imaging Library.

8.0 Content of Safety Operating Instructions

The Safety Operating Instructions contain:

- A title.
- The date of issue.
- A sequential SOI number assigned by the DIVP Safety Coordinator.
- Page numbers.
- A body with at least a scope and policy or procedure section.
- Approval by the Digital Imaging Manager.

Digital Imaging Venture Project Safety Operating Instructions

| Title | Date Issued | OI Number |
|--|-------------|-----------|
| Generation, Control, and Distribution of Safety Operating Instructions | | SOI001 |

9.0 Index

An Index of the Safety Operating Instructions is maintained and a new copy is distributed each time an Operating Instruction changes or is added. The index contains:

- The date of issue of the Index.
- A table of the currently active OI's and the date of the currently active Operating Instruction.

10.0 Approval

J. B. Harrod
Executive Vice President
Corporate Staff
Manager, Corporate Venture Projects

| Title | Date Issued | OI Number |
|-------------|-------------|-----------|
| LAMP SAFETY | | SOI002 |

1.0 SCOPE

This document describes the current safety policy and practice for handling or operating all lamps used by Digital Imaging Venture Products (DIVP) projects. For specific information concerning lamp handling and operation refer to the lamp safety data sheet. The objective is to minimize unsafe acts and conditions that may cause serious injury or illness to personnel or damage to property and equipment.

2.0 HAZARDS

WARNING

Serious hazards exist in the handling and operation of lamps. The operation of lamps involves one or more of the following hazards, any one of which could result in serious harm to personnel. Proper safety precautions must be followed when handling or operating lamps.

2.1 High Voltage

Ignition voltages of lamps can be deadly. Portions of the lamp may be exposed and caution must be used in the setup and operation of the DIVP illumination system. Never operate a lamp above the manufacturers suggested power rating. As with all electrical equipment, the input power must be disconnected before attempting any service of the lamp. Even when disconnected, some residual energy may be stored in the power source. For additional handling information, refer to the lamp safety data sheet.

2.2 Explosion

Some lamps are filled at high pressure. A hazard exists if the window or ceramic fractures. The resulting explosion could cause serious bodily injury or death. Only qualified and trained personnel may handle and/or assemble high pressure lamps. The possibility of lamp failure is greater during startup and operation. Face shields and protective clothing, designed to withstand explosive failure, are required during all handling and maintenance of unshielded high pressure lamps.

2.3 Infrared and Ultraviolet Radiation

Infrared radiation may be emitted from some lamps. Infrared radiation causes heating of the tissues and prolonged exposure may damage the eyes. Some lamps emit ultraviolet radiation. Exposure of the unprotected skin to ultraviolet radiation may cause painful skin burns. Exposure of unprotected eyes to ultraviolet radiation may cause permanent injury. The eyes also can be damaged from ultraviolet radiation reflected from other surfaces. Protective, ultraviolet-absorbing, dark, safety glasses must be worn while working in an open exposure cabinet when the lamp is illuminated. In addition, protect skin with clothing, and do not expose skin area to ultraviolet light, as burns will result from overexposure to ultraviolet or infrared energy. All protective covers and baffles must be installed around the light source prior to working within the exposure cabinet.

| Title | Date Issued | OI Number |
|-------------|-------------|-----------|
| LAMP SAFETY | | SOI002 |

2.4 Bright Light

The bright light emitted by the lamp can cause permanent damage to the eyes. Never look into a bright light source of any kind (lamp, laser, the sun, etc.). All protective covers and baffles should be installed around the light source prior to working within the exposure cabinet. If you cannot avoid exposure to the lamp output, protective dark safety glasses must be worn.

2.5 Hot Surfaces

During operation and immediately after turnoff, exterior surfaces of the lamp are hot enough to cause burns. All lamp surfaces remain hot for an extended time after lamp turnoff. To prevent serious burns, use care to prevent bodily contact with the lamp surfaces during operation and for a cool-down period after turnoff.

2.6 Fire

A fire hazard exists if combustible materials are in or near the illumination path. When chemicals have been used for cleaning purposes, ensure all excess solution has been removed and the chemical is dried before operation of the illumination system. Do not attempt to clean any illumination system which may still be hot from previous operation. Use cleaning chemicals in adequate ventilation and avoid prolonged or repeated breathing of vapors. Keep cleaning tissues and all other materials away from the illumination source/path to prevent sources of flame or ignition.

3.0 OPERATING INSTRUCTIONS

3.1 General Instructions

This information is provided to help establish safe operating conditions for the operator and the illumination system. Questions regarding lamp operation or safety matters should be addressed to the site safety coordinator and/or lamp supplier.

Only qualified personnel who have been trained in the safe operation of illumination systems may operate such equipment. The operation of the illumination system should begin only when the protective enclosure and cover has been installed and only after the operator has performed a safety inspection of all related equipment (reference lamp safety data sheet).

Protective, ultraviolet-absorbing, dark, safety glasses must be worn while working in an open exposure cabinet when the lamp is illuminated. Serious eye damage can result from looking at ultraviolet or infrared energy with unprotected eyes. All protective covers and baffles must be installed around the light source prior to working within the exposure cabinet.

3.2 Handling and Storage

High pressure lamps should be handled and stored with the same caution given any vessel containing extremely high pressure levels. Appropriate care must be taken when handling lamps.

| Title | Date Issued | OI Number |
|-------------|-------------|-----------|
| LAMP SAFETY | | SOI002 |

Protective eye wear only provides minimum protection. Face shields and protective clothing, designed to withstand explosive failure, are required during all handling and maintenance of unshielded high pressure lamps. These lamps, if dropped or cracked, can explode with force, projecting glass fragments outward with sufficient force to cause injury or death.

3.3 Assembly of Lamps

Only qualified and trained personnel may handle and/or assemble high pressure lamps. Refer to the lamp safety data sheet for specific assembly and/or handling instructions.

4.0 LAMP SAFETY DATA SHEET

Each lamp type will have a lamp safety data sheet before it is used. The lamp safety data sheet will have the following minimum information:

- manufacturers part number
- manufacturers data sheet
- manufacturers safety instructions
- special operating and/or handling instructions
- radiation evaluation report from TI Safety

5.0 WARNING SIGNS AND LABELS

Each laboratory and illumination system will have the appropriate warning signs and labels.

6.0 APPROVAL

J. B. Harrod
 Executive Vice President
 Corporate Staff
 Manager, Corporate Venture Projects

LAMP SAFETY DATA SHEET

MANUFACTURER: COUGAR
LAMP PART NUMBER: CSL-R 100
LAMP DESCRIPTION: 100 WATT
DATA SHEET: Appendix A
SAFETY INSTRUCTIONS: Not Available
ASSEMBLY INSTRUCTIONS: Not Applicable

HAZARDS: (RISK: 1=Low, 2=Moderate, 3=High)

| | | |
|--------------------|-----|--|
| High Voltage: | (3) | Install all protective covers. Disconnect power prior to service. |
| Explosion: | (1) | Wear protective safety glasses. |
| IR & UV Radiation: | (2) | Install all protective baffles. Wear UV absorbing, dark, safety glasses. |
| Bright Light: | (2) | Do not stare into light source. |
| Hot Surfaces: | (2) | Prevent bodily contact with lamp surfaces. |
| Fire: | (2) | Keep combustible materials away from illumination source/path. |

GENERAL INFORMATION:

The greatest potential for harm in working with the Cougar 100 Watt lamp is the danger of electrical shock. Portions of the circuit may be exposed and caution must be used in the setup and operation of the system.

PROTECTIVE EQUIPMENT:

SYSTEM OPERATION:

The Cougar lamp does not present any significant potential for explosion. Explosion protective shields are not required for the operation of this lamp. Protective baffling for IR and UV radiation shall be installed prior to operating the illumination system. Protective, ultraviolet absorbing, dark, safety glasses must be worn when working within the exposure cabinet when the lamp is illuminated. All protective covers must be installed prior to operating the illumination system.

HANDLING AND MAINTENANCE:

Protective safety glasses shall be worn when handling the Cougar lamp. In the event that a lamp is broken, protective gloves shall be worn when handling the glass fragments.

LAMP ASSEMBLY:

Not Applicable

STORAGE:

Lamps when not in use must be stored in a secure location in their original shipping container or within a foam lined enclosure.

**COUGAR CSL-R 100
DATA SHEET**

CONFIDENTIAL
(See Jim Florence or Jack Gregory)

Appendix A

LAMP SAFETY DATA SHEET

MANUFACTURER: ILC
LAMP PART NUMBER: CERMAX LX1000-CF
LAMP DESCRIPTION: 1000 WATT XENON LAMP
DATA SHEET: Appendix A
SAFETY INSTRUCTIONS: Appendix B
ASSEMBLY INSTRUCTIONS: Appendix C
INSTALLATION INSTRUCTIONS: Appendix D
POWER SUPPLY OPERATION: Appendix E

HAZARDS: (RISK: 1=Low, 2=Moderate, 3=High)

High Voltage: (3) Install all protective covers. Disconnect power prior to service.
Explosion: (3) Install all protective covers. Wear appropriate safety clothing.
IR & UV Radiation: (2) Wear UV absorbing, dark, safety glasses.
Bright Light: (2) Do not stare into light source.
Hot Surfaces: (2) Prevent bodily contact with lamp surfaces.
Fire: (2) Keep combustible materials away from illumination source/path.

GENERAL INFORMATION:

The greatest potentials for harm in working with the ILC Xenon pressurized lamps is the danger of electrical shock and explosion. Ignition voltages of the lamp can be deadly. Portions of the lamp may be exposed and caution must be used in the setup and operation. The Xenon lamp listed above is classified as a high pressure lamp and should be handled accordingly. The possibility of violent failure of the lamp is greatest during start-up and operation. A hazard exists if the lamp is dropped or damaged. If the window or ceramic fractures the resulting explosive failure could cause serious bodily injury or death. Only qualified and trained personnel may handle and/or assemble Xenon high pressure lamps.

Possible explosions may be caused by the following conditions:

- a) Overpowering the lamp above rated power (i.e. 1000 Watts).
- b) High peak power lasting several milliseconds. Resulting high thermal gradients can cause ceramic failures.
- c) Operating lamps without a fan or failure of the fan could cause high thermal gradients which can cause ceramic failures.
- d) Excessive clamping of heatsinks, especially on the ceramic to metal sleeve interface can cause ceramic failures.

PROTECTIVE EQUIPMENT:

SYSTEM OPERATION:

All protective shields, covers and/or baffles must be installed around the light source prior to working within the exposure cabinet. Protective, ultraviolet absorbing, dark, safety glasses shall be worn when working within the exposure cabinet when the lamp is illuminated.

HANDLING AND MAINTENANCE:

Protective safety glasses, face shields, gloves, arm shields, and protective clothing, designed to withstand explosive failure, must be worn during all handling and maintenance of unshielded lamps.

LAMP ASSEMBLY:

Protective safety glasses, face shields, gloves, arm shields, and protective clothing, designed to withstand explosive failure, must be worn when assembling lamps. The lamps must be assembled within the lamp assembly fixture (JG-BMB-100).

STORAGE:

Unassembled lamps must be stored in a secure location in their original shipping container or within a foam lined metal enclosure.

LAMP SAFETY DATA SHEET

MANUFACTURER: ILC
LAMP PART NUMBER: CERMAX LX300F
LAMP DESCRIPTION: 300 WATT XENON LAMP
DATA SHEET: Appendix A
SAFETY INSTRUCTIONS: Appendix B
ASSEMBLY INSTRUCTIONS: TBD
INSTALLATION INSTRUCTIONS: TBD
POWER SUPPLY OPERATION: TBD

HAZARDS: (RISK: 1=Low, 2=Moderate, 3=High)

High Voltage: (3) Install all protective covers. Disconnect power prior to service.
Explosion: (3) Install all protective covers. Wear appropriate safety clothing.
IR & UV Radiation: (2) Wear UV absorbing, dark, safety glasses.
Bright Light: (2) Do not stare into light source.
Hot Surfaces: (2) Prevent bodily contact with lamp surfaces.
Fire: (2) Keep combustible materials away from illumination source/path.

GENERAL INFORMATION:

The greatest potentials for harm in working with the ILC Xenon pressurized lamps is the danger of electrical shock and explosion. Ignition voltages of the lamp can be deadly. Portions of the lamp may be exposed and caution must be used in the setup and operation. The Xenon lamp listed above is classified as a high pressure lamp and should be handled accordingly. The possibility of violent failure of the lamp is greatest during start-up and operation. A hazard exists if the lamp is dropped or damaged. If the window or ceramic fractures the resulting explosive failure could cause serious bodily injury or death. Only qualified and trained personnel may handle and/or assemble Xenon high pressure lamps.

Possible explosions may be caused by the following conditions:

- a) Overpowering the lamp above rated power (i.e. 300 Watts).
- b) High peak power lasting several milliseconds. Resulting high thermal gradients can cause ceramic failures.
- c) Operating lamps without a fan or failure of the fan could cause high thermal gradients which can cause ceramic failures.
- d) Excessive clamping of heatsinks, especially on the ceramic to metal sleeve interface can cause ceramic failures.

PROTECTIVE EQUIPMENT:

SYSTEM OPERATION:

All protective shields, covers and/or baffles must be installed around the light source prior to working within the exposure cabinet. Protective, ultraviolet absorbing, dark, safety glasses shall be worn when working within the exposure cabinet when the lamp is illuminated.

HANDLING AND MAINTENANCE:

Protective safety glasses, face shields, gloves, arm shields, and protective clothing, designed to withstand explosive failure, must be worn during all handling and maintenance of unshielded lamps.

LAMP ASSEMBLY:

Protective safety glasses, face shields, gloves, arm shields, and protective clothing, designed to withstand explosive failure, must be worn when assembling lamps. The lamps must be assembled within the lamp assembly fixture (JG-BMB-100).

STORAGE:

Unassembled lamps must be stored in a secure location in their original shipping container or within a foam lined metal enclosure.

LAMP SAFETY DATA SHEET

MANUFACTURER: ILC
LAMP PART NUMBER: CERMAX Y1285 (Experimental Lamp)
LAMP DESCRIPTION: 1200 WATT XENON LAMP
DATA SHEET: Not Applicable
SAFETY INSTRUCTIONS: Appendix B
ASSEMBLY INSTRUCTIONS: Appendix C
INSTALLATION INSTRUCTIONS: Appendix D
POWER SUPPLY OPERATION: Appendix E

HAZARDS: (RISK: 1=Low, 2=Moderate, 3=High)

High Voltage: (3) Install all protective covers. Disconnect power prior to service.
Explosion: (3) Install all protective covers. Wear appropriate safety clothing.
IR & UV Radiation: (2) Wear UV absorbing, dark, safety glasses.
Bright Light: (2) Do not stare into light source.
Hot Surfaces: (2) Prevent bodily contact with lamp surfaces.
Fire: (2) Keep combustible materials away from illumination source/path.

GENERAL INFORMATION:

The greatest potentials for harm in working with the ILC Xenon pressurized lamps is the danger of electrical shock and explosion. Ignition voltages of the lamp can be deadly. Portions of the lamp may be exposed and caution must be used in the setup and operation. The Xenon lamp listed above is classified as a high pressure lamp and should be handled accordingly. The possibility of violent failure of the lamp is greatest during start-up and operation. A hazard exists if the lamp is dropped or damaged. If the window or ceramic fractures the resulting explosive failure could cause serious bodily injury or death. Only qualified and trained personnel may handle and/or assemble Xenon high pressure lamps.

Possible explosions may be caused by the following conditions:

- a) Overpowering the lamp above rated power (i.e. 1200 Watts).
- b) High peak power lasting several milliseconds. Resulting high thermal gradients can cause ceramic failures.
- c) Operating lamps without a fan or failure of the fan could cause high thermal gradients which can cause ceramic failures.
- d) Excessive clamping of heatsinks, especially on the ceramic to metal sleeve interface can cause ceramic failures.

PROTECTIVE EQUIPMENT:

SYSTEM OPERATION:

All protective shields, covers and/or baffles must be installed around the light source prior to working within the exposure cabinet. Protective, ultraviolet absorbing, dark, safety glasses shall be worn when working within the exposure cabinet when the lamp is illuminated.

HANDLING AND MAINTENANCE:

Protective safety glasses, face shields, gloves, arm shields, and protective clothing, designed to withstand explosive failure, must be worn during all handling and maintenance of unshielded lamps.

LAMP ASSEMBLY:

Protective safety glasses, face shields, gloves, arm shields, and protective clothing, designed to withstand explosive failure, must be worn when assembling lamps. The lamps must be assembled within the lamp assembly fixture (JG-BMB-100).

STORAGE:

Unassembled lamps must be stored in a secure location in their original shipping container or within a foam lined metal enclosure.

LAMP SAFETY DATA SHEET

MANUFACTURER: ILC
LAMP PART NUMBER: CERMAX Y1343 (Experimental Lamp)
LAMP DESCRIPTION: 700 WATT XENON LAMP (Extremely High Pressure)
DATA SHEET: Not Applicable
SAFETY INSTRUCTIONS: Appendix B
ASSEMBLY INSTRUCTIONS: Appendix C
INSTALLATION INSTRUCTIONS: Appendix D
POWER SUPPLY OPERATION: Appendix E

HAZARDS: (RISK: 1=Low, 2=Moderate, 3=High)

High Voltage: (3) Install all protective covers. Disconnect power prior to service.
Explosion: (3) Install all protective covers. Wear appropriate safety clothing.
IR & UV Radiation: (2) Wear UV absorbing, dark, safety glasses.
Bright Light: (2) Do not stare into light source.
Hot Surfaces: (2) Prevent bodily contact with lamp surfaces.
Fire: (2) Keep combustible materials away from illumination source/path.

GENERAL INFORMATION:

The greatest potentials for harm in working with the ILC Xenon pressurized lamps is the danger of electrical shock and explosion. Ignition voltages of the lamp can be deadly. Portions of the lamp may be exposed and caution must be used in the setup and operation. The Xenon lamp listed above is classified as a high pressure lamp and should be handled accordingly. The possibility of violent failure of the lamp is greatest during start-up and operation. A hazard exists if the lamp is dropped or damaged. If the window or ceramic fractures the resulting explosive failure could cause serious bodily injury or death. Only qualified and trained personnel may handle and/or assemble Xenon high pressure lamps.

Possible explosions may be caused by the following conditions:

- a) Overpowering the lamp above rated power (i.e. 700 Watts).
- b) High peak power lasting several milliseconds. Resulting high thermal gradients can cause ceramic failures.
- c) Operating lamps without a fan or failure of the fan could cause high thermal gradients which can cause ceramic failures.
- d) Excessive clamping of heatsinks, especially on the ceramic to metal sleeve interface can cause ceramic failures.

PROTECTIVE EQUIPMENT:

SYSTEM OPERATION:

All protective shields, covers and/or baffles must be installed around the light source prior to working within the exposure cabinet. Protective, ultraviolet absorbing, dark, safety glasses shall be worn when working within the exposure cabinet when the lamp is illuminated.

HANDLING AND MAINTENANCE:

Protective safety glasses, face shields, gloves, arm shields, and protective clothing, designed to withstand explosive failure, must be worn during all handling and maintenance of unshielded lamps.

LAMP ASSEMBLY:

Protective safety glasses, face shields, gloves, arm shields, and protective clothing, designed to withstand explosive failure, must be worn when assembling lamps. The lamps must be assembled within the lamp assembly fixture (JG-BMB-100).

STORAGE:

Unassembled lamps must be stored in a secure location in their original shipping container or within a foam lined metal enclosure.

CERMAX[®] XENON ILLUMINATORS



ILC Technology

399 JAVA DRIVE • SUNNYVALE, CALIFORNIA 94089
PHONE (408) 745-7800 • TWX 910-338-9388 • FAX 408-744-0829

Features.

- Rugged and compact ceramic-to-metal construction
- Optically prealigned
- Safer than conventional (quartz bulb) xenon lamps
- Ozone-free versions available
- Daylight color (5600 K)
- UV-enhanced lamps available
- High efficiency integral reflector
- Parabolic or elliptical reflectors
- IR suppressed version available.

Applications.

Fiber optic illumination
Analytical instrumentation
Spectroscopy
Audio-visual systems
Microscopy
Character recognition
Data projection
Infrared and visual searchlights
Infrared and ultraviolet systems

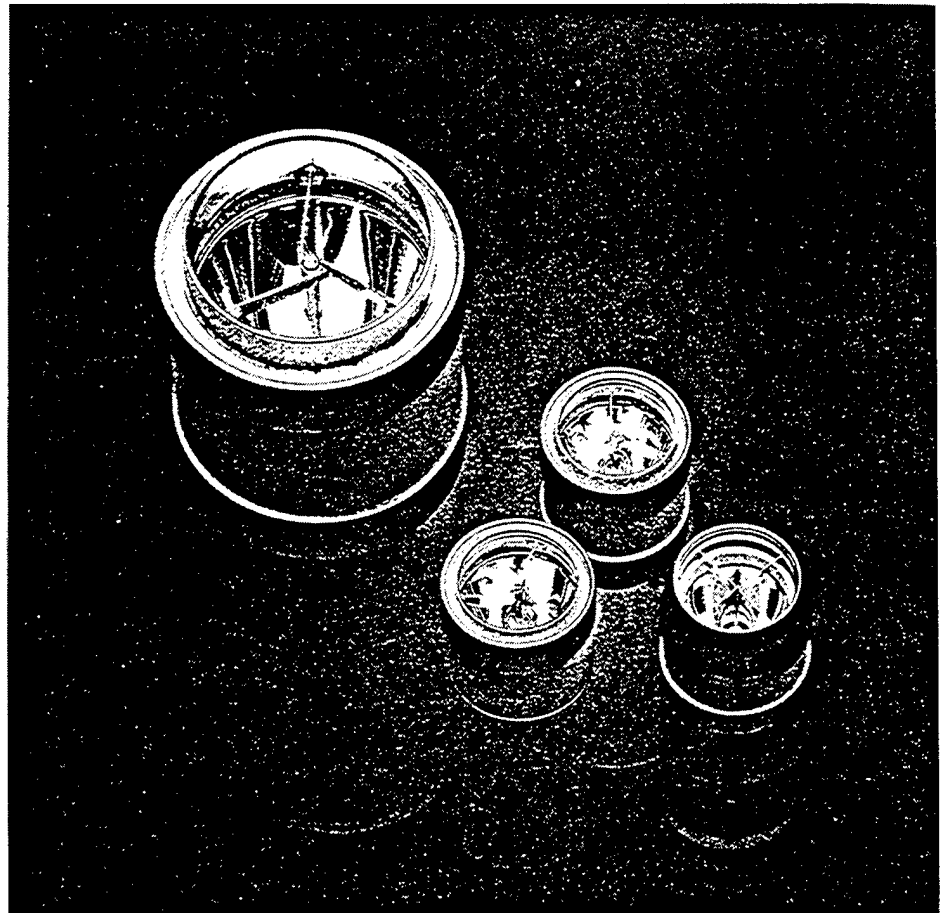
ILC's CERMAX[®] high intensity narrow beam light sources are compact and rugged xenon short arc lamps with fixed internal reflectors. They are reliable and efficient sources of broadband ultraviolet, visible and infrared radiation.

CERMAX lamps combine xenon short arc technology with ILC's unique ceramic-to-metal sealing techniques. The mechanical integrity of these lamps far exceeds that of any other type of short arc lamp.

The internal reflector is prealigned and requires no adjustment. Optimal reflector design results in a large collection angle around the arc, maximizing efficiency of output.

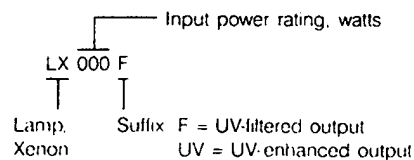
The single-crystal sapphire windows used in every CERMAX lamp have excellent transmission from the ultraviolet deep into the infrared.

CERMAX lamps solve the problems associated with quartz arc lamps, fragility, devitrification, and the need for external reflector adjustment. You will find them much easier to incorporate into your design and use.



LX Series Lamps.

The following nomenclature is used to describe the ILC CERMAX lamps:



The reflectors of CERMAX lamps are vacuum deposited on the precision ceramic surface. The LX75 F/UV lamps employ a precisely stamped aluminum reflector which is overcoated with high reflectivity aluminum or silver. The lamp bodies are of high density alumina ceramic. The windows are of single crystal sapphire. Mounting is normally by means of the bolt circle in the anode plate and by the cathode ring (OD).

Power Supply Information.

It is recommended that the lamps be operated with the input power limits indicated in Table A. Overpowering a lamp will cause rapid electrode wear and may even lead to structural failure. Underpowering may cause arc instability and, eventually, hard starting. Current-regulated or power-regulated supplies with output ripples of less than 5% are recommended for all lamps. Monopolar single shot ignition pulses are advised because radio frequency starters may damage the lamp's internal reflectors.

Please review the detailed operating safety sheet enclosed with each lamp, and available on request from ILC.

Table A: TYPICAL CHARACTERISTICS—CERMAX LAMPS

| LAMP TYPE | 75W | 150W | 300W | 500W | 1000W |
|---|----------------------|-----------------------|-----------------------|----------------------|-----------------------|
| Nominal Operating Power (watts) | 75 | 150 | 300 | 500 | 1000 |
| Operating Power Range (watts) | 60-75 | 90-180 | 180-320 | 340-575 | 850-1050 |
| Nominal Operating Current (amps dc) | 7 | 13 | 21 | 20 | 48-54 |
| Operating Current Range (amps dc) | 6-8 | 8-15 | 10-22 | 20-32 | 48-54 |
| Nominal Operating Voltage (volts dc) | 10.7 | 12 | 14 | 18.5 | 19.5 |
| Operating Voltage Range (volts dc) | 9.5-13 | 11-13.5 | 13-16 | 16-21 | 18.5-21 |
| Ignition Voltage (kilovolts) | 17 | 17 | 23 | 35 | 35 |
| Beam Geometry—Half Angle at 0/100/1000 hrs. (degrees) | 5/7/10 | 4.5/5/6 | 5/6/7 | 3/4/5 | 4/5/6 |
| Radiant Beam Characteristics (nominal values) | | | | | |
| Peak Intensity (candelas) | | | | | |
| (F suffix) | 50 x 10 ³ | 330 x 10 ³ | 515 x 10 ³ | 24 x 10 ³ | 3.8 x 10 ³ |
| (UV suffix) | 47 x 10 ³ | 310 x 10 ³ | 460 x 10 ³ | 17 x 10 ³ | 2.7 x 10 ³ |
| Radiant Output (watts) | 8.5 | 21 | 50 | 112 | 250 |
| UV Output* | | | | | |
| (F suffix) | 0.4 | 1.0 | 2.6 | 5.5 | 13 |
| (UV suffix) | 1.0 | 2.8 | 6.6 | 11.5 | 25 |
| Visible Output (lumens)** | | | | | |
| (F suffix) | 525 | 1,900 | 5,000 | 10,500 | 24,000 |
| (UV suffix) | 485 | 1,750 | 4,500 | 9,600 | 22,000 |
| IR Output (watts)*** | | | | | |
| (F suffix) | 5 | 12 | 28.8 | 65 | 137 |
| (UV suffix) | 4.8 | 11.5 | 26.8 | 62 | 133 |
| Reflection Geometry | | | | | |
| P = Parabola | P | P | P | P | P |
| Reflector Coating | | | | | |
| S = Silver, A = Aluminum | | | | | |
| (F suffix) | S | S | S | S | S |
| (UV suffix) | A | A | A | A | A |
| UV Reflective Window Coating | | | | | |
| (F suffix) | Yes | Yes | Yes | Yes | Yes |
| (UV suffix) | No | No | No | No | No |

*UV ≤ 390 **390nm ≤ VIS ≤ 770nm ***IR ≥ 770nm

Figure 2: DEFINITION OF BEAM ANGLE

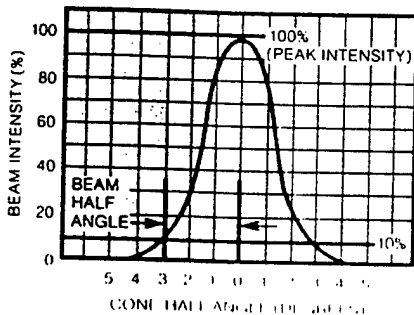


Figure 3: TYPICAL BEAM PROFILES

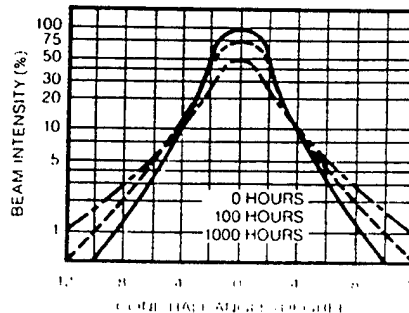
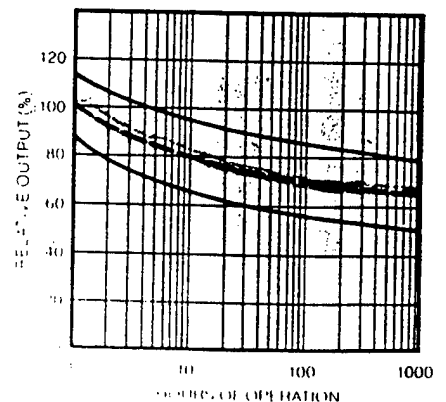


Figure 4: OUTPUT VS. TIME



Safety Notes.

Proper use of CERMAX lamps and safe operating practices are the responsibility of the manufacturers who incorporate the lamps into their equipment and of the users of their equipment.

Operation of xenon short arc lamps involves the following hazards:

- High pressure in the lamps can cause explosive mechanical failure.
- High voltage is required for ignition.
- Infrared and ultraviolet radiation generated by the lamp can cause skin burns and eye damage.
- Ultraviolet radiation can generate ozone.
- Portions of the lamp can reach temperatures of almost 200°C.

Engineering Notes.

Engineering notes are available for CERMAX lamps to help designers and experimenters make optimal use of CERMAX lamps. Contact an ILC Technology applications engineer for details.

Optical Characteristics.

CERMAX lamps have highly collimated output beams with essentially Gaussian beam profiles. The peak intensity data in Table A refer to intensity along the optical axis, measured in the far field. The beam angle in Table A is defined as the half angle in which the beam intensity falls to 10% of its peak value (Figure 2). Lamps with elliptical reflectors also have Gaussian intensity distributors in their focal planes, but far field peak beam intensity and beam angle are unspecified.

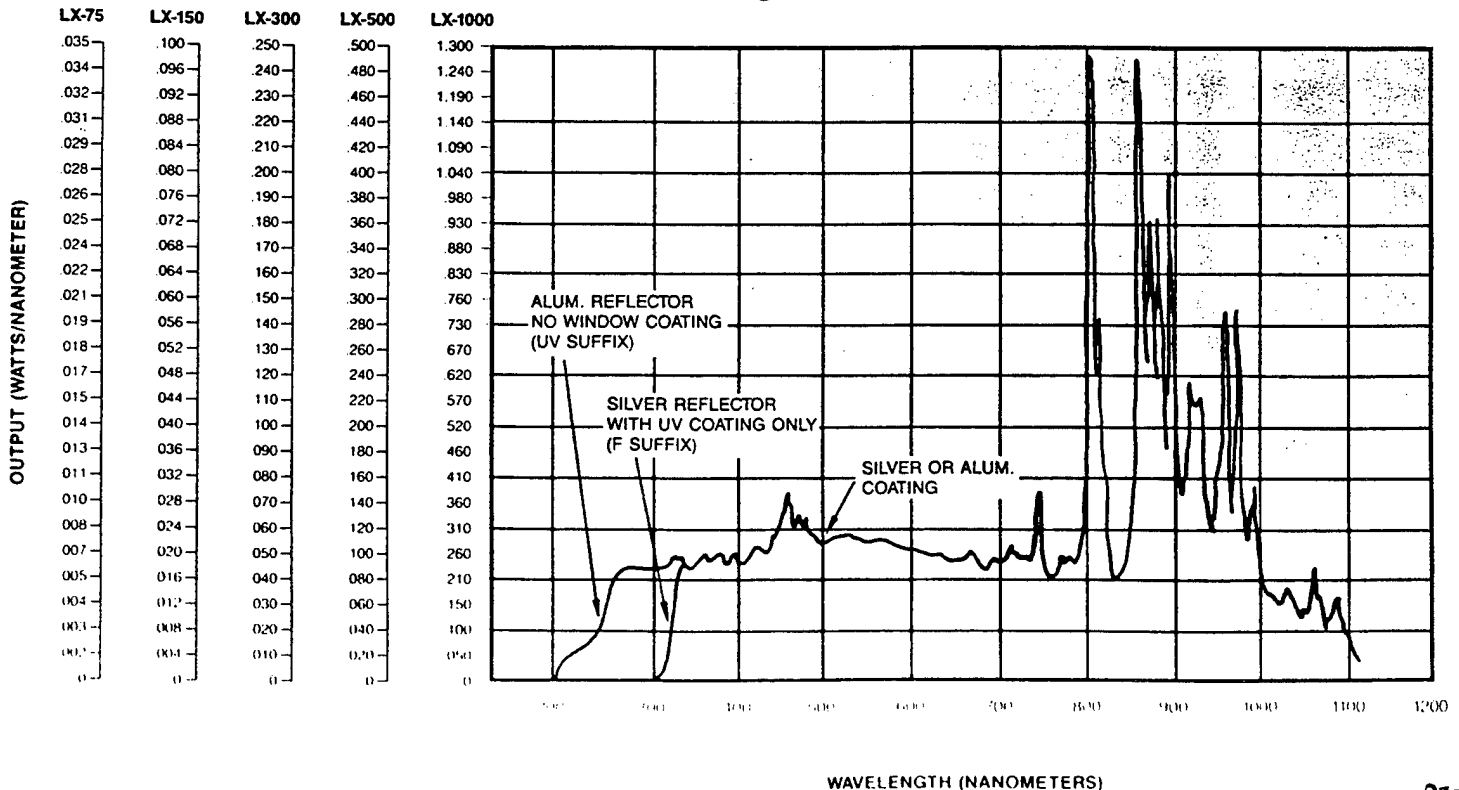
The values of radiant flux given in Table A represent total CERMAX lamp output. This output is also reported in three spectral bands: UV, visible and IR. The UV-filtered lamps have initial color temperatures of 5600°K. This value will drop slightly over lamp's lifetime, to about 5400°K. The UV-enhanced lamps have a color temperature of approximately 5100°K. The spectral distribution of CERMAX lamp types may be compared in Figure 1.

The lamp output will decline with time due to evaporation of tungsten on to the

reflector and window surfaces. Figure 4 gives a typical rate of decay. This rate is dependent on many factors: high number of starts, high lamp current, modulation and poor cooling will all contribute to decreased output.

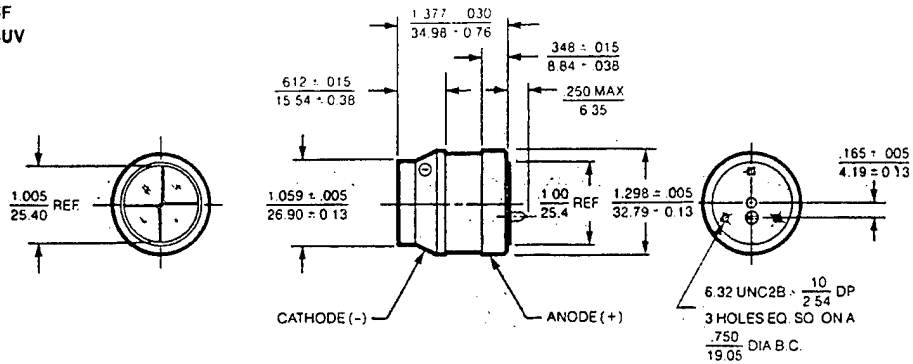
The lamps should not be operated with the window facing upwards within 45° of vertical, a position which can lead to arc instability and window fracture from convective heating. All other mounting positions are acceptable as long as proper care is taken in cooling the lamp: ceramic/metal seal temperatures should normally not exceed 150°C.

Figure 1: SPECTRAL DISTRIBUTION

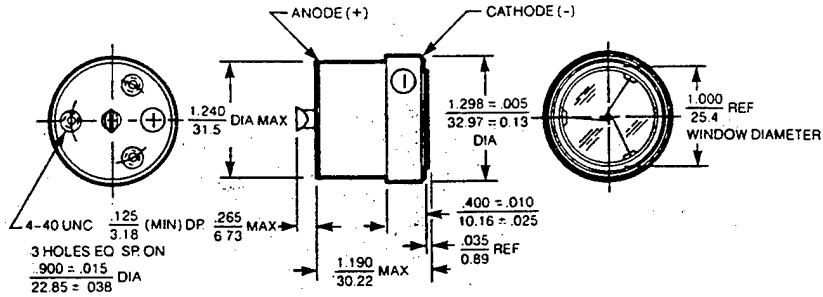


CERMAX[®] Lamp Mechanical Details

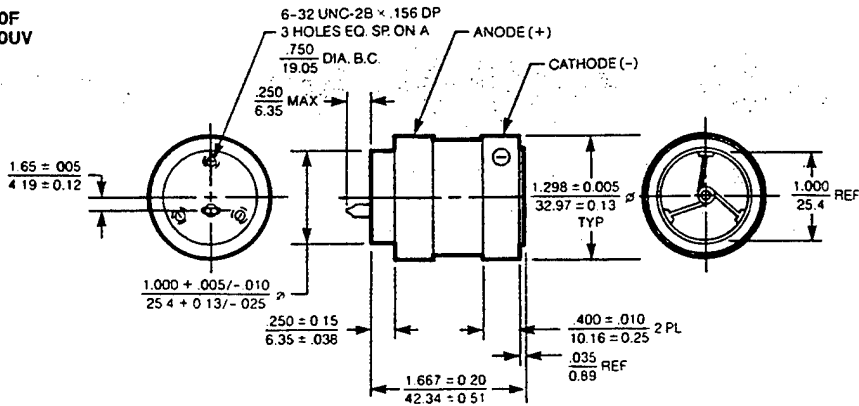
LX75F
LX75UV



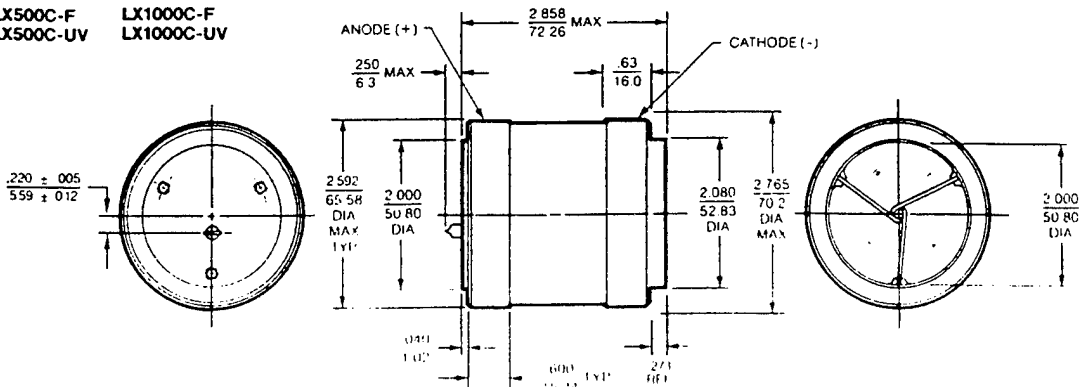
LX150F
LX150UV



LX300F
LX300UV



LX500C-F LX1000C-F
LX500C-UV LX1000C-UV





OPERATING HAZARDS

READ THE FOLLOWING INSTRUCTIONS AND
TAKE ALL NECESSARY PRECAUTIONS

SHORT ARC XENON ILLUMINATORS AND ILLUMINATOR SYSTEMS
PROPER USE AND SAFE OPERATING PRACTICES WITH RESPECT TO HIGH
INTENSITY ILLUMINATORS AND ILLUMINATOR SYSTEMS ARE THE RESPON-
SIBILITY OF EQUIPMENT MANUFACTURERS WHO INCORPORATE THE IL-
LUMINATOR INTO EQUIPMENT AND USERS OF SUCH ILLUMINATORS AND
EQUIPMENT. THE SUPPLIER OF THIS ILLUMINATOR PROVIDES INFORMA-
TION ON ITS PRODUCTS AND ASSOCIATED HAZARDS, BUT IT ASSUMES NO
RESPONSIBILITY FOR AFTER-SALE OPERATING AND SAFETY PRACTICES.
LIMITED USE AND RANDOM FAILURES ARE INHERENT CHARACTERISTICS
OF XENON ILLUMINATORS. TAKE APPROPRIATE ACTION THROUGH BAF-
FLES, LIGHT SHIELDS, INTERLOCK SWITCHES OR OTHER SAFEGUARDS TO
PROTECT PERSONNEL AND PROPERTY FROM HARM DUE TO OPERATION
AND/OR FAILURE OF THE ILLUMINATOR.

ALL PERSONS WHO WORK WITH OR ARE EXPOSED TO ILLUMINATORS OR
EQUIPMENT WHICH UTILIZES SUCH ILLUMINATORS MUST TAKE PRECAU-
TIONS TO PROTECT THEMSELVES AGAINST POSSIBLE SERIOUS BODILY IN-
JURY. DO NOT BE CARELESS AROUND SUCH PRODUCTS.

OPERATING INSTRUCTIONS

This information is provided to help you establish safe operating conditions for
both you and your illuminator or illuminator system.

Do not operate this illuminator except in accordance with proper operating in-
structions, these precautions and any additional information provided by the
manufacturer.

Questions regarding illuminator operation or safety matters should be address-
ed to your illuminator supplier.

WARNING:

SERIOUS HAZARDS EXIST IN THE OPERATION OF ILLUMINATORS

Operation of illuminators involves one or more of the following hazards, any
which, in the absence of safe operating practices and precautions, could
be in serious harm to personnel:

EXPLOSION—High internal pressure in the illuminator, as with any
pressure vessel, can cause explosive failure resulting in serious bodily in-
jury or death.

HIGH VOLTAGE—Ignition voltage of some illuminator models is high and
can be deadly.

INFRARED RADIATION—Infrared radiation generated by the illuminator
can cause skin burns and eye damage.

ULTRAVIOLET RADIATION—Ultraviolet radiation generated by the il-
luminator can cause skin burns and eye damage.

OZONE—Some illuminators generate toxic ozone gas by virtue of the
ultraviolet radiation.

HOT SURFACES—Portions of the illuminator can reach temperatures of
several hundred degrees centigrade and cause serious burns if touched.

Additional specific information about illuminator hazards:

EXPLOSION

The illuminators are filled with xenon gas at very high pressure: over 200 psi (ap-
proximately 14 atmospheres) when cold and approaching 450 psi (approximate-
ly 30 atmospheres) when operating. Illuminators must be handled with the
same care and caution given any vessel containing these levels of pressure. A
hazard exists if the window or ceramic fractures. The resulting explosive failure
could cause serious bodily injury or death. Adequate shielding must be provid-
ed to prevent persons and/or objects from being hit by flying particles in the
event of an explosive failure. The illuminator enclosure must be designed with
baffles and shields to contain such particles in the event of failure. This
enclosure should also contain stray radiation of light. Protective eyewear is on-
ly a minimum protection. Face shields and protective clothing, designed to
withstand explosive failure, are strongly recommended for safety during all
handling operations. The possibility of violent failure is greater during starting
and operation.

HIGH VOLTAGE

High voltage, as high as 40 kilovolts, is applied to the illuminator during
operation. The high voltage starting pulse lead should be adequately insulate-
shielded to prevent accidental contact or shorting. Portions of the circuit
exposed and caution must be used in setup and operation of the system. Il-
luminators must be operated in well grounded and/or well insulated hous-
ing for protection from electrical shock. The input power supplied to the sys-
tem power supply must have a properly functioning earth ground. The input po-
wer must be disconnected from the power outlet before attempting any service
to the illuminator.

INFRARED RADIATION

Infrared radiation will cause heating of tissues and will penetrate the eye. Prolonged
infrared exposure may damage the eye.

ULTRA-VIOLET RADIATION

Some xenon lamps are manufactured for applications requiring ultraviolet
radiation. When using these lamps painful skin burns can result if the skin is
exposed to the ultraviolet radiation. Exposure of the unprotected eye to ultraviolet
radiation will cause injury to the eye which may be permanent. The eye can be
damaged through reflection of ultraviolet radiation from surfaces. Out-
going wavelengths of less than 320 nm (3200 Å) will cause this effect.

OZONE

When using lamps manufactured for ultraviolet applications ozone, a toxic gas,
will be generated. Ozone is very irritating to all mucous membranes. Continu-
ous exposure of personnel to concentrations of ozone exceeding .04 parts per
million is inadvisable and considered a health hazard. The accepted thresh-
old limit value for a daily 8 hour exposure is 0.1 parts per million (American Con-
ference of Governmental Industrial Hygienists, 1967). A lamp which gives off
ozone must be operated in a well ventilated area.

HOT SURFACES

During operation and immediately after shut-down, exterior surfaces of the
illuminator are hot enough to cause burns. All hot surfaces may remain hot for an
extended time after the illuminator is shut off. To prevent serious burns, take
care to prevent and avoid any bodily contact with these surfaces both during
and for a reasonable cool-down period after operation.

LAMP ASSEMBLY PROCEDURE

ILC 700/1000/1200 WATT XENON LAMP

GENERAL INFORMATION:

The ILC Xenon lamps are classified as a high pressure lamps and should be handled accordingly. A hazard exists if the lamp is dropped or damaged. If the window or ceramic fractures the resulting explosive failure could cause serious bodily injury or death. Only qualified and trained personnel may handle and/or assemble Xenon high pressure lamps.

PROTECTIVE EQUIPMENT:

Protective safety glasses, face shields, gloves, arm shields, and protective clothing, designed to withstand explosive failure, must be worn when handling and/or assembling lamps. The lamps must be assembled within the lamp assembly fixture (JG-BMB-100).

ASSEMBLY PROCEDURE:

1. Install protective eye glasses, face shield, arm shields, gloves and other protective clothing prior to removing lamp from manufacturers shipping container.
2. With protective clothing installed, remove unassembled lamp from shipping container and place in the lamp assembly fixture (JG-BMB-100). Keep the lamp window pointed away from personnel.
3. Remove the electrical safety cover from the lamp housing, by removing the two red thumb screws. Set cover and thumb screws aside for later use.
4. Remove lamp housing from lamp mounting bracket by unscrewing the four red thumb screws. Set lamp mounting bracket and thumb screws aside for later use.
5. Remove heat sinks from the lamp housing. Do not remove the fan assembly from the lamp housing.
6. Clean any foreign material from the heat sinks.
7. While working within the lamp assembly fixture, clean any foreign material from the lamp base.
8. Apply a very thin, even coat of heat transfer compound (EG&G Wakefield, Series 120 or GE "INSULGREASE", G.E.#G642) to the cathode (positive) surface of the lamp and to the heat sink base. Do not apply heat transfer compound to the internal threads of the lamp.
9. Insert lamp into the heat sink base. Align the clearance holes in the heat sink base to the tapped holes and pinch off tube in the lamp base.
10. Install the three socket headed screws provided. The screws should be tightened evenly. The maximum torque shall not exceed 12 inch lbs.
11. Insure the heat sink is fully seated on the lamp base. Install copper clip provided to the heat sink base.
12. Apply a very thin, even coat of heat transfer compound to the anode (negative) surface of the lamp and to the inside diameter of the middle heat sink.
13. Insert the middle heat sink over the anode (negative) surface of the lamp until the top surface of the heat sink is flush with the top edge of the anode surface.
14. Align the tapped hole in the middle heat sink with the tapped hole in the heat sink base.
15. Install copper clip provided to the middle heat sink.
16. Insert the top heat sink (which has four tapped holes on the front surface) over the lamp rim until it is flush with the top of the middle heat sink. Do not apply thermal compound to mating surfaces.
17. Align short fins of the top heat sink with the short fins of the middle heat sink.
18. Install copper clip provided to side of top heat sink.
19. Place window of lamp/heat sink assembly facing downward on floor of lamp assembly fixture.
20. Insert lamp housing over lamp/heat sink assembly until the lamp base heat sink rests on the interior shoulder of the lamp housing. Place assembly in horizontal position being careful not to let the lamp assembly slide out of the lamp housing.
21. Align the tapped holes of the heat sinks with the clearance holes of the lamp housing. These are the electrical connections.

APPENDIX C

LAMP ASSEMBLY PROCEDURE ILC 700/1000/1200 WATT XENON LAMP

ASSEMBLY PROCEDURE: continued

22. Install the lamp heat sink retaining ring (JG-BMB-101) to the lamp housing using the screws provided (#6 x 1/2 long flat heat screws).
23. Orient flat surfaces of retaining ring with flat surfaces to the lamp housing. The single retaining ring clamp should be at the top of the lamp assembly (near electrical connections).
24. Remove lamp assembly from lamp assembly fixture. Keep the window of the lamp pointed away from personnel.
26. Install the lamp into the lamp mounting bracket by using the four red thumb screws.
27. Install the philips head connector screws provided to the tapped holes of the heat sink.
28. Install the electrical safety cover to the lamp housing using the two red thumb screws.
29. Place the lamp into a foam lined metal enclosure.
30. Remove protective equipment and clothing.

LAMP INSTALLATION PROCEDURE ILC 700/1000/1200 WATT XENON LAMP

GENERAL INFORMATION:

The ILC Xenon lamps are classified as high pressure lamps and should be handled accordingly. A hazard exists if the lamp is dropped or damaged. If the window or ceramic fractures the resulting explosive failure could cause serious bodily injury or death. The possibility of lamp failure is greatest during startup and operation. Only qualified and trained personnel may handle and/or assemble Xenon high pressure lamps. In the event the lamp has been dropped, it is to be returned to the manufacturer for evaluation and proper disposition.

PROTECTIVE EQUIPMENT:

Protective safety glasses, face shields, gloves, arm shields, and protective clothing, designed to withstand explosive failure, must be worn when handling and/or assembling lamps.

INSTALLATION PROCEDURE:

1. Install protective eye glasses, face shield, arm shields, gloves and other protective clothing prior to removing lamp from container.
2. With protective clothing installed, remove the lamp from storage container. Keep the lamp window pointed away from personnel.
3. Remove two red thumb screws that secure the electrical safety cover to the lamp housing. Set aside cover and screws for later use.
4. Remove the four red thumb screws that retain the lamp housing to the lamp mounting bracket. Set aside screws for later use.
5. Install lamp mounting bracket to lamp fixture within the illumination system.
6. Install lamp housing to the lamp mounting bracket using the four red thumb screws.
7. Install the electrical connections with the two philips screws provided.
8. Install the electrical safety cover to the lamp housing using the two red thumb screws.
9. Install all protective covers, shields, and/or baffles around the light source.
10. Remove all safety equipment except for the protective eye glasses.

APPENDIX D

XENON ARC LAMP
POWER SUPPLY

PS500SW-1
PS800SW-1
PS1000SW-1

OPERATING INSTRUCTIONS

APPENDIX E

TABLE OF CONTENTS

| | | |
|--------------------|---|--------|
| SECTION I | GENERAL INFORMATION | |
| 1.1 | Introduction | Page 1 |
| 1.2 | Specifications | 2 |
| SECTION II | INSTALLATION | |
| 2.1 | Initial Inspection | 4 |
| 2.2 | Mechanical Check | 4 |
| 2.3 | Power Requirements | 4 |
| 2.4 | Cooling | 4 |
| 2.5 | Connecting Power Supply to Lamp | 5 |
| 2.6 | Range Selection | 5 |
| 2.7 | External Current Control | 5 |
| 2.8 | Pulse Modulation | 5 |
| 2.9 | Performance Testing Procedure | 6 |
| SECTION III | OPERATING THEORY | |
| 3.1 | Introduction | 7 |
| 3.2 | Power Flow | 7 |
| 3.2.1 | Ignitor Circuit Power Flow | 8 |
| 3.3 | Signal Flow | 8 |
| 3.4 | A300 Drive Board | 11 |
| SECTION IV | GENERAL MAINTENANCE AND CALIBRATIONS | |
| 4.1 | General Maintenance | 12 |
| 4.2 | Inspection and Cleaning | 12 |
| 4.3 | Calibrations | 13 |
| 4.3.1 | Checking Pulse Width Modulator | 14 |
| 4.3.2 | Calibration of Current Meter | 14 |
| 4.3.3 | Shunt Sense Calibration | 14 |
| 4.3.4 | Final Calibration | 15 |
| SECTION V | PARTS LISTS | 16 |
| SECTION VI | SCHEMATICS | 17 |

SECTION I GENERAL INFORMATION

1.1 INTRODUCTION

This manual contains operating and maintenance instructions for the PS500SW-1, PS800SW-1 and PS1000SW-1 xenon arc lamp power supplies. The power supply is intended for ignition and operation of CERMAX xenon short arc lamps rated at either 500, 800 or 1000 watts.

The power supply not only provides a stable light output but has other special capabilities which are listed below:

- Contains a regulated adjustable constant current source with an adjustable range to either 500, 800 or 1000 watts at 20 volts.

- Provides a high voltage ignition circuit and the boost of "open circuit" voltage required for starting the arc lamp.

- Internal security switching for power range selection.

- provides ac turn-on/off and circuit protection by means of UL rated input circuit breaker.

- Push button start lamp power ignition.

- AC connection on the back of the supply for an external fan (115V output).

- External 0-5 volt current control.

- External triggered adjustable amplitude and duration pulse modulation increases output current over the preset output of the unit.

- Lamp hour monitor.

- Unit is fan cooled and thermostatically protected. Air enters at sides and exits at the rear. Consequently, no heat will be applied to other equipment above or below the power unit.

- 7 1/2 foot input ac power cord.

1.2 SPECIFICATIONS

AC INPUT:

100-130V AC signal phase 50/60 Hz
115V AC Input:

10.3 A RMS @ 500 W Typical
13.7 A RMS @ 800 W Typical
15.0 A RMS @ 1000 W Typical

200-260V AC signal phase 50/60 Hz
(Internal wiring change required)

230V AC Input:

4.5 A RMS @ 500 W Typical
6.5 A RMS @ 800 W Typical
8.0 A RMS @ 1000 W Typical

LAMP OUTPUT BOOST VOLTAGE:

200V DC (nominal) stored in two
820uf capacitors through 2.5 ohm
resistors.

Additional boost at 40 volts stored
in 1400uf capacitors.

IGNITION VOLTAGE:

30KV peak, 1.0us at half amplitude
at 0.1us rise time.

LAMP OPERATING POWER:

(Internal range switch shipped from
factory as labeled on front panel)

Up to 20 V DC

Normal Current - 1000 watt mode -
37-54 Amps.

Normal Current - 800 watt mode
29-43 Amps.

Normal Current - 500 watt mode
20-36 Amps.

Pulse Duration - 1-250us (approx.)
with a ten turn potentiometer.

External Trigger - 0 to +5 volts

External Programming - 0 to +5 volts
with front panel current control
fully CCW. Duplicates range of front
panel control.

REGULATION:

Output current will not vary more than 1% with line variation of 100 to 130 or 200 to 260 V AC.

RIPPLE:

Below 20KHz, 1% RMS maximum.

FAN OUTPUT VOLTAGE:

115V 25VA maximum.

SIZE:

Height - 5.843" with feet
- 5.343" without feet

Width - 11.875"

Length - 17.50" (Does not include external controls or input/output connections.)

WEIGHT:

33 1/4 pounds.

COOLING:

Forced air cooled.

SECTION II INSTALLATION AND OPERATION

2.1 INITIAL INSPECTION

Before shipment this instrument was inspected and was free of mechanical and electrical defects. As soon as the unit is unpacked, inspect for any damage that may have occurred in transit. Check for broken knobs or connectors, also that the external surface is not scratched or dented, the meter face is not damaged and that all controls move freely. Any external damage may be indication of internal problems.

2.2 MECHANICAL CHECK

1. Remove five 6/32 machine screws from each side of the top cover plus two from the top.
2. Remove cover.
3. Inspect for loose hardware, damaged components or broken wires.
4. Check operation of controls.

NOTE: If any damage is found, follow the "Claim for Damage in Shipment" instruction in the warranty section of this manual.

5. Replace cover and attaching hardware.

2.3 POWER REQUIREMENTS

A normal dedicated 15A source is sufficient unless the unit is to be used in the pulsed mode. In this mode it is usually easier to use 220V service to power the unit.

2.4 COOLING

The supply enclosure is cooled by a fan exhausting warm air to the rear. Fresh air intake is from each side. None of the surfaces of the supply radiates heat to adjacent equipment. At least five inches of space should be allowed behind the supply and one inch along each side in the vicinity of the air inlet holes for unimpeded air flow.

NOTE: Do not operate the supply continuously with the covers removed since the air flow pattern within the chassis is adversely affected.

2.5 CONNECTING POWER SUPPLY TO LAMP

1. Connect high voltage terminal marked POS HV to anode of the lamp using cable suitable for carrying 83 or more amps with insulation capable of withstanding 30K pulse voltage.
2. Connect terminal of power supply marked NEG GND to negative side of the lamp.
3. Plug ac cord provided into appropriate voltage.
4. Flip the circuit breaker to the "ON" position.
5. Push start button and hold in until lamp starts. (Several seconds)

2.6 RANGE SELECTION

1. Factory set to range marked on front panel.
2. To change range remove top cover. Switch is located on A600 PCB on right side near front of power supply.

2.7 EXTERNAL CURRENT CONTROL

An external 0-5 volt may be used to control the unit instead of the front panel current control.

1. Turn the "CURRENT ADJUST" control fully counterclockwise.
2. Connect an external 0 to +5 volts to connection labeled "EXTERNAL PROGRAM"

2.8 PULSE MODULATION

Applying an external trigger pulse will increase the preset current output.

1. Apply a pulse voltage of +5 volts through the external connector marked "PULSE TRIGGER".
2. PULSE AMPLITUDE CONTROL - Controls amount of current output over the preset amount of the "CURRENT ADJUST" control.

PULSE WIDTH - Sets duration of pulse from 1 to 250us

2.9 PERFORMANCE TESTING PROCEDURE

Equipment Required - Ammeter, 0 to 86 amps
- Power Supply, 0 to +5 volts DC

1. Connect power supply to suitable ac power input.
2. Turn circuit breaker to "ON" position.
3. Push the "START" button. You should hear the spark gap.
4. Turn power supply circuit breaker to "OFF" position.
5. Connect xenon lamp to the power supply output terminals marked POS +HV and NEG GND observing polarities.
6. Connect an ammeter in the negative leg between the power supply and lamp.
7. Turn power supply circuit breaker to "on" position.
8. Current should vary up and down at load when varying "CURRENT ADJUST" control.
9. Turn the "CURRENT ADJUST" control fully counterclockwise.
10. Connect an external 0 to +5 volts to connection labeled "EXTERNAL PROGRAM".
11. Current at load should vary up and down with variation of the external voltage.
12. Connect an external positive 0-5 volt pulse to connection labeled "PULSE TRIGGER".
13. Set the "CURRENT ADJUST", the "PULSE WIDTH" and the "PULSE AMPLITUDE" controls to desired output.
14. At each pulse trigger the current set by the "CURRENT ADJUST" will increase.

SECTION III OPERATION THEORY

3.1 INTRODUCTION

This section describes the Theory of Operation of the PS800SW-1 Arc Lamp Power Supply. Major areas will include the power flow circuitry and circuit functions of the print circuits. References to schematic symbol numbers of schematic diagrams included are made to ease understanding.

3.2 POWER FLOW (Figure 3.1)

At turn-on, single phase 115V AC is rectified by FWB CR1 and doubled by capacitor action of C1 and C2. (See Figure 3.2) Capacitor C2 charges during the negative cycle at supply voltage and C1 during the positive cycle. This produces from 250 to 350V DC (due to ac input line fluctuation) across the combined resistance of R1 and R2. At 230V AC input rectification is not doubled as it is on 115V AC inputs.

Thermistor RT1 and RT2 guard against the large current inrush that would otherwise occur because of the initially low impedance of capacitors C1 and C2.

L701, C702 and C703 form the RFI low pass filter between the bridge network and the chopper circuit input. A fuse is provided at the positive dc output of the bridge network for circuit protection.

The basic 20kHz switching rate of the chopper networks are developed by IC201, a pulse width modulator. (IC201 is a major component of the Control Board.) As illustrated in Figure 3.3, chopping action occurs during alternate pulse cycles, when the diagonally opposite transistors Q701 and Q704 or Q702 and Q703 are on simultaneously. Regulation of output power is accomplished in the chopper unit by variation of the pulse widths. The actual control of the pulse widths is performed by circuitry on the A200 Control Board. The alternating waveform frequency (regardless of pulse width) is approximately 20K Hz. An 150V AC rectangular waveform is produced at each cycle to the input of transformer T1401. The signal is referenced to zero volts between each cycle by the capacitive action of C1401. This voltage is transformer coupled through T1401, rectified and filtered to produce the dc output voltage of the power supply.

3.2.1 IGNITOR CIRCUIT POWER FLOW (See Figure 3.4)

When the start button is pressed the following actions occur:

Transformer T3 produces about 390 volts ac between terminals 7 and 8. This voltage is applied to a three stage voltage multiplier circuit consisting of diodes CR401 thru CR406, which charges the energy storage capacitor (C3). When this voltage reaches 2000V DC, the spark gap (V401) shorts discharging C3 thru the primary of ignitor step-up power transformer T2. This voltage is stepped-up to approximately 30KV which is the ignition pulse for the lamp. The igniter will continue to produce pulses at a rate determined by its own recovery time until either the arc lamp ignites or the start button is released.

When the lamp is arced, a great deal of energy is required for a short period to sustain an arc once it has been established. A boost capacitor provides this energy. A special step-up winding of transformer T1401 provides the 200 volts to charge the boost capacitors C1409 and C1410. An additional 150 volts off transformer T3 helps to charge them at a faster rate. Blocking diode CR712 keeps this 200 volts from returning into the filter and rectifier sections.

3.3 SIGNAL FLOW (See Figure 3.5)

The Low Voltage Inhibit Circuit holds the Soft Start Circuit off until the bias voltage reaches +30 volts. This allows for stability of the drive signal to be attained before the power supply output transistors are operational. The slowly rising voltage of the Soft Start Circuit allows the output capacitors to charge at a gradual rate. Output power will also be rising at a steady rate until operation output power is reached.

Low Voltage Inhibit

At ac turn on transistor Q205 is conducting, holding pin 9 of IC201 at a low state.

NOTE: Most safety circuitry or fault detection operates to place a low voltage at pin 9 of IC201 (pulse width modulator) which eliminates or minimizes pulse to the chopper network. This causes output power to cease.

When the voltage across zener diode CR220 attempts to rise above 12 volts the following action takes place: Q201 attempts to turn on but collector current is held down by Q203 being off. As +30V supply continues to rise zener diode CR220 starts conducting causing CR219 to start conducting turning on Q203. This turns on transistor Q204 which through R204 latches on Q203. Q204 also turns on Q202 which removes base signal from Q205.

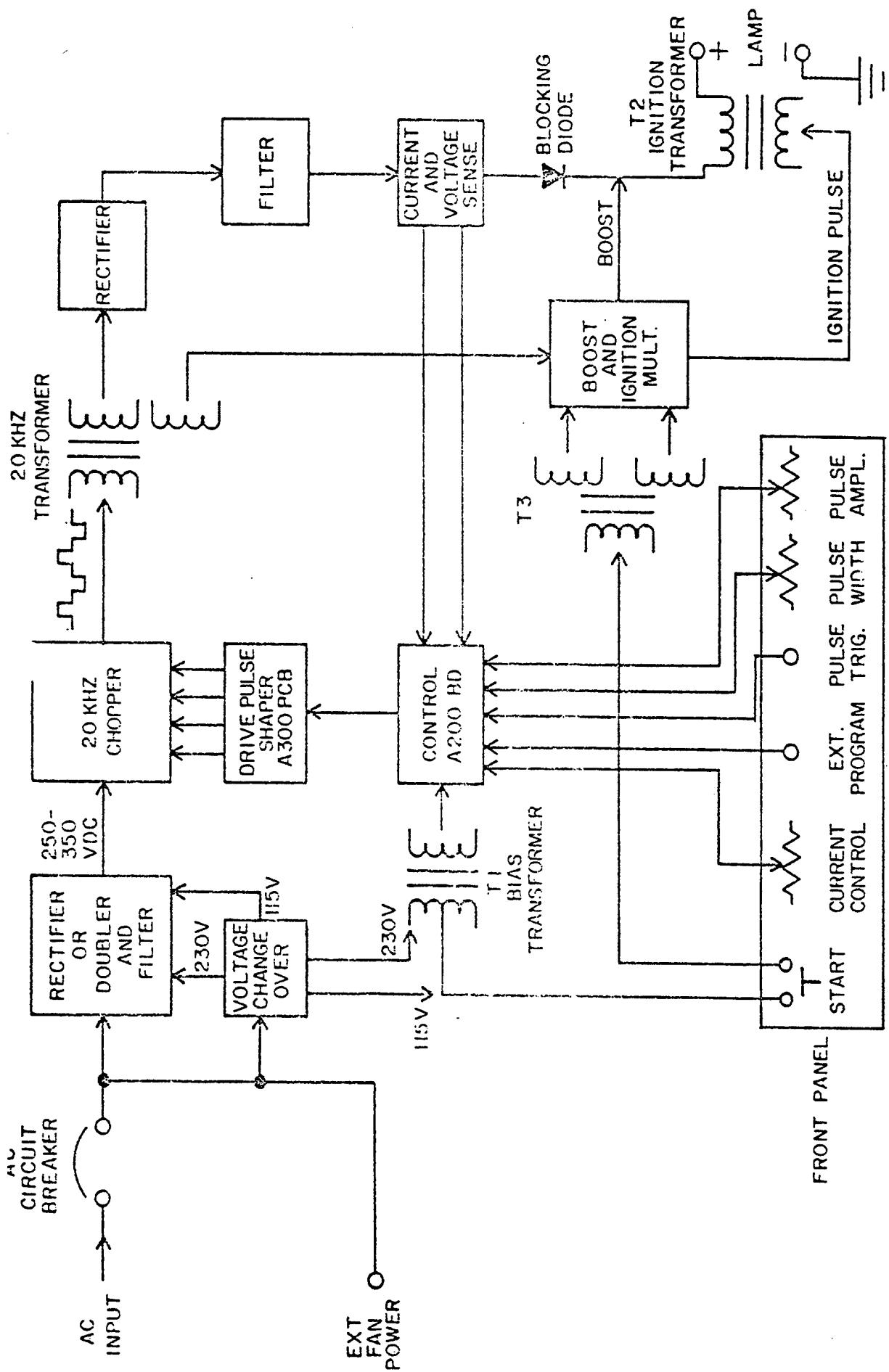
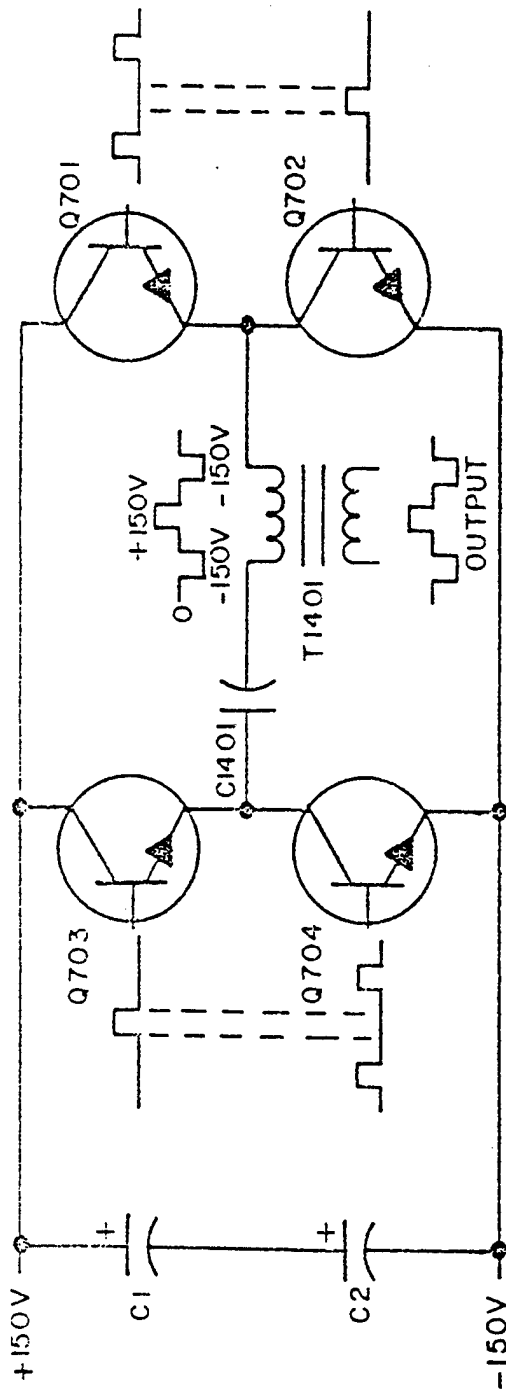
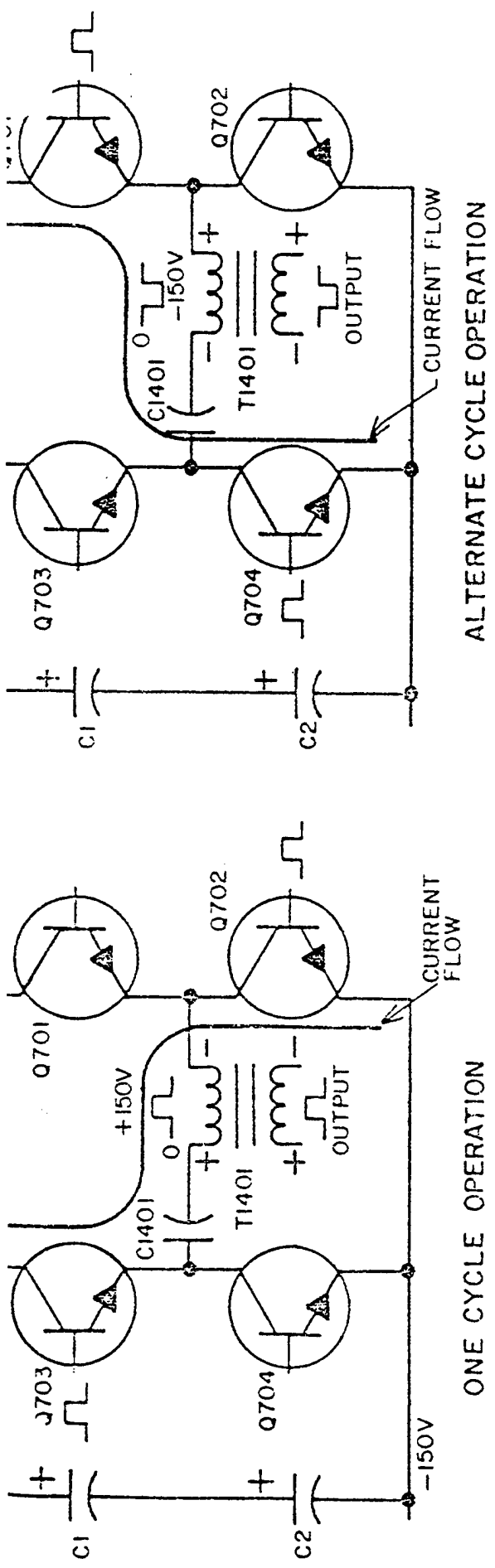


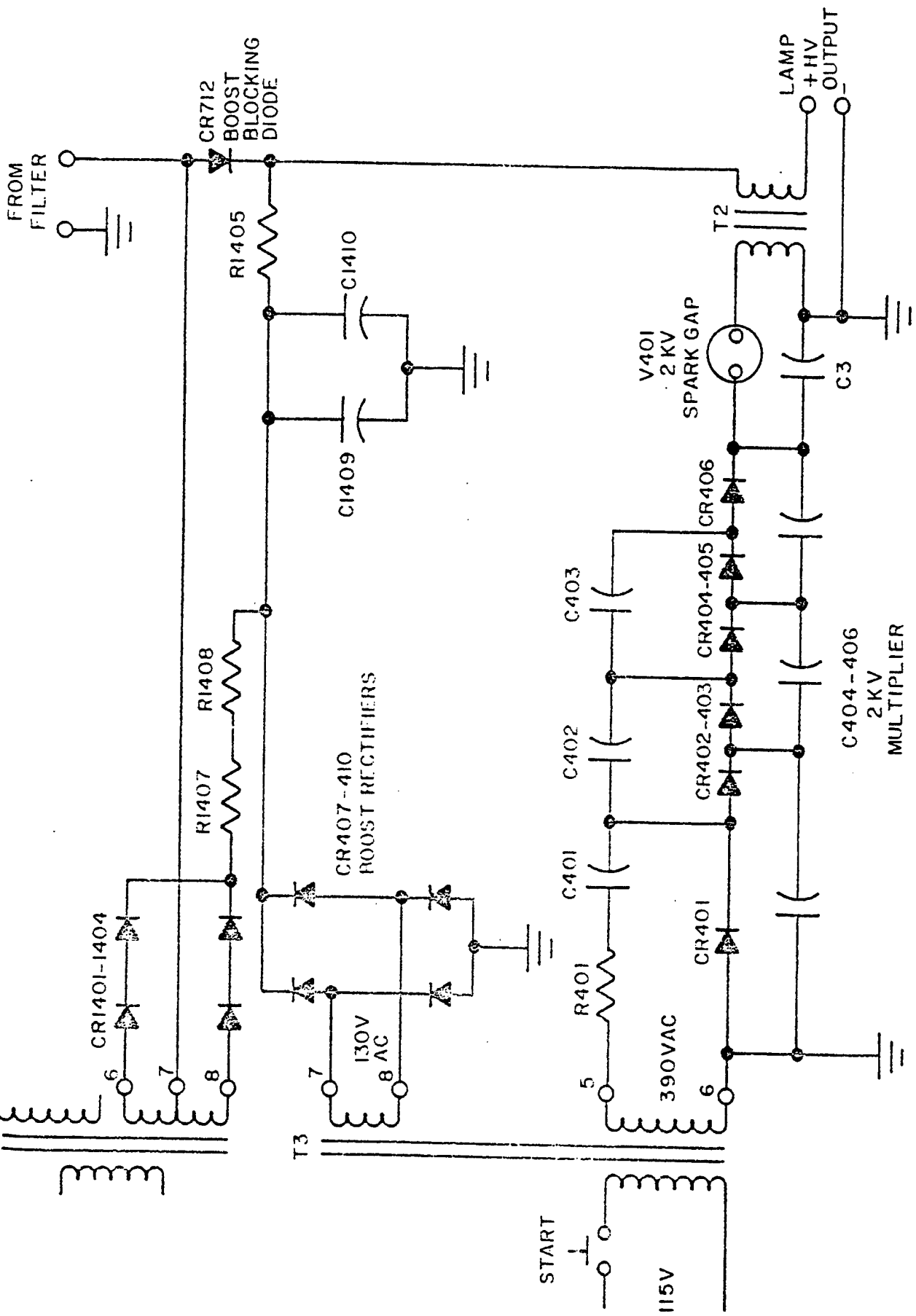
Figure 3.1



ALTERNATE CYCLE OPERATION

COMBINED OPERATION

Figure 3.3



IGNITOR & BOOST

Figure 3.4

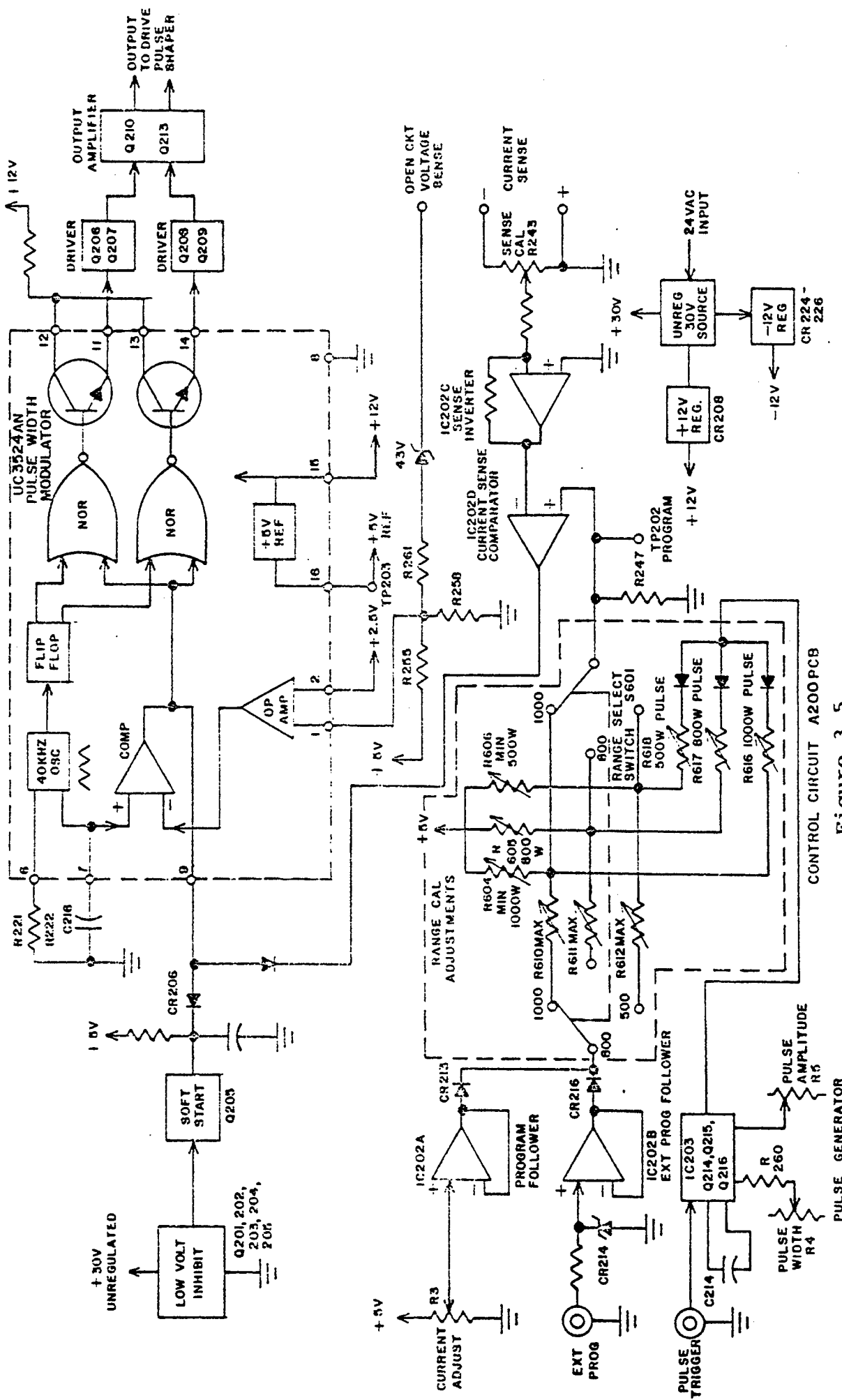


Figure 3.5

Soft Start

Prior to start-up capacitor C202 is discharged. When Q205 turns off it allows C202 to start charging through R215. As the capacitor charges, the input voltage at pin 9 of IC201 is also rising. This allows the output pulses of IC201, which are initially narrow, to gradually become wider until regulation is achieved.

Shut Down

As the +30V supply decreases CR219 stops conducting and attempts to turn off Q203. However Q203 is being held on by the conduction of Q204. As a result nothing occurs. As the +30V supply further decreases CR220 stops conducting turning off Q201, thus turning off Q203, Q204 and Q202 and turning on Q205. This pulls pin 9 of IC201 low, halting output of the pulse width modulator.

Pulse Width Modulation

The function of pulse width modulation is provided by IC201. It varies the width of rectangular pulses on response to a dc signal from the error amplifier. Specifically, the leading edges of the pulses are triggered by the 20K Hz clock signal. The trailing edges of the rectangular pulses are then determined by the error signal which originates from IC201D. The pulse-width modulated available from pin 7 of IC201, has a repetition rate of 40K Hz, rather than 20K Hz. (The oscillator frequency is controlled by an RC time constant consisting of R221, R222 and C216.) This frequency doubling is necessary in order that the ultimate switching rate of two internal output transistors at pin 11 and 14 of IC201 will be 20K Hz due to the configuration of the output chopper transistors.

Each output of IC201 pins 11 and 14 operate a pair of drive transistors (Q206, Q207 or Q208, Q209) which in turn drive a pair of output amplifier transistors (Q210, Q211 or Q212, Q213). These signals are fed through transformer T301 to produce base drive for the chopper transistors Q701-Q704. A quiescent period (dead time) established by R217, R264 and R218 between each output phase avoids problems of simultaneous conduction of both sets of power transistors.

Open Circuit Voltage Limiting

Open circuit voltage limiting is accomplished by using IC201's internal comparator whose inputs are pins 1 and 2. Pin 2 is biased to 2.5V by R254 and R255 from the 5 volt reference. A sample of the open circuit power supply voltage is applied to pin 1 through R261 and zener diode CR222. When the power supply voltage exceeds the zener voltage +2.5 volts, the comparator causes pin 9 to go low thus controlling the output voltage.

Sense Invertor

The negative current sensing voltage from R1401 must be inverted to a positive voltage to be compatible with the positive programming voltage at TP202. This is accomplished by a unity gain invertor amplifier IC202C. Sense Calibration Resistor R271 allows for variations in the manufacturing tolerance of R1404.

Program Followers

Adjustment of the power supply output current can be accomplished in two ways.

1. A front panel current control pot.
2. An external 0 to +5V analog signal.

When using the external analog signal the front panel control should be turned fully counterclockwise. Two unity gain program followers (IC202A and IC202B) are used to isolate the programming signals from each other. The front panel control (R3) supplies 0 to +5 volts to IC202A. The external program jack supplies 0 to +5 volts to IC202B. CR214 clamps the input voltage to prevent over driving the power supply. The outputs are fed through CR213 and CR216 to one section of the range switch (S2). The outputs of this section of the switch are connected to a network of calibration adjustment resistors to set the maximum and minimum current of each range. The outputs of the pulse generator are also connected at this point.

Pulse Generator

The pulse modulation signal is generated by a monostable timer IC203. The circuit is initiated by the triggering by the users input pulse. The output pulse width is determined by components (R5, R260, and C204) connected to pins 6 and 7 which are the R-C time constant. Both threshold terminals (pin 6) and the discharge transistor terminal (pin 7) are connected together in this mode.

Once the internal flip-flop of IC203 has been triggered by an input signal, it cannot be retriggered until the timing period has been completed. When the input voltage to the trigger comparator falls below $1/3 V_{cc}$, the comparator output (5V) triggers the flip-flop so that its output sets low. This turns the capacitor discharge transistor "OFF" and drives the digital output to the high state. This rate is set by the R-C constant. When the capacitor voltage reaches $2/3 V_{cc}$ the threshold comparator resets and returns the digital output to the low state. Front panel control R5 adjusts the pulse width from approximately 1us to 250us. The amplitude of the pulse may be adjusted from no pulse width to approximately twice normal maximum output current.

Note: The timer IC203's output is high during the monostable "on" time and "low" otherwise.

Current Sense Comparator

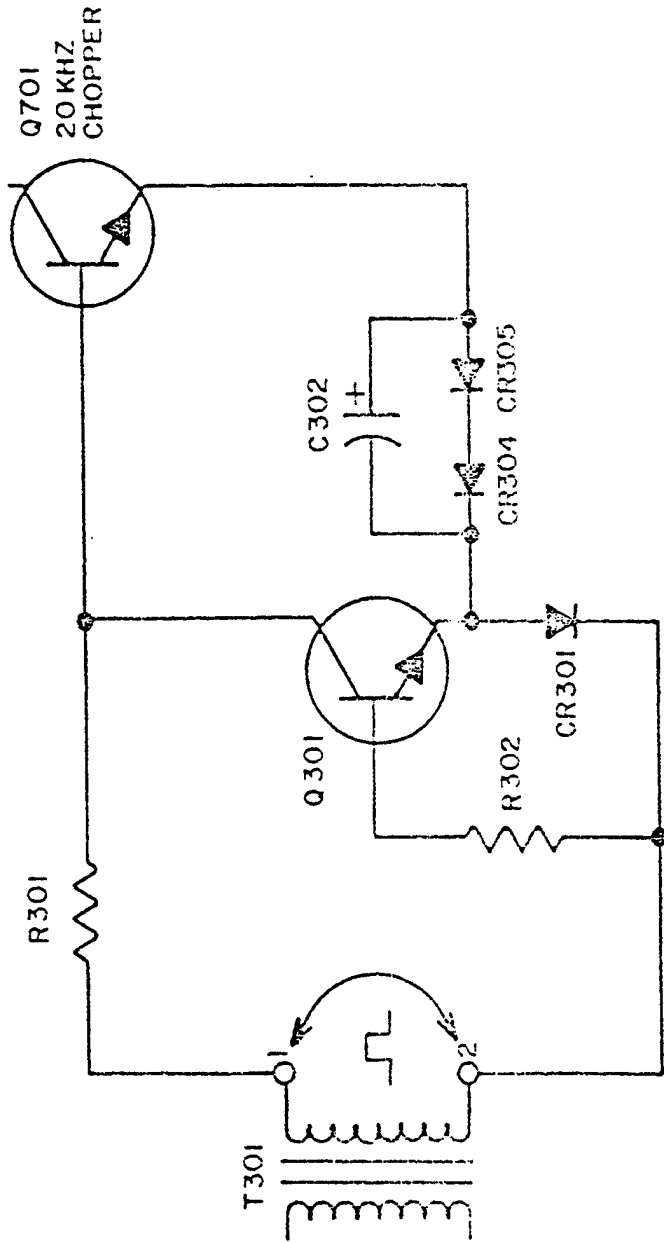
The select programming voltage at TP202 is applied to one input of the current sense comparator IC202D. The sensed current voltage from IC202C is applied to the other input of the comparator. Any difference in these voltages will cause the output of the comparator to generate an error voltage, which is applied to pin 9 of the pulse width modulator IC201. This causes a change in the pulse width generated to the chopper to bring the current of the power supply back to that set by the programming.

3.4 A300 DRIVE BOARD (Figure 3.6)

The A300 Drive Network is not the conventional buffer or drive stages ordinarily encountered. Rather, their function is also one of pulse shaping. Specifically, these transistors provide a low impedance source of negative-going base turn-off pulses for the inverter power switches. In this way the stored charges in transistors Q701-Q704 are much more rapidly depleted at turn-off time than would be the case if Q301, Q301A, Q302 and Q302A were not in the circuit.

Circuit operation is as follows: During turn on of Q701, T301 terminal 1 is positive with respect to terminal 2. Current flows through current limiting resistor R301 into base of Q701. Q701's emitter voltage goes through CR305, CR304 and CR301 back to T301 terminal 2. C302 is charged to approximately 1.5-2.0V by the voltage drop across CR304 and CR305. Q301 is held non-conductive by the drop across CR301.

During turn-off the polarity of T301 reverses. Terminal 1 is negative with respect to terminal 2. Q301 base becomes positive with respect to its emitter causing collector current to flow. This causes the negative charge in C302 to be transferred to the base of Q701 resulting in negative base current flow. A separate shaper is used for each chopper transistor.



TYPICAL
(1 OF 4)

DRIVE PULSE SHAPER

Figure 3.6

SECTION IV GENERAL MAINTENANCE AND CALIBRATION

4.1 GENERAL MAINTENANCE

A regular scheduled preventive maintenance program is recommended for the power supply. As a minimum, maintenance should consist of a thorough cleaning of interior and a visual inspection of components on printed circuit boards. The interval of these inspections will depend on the operational environment. Even a relatively clean location requires at least one inspection every six months.

4.2 INSPECTION AND CLEANING

Always unplug power supply from ac line before removing cover.

1. Remove 5 6/32 machine screws from each side of the top cover plus two from the top.
2. Remove cover.
3. Check for loose wires, burn marks, etc.
4. A200 Control Board unplugs so it may be checked external to the enclosure.
5. Remove dust from between parts with small long bristled brush or compressed air.

Equipment Required for Calibrations

Use test equipment listed or an equivalent.

1. Oscilloscope - dual trace - 20K Hz bandwidth - Isolated from ground (Tektronix 2213 with 10x voltage probe)
2. Digital Multimeter - 100 volts DC - 4000 volts AC (Hewlett Packard - HP-3465A)
3. Power Supply - 10 volts DC
4. Variable voltage source - 60 Hz 0V to 130V
5. Ammeter - 0 to 86 amps
6. Resistive Loads - 1.000 Ohm
.555 Ohm
.629 Ohm
.465 Ohm
.400 Ohm

4.3 CALIBRATIONS

All controlling signals are generated by the A200 Control Board and A600 Range Calibration Board. Reference schematic diagrams while making the following calibrations:

1. Remove A200 Control Board from unit.
2. Unplug connections J201 and J203 and leave others connected.
3. Set all potentiometers on the Range Calibration Board to midpoint.
4. Connect a 24V AC power supply source to J201.
5. Connect a digital meter to TP202 (A200 PCB).

CALIBRATION TABLE

| RANGE SWITCH | | INTERNAL POTS : BEING ADJUSTED | POSITION OF EXTERNAL : POTENTIOMETERS | Current : Adjust | Pulse : Amplitude | CALIBRATION MEASUREMENTS : on TP202 |
|--------------|-----|--------------------------------|---------------------------------------|------------------|-------------------|-------------------------------------|
| 500 W | MIN | R606 | CCW | : | : | 100 MV (20A) |
| | MAX | R612 | CW | : | : | 180 MV (36A) |
| 800 W | MIN | R605 | CCW | : | : | 145 MV (29A) |
| | MAX | R611 | CW | : | : | 215 MV (43A) |
| 1000 W | MIN | R604 | CCW | : | : | 185 MV (37A) |
| | MAX | R610 | CW | : | : | 270 MV (54A) |

7. Connect short between the collector of Q215 and ground.
- | | | | | | | |
|--------|-------|------|----|---|----|--------------|
| 500 W | PULSE | R618 | CW | : | CW | 320 MV (64A) |
| 800 W | PULSE | R617 | CW | : | CW | 410 MV (82A) |
| 1000 W | PULSE | R616 | CW | : | CW | 410 MV (82A) |
8. Remove short from Q215 collector.
 9. Turn the "CURRENT ADJUST CONTROL" CCW. Apply +5 volts dc external analog signal* to the "EXTERNAL PROGRAM" jack located on the front panel.
 10. Check 500 W MAX, 800 W MAX and 1000 W MAX reference Calibration Table.

NOTE: A 0 to +5 volt external power supply may be used or a 1K pot. connected between the 5 volt reference and ground on the control board.

4.3.1 CHECKING PULSE WIDTH MODULATOR

1. Connect oscilloscope to collector of Q215.
2. Apply a +5 volt pulse to "PULSE TRIGGER" jack.
3. A. Turn "PULSE WIDTH" control adjustment fully CW. - A negative 250us pulse will appear with each trigger.
B. Turn "PULSE WIDTH" control adjustment fully CCW. - A negative 1us pulse will appear with each trigger.
4. Disconnect external ac source from control board.
5. Reconnect plugs J203 to P301 and P1 to J201.
6. Connect a resistive load in series with an external ammeter across the output of the power supply.
7. Plug ac cord into ac source and turn AC switch to "ON".

4.3.2 CALIBRATION OF LAMP CURRENT METER

1. Turn power supply "OFF", zero the lamp current meter.
2. Set range select switch to 1000W.
3. Connect a .400 ohm 1000W resistive load in series with an external ammeter across the output of the power supply.
4. Turn power supply circuit breaker "ON".
5. Turn "CURRENT ADJUST" until external meter reads 50 amps.
6. Adjust current meter potentiometer R7 for the same reading as external ammeter (50 amps).

4.3.3 SHUNT SENSE CALIBRATION

1. Connect a digital meter to the junction of R244 and R245.

SECTION V

PARTS LISTS

PAGE 16

5.1 GENERAL

This section contains a list of replacement parts for the and names of the typical manufacturers of these parts.

2 LIST OF MANUFACTURERS

The following list contains the key to the abbreviations in the parts list, company name and address.

| ABV | COMPANY NAME | COMPANY ADDRESS |
|-----|-------------------------------|--|
| AB | ALLEN-BRADLEY | 1201 South 2nd Street Milwaukee, WI 53204 |
| AL | ALCDSWITCH | 1551 Osgood St. N. Andover, MA 01845 |
| AM | AMPHENOL | Distribution Marketing 2875 S. 25th Avenue Boardway, IL 60153 |
| AP | AIRPAX | North American Philips Control Corp. Cambridge Division Cambridge, Maryland 21613 |
| AT | AMETEK | Rodan Division 2905 Blue Star Street Anaheim, CA 92806 |
| BK | BECKMAN | 2500 Harbor Boule. Fullerton, GA 92634 |
| BO | BOURNS | Trimparts Products Division 1200 Columbia Avenue Riverside, CA 92507 |
| CD | CORNELL DUBILIER ELEC. CO. | 150 Avenue "L" Newark, N.J. 07105 |
| CL | CP CLARE | |
| CTS | CTS CORPORATION | 905 N. West Blvd. Elkhart, Indiana 46514 |
| CU | CURTIS INSTRUMENTS, INC. | 200 Kisco Avenue Mt. Kisco, N.Y. 10549 |
| DA | DALE ELECTRONIC INC. | Box 785 Columbus, NE 68601 |
| EC | ELECTRONIC CONCEPTS INC. | P.O. Box 627 Eatontown, New Jersey 07724 |
| EM | ELECTRONIC MEASUREMENTS, INC. | 405 Essex Road Neptune, N.J. 07753 |

| | | |
|-----------------|---|--|
| ETI | ELECTRO TECHNIQUES INC. | 215 Via Del Norte Oceanside, CA 92054 |
| GE | GENERAL ELECTRIC | 1 Plastic Avenue Pittsfield, MA 01210 |
| ICC | INTERNATIONAL COMPONENTS CO. | 105 Maxess Road Melville, N.J. 11746 |
| KE | KEMET, UNION CARBIDE INC. | P.O. Box 5928 Greenville, SC 29606 |
| LE | LEECRAFT MANUFACTURING INC. | 21-02 44th Road Long Island City, N.Y. 11101 |
| LF | LITTLE FUSE | 800 E. North Highway DesPlaines, IL 60532 |
| ME | MEPCO/ELECTRA | 6071 St. Andrews Road Columbia, S.C. 29210 |
| MO | MOTOROLA INC. | P.O. Box 20912 Phoenix, AZ 85036 |
| CDE, RKO ERO | ROEDERSTEIN | 2100 West Front Street Stateville, NC 28677 |
| SG | SILICON GENERAL | 11651 Monarch Street Garden Grove, CA 92641 |
| | SIEMENS CORPORATION | Colorado Components Division 800 Hoyt Street, Broomfield, Colorado 80020 |
| ST | UNITED TECHNOLOGIES HAMILTON STANDARD CONTROLS | Stancor Products 131 Godfry Street Logansport, IN 46947 |
| SU | SUPERIOR ELECTRIC COMPANY | 383 Middle Street Bristol, CT 06790 |
| TH | THERM-O-DISC INC | 1320 S. Main Street Mansfield, Ohio 44907 |
| TO | TORIN CORPORATION | 100 Franklin Drive Torrington, Connecticut 06970 |
| UC | UNION CARBIDE | Component Department P.O. Box 5928 Greenville, S.C. 29606 |
| UN | UNITRODE CORPORATION | 5 Forbes Road Lexington, MA 02173 |
| VA | VARO SEMICONDUCTOR, INC | 2900 W. Kingsley Drive Garland, Texas 75040 |

5.3 PARTS LIST

NOTE: WW stands for wire-wound.

RESISTORS

| CIRCUIT REF. | DESCRIPTION | MFR PARTS NO. | MFR CODE |
|------------------|-------------------|---------------|-------------------|
| R1,R2 | 33K 1W 5% COMP | 67003066 | GB3335 AB |
| R3,R5 | 1K 1T 10% POT | 67054002 | 3852A-282-102A DA |
| R4 | 100K 10T POT 10% | 67055004 | 850-100K ETI |
| R6,1407, 1408 | 500 ohm 25W 5% ww | 67023048 | HL-25-06Z 500 DA |

A200 CONTROL BOARD

| | | | |
|--|--------------------|----------|---------------|
| R201,6,9, 10,24,30, 35,51,59, 66,67 | 1K 1/2W 5% COMP | 67002013 | EB1025 AB |
| R203,11, 62,63 | 10K 1/2W 5% COMP | 67002014 | EB1035 AB |
| R261 | 3.3K 1/2W 5% COMP | 67002065 | EB3225 AB |
| R204,17, 38,39,40, 41,42,45, 46,50,57, 65,68 | 4.7K 1/2W 5% COMP | 67002075 | EB4725 AB |
| R205 | 2.7K 1/2W 5% COMP | 67002060 | EB2725 AB |
| R207,12 | 2.2K 1/2W 5% COMP | 67002049 | EB2225 AB |
| R208,15, 20 | 15K 1/2W 5% COMP | 67002030 | EB1535 AB |
| R213 | 22K 1/2W 5% COMP | 67002080 | EB2135 AB |
| R214,70 | 6.8K 1/2W 5% COMP | 67002090 | EB6825 AB |
| R216 | 47 1/2W 5% COMP | 67002006 | EB4705 AB |
| R218 | 3.9K 1/2W COMP | 67002070 | EB3925 AB |
| R219 | 220 1/2W 5% COMP | 67002048 | EB2215 AB |
| R222,602 | 2.74K 1/4W 1% FILM | 67006038 | RN60C274IF DA |

| | | | | |
|---------------------------------|--------------------|------------|------------|----|
| R223 | 390 2W R% COMP | 67004069 | HB3915 | AB |
| R225,233 | 270 2W 5% COMP | 67004059 | HB2715 | AB |
| R227,228, 234,237 | 1.5K 1/2W 5% COMP | 67002029 | EB1525 | AB |
| R229,236 | 470 1/2W 5% COMP | 67002074 | EB4715 | AB |
| R230 | 47 2W 5% COMP | 67004006 | EB4705 | AB |
| R231,232 | 1 3W 5% WW | 67019001 | CW-2B-1 | DA |
| R243,244 | 1K 1/4W 1% FILM | 67006001 | RN60C1001F | AB |
| R247,272 | 100 1/4W 1% FILM | 67006094 | RN60C1000F | AB |
| R254,255, 256 | 4.99K 1/4W 1% FILM | 67006053 | RN60C4991F | AB |
| R258,603, 607 | 4.32K 1/4W 1% FILM | 67006097 | RN60C4321F | AB |
| R260 | 390 1/2W 5% COMP | 67002069 | EB3915 | AB |
| R264,604, 605,606 | 1K TRIM POT | 67063007 | 72LPRIK | BK |
| R269 | 1.5M 1/2W 5% COMP | 67002032 | EB1055 | AB |
| R271 | 20 Ohm TRIM POT | 67-063-006 | 72LPR20 | BK |
| R283 | 560 1/2w 5% COMP | 67002084 | EB5615 | AB |
| R301,301A, 304,304A, 1402 | 10 5W 5% WW | 67020012 | CW5-105 | DA |
| R302,302A, 305,305A | 100 1/2W 5% COMP | 67002012 | EB1015 | AB |
| R401 | 10K 2W 5% COMP | 67004014 | CW2-10K5 | DA |
| R402,403, 404 | 8.2M 1W 5% | 67003098 | CW1-8.2M5 | DA |
| R601,613, 615 | 2.99K 1/8W 1% FILM | 67005030 | RN60C1001F | DA |
| R608 | 5.62K 1/8W 1% FILM | 67005073 | RN55C5621F | DA |
| R609 | 3.92K 1/4W 1% FILM | 67006047 | RN60C3921F | DA |
| R610,611, 612 | 5K TRIM POT | 67063006 | 72PLR5K | BK |
| R614 | 1.5K 1/4W 1% FILM | 67006012 | RN60C1501F | DA |

| | | | | |
|----------------------|---------------------|----------|---------------|-----|
| R615 | 2.21K 1/4W 1% FILM | 67006030 | RN60C2211F | DA |
| R616,617, 618 | 500 Ohm TRIMPOT | 67063002 | 72PLR500 | BK |
| R701,702, 703,704 | 250 OHM 3W 5% WW | 67019040 | CW-2B-250 | DA |
| R705 | 100 OHM 25W 5% WW | 67023026 | HL-25-06Z-100 | DA |
| R1401 | 300 5W 5% | 67020043 | CW5-3005 | DA |
| R1403 | 5 5W 5% | 67020009 | CW5-55 | DA |
| R1404 | 50A 250mV Shunt | 70013001 | 70013001 | EM |
| R1405 | 2.5 5W 5% | 67020018 | CW5-2.55 | DA |
| R1406 | 56K 2W | 67004086 | CW2-56K5 | AB |
| R1409 | 42.2 OHM 1/4W 1% FM | 67006085 | RN60C42R2F | DA |
| R1410 | 10 OHM TRIM POT | 67058003 | 117A-10A | CTS |
| R1411 | 250 OHM 10W 5% | 67022040 | RS10-250-10 | DA |

Capacitors

| | | | | |
|---|--------------------|----------|---------------|-----|
| C1,C2 | 5K uF 200V Elec | 54046008 | 318GGE512T200 | ME |
| C3 | 1uF 660ufacV Oil | 54021001 | 26f6616 | GE |
| C101,102, | 2200PF 400V DISC | 54068002 | RK0600 | ERO |
| C103,104 | .47uF 250V Film | 54066001 | F1173-447-200 | ERO |
| C201 | 2200 uF - 40V Elec | 54034003 | DIN 41 316 | ERO |
| C202 | 10 UF - 25V Elec | 54026003 | SM25VB100 | UC |
| C203,205, 211,223, 702,3,5, 7,9,11 | .005uF - 1KV Disc | 54003004 | 5HK-050 | SP |
| C204,212 | 10 uF - 50V Elec | 54023001 | SM50V910 | UC |
| C206,7,8, 13,15,19, 21,22 | .01uF - 100V Disc | 54002002 | TG-510 | SP |
| C209,10, 26 | .001uF - 1KV Disc | 54003002 | EGA-D10 | SP |
| C214 | 2.2uF - 35V Tant. | 54017002 | T11B225M035AS | KE |

| | | | | |
|----------------------|--------------------|-----------------|----------------|-----|
| C216 | .01uF - 100V Film | 54006008 | WMF1S1 | CDE |
| C217,18 | 50uF - 100V Elec | 54025002 | PDA100MFD | ICC |
| C225 | 470pF - 500V | 54024002 | DM15-471J | CD |
| C302,02A, 04,04A, | 22uF 15V Tant. | 54016002C401-06 | T110B226J015AS | KE |
| C305,05A, | .1uF 100V DISC | 54002001 | T110B226J015AS | KE |
| C401-6 | .22uF - 1KV Film | 54009001 | ME2-2186K | EC |
| C702,03 | .005uF - 1KV | 54003004 | 5HK-D50 | SP |
| C701,1401 | 4 uF 400V FILM | 54008002 | ME2-0729K | EC |
| C1402 | .001uF - 500V Mica | 54014001 | CM20C102J | CD |
| C1404 | .022uF - 660V Film | 54010001 | MKT1813 | ERO |
| C1405,06 | 1400uF 1KV Elec | 54045001 | 3186BA142U050A | ME |
| C1407,11 | .02uF 1KV Disc | 54003003 | SGA-D50 | SP |
| C1408 | 1uF - 250V Film | 54007001 | YM10000-2A | ICC |
| C1401,9, 10 | 820uF - 200V Elec | 54046007 | CGS821T200L | MA |

DIODES

| | | | | |
|--|-----------------|----------|-----------|----|
| CR1 | 600V 25A FWB | 60028001 | KBPC25-06 | GI |
| CR201,2, 3,4 | 200V 3 Amp | 60007001 | V332 | VA |
| CR205,6, 7,10,11, 21,23,25, 26 | 200V 1 Amp | 60006001 | IN4003 | GE |
| CR208,19, 20,24 | 12V Zener | 60001004 | IN4742 | MO |
| CR209 | 5.6V Zener | 60001007 | IN4734 | MO |
| CR212,13, 15,16,28, 29,601,2, 3,17,27 | 100V 1 Amp | 60005002 | IN4148 | MO |
| CR214,18 | 6.2V Zener | 60003002 | IN823A | MO |
| CR222 | 27V Zener 1W 5% | 60001009 | IN4750A | MO |

| | | | |
|-----------------------|----------|-------------|----|
| CR301, 1A, 400V 3 Amp | 60007005 | V334X | VA |
| 02, 02A, 4, | | | |
| 4A, 5, 5A, | | | |
| 8, 8A, 11, | | | |
| 11A, 701, | | | |
| 02, 03, 04, | | | |
| 05, 06, 07, | | | |
| 08, 1401, | | | |
| 02, 03, 04 | | | |
| CR401-10 1000V 1A | 67006005 | IN4007 | MO |
| CR709 600V 30A FWB | 60028001 | MB12A25-V60 | WE |
| CR710, 11 150V 50A | 60018001 | D621ED25S | SI |
| CR712 1000V 85A | 60014003 | S37100 | SI |

TRANSISTORS

| | | | |
|---------------------------|----------|-----------|-----|
| Q201, 2, 3, PNP Signal | 62001001 | 2N2907A | MO |
| 16 | | | |
| Q204, 5, 7, NPN Signal | 62001002 | 2N2222A | MO |
| 9, 14, 15 | | | |
| Q206, 8 NPN | 62002004 | 2N3053 | MO |
| Q210, 11, NPN | 62002006 | F7771 | EM |
| 12, 13, 301 | | | |
| 01A, 2, 2A | | | |
| Q701-704 NPN HV Switching | 62005008 | D64VS5 or | GE |
| | | 2N6678 | RCA |

INTERGRATED CIRCUITS AND VOLTAGE REGULATORS

| | | | |
|------------------------|----------|---------|----|
| IC201 Pulse Width Mod. | 64006001 | SG3524N | SG |
| IC202 Operation Ampl. | 64003016 | LM324N | MO |
| IC203 Timer | 64002003 | NE555V | MO |

GENERAL PARTS

| | | | |
|-------------------------------|----------|-------------------|----|
| CB1 Circuit Breaker 2P 250V | 56016001 | UPGH 11-1-6250201 | AP |
| S1, S3 Switch Pushbutton .25A | 68028000 | 903 | SW |
| S601 Switch Rotary 3P 3T | 68041000 | MRSB-3-3K-FC | AL |
| J1 Jack 50A | 35023002 | RF50GR | SU |

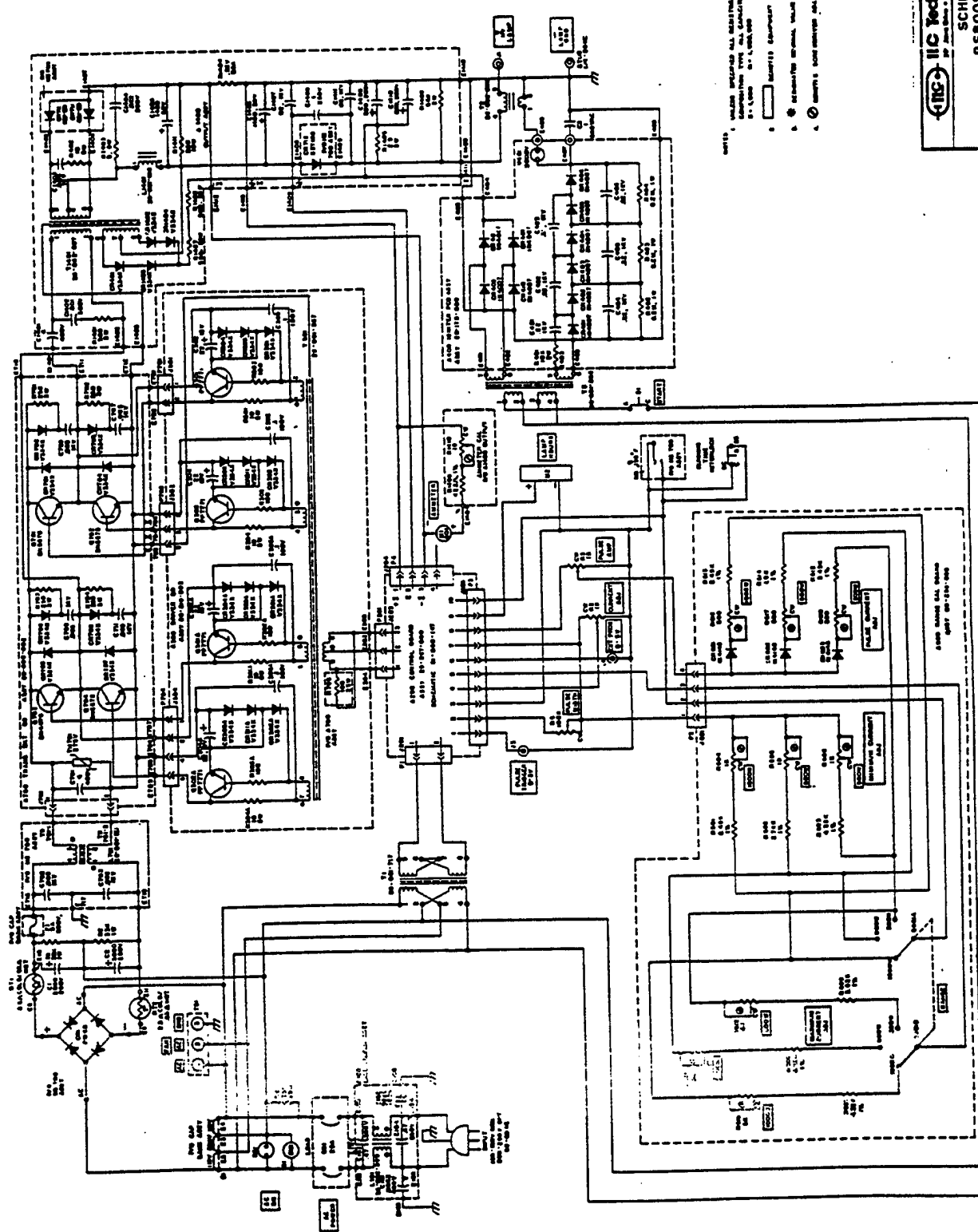
| | | | | |
|-------|-------------------------------|----------|------------------|----|
| | Plug 50A | 35024002 | PS50GR | SU |
| J3,4 | Connector BNC | 72112000 | UG625-31-256 | AM |
| T1,2 | Thermistor 15A | 67066002 | SG-160 | AT |
| M1 | Meter 50MV Special Scale | 66096001 | | EM |
| M2 | Elapsed Time Indicator 1000HR | 66079000 | Model 120-PC | CU |
| TS701 | Thermostat N/D 197 F | 68001001 | 36T22 Style 9225 | TH |
| DS1 | Lamp Neon Red | 57002001 | 36U2311-125V | LE |
| V401 | Spark Gap 2KV | 69007001 | SP2.0 | CL |
| B1 | FAN 4 11/16" 115V | 51002001 | A28678-10 TA450 | TO |
| T1 | Transformer 115/230V 12/24V | 28001717 | P6377 | ST |
| T2 | Transformer Ignitor | 28002008 | | EM |
| T3 | Transformer Boost | 28001888 | | EM |
| T301 | Transformer Driver | 28001287 | | EM |
| T1401 | Transformer Power | 28002007 | | EM |
| L701 | Choke Filter | 28001121 | | EM |
| L1401 | Choke Filter | 28001120 | | EM |
| L101 | Choke RFI | 28002599 | | EM |

PRINTED CIRCUIT CARDS AND OTHER ASSEMBLIES WITH PARTS

| Board Ref. | Description | Order Part Number |
|------------|----------------------------------|-------------------|
| A100 | Line Filter Assy. | 26142000 |
| A200 | PCB Control Circuit | 20267000 |
| A300 | PCB Drive Circuit | 20010002 |
| A400 | PCB Igniter Circuit | 20178000 |
| A600 | PCB Range Cal. | 20268000 |
| A700 | Assy. PCB Transistor Socket | 20090002 |
| HS700 | Heatsink Assy plus A300 and A700 | 23049000 |
| A1400 | Assy. Output Plate | 24067000 |
| | Assy. Front Panel | 25532000 |
| | Assy. Cap MTG. Plate | 24460010 |

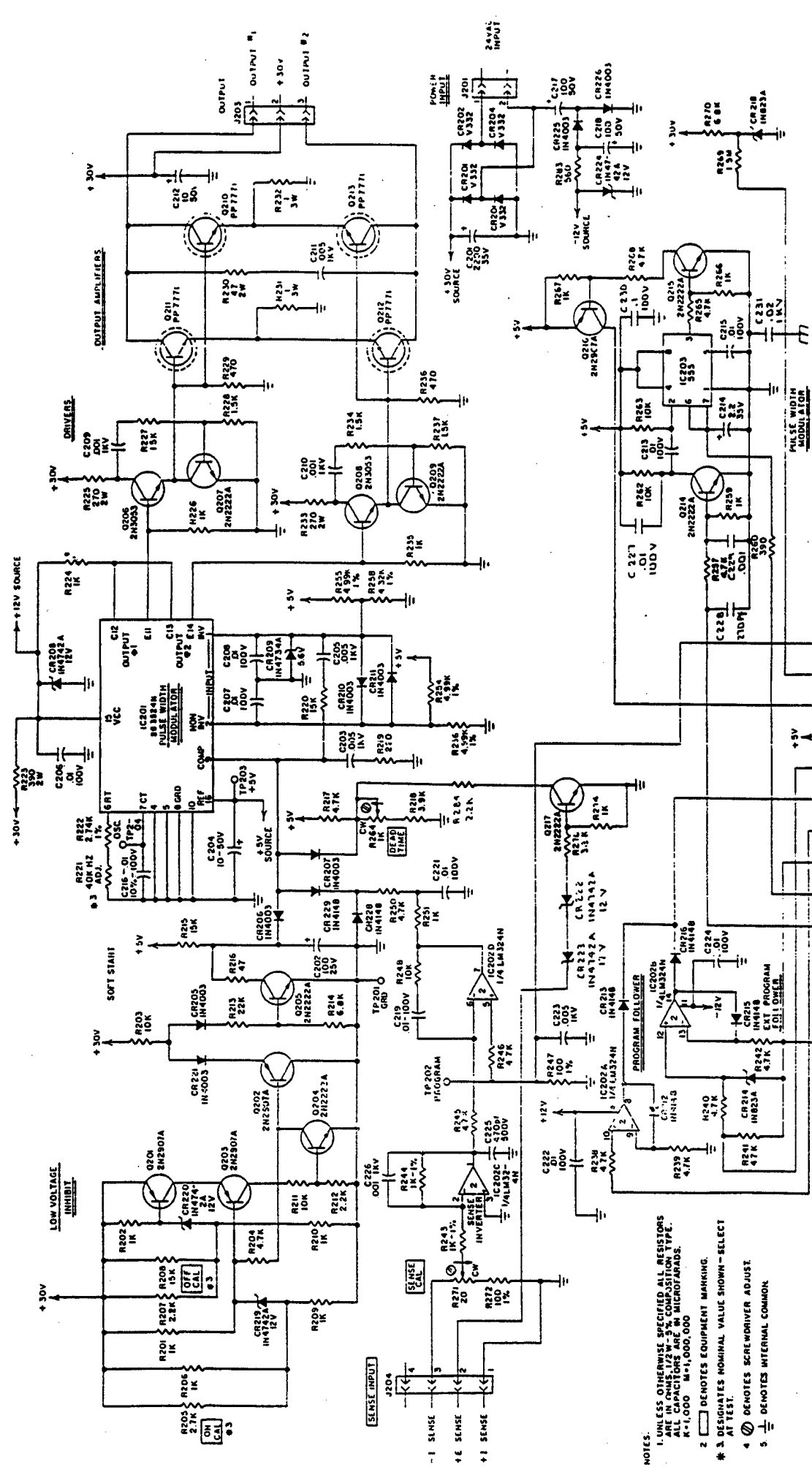
SECTION VI

SCHEMATICS



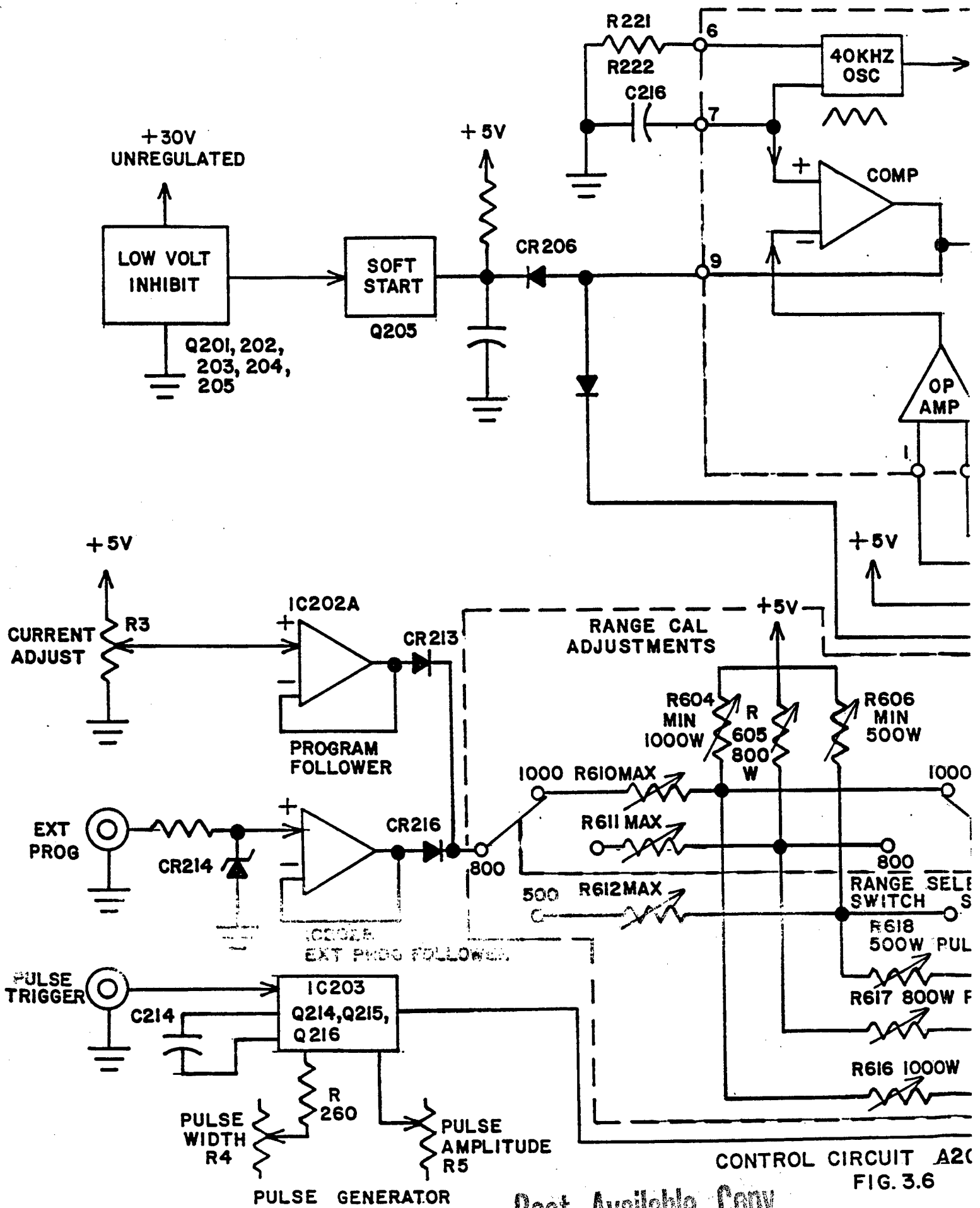
NOTES:
 1. VALUES INDICATED ARE UNLESS OTHERWISE NOTED. U.S.P. S.I. UNITS.
 2. RESISTOR VALUES: ALL UNLESS OTHERWISE NOTED.
 3. CAPACITOR VALUES: ALL UNLESS OTHERWISE NOTED.
 4. RESISTOR TOLERANCE: UNLESS OTHERWISE SPECIFIED.
 5. CAPACITOR TOLERANCE: UNLESS OTHERWISE SPECIFIED.
 6. RESISTOR TYPE: UNLESS OTHERWISE SPECIFIED.

IIC Technology, Inc.
 10000 E. 10th Avenue, Suite 100, Denver, CO 80231, U.S.A.
SCHEMATIC
PS800SW-1



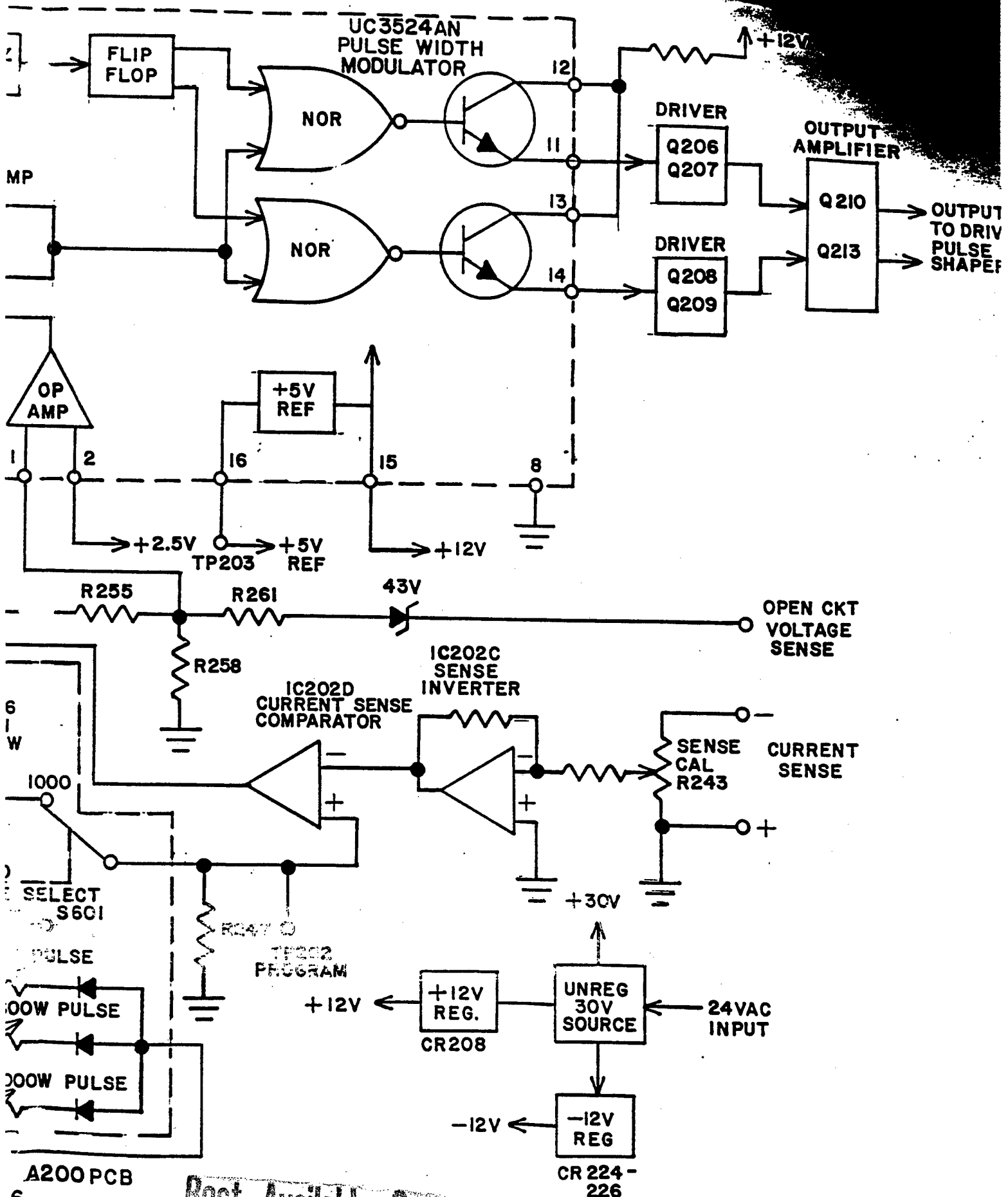
ILC Technology, Inc.
 A200 SCHEMATIC
 P-5800SW-1

- NOTES:
1. UNLESS OTHERWISE SPECIFIED ALL RESISTORS ARE IN OHMS, 1/2W-5% COMPOSITION TYPE. ALL CAPACITORS ARE IN MICROFARADS.
 2. □ DENOTES EQUIPMENT MARKING.
 3. * 3 DESIGNATES NOMINAL VALUE SHOWN - SELECT AT TEST.
 4. ⊕ DENOTES SCREWDRIVER ADJUST.
 5. ⊖ DENOTES INTERNAL COMMON.



CONTROL CIRCUIT A2C
FIG. 3.6

Best Available Copy



A200 PCB
6

Best Available Copy

References

- Ando, K., M. Ohki, M. Ohta, M. Ogino, and E. Yamazaki, *Projection Display Series for High-Definition TV*, Proc. SPIE 1081, 38, (1989).
- Born, M. and E. Wolf, *Principles of Optics* (1975), Table XIX, p394., (Pergamon, New York)
- Breen Jr, P.T., *Function Requirements for C³I Large Screen Displays*, Proc. SPIE 1081, 1 (1989).
- Bruce, R.H., *Active-Matrix Liquid-Crystal Displays* in SID Seminar Lecture Notes, F3, (1991), Vol. II, and the references therein.
- Campbell, F.W. and D.G. Green, *Optical and Retinal Factors Affecting Visual Resolution*, J. Physiol. 187, 576, (1965).
- Demos, G., *Computing Needs for High Resolution Synthetic Images*, Proc. SPIE 1081, 122 (1989).
- Goede, W.F., *Status of Electronic Displays* in SID Seminar Lecture Notes, (1991), Vol. I.
- Good, W.E. et al., *System Concepts and Recent Advancements in a Light Valve Color-TV Projector*, Digest of Technical Papers, SID International Symposium, 24 (1971).
- Goodman, J.W., *Introduction to Fourier Optics*, (1968), (McGraw-Hill, New York)
- Holmes, R.E., *VideoramaTM-a new concept in juxtaposed large screen displays*, Proc. SPIE 1081, 15 (1989).
- Hopkins, R. and K.P. Davies, *Development of HDTV Emission Systems in North America* in SID Seminar Lecture Notes, (1991), Vol. I.
- Jones, P., A. Tomita and M. Wartenberg, *Performance of NCAP projection displays*, SPIE/SPSE 1456, Conf., San Jose, Feb 26, 1991.
- Klein, M.V., *Optics*, (1970), p.300 ff, (John Wiley and Sons, New York).
- de Lang, H. and G. Bouwhuis, *Colour Separation in Colour-Television Cameras*, Phillips Technical Review, 24, 263, (1963).
- Longhurst, R.S., *Geometrical and Physical Optics*, (1964), p24, (John Wiley and Sons, New York).
- Masterman, H., C. Johnson, and M. Silverstein, *How to Select a CRT Monitor*, Beta Review Inc, Millwood VA (1990 and 1991).
- Matthies, D.L., and P. Heyman, *Projection displays*, in Commercial Technology Assessment, NIDL at the David Sarnoff Research Center, (S. Miller ed.), (May 9, 1991).
- Miyasaka, T., H. Kamakura, J. Shinozaki, and S. Morozumi, *Full-color projector with poly-Si thin film transistor (TFT) lightvalves*, Proc. SPIE 1081, 64 (1989).

Mori, Y., K. Funahata, Y. Nagae, and H. Kawakami, *Optical System of a Multicolor Laser-Addressed Liquid-Crystal Projection Display*, Digest of Technical Papers, SID International Symposium XIX, 102, (1988).

Optical Society of America, Handbook of Optics, W.G. Driscoll ed., Section 12, (1978), (McGraw-Hill, New York).

Scheuble, B.S., *Liquid Crystal Displays with High Information Content*, SID Seminar Lecture Notes, F2 (1991), Vol. II and the references therein.

Schlam, E., *Overview of Flat Panel Displays* in SID Seminar Lecture Notes, (1991), Vol II.

Smith, W.J., Modern Optical Engineering, Second ed. (1990), (McGraw-Hill, New York)

SMPTE Journal, February and March 1980.

Stanley, E.H., Introduction to Phase Transitions and Critical Phenomena, (1971), (Oxford University Press, New York).

Stroomeer, M.V.C., *CRT and LCD Projection TV; A Comparison*, Proc. SPIE 1081, 136 (1989).